

# **Interstitial Cells In Human Paediatric Colon Of Hirschsprung Disease**

**Hanan Issa Ali El-Kuwaila**

Submitted in accordance with the requirements for the degree of  
Doctor of Philosophy

The University of Leeds  
School of Biomedical Sciences

The candidate confirms that the work submitted is her own and that appropriate credit has been given where reference has been made to the work of others.

This copy has been supplied on the understanding that it is copyright material and that no quotation from the thesis may be published without proper acknowledgement.

## **Dedication**

I am dedicating this thesis to my beloved Dad who has meant and continue to mean so much to me. Although he is no longer of this world, his memories continue to regulate my life. His love for me knew no bounds, and he taught me the value of hard work. I will never forget you. I will make sure your memory lives on as long as I shall live. I love you and miss you beyond words. You never had the chance to see me complete this work. I know that you would be proud.

## **Acknowledgements**

First and foremost, I would like to acknowledge the support and guidance of my supervisor Professor. Jim Deuchars. You were always willing to meet to share ideas, give advice, and address any concerns I may have had.

I would like to thank my second supervisor Mr. Jonathan Sutcliffe for his efforts over the 4 years of my study, I will never forget my weekly meetings with you and your valuable help and support which kept me on track . To my third supervisor Andrew Smith, thank you very much for your help.

I am grateful to all members of the Deuchars lab that I had the honour to work with, including Susan Deuchars for her support during my hard times she was the first person to talk to when I feel down, thank you very much. Also cannot forget Emily Johnson with her beautiful face for the kind support, thanks for lending a helping hand when it was needed. I want to make special mention of Christian Nathan for his incredible help, whether I needed help with protocols and techniques.

Massive thanks to the Leeds General Infirmary (LGI) Hospital, Paediatric surgery department staff for their help, especially Mr. Ian Sugarman, and I must also thank the team in the histopathology department at St James Hospital especially Dr Kerry Turner for her incredible help and support.

To my best friend Safia Younis, thank you very much for being my sister and support me throughout my study.

To my family, my mum, my sisters and brothers thanks for all your support, for believing in me and being there whenever I needed you, no matter how far we are.

Lastly, I would like to thank my small family, my beautiful daughters Rayan, Bnan, and my little one Khadiga for all their love and encouragement. Without you being with me this work would never had finished, I love you all so much.

This work was kindly funded by my country Libya through Libyan Embassy in London.

## Abstract

Interstitial Cells originate from mesenchymal embryonic layer communicate with smooth muscle cells in many organs and provide important regulatory functions. Two different classes of Interstitial Cells (ICs) namely, cKit<sup>+</sup> and PDGFR $\alpha$ <sup>+</sup> ICs have been described in detail in the gut tissue. They represent distinct groups of cells with distinctive ultrastructure. Both cell types are electrically coupled to smooth muscle cells (SMCs) and enteric neuronal cells, together forming an integrated unit called the SIP syncytium. SIP cells express a range of receptors and ion channels such as Ca<sup>2+</sup>- activated Cl<sup>-</sup> channel (Ano1) and Ca<sup>2+</sup>-activated K<sup>+</sup> channels (SK3), changes in the conductance of any type of SIP cells affect the excitability of the whole syncytium unit. cKit<sup>+</sup> ICs provide pacemaker activity, slow wave propagation pathways and motor neurons input transduction. Loss of ICs has been associated with gut motility disorders. However, the pathophysiological roles of these cells were not clearly defined in most cases. Gastrointestinal smooth muscles produce electrical activity (slow waves) that is not dependent on nerve input. Intrinsic pacemaker activity comes from cKit<sup>+</sup> ICs, which are electrically coupled to SMCs via gap junctions. Abnormalities in ICs numbers and networks has been linked to several gastrointestinal motility disorders.

Hirschsprung disease (HD) is a congenital malformation of the enteric nervous system (ENS). The diagnosis is generally established by an experienced pathologist based on histopathological studies of rectal biopsies. Obstructive symptoms such as constipation or recurrent intestinal dysmotility problems are

common after definitive surgery. Defining how ICs are affected in HD allows insights into the interdependence of the ENS and ICs. Furthermore, these post-operative complications have led researchers to consider alternative therapies based on understanding the role of ICs in developing the HD.

This project describes different protocols including, immunohistochemistry, *in situ hybridization*, qPCR and RNAseq for identifying ICs in a step toward understanding their contributions in gut motility disorder especially HD. However, further experiments and computational techniques are required to confirm the function of ICs in HD.

## Table of Contents

<b>Dedication</b> .....	<b>I</b>
<b>Acknowledgements</b> .....	<b>ii</b>
<b>Abstract</b> .....	<b>iv</b>
<b>Table of Contents</b> .....	<b>vi</b>
<b>List of Figures</b> .....	<b>xi</b>
<b>List of Tables</b> .....	<b>xv</b>
<b>Abbreviations</b> .....	<b>xvi</b>
<b>Chapter 1 General Introduction</b> .....	<b>1</b>
1.1 Gastrointestinal function .....	1
1.2 Histology of human gut.....	1
1.3 What are Interstitial Cells?.....	3
1.4 Immunomarkers for cKit <sup>+</sup> ICs.....	4
1.5 Immunomarkers for PDGFR $\alpha$ <sup>+</sup> ICs .....	6
1.6 Embryological development of Interstitial Cells .....	10
1.7 Ultrastructural feature of ICs and their distribution throughout the gut 13	
1.8 IC distribution within the human gut .....	14
1.8.1 IC distribution in human stomach .....	16
1.8.2 IC distribution in human small intestine .....	16
1.8.3 IC distribution in human colon .....	17
1.9 IC and enteric innervation.....	18
1.10 IC function in gastrointestinal motility .....	20
1.11 The SIP syncytium .....	23
1.11.1 Glial cells in SIP .....	25
1.12 Mechanism of slow wave generation in the smooth muscle .....	27
1.13 Involvement of IC in smooth muscle contractility .....	28
1.13.1 Excitatory enteric innervation and smooth muscle contraction in the gut (cholinergic neurotransmission).....	28
1.13.2 Inhibitory enteric innervation and smooth muscle relaxation in the gut (purinergic neurotransmission).....	33
1.14 The role of IC in gastrointestinal disease.....	37

1.15 Hirschsprung disease .....	39
1.15.1 Distribution of cKit <sup>+</sup> ICs in HD.....	41
1.15.2 Distribution of PDGFR $\alpha$ <sup>+</sup> ICs in Hirschsprung disease.....	42
1.15.3 Genetics of Hirschsprung disease.....	43
1.16 Expressions of gene encoding tyrosine kinase protein and ion channels in ICs.....	45
1.17 Aims of the study .....	47
<b>Chapter 2 Optimising Methods of Fixation and Processing for Immunostaining in Fresh Tissue and Evaluating Methods of Quantification .....</b>	<b>49</b>
2.1 Introduction.....	49
2.2 Tissue fixation .....	49
2.2.1 Types of fixation .....	50
2.3 Quantification Procedures .....	52
2.4 Aims and objectives.....	57
2.5 Materials and methods .....	58
2.5.1 Specimen collection .....	58
2.5.2 Fixation and Sectioning.....	59
2.5.3 Immunohistochemistry .....	61
2.5.4 Imaging and quantification analysis .....	64
2.5.5 Quantification Methods .....	64
2.5.6 Quantification using automated software .....	65
2.6 Statistical analysis .....	66
2.7 Results .....	67
2.7.1 Labelling of ICs in fresh tissue is fixative dependent.....	67
2.8 Quantification Results.....	75
2.8.1 Semi-quantification method.....	75
2.8.2 Computational quantification of stained disease control samples.....	79
2.9 Discussion .....	89
2.9.1 Optimized methodology of labelling and assessing IC networks	
2.10 Conclusion.....	94

<b>Chapter 3 Testing Immunohistochemical and <i>In Situ hybridisation</i> protocols in human archived formalin fixed paraffin-embedded Hirschsprung disease tissue samples .....</b>	<b>95</b>
3.1 Introduction.....	95
3.2 Fresh Frozen vs FFPE tissue samples.....	97
3.3 Issues of standardisation and the use of antigen retrieval.....	99
3.4 Analysis of genetic material.....	100
3.5 Aims and objectives.....	102
3.6 Material and methods.....	103
3.6.1 Formalin - fixed paraffin embedded (FFPE) archived samples	103
3.6.2 Preparing FFPE sections for immunostaining .....	103
3.6.3 Immunofluorescent staining .....	104
3.6.4 Chromogenic DiaminoBenzidine (DAB) staining .....	104
3.6.5 <i>In Situ Hybridisation</i> (ISH) using RNAscope technique.....	107
3.6.6 Quantification of the RNA expression .....	109
3.7 Results and conclusion.....	109
3.7.1 Antigen Retrieval and immunostaining of FFPE .....	109
3.7.2 Immunoperoxidase chromogenic immunostaining .....	113
3.7.3 RNAscope <i>In Situ Hybridisation</i> (ISH).....	117
3.8 Discussion .....	120
3.8.1 Immunostaining of FFPE archived HD samples.....	120
3.8.2 Detection of RNA in FFPE tissue .....	122
3.9 Conclusion.....	123
<b>Chapter 4 cKit<sup>+</sup> and PDGFR<math>\alpha</math><sup>+</sup> Interstitial Cells in Hirschsprung Disease .....</b>	<b>124</b>
4.1 Introduction.....	124
4.2 Aims .....	131
4.3 Material and Methods.....	132
4.3.1 Tissue processing for Hematoxylin and Eosin staining .....	132
4.3.2 Immunohistochemical staining .....	133
4.3.3 Protein receptor markers of ICs colocalization with the functional ion channels expressed by ICs .....	134
4.3.4 Statistics.....	134
4.4 Results .....	134
4.4.1 Hirschsprung disease histopathology conformation .....	134

4.4.2	Immunohistochemical staining .....	135
4.4.3	Distribution of cKit <sup>+</sup> and Ano1 <sup>+</sup> ICs in HD .....	140
4.4.4	Distribution of PDGFR $\alpha$ <sup>+</sup> and SK3 <sup>+</sup> ICs in HD .....	143
4.5	Discussion .....	149
4.5.1	Distribution of Interstitial Cells as compared to other studies in HD .....	149
4.5.2	Hirschsprung Disease and Disease Control samples difference... 152	
4.5.3	Ratio of different types of IC target PDGFR $\alpha$ <sup>+</sup> cells .....	154
4.6	Conclusion.....	154
<b>Chapter 5 Gene expression in Hirschsprung Disease.....</b>		<b>155</b>
5.1	Introduction.....	155
5.2	Aims of the study .....	159
5.3	Material and methods: .....	160
5.3.1	Sample collection .....	160
5.3.2	RNA extraction, reverse transcription and quantitative polymerase chain reaction (qPCR) .....	160
5.3.3	Interstitial Cell isolation using Fluorescence-Activated Cell Sorting (FACS).....	165
5.3.4	Manual isolation of ICs using micro- electrode techniques .	168
5.3.5	Targeted RNA sequencing of specific colon wall layers .....	170
5.3.6	cDNA synthesis.....	173
5.3.7	cDNA amplification by PCR.....	174
5.3.8	Purification of amplified cDNA.....	174
5.4	Statistical analysis .....	175
5.5	Results .....	175
5.5.1	Cell isolation using Fluorescence-Activated Cell Sorting ....	175
5.5.2	Quantitative Polymerase Chain Reaction (qPCR).....	176
5.5.3	RNAseq: Validation of cDNA from targeted RNA using Agilent 2100 Bioanalyzer .....	180
5.5.4	Library preparation for sequencing.....	183
5.5.5	Unmapped read data (FASTQ) .....	185
5.5.6	Assessing quality using FAST-QC .....	185
5.5.7	Calculating expression levels .....	188
5.5.8	Visualizing gene expression.....	190

5.5.9	Functional analysis of differentially expressed genes (DEG) and identifying the most upregulated and downregulated genes .....	192
5.5.10	Kyoto Encyclopedia of Genes and Genomes (KEGG) pathway analysis .....	194
5.5.11	Known genes contributing to HD development .....	196
5.5.12	Genes expressed in the ICs .....	199
5.5.13	Genes related to Ion channels proteins.....	202
5.6	Discussion .....	206
<b>Chapter 6 General Discussion and Future perspectives.....</b>		<b>213</b>
6.1	General Discussion .....	213
6.2	Future perspectives .....	217
6.2.1	How can these findings help future HD patients?.....	217
6.2.2	Can IC and/or neurons be replaced as a future treatment ..	218
6.3	General Conclusion .....	220
<b>Chapter 7 Appendix .....</b>		<b>221</b>
7.1	Appendix (1): Ethical Approval and Consent Forms .....	222
7.2	Appendix (2): Supplementary Figures .....	233
7.3	Appendix (3): Supplementary Tables .....	242
7.4	Appendix (4): Interstitial cell marker gene sequences .....	247
<b>References.....</b>		<b>263</b>

## List of Figures

<b>Figure 1.1</b> Histological structure of the gut wall.....	<b>2</b>
<b>Figure 1.2</b> Schematic diagram illustrating close relationship between ICs.....	<b>8</b>
<b>Figure 1.3</b> The distribution of different IC populations and their location throughout the gut wall .....	<b>15</b>
<b>Figure 1.4</b> The major pathways of purinergic and cholinergic neurotransmission in ICs.....	<b>25</b>
<b>Figure 2.1</b> Flow chart illustrating the main techniques of the common fixatives used in histopathological and research.....	<b>52</b>
<b>Figure 2.2</b> The processing of the human samples for immunohistochemistry workflow.....	<b>59</b>
<b>Figure 2.3</b> Confocal image of the disease control sample.....	<b>68</b>
<b>Figure 2.4</b> Confocal images of cKit and PDGFR $\alpha$ immunoreactivity in rat colon fixed in different fixation.....	<b>70</b>
<b>Figure 2.5</b> Human colon tissue fixed in AE and stained with cKit and Ano1. ...	<b>71</b>
<b>Figure 2.6</b> Confocal images of rat colon show the difference in the immunostaining intensity of Ano1 protein marker in different fixatives.....	<b>71</b>
<b>Figure 2.7</b> Rat fixed colon shows immunoreactivity of the SK3 antibody in three different fixatives.....	<b>72</b>
<b>Figure 2.8</b> Confocal images show a split view of a AE fixed mouse colon section. ....	<b>73</b>
<b>Figure 2.9</b> Ano1 networks in rat colon tissues AE fixed and treated with 0.2% tween and triton .....	<b>73</b>
<b>Figure 2.10</b> Immunofluorescence of cKit <sup>+</sup> ICs in human colon fixed in AE, PFA or ZBF from a stoma-closure sample patient.....	<b>74</b>
<b>Figure 2.11</b> Semi-quantative analysis of z-stack confocal images compared to maximum intensity projection image.....	<b>76</b>
<b>Figure 2.12</b> Graph illustrating observer agreement according to the number of cases analysed.....	<b>77</b>
<b>Figure 2.13</b> ImageJ and IMARIS analyses of cKit <sup>+</sup> ICs and Ano1 <sup>+</sup> ICs stained disease control samples show similar positive counts. ....	<b>81</b>
<b>Figure 2.14</b> IMARIS and ImageJ analyses of cKit and PDGFR $\alpha$ stained disease control samples.....	<b>84</b>
<b>Figure 2.15</b> IMARIS and Image J show no significant differences between the two tools used to analysis the tested sections. ....	<b>85</b>

<b>Figure 2.16</b> Creation of 3D images has no effect on the consistency and reproducibility of ImageJ and IMARIS analysis of cKit and PDGFR $\alpha$ stained cells. ....	<b>88</b>
<b>Figure 3.1</b> Mechanism of Formaldehyde fixation.....	<b>96</b>
<b>Figure 3.2</b> The main steps of the RNAscope protocol.....	<b>102</b>
<b>Figure 3.3</b> Flow chart of the work flow of the immunostaining steps using FFPE samples. ....	<b>106</b>
<b>Figure 3.4</b> Flow chart of the main working steps of the RNAscope.....	<b>108</b>
<b>Figure 3.5</b> Immunofluorescence staining for cKit in FFPE using different antigen retrieval solutions. ....	<b>112</b>
<b>Figure 3.6</b> Chromogenic immunostaining of FFPE sections. ....	<b>115</b>
<b>Figure 3.7</b> Confocal images of PDGFR $\alpha$ <sup>+</sup> cells in fresh fixed tissue and FFPE tissue. ....	<b>116</b>
<b>Figure 3.8</b> The statistical difference in the numbers of ICs in two different tissue types. ....	<b>117</b>
<b>Figure 3.9</b> RNAscope detection of mRNA for Kit gene in FFPE Hirschsprung disease samples. ....	<b>119</b>
<b>Figure 4.1</b> Regulation of gut motility, schematic drawing shows the interaction between the CNS and the ENS with the ICs.....	<b>125</b>
<b>Figure 4.2</b> The changes in intracellular Ca <sup>2+</sup> levels responsible for pacemaker activity in cKit <sup>+</sup> ICs. ....	<b>128</b>
<b>Figure 4.3</b> Haematoxylin-Eosin staining of the proximal (A) and distal (B) parts of HD sample.....	<b>135</b>
<b>Figure 4.4</b> Confocal images of ICs showing the morphological feature of these cells. ....	<b>136</b>
<b>Figure 4.5</b> 3D images of cKit <sup>+</sup> ICs show complex networks around the myenteric plexus area.....	<b>137</b>
<b>Figure 4.6</b> Confocal images show the complete co-localization of the two types of ICs with their functional ion channels.....	<b>137</b>
<b>Figure 4.7</b> Confocal images show the complex network formed by the two different types of ICs.....	<b>138</b>
<b>Figure 4.8</b> Confocal images for ICs in the MP area show the close apposition of these cells and the enteric neurons and ganglion.....	<b>139</b>
<b>Figure 4.9</b> Confocal tile scans of the human colon sample show the distribution of the PDGFR $\alpha$ <sup>+</sup> ICs around the MP.....	<b>139</b>

<b>Figure 4.10</b> Confocal images of the cKit and Ano1 immunostaining show complete co-localization of these two protein markers and the network around the ganglionic area .....	<b>141</b>
<b>Figure 4.11</b> Number of cKit <sup>+</sup> ICs in the three different histological layers of the colon of HD and DC samples.....	<b>141</b>
<b>Figure 4.12</b> Number of Ano1 <sup>+</sup> ICs in the three different histological layers of the colon of HD and DC samples.....	<b>142</b>
<b>Figure 4.13</b> Confocal images of PDGFR $\alpha$ immunostaining.....	<b>144</b>
<b>Figure 4.14</b> Confocal images show the immunolabelling of SK3.....	<b>144</b>
<b>Figure 4.15</b> Number of PDGFR $\alpha$ <sup>+</sup> ICs in the three different histological layers of the colon of HD and DC samples.....	<b>145</b>
<b>Figure 4.16</b> Number of SK3 <sup>+</sup> ICs in the three different histological layers of the colon of HD and DC samples.....	<b>146</b>
<b>Figure 4.17</b> Ratio between the two IC subtypes as expressed by their specific markers and the functional protein markers.....	<b>148</b>
<b>Figure 5.1</b> Sample preparation and workflow of qPCR experiments .....	<b>165</b>
<b>Figure 5.2</b> Work-flow for the human colon tissue cell enzymatic dissociation	<b>167</b>
<b>Figure 5.3</b> Microelectrode IC aspiration. ....	<b>170</b>
<b>Figure 5.4</b> RNA Sequencing Workflow.....	<b>171</b>
<b>Figure 5.5</b> qPCR revealed significantly decreased relative mRNA expression levels of ICs marker genes in the proximal HD specimen compared to the distal specimen .....	<b>177</b>
<b>Figure 5.6</b> Relative normalized IC genes expression in the two different parts of HD as compared to the DC samples. IC- Interstitial Cells, HD- Hirschsprung Disease, DC- disease control .....	<b>179</b>
<b>Figure 5.7</b> Agilent 2100 bioanalyzer results of the HD sample.....	<b>182</b>
<b>Figure 5.8</b> The work-flow of RNAseq experiment.....	<b>183</b>
<b>Figure 5.9</b> Summary of RNAseq experiment steps .....	<b>184</b>
<b>Figure 5.10</b> Principal component analysis plot describes the similarities between gene expression values of Hirschsprung disease samples. ....	<b>189</b>
<b>Figure 5.11</b> Heat map of 9 samples from HD for the selected genes.....	<b>191</b>
<b>Figure 5.12</b> The Gene Ontology term analysis of biological process for the top 20 most downregulated genes between the distal and proximal HD segments. ....	<b>193</b>
<b>Figure 5.13</b> The Gene Ontology term analysis of biological process for the top 20 most upregulated genes between the distal and proximal HD segments. ....	<b>194</b>

<b>Figure 5.14</b> The Kyoto Encyclopaedia of Genes and Genomes pathway analysis for the upregulated (red) and downregulated (green) genes of the distal vs proximal HD segments.....	<b>195</b>
<b>Figure 5.15</b> The RPKM for the genes known to contribute to the HD development in the proximal, transitional and distal segments of HD.....	<b>197</b>
<b>Figure 5.16</b> The RPKM for the genes known to contribute to the HD development in the distal compared to the proximal different histological layers of HD colon. ....	<b>198</b>
<b>Figure 5.17</b> The RPKM for the genes known to contribute to the HD development in the different histological layers of the wall of the colon of HD. ....	<b>199</b>
<b>Figure 5.18</b> The RPKM for the genes highly expressed in the ICs.....	<b>201</b>
<b>Figure 5.19</b> The RPKM for the genes highly expressed in the ICs.....	<b>201</b>
<b>Figure 5.20</b> RPKM values of genes that are exclusively expressed by ICs....	<b>202</b>
<b>Figure 5.21</b> The log <sub>2</sub> fold change of certain functional genes in the distal vs proximal segments of HD colon. ....	<b>204</b>
<b>Figure 5.22</b> The log <sub>2</sub> fold change of certain functional genes in the distal myenteric plexus vs proximal myenteric plexus of HD colon. ....	<b>205</b>

## List of Tables

<b>Table 1.1</b> History of ICs in the gastrointestinal tract .....	<b>9</b>
<b>Table 1.2</b> Examples of studies used different ICs identification methods in human tissue in various pathological conditions including HD.....	<b>38</b>
<b>Table 1.3</b> Genes reported in the literature with an established role in the development of the HD .....	<b>45</b>
<b>Table 2.1</b> Summary of the protocols established for the use of different fixatives and their appropriate method of cryo-protection by incubation in sucrose.	<b>61</b>
<b>Table 2.2</b> Properties and manufacturer details of antibodies used .....	<b>63</b>
<b>Table 2.3</b> Semi- qualitative patterns of staining of different protein markers according to method of fixation .....	<b>67</b>
<b>Table 2.4</b> Frequency of agreement between the two observers .....	<b>77</b>
<b>Table 3.1</b> The main difference considered between fresh frozen (FF) and formalin fixed paraffin embedded (FFPE) samples .....	<b>98</b>
<b>Table 3.2</b> Semi-quantitative assessment of RNAscope staining.....	<b>109</b>
<b>Table 4.1</b> IC numbers for the four different protein markers in the same ROI area performed using Image J software .....	<b>147</b>
<b>Table 5.1</b> Human Interstitial Cell primer pairs sequences. ....	<b>161</b>
<b>Table 5.2</b> The volumes to make 20 µl per reaction for cDNA synthesis .....	<b>163</b>
<b>Table 5.3</b> Summary of the quality control for sequencing data .....	<b>187</b>

## Abbreviations

<b>°C</b>	Celsius
<b>µm</b>	Micrometre
<b>2D</b>	Two Dimensional
<b>3D</b>	Three Dimensional
<b>Ach</b>	Acetylcholine
<b>AchE</b>	Acetylcholinesterase
<b>ACK2</b>	cKit neutralizing antibodies
<b>ACSF</b>	Artificial Cerebrospinal Fluid
<b>AE</b>	Acetic Ethanol
<b>Ano1</b>	TMEM16A
<b>AR</b>	Antigen Retrieval
<b>ATP</b>	Adenosine Tri-Phosphate
<b>BSA</b>	Bovine Serum Albumin
<b>Ca<sup>2+</sup></b>	Calcium
<b>CaCl<sub>2</sub></b>	Calcium chloride
<b>CD34</b>	Cluster of Differentiation 34
<b>cDNA</b>	Complementary DNA
<b>cGMP</b>	Cyclic Guanosine Monophosphate
<b>ChAT</b>	Choline acetyltransferase
<b>cKit</b>	Tyrosine kinase receptor
<b>cKit<sup>+</sup> ICs</b>	cKit positive Interstitial Cells
<b>Cl<sup>-</sup></b>	Chloride
<b>DAB</b>	Diaminobenzidine
<b>dapB</b>	Hydroxy-Tetrahydrodipicolinate Reductase
<b>DAPI</b>	4', 6-DiAmidino-2-Phenyl-Indole
<b>DC</b>	Disease Control
<b>DEG</b>	Differentially Expressed Gene
<b>dH<sub>2</sub>O</b>	Distilled Water

<b>DMP</b>	Deep Muscular Plexus
<b>DNA</b>	Deoxyribonucleic acid
<b>dNTP</b>	deoxy ribonucleotide triphosphate
<b>DPX</b>	Distyrene- Plasticiser and Xylene mounting medium
<b>EDNRB</b>	Endothelin- B- receptor
<b>EDTA</b>	Ethylene Diamine Tetra Acetic acid
<b>eGFP</b>	Enhanced Green Fluorescent Protein
<b>EJPs</b>	Excitatory Junction Potentials
<b>ENS</b>	Enteric Nervous System
<b>ER</b>	Endoplasmic Reticulum
<b>FACS</b>	Fluorescence Activated Cell Sorting
<b>FF</b>	Fresh Frozen
<b>FFPE</b>	Formalin-Fixed Paraffin Embedded
<b>FIJP</b>	Fast Inhibitory Junction Potentials
<b>FITC</b>	Fluorescein isothiocyanate
<b>FLCs</b>	Fibroblast-like cells
<b>GAPDH</b>	Glyceraldehyde 3-phosphate dehydrogenase
<b>GDNF</b>	Glial Cell Line Derived Neurotrophic Factor
<b>GFAP</b>	Glial Fibrillary Acidic Protein
<b>GI tract</b>	Gastro-Intestinal tract
<b>GO</b>	Gene Ontology
<b>H&amp;E</b>	Hematoxylin-Eosin
<b>H<sub>2</sub>O<sub>2</sub></b>	Hydrogen peroxide
<b>HBSS</b>	Hanks' Balanced Salt Solution
<b>Hcn4</b>	Hyperpolarization- activated cyclic nucleotide- gated K <sup>+</sup> channel 4
<b>HD</b>	Hirschsprung Disease
<b>hM3Dq</b>	Chemogenetic Receptors
<b>ICC</b>	Interstitial Cells of Cajal
<b>IC-CM</b>	Interstitial Cells- Circular Muscle
<b>IC-DMP</b>	Interstitial Cells within the deep muscular plexus
<b>IC-IM</b>	Interstitial Cells- Intramuscular

<b>IC-LM</b>	Interstitial Cells- Longitudinal Muscle
<b>IC-MP</b>	Interstitial Cells -Myenteric Plexus
<b>ICs</b>	Interstitial Cells
<b>IC-SM</b>	Interstitial Cells - Submucosal
<b>IGF-1</b>	Insulin Growth Factor 1
<b>IMARIS</b>	Microscopy Image Analysis Software
<b>InsP3R</b>	Inositol trisphosphate receptor
<b>IP3</b>	Inositol trisphosphate
<b>ISH</b>	In Situ Hybridization
<b>K</b>	Cohen's Kappa coefficient
<b>KCl</b>	Potassium Chloride
<b>M</b>	Molarity
<b>M2,M3</b>	Muscarinic Receptors (2,3)
<b>mAChRs</b>	Muscarinic Acetylcholine receptor
<b>MgCl<sub>2</sub></b>	Magnesium chloride
<b>MgSO<sub>4</sub>.7H<sub>2</sub>O</b>	Magnesium sulfate heptahydrate (Epsom salts)
<b>mm<sup>2</sup></b>	Square Millimeter
<b>MP</b>	Myenteric Plexus
<b>mRNA</b>	Messenger RNA
<b>N</b>	Number
<b>NA</b>	Norepinephrine
<b>nAChRs</b>	Nicotinic acetylcholine receptors
<b>NaCl</b>	Sodium chloride
<b>NaH<sub>2</sub>PO<sub>4</sub></b>	Anhydrous monobasic sodium phosphate
<b>NaHCO<sub>3</sub></b>	Sodium bicarbonate
<b>NANC</b>	Non- Adrenergic, Non-Cholinergic
<b>NCX</b>	Sodium-Calcium Exchanger
<b>Nm</b>	Nanometres
<b>NO</b>	Nitric Oxide
<b>OCT</b>	Optimised Cutting Temperature Compound
<b>OD</b>	Optical Density
<b>P<sub>2</sub>RY<sub>1</sub></b>	Purinergic Receptor 1

<b>P<sub>2</sub>RY<sub>2</sub></b>	Purinoceptor 2
<b>PB</b>	Phosphate Buffer
<b>PBS</b>	Phosphate Buffer Saline
<b>PBST</b>	Phosphate Buffer Saline with Triton
<b>PC</b>	Principle Component
<b>PDGFR<math>\alpha</math><sup>+</sup></b>	Platelet- Derived Growth Factor Receptor Alpha positive
<b>ICs</b>	Interstitial Cells
<b>Pe</b>	Expected Agreement
<b>PE</b>	Phycoerythrin conjugated antibody
<b>PFA</b>	Paraformaldehyde
<b>Pg</b>	Picogram
<b>PKC</b>	protein kinase C
<b>PMCA</b>	Plasma membrane Ca <sup>2+</sup> ATPase
<b>Po</b>	Observed Agreement
<b>PPIB</b>	Peptidylprolyl Isomerase B
<b>PPP</b>	Percentage of Positive Pixels
<b>QC</b>	Quality Control
<b>qPCR</b>	Quantitative PCR
<b>RER</b>	Rough Endoplasmic Reticulum
<b>RET</b>	Proto-Oncogene
<b>RNA</b>	Ribonucleic acid
<b>RPKM</b>	Reads Per Kilo base Million
<b>RPMI</b>	Growth media
<b>RT</b>	Room Temperature
<b>RT-PCR</b>	Reverse Transcription Polymerase Chain Reaction
<b>RYR3</b>	Ryanodine receptor 3
<b>SCF</b>	Stem Cell Factor
<b>scRNAseq</b>	Single-cell RNA sequencing
<b>SD</b>	Standard Deviation
<b>SEM</b>	Standard Error of the Mean
<b>SER</b>	Smooth Endoplasmic Reticulum
<b>SERCA</b>	Sarco-Endoplasmic Reticulum Ca <sup>2+</sup> ATPase

<b>SIP</b>	Smooth muscle- ICC- PDGFR $\alpha$ Syncytium
<b>SK3</b>	Calcium-activated Potassium channel
<b>SMCs</b>	Smooth Muscle Cells
<b>SP</b>	Submucosal Plexus
<b>STD</b>	Spontaneous Transient Depolarization
<b>STICs</b>	Spontaneous Transient Inward Currents
<b>STOCs</b>	Spontaneous Transient Outward Currents
<b>SV2</b>	Synaptic Vesicle Glycoprotein 2
<b>TBE</b>	Tris/Borate/EDTA
<b>TEM</b>	Transmission Electron Microscopy
<b>Thbs4</b>	Thrombospondin-4
<b>Tm</b>	Melting Temperature
<b>TMEM16a</b>	Calcium-activated Chloride channel
<b>TRIZOL</b>	Guanidinium thiocyanate
<b>TTX</b>	Tetrodotoxin
<b>UC</b>	Ulcerative Colitis
<b>UV</b>	Ultra Violet
<b>vAChT</b>	Vesicular Acetylcholine Transporter
<b>VOC</b>	Voltage Operated Calcium Channel
<b>W/W<sup>v</sup></b>	Kit mutant mice
<b>ZBF</b>	Zinc Based Fixative
<b>Zn<sup>2+</sup></b>	Zinc
<b><math>\beta</math>-NAD</b>	$\beta$ -Nicotinamide Adenine Dinucleotide

## Chapter 1 General Introduction

### 1.1 Gastrointestinal function

The gastrointestinal tract functionally provides nutrients, electrolytes and water to the body, including the gut itself, by performing different tasks: motility, secretion, digestion, absorption and storage in addition to the endocrine function (Johnson, 1977, Rehfeld, 1998). The gut performs these functions through intrinsic and extrinsic control systems. The intrinsic control system is situated between the different histological layers of the gut and consists of two main parts: the enteric nervous system (ENS) and gut hormones. The extrinsic control system resides outside the wall of the gut and consists of the vagus and splanchnic nerves and hormones, such as aldosterone (Singh et al., 2016, Sayegh and Washington, 2012).

### 1.2 Histology of the human gut

The wall of human gut is made up of four layers; the mucosa, submucosa, muscularis and serosa (**Figure 1.1**). The mucosa forms the gastrointestinal tract's innermost layer, which comes in direct contact with digested food. It consists of epithelium, responsible for digestive, absorptive and secretory processes, and goblet cells that produce mucus that protects the epithelial surface. In addition to this, the intestinal epithelium is actively involved in antigen processing and immune cell regulation (Henderson et al., 2010). The sub-mucosa is a dense connective tissue made up of blood vessels, lymph

vessels, and nerves. The muscle layer (muscularis) is a thin layer of smooth muscle that forms an external longitudinal muscle (LM) layer and an internal circular muscle (CM) layer. The CM layer prevents intestinal content from backward movement, whereas the LM layer helps in peristalsis. A dense network of neuronal cells, the myenteric plexus (MP) separates these two layers. The serosa (outermost layer), consists of a thin layer of secretory epithelial cells, with underneath connective tissue (Anthony, 2016).

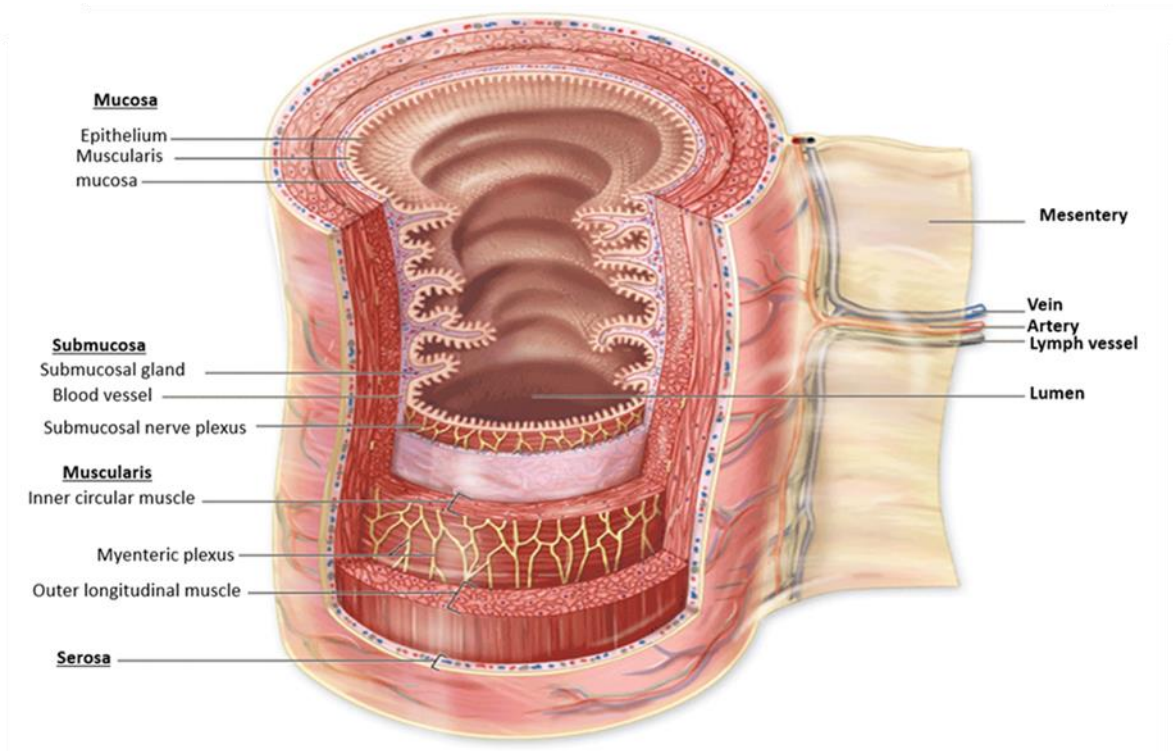


**Figure 1.1 Histological structure of the gut wall.**

The wall of the gut consists of four layers (mucosa, submucosa, muscularis and serosa). Adapted from Basic Histology: Text and Atlas, 12th Edition.

### 1.3 What are Interstitial Cells?

Interstitial Cell (IC) is a term applied to different kind of cells of different origins and phenotypes occupying spaces within the interstitium (Wiig and Swartz, 2012). Although in the smooth muscle wall of the digestive tract, this group includes fibroblasts, mast cells, and macrophages (Mikkelsen, 2010), it is those involved in regulating motility that has become known as Interstitial Cells (ICs).

ICs have been an area of growing interest in the gut since their discovery in the late 19<sup>th</sup> century by Cajal. Ramón y Cajal, a Spanish neuroanatomist, found the Interstitial Cells when he was studying the intestinal plexus of amphibians (Junquera et al., 2007). These cells were first described as nerve-like cells located along the gastrointestinal tract and were named as Interstitial Cells of Cajal (ICC) (Faussonne-Pellegrini and Thuneberg, 1999, Thuneberg, 1999) and will be referred to as cKit<sup>+</sup> ICs in our study.

Cajal discovered these cells by using histological staining methods such as silver impregnation and Ehrlich's vital methylene blue (Blair et al., 2014, Huizinga et al., 2013). Because these methods were widely used to stain neurons, Cajal proposed that these cells were accessory neurons (Blair et al., 2014). Cajal speculated that cells were affected by the components of the enteric nervous system (ENS) and influence the contractile activity of the neighbouring smooth muscle cells (Blair et al., 2014). However, for a long time, the nature and physiological role of these cells have remained unclear, and their function is still under investigation (Vannucchi et al., 1997).

The most popular hypothesis regarding the function of cKit<sup>+</sup> ICs is their contribution to the normal vascular and gut smooth muscle motility. Loss of

these cells has been associated with a range of motility disorders (Sanders et al., 2014). The electrical activity of the gut results from the integrated behaviour of different IC subtypes and smooth muscle cells (SMCs), with changes in the electrical activity of one cell influencing the excitability of the other cells (Ward et al., 1994a, Sanders et al., 2004, Ward et al., 1994b, Sanders et al., 2014, Van Helden et al., 2010). Studies investigating the structure and function of IC have broadened our understanding of their role in the complex mechanism regarding the coordination of motor activity in the gastrointestinal tract (Thuneberg, 1999). More recently, sub-types of IC have been recognised. Experimental evidence has demonstrated these sub-types using protein markers expressed by these cells, namely cKit protein (Maeda et al., 1992) and platelet-derived growth factor receptor alpha (PDGFR $\alpha$ ) protein (Grover et al., 2012). These two different classes of ICs run close to each other and near to enteric neurons as well as to the SMCs (Thuneberg, 1999, Hanani and Freund, 2000a, Blair et al., 2014). Although the protein markers themselves are not very specific, each of the two cell types expresses more reliable and specific ion channels, described below.

#### **1.4 Immunomarkers for cKit<sup>+</sup> ICs**

In the tunica muscularis, cKit<sup>+</sup> ICs constitute only a fraction of total cells, and there were no specific labels for them, making them difficult to investigate. Several histological stains, such as methylene blue (Miyamoto-Kikuta et al., 2009, Nakahara et al., 1998), silver impregnation (Kobayashi et al., 1989) were used to highlight ICs, none of these methods was specific to cKit<sup>+</sup> ICs, and only in some regions of the intestine and in certain species they were successfully

stained (Rumessen, 1994). Previously, the most reliable technique for identifying cKit<sup>+</sup> ICs was transmission electron microscopy (TEM), which identified the ultrastructural criteria of these cells (Xue et al., 1993). A study of canine small intestine found that vimentin filaments were predominant in cKit<sup>+</sup> ICs within the deep muscular plexus (IC-DMP) (Torihashi et al., 1993). Vimentin became the first immunolabel for cKit<sup>+</sup> ICs and was commonly used in the identification of these cells in many organs. Vimentin does not, however, differentiate between cKit<sup>+</sup> and PDGFR $\alpha$ <sup>+</sup> IC classes, besides being expressed by fibroblast cells (Eckes, 1998).

Researchers using Kit mutant ( $W/W^V$ ) mice hematopoietic cells, melanocyte and germ cells, noted that cKit was expressed in a variety of cells (Geissler et al., 1988, Chabot et al., 1988). To understand cKit function, neutralizing antibodies (ACK2) were administered to neonatal mice (Maeda et al., 1992) which resulted in severe bowel motility defects described as paralytic ileus. An abnormality in the contractile patterns in the ileal muscle of  $W/W^V$  mice as a response to agonists (bradykinin and acetylcholine) was observed, but no morphological defects were apparent in the ENS or SMCs (Maeda et al., 1992). Identification of cKit<sup>+</sup> ICs in the gut was achieved by methylene blue and immunocytochemistry (Torihashi et al., 1995). Treatment of new-born mice with neutralizing cKit antibodies results in cells with ultrastructural features of cKit<sup>+</sup> ICs to be decreased in numbers (Torihashi et al., 1995). Studies have shown that the cells in the MP region labelled with cKit antibodies were reduced in the gut wall of  $W/W^V$  mice (Ward et al., 1994b, Hulzinga et al., 1995). Although mast cells are also labelled with cKit antibodies, cKit antibodies labelling has become

the standard method for studying and identifying cKit<sup>+</sup> ICs. This method has been widely used in developmental research, pathological assessments and molecular and physiological studies over the past two decades. The progress of IC research has depended on development and application of different technology summarised in **(Table 1.1)**.

A striking advance occurred when a gene array screen of transcripts, demonstrated for the first time that Ano1 (TMEM16a), Ca<sup>2+</sup>-activated Cl<sup>-</sup> channel, is one of the cKit<sup>+</sup> ICs most highly expressed genes (Chen et al., 2007a), and expressed robustly and exclusively by cKit<sup>+</sup> ICs throughout the gut (Blair et al., 2012b, Gomez-Pinilla et al., 2009, Hwang et al., 2009). An advantage of labelling of cKit<sup>+</sup> ICs with Ano1 antibodies is that mast cells are not labelled, and therefore, this method may be considered superior to cKit labelling.

## **1.5 Immunomarkers for PDGFR $\alpha$ <sup>+</sup> ICs**

Cells known as PDGFR $\alpha$ <sup>+</sup> IC were initially referred to as fibroblast-like cells (FLC), where TEM provided a description of FLC's ultrastructural features and close appositions of these cells to other cellular components of the SIP (SMCs, ICC and PDGFR $\alpha$ ) syncytium (Komuro et al., 1999). Histological methods could not correctly recognise FLCs, initially, CD34 immunomarkers were found to label FLC adjacent to cKit<sup>+</sup> ICs, but constitute a different population of cells (Pieri et al., 2008, Robinson et al., 2000, Vanderwinden et al., 2000, Vanderwinden et al., 1999). Cells with CD34<sup>+</sup> immunoreactivity were identified as cKit negative FLC in the small intestine of humans. CD34 has thus become a

first immunolabel for FLC, but it has also been recognized that CD34 is not a specific FLC labelling in the intestinal wall, where other types of mesenchymal cells also express this antigen (Vanderwinden et al., 2000, Vannucchi et al., 2013). Guinea pig gut IC was found to express small conductance  $Ca^{2+}$  activated  $K^{+}$  channels (SK3), and SK3<sup>+</sup> cells were found to be cKit negative cells in the MP region and within the CM layers of the gut wall (Klemm and Lang, 2002, Vanderwinden et al., 2002, Fujita et al., 2003). Significant progress was made when FLC was found to express PDGFR $\alpha$  throughout the gut wall (Iino et al., 2009, Iino and Nojyo, 2009). PDGFR $\alpha$ <sup>+</sup> ICs are different from cKit<sup>+</sup> ICs as they are not affected in cKit deficient *W/W<sup>v</sup>* mutant mice in which cKit<sup>+</sup> ICs are significantly reduced. In the MP region, PDGFR $\alpha$ <sup>+</sup> ICs form networks adjacent to cKit<sup>+</sup> ICs and intertwine with cKit<sup>+</sup> ICs and enteric neurons processes in muscle layers (Iino et al., 2009, Kurahashi et al., 2011). An increase in the amount of research investigating the distribution and function of PDGFR $\alpha$ <sup>+</sup> ICs alongside cKit<sup>+</sup> ICs, within the gastrointestinal (GI) tract has led to an improved understanding of the role these cells play as part of pacemaker system (Chan et al., 2010) (**Figure 1.2**).

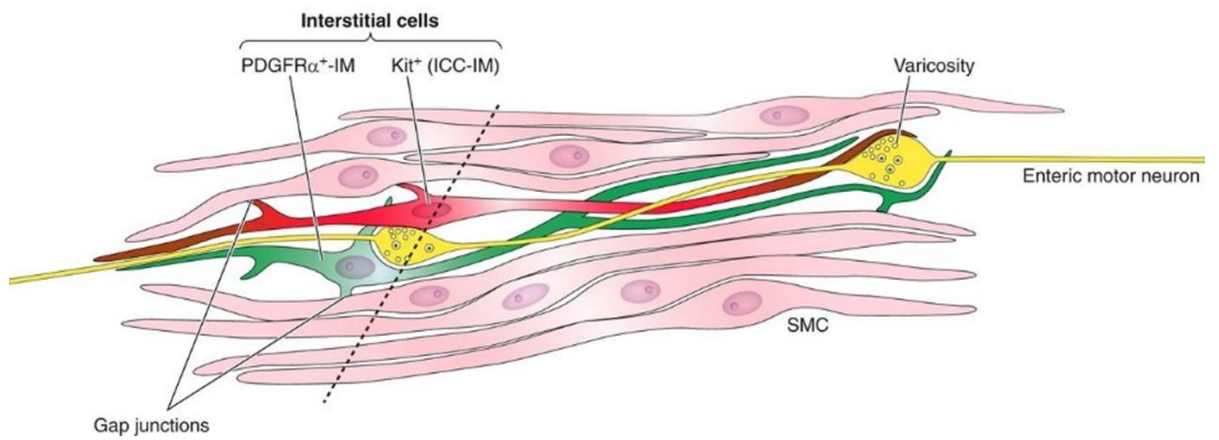


**Figure 1.2 Schematic diagram illustrating close relationship between ICs (cKit<sup>+</sup> and PDGFR $\alpha$ <sup>+</sup>).**

These cells run in the same anatomical space in adjacent to each other and to the enteric nerve varicosity. Adapted from *Physiol Rev* 94:859-907, 2014 (Sanders et al., 2014) .

**Table 1.1 History of ICs in the gastrointestinal tract**

<b>Year of the study</b>	<b>Main finding</b>	<b>References</b>
<b>1911</b>	Ramón y Cajal used methylene blue and silver impregnation to stain cells similar to neural tissue in the rabbit small intestine	(Huizinga et al., 2013)
<b>1985</b>	Morphological studies of ICs, EM considered the "gold standard" for identifying ICs.	(Zhou and Komuro, 1992b, Zhou and Komuro, 1992a)
<b>1992</b>	Use of cKit mutants and cKit neutralization to study physiological functions of cKit <sup>+</sup> ICs.	(Maeda et al., 1992, Ördög et al., 2004, Torihashi et al., 1999b, Ward et al., 2000b, Ward et al., 1995)
<b>1980-1994</b>	Whole muscle experiments and selectively destroy ICs function	(Bauer et al., 1985, Berezin et al., 1988, Liu et al., 1994, Smith et al., 1987)
<b>1994</b>	Kit immunohistochemistry as specific method to identify and characterize cKit <sup>+</sup> ICs networks and their role in electrical rhythmicity.	(Torihashi et al., 1995, Ördög et al., 1999, Goto et al., 2004, Chess-Williams et al., 2001, Burns et al., 1997)
<b>1996</b>	cKit <sup>+</sup> ICs loss associated with pathological conditions.	(Knowles and Farrugia, 2011, Lyford et al., 2002, Mazzone et al., 2011, Pardi et al., 2002)
<b>1998-2009</b>	cKit <sup>+</sup> ICs culture for detailed physiological studies.	(Koh et al., 1998, Ward et al., 2000a)
<b>2004</b>	Use of FACS to purify immunolabelled cKit <sup>+</sup> ICs. An activation of ICs and propagation of pacemaker activity with digital imaging of Ca <sup>2+</sup> transients.	(Yamazawa and Iino, 2002, Park et al., 2006, Ördög et al., 2004, Lee et al., 2007, Lee et al., 2009, Horváth et al., 2006, Chen et al., 2007a)
<b>2005</b>	Proof of cKit <sup>+</sup> ICs role as stretch receptors .	(Kraichely and Farrugia, 2007, Kubota et al., 2004)
<b>2007-2009</b>	Recognition of Ano1 significance in cKit <sup>+</sup> ICs	(Chen et al., 2007a, Gomez-Pinilla et al., 2009, Hwang et al., 2009, Zhu et al., 2009)
<b>2009</b>	Identification of PDGFR $\alpha$ as FLC particular marker.	(Iino et al., 2009, Iino and Nojyo, 2009)
<b>2011</b>	PDGFR $\alpha$ <sup>+</sup> cells were isolated and physiological studies indicating their function in neurotransmission inhibitory.	(Klein et al., 2013, Groneberg et al., 2013)
<b>2012- 2019</b>	Studies continue with more advanced techniques range from creating animal model for HD and stem cell transplant to the use of NGS and transcriptome sequencing.	(Liu et al., 2012, Tang et al., 2012, Fernández et al., 2013, Julie E. Cooper et al., 2016, Lee et al., 2016, Malysz et al., 2016, Breland et al., 2019, O'Donnell et al., 2019b)

## 1.6 Embryological development of Interstitial Cells

Although ICs were described toward the end of last century, until recently, the embryological origin of ICs was uncertain (Young, 1999, Vannucchi and Traini, 2016). They were first identified in 1889 by Santiago Ramón y Cajal after whom they are named (Faussonne-Pellegrini and Thuneberg, 1999).

Cajal was unclear whether ICs arise from the neural crest or from the mesenchyme, because ICs have some characteristics in common with cells of neural crest origin (neurons and glial cells) and some attributes in common with cells of mesenchymal origin such as fibroblast and SMCs (Lecoin et al., 1996, Radenkovic et al., 2018). Although cells with similar characteristics do not necessarily have similar developmental origins, similarities between ICs and neurons, neuronal support cells, fibroblasts and smooth muscle cells had raised the possibilities that ICs could be either of neuronal crest or mesenchymal origin (Christensen, 1992, Radenkovic et al., 2018). Since then, the neuronal or non-neuronal nature of ICs has been a matter of debate (Thuneberg et al., 1982, Timmermans, 2001).

Cajal (1893-1911) and many other scientists considered ICs as primitive nerve cells because, like neurons, they could be stained with methylene blue or with silver chromate, and they also formed intimate relationships with nerves (Dupont and Sprinz, 1964), where others considered them as glial cells (Lecoin et al., 1996). These hypotheses were much debated in the years following the discovery, with many scientists alternatively arguing that ICs were connective tissue cells or indeed a type of glia, such as Schwann cells (Sircar et al., 1999).

A complete aneural intestinal segment was constructed in the avian gut, this study clearly showed that in the absence of the neural crest-derived enteric plexus, ICs appear in the gut of avian. This observation rules out the possibility that ICs are of neural crest origin and show that ICs are derived from the mesoderm of the gut wall (Lecoin et al., 1996).

Faussone-Pellegrine examined the ultra-structural histogenesis of the cKit<sup>+</sup> ICs at the level of the MP and the deep muscular plexus in the mouse small intestine. The study identified cKit<sup>+</sup> IC precursor cells in early post-natal mice that were closely associated with nerve fibres of the myenteric plexus, but she was unable to determine whether the precursor cells were of neural crest or of mesenchymal origin (Faussone-Pellegrini MS et al., 1989, Faussone-Pellegrini et al., 1990b, Faussone-Pellegrini and Thuneberg, 1999). The results from two more studies suggest that ICs arise from mesenchymal cells and have common precursors with SMCs (Klüppel et al., 1998, Torihashi et al., 1997).

Torihashi et al. (1997) examined the development of immunoreactivity to cKit, a member of tyrosine kinase family, smooth muscle markers (actin, myosin, desmin) and a marker of neural crest-derived cells in the small intestine of embryonic and neonatal mice. They found that cKit immunoreactive cells were first detected in the outer layers of the murine gut, these cells were undifferentiated in appearance and lacked the morphological feature of both ICs and muscle cells (Torihashi et al., 1997). cKit<sup>+</sup> cells were peripheral to and did not overlap with, the developing myenteric ganglion cells. The CM layer started to show actin-myosin immunoreactivity, whereas LM layer was cKit<sup>+</sup>, but actin and myosin negative. This finding suggested that ICs and longitudinal

smooth muscle cells develop from common cKit<sup>+</sup> precursor cells in the outer layers of the gut. Those cells in which cKit receptor is activated with stem cell factor (SCF) released from neural cells will differentiate into ICs, whereas those cells without direct appositions with neural cells will differentiate into longitudinal SMCs and downregulate the expression of cKit (Sanders et al., 2014).

A significant development arose following the discovery that the receptor tyrosine kinase, cKit, is required for IC development (Maeda et al., 1992). During the development of the human digestive tract, cKit<sup>+</sup> cells, morphologically different from mature cKit<sup>+</sup> ICs, appear late during the embryonic stage. cKit<sup>+</sup> ICs appear first in the oesophagus and stomach, then in the small bowel and finally in the large intestine (Wallace and Burns, 2005, Radenkovic et al., 2010a, Radenkovic et al., 2010b, Abramovic et al., 2014). cKit<sup>+</sup> cells emerge along the digestive tube following the rostrocaudal gradient, in the same way as neural crest cells colonise the digestive tube (Wallace et al., 2005).

Stem cell factor (SCF) is the natural ligand for cKit and also known as steel factor, a study on mice with mutations affecting the gene encoding SCF display phenotypic changes similar to those with cKit mutations (Ward et al., 1995). It was, therefore, suggested that the SCF-cKit signalling pathway critical for the development and survival of cKit<sup>+</sup> ICs (Sanders, 1996, Torihashi et al., 1995, Ward et al., 1995). In addition to its role in the development of cKit<sup>+</sup> ICs, cKit signalling may stabilize the phenotype of cKit<sup>+</sup> ICs, when cKit or downstream signalling elements are blocked, ICs may revert to the smooth muscle

phenotype, in that they possess a few rough endoplasmic reticulum (RER), but more smooth endoplasmic reticulum (SER). This hypothesis suggests inherent plasticity between cKit<sup>+</sup> ICs and SMCs that might be used in the clinical conditions in which cKit<sup>+</sup> ICs are reduced in number (Ward et al., 1994a, Hanani and Freund, 2000a, Hanani and Freund, 2000b).

However, one significant limitation is that many of these studies used cKit, which is a non-specific marker that does not distinguish between mast cells and ICs. It was not until recent years that Ano1, an ion channel expressed exclusively in cKit<sup>+</sup> ICs, was discovered and use of this may have been more selective for the cKit<sup>+</sup> ICs.

### **1.7 Ultrastructural feature of ICs and their distribution throughout the gut**

Morphologically, cKit<sup>+</sup> ICs have small cell bodies, exhibit caveolae, abundant mitochondria, RER, SER, a discontinuous basal lamina, a moderately developed Golgi apparatus, characterized by an ovoid nucleus, extend intermediate cell processes organized in networks, they are interspersed between nerve fibres and muscle cells and are considered responsible for the pacemaker activity of the gut (Lecoin et al., 1996, Sanders et al., 2014).

PDGFR $\alpha$ <sup>+</sup> ICs have morphological features distinct from cKit<sup>+</sup> ICs. The cytoplasm has moderate to high electron density, well-developed RER and they do not have basal lamina or caveolae, but they form gap junctions with circular and longitudinal SMCs (Horiguchi and Komuro, 2000).

## **1.8 IC distribution within the human gut**

There are several IC subclasses present throughout the entire bowel, although, their relative numbers vary considerably throughout the different organs. Many earlier studies on ICs were performed using animal models, and these studies have shaped our fundamental understanding of IC function within the gut.

Nonetheless, human studies have become more prevalent in recent years, and many have been published describing the morphology, distribution and function of ICs in the human gut (**Figure 1.3**).

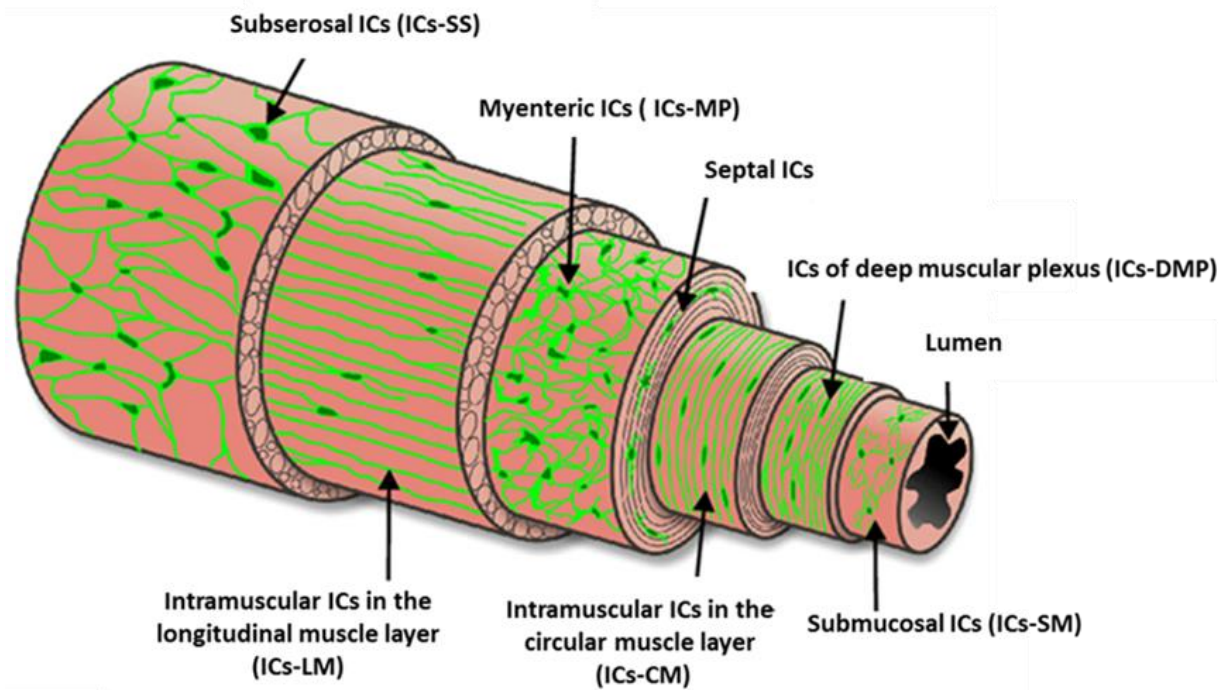


Figure 1.3 The distribution of different IC populations and their location throughout the gut wall (Blair et al., 2014)

### **1.8.1 IC distribution in the human stomach**

An immunohistochemistry study by Manneschi et al. (2004) provided excellent detail on the morphology and distribution of ICs in the human stomach. By using immunohistochemistry, cKit<sup>+</sup> ICs were demonstrated throughout the human stomach, although their density and morphology varied according to region. ICs were abundant in the fundus interspersed among SMCs of the longitudinal and circular muscle layers (IC-IM), these cells were especially abundant in area of myenteric plexus region (IC-MP) (Manneschi et al., 2004, Hulzinga et al., 1995, Torihashi et al., 1995, Ward et al., 1994a, Ward et al., 1994b). However, this finding comes in direct conflict with Torihashi et al. (1999), who states that no cells were observed at the level of MP (Torihashi et al., 1999a). Furthermore, a study conducted by Yun et al. (2010), verified that ICs were found ubiquitously in human stomach and the density of ICs was considerably smaller in both fundus and corpus muscularis mucosa and greater in the gastric fundus submucosa than corpus (Yun et al., 2010).

### **1.8.2 IC distribution in the human small intestine**

In a series of studies by Rumessen and colleagues a detailed distribution of ICs in the small intestine of human was demonstrated (Rumessen and Thuneberg, 1991, Rumessen et al., 1992, Rumessen et al., 1993, Rumessen, 1994). IC-MP are organized in bundles which extend into both the LM and CM layers (Rumessen, 1994). IC-MP bundle density was reported to be highest in the duodenum (Rumessen and Thuneberg, 1991). IC-IM were found in the small intestine circular and longitudinal muscle layers and enriched in the MP region (Wang et al., 2003). However, while IC-IM in the small intestine are frequently

opposed to nerves, no specialized contacts were observed between IC-IM and enteric nerve endings (Wang et al., 2003). Within the small intestine wall, IC-DMP were found by using TEM to form close synapse-like contacts with nerve ending (Rumessen et al., 1992). Moreover, IC-DMP were reported to form numerous gap junctions with each other and with SMCs (Rumessen et al., 1993). Wang et al. also reported the presence of specialized contact between IC-DMP and both enteric neurons and SMCs (Wang et al., 2003).

Observations in subsequent studies (Rømer and Mikkelsen, 1998, Al-Shboul, 2013) however, sometimes conflicted with earlier research. Romert & Mikkelsen (1998) reported that there are identical IC distribution patterns in the duodenum, jejunum and ileum, but acknowledge that there is a higher density of IC-MP in the ileum. Vanderwiden et al. (1998) on the other hand, state that the first part of the duodenum has a distinctive IC distribution that is different from the rest of the intestine, here IC-MP and numerous ICs are present in the CM layer, but no IC-DMP were observed (Kenny et al., 1998). Despite the existence of conflicting studies, it is clear that the small intestine shows an abundant expression of IC-MP, IC- DMP and IC-IM.

### **1.8.3 IC distribution in the human colon**

Several groups have detailed the distribution of ICs within the human colon (Faussone-Pellegrini et al., 1990a, Faussone-Pellegrini et al., 1990b, Rumessen et al., 2009, Rumessen et al., 2013, Mazzia et al., 2000, Torihashi et al., 1999a). Mazzia et al. (2002) recorded ICs within the longitudinal and circular muscle layers, within the septa, at the interface between circular muscle and submucosa, and in the myenteric plexus. IC-LM and IC-CM

demonstrated long cytoplasmic processes and were aligned parallel to muscle fibres and formed an interconnected network. Torihashi et al. identified multipolar and bipolar ICs characterized by numerous branches that were specific to the colon (Torihashi et al., 1999a). Gap junctions were noted between the ICs and SMCs in myenteric plexus (Rumessen et al., 2013).

Although IC-MP and IC-IM, have all been recorded in the colon (Rumessen et al., 1993, Mazzia et al., 2000), regional differences in the pattern of distribution of each IC types have been reported (Fauscione-Pellegrini et al., 1990b, Horisawa et al., 1998). The distribution was assessed by immunostaining of the whole mount tissue sections and revealed that, in the ascending colon, ICs were mainly in the circular and longitudinal muscle layers (Horisawa et al., 1998). In the sigmoid and transverse colon, however, submucosal ICs (IC-SM) were the most abundant. IC-MP were confined to the descending colon (Horisawa et al., 1998). Yet, conflicting reports have been published, and researchers do not agree on the exact regional distribution of ICs in the colon.

## **1.9 IC and enteric innervation**

The enteric nervous system (ENS), often referred to as “the second brain” (Gershon, 1999, Lake and Heuckeroth, 2013), provides intrinsic innervation for the GI tract (Hwang et al., 2012), and plays an essential role in gastrointestinal functions such as motility and secretion (Hwang et al., 2012, Chalazonitis and Rao, 2018). The ENS comprises two layers of ganglia; the MP and the submucosal plexus (SP) embedded within GI organs from the oesophagus to the anus (Hwang et al., 2012, Saffrey, 2013). The SP predominantly supplies

innervation to the mucosa, the main role is to regulate the configuration of the luminal surface, control glandular secretions, alter electrolyte and water transport, and regulate local blood flow (Costa et al., 2000). The MP located between the CM and LM layers regulates motility and secretion (Hwang et al., 2012, Saffrey, 2013, Chalazonitis and Rao, 2018, Lake and Heuckeroth, 2013). All enteric neurons are either classified as afferent neurons, interneurons or motor neurons (Benarroch, 2007, Furness, 2000).

The excitatory and inhibitory enteric nervous system control contraction and relaxation of gastrointestinal smooth muscle, respectively, coordinating regulation of gastric motility of the gut. However, evidence suggests that the concerted actions of the ENS, ICs, and SMCs are required for the proper functioning of the gut. The close apposition between Interstitial Cells of Cajal (cKit<sup>+</sup> ICs) and nerve fibres within the tunica muscularis of the gut organs has been noted by different morphologists numerous times over the past 100 years (Ward and Sanders, 2001). Moreover, Immunohistochemical experiments and molecular studies using Reverse transcription polymerase chain reaction (RT-PCR) confirm the expression of neurotransmitter receptors such as muscarinic receptors (M2 and M3) in freshly dispersed and cultured ICs from the murine gut (Ward and Sanders, 2001, Epperson et al., 2000). The first indication that ICs were functionally innervated came from monitoring changes in the second messenger content after nitrenergic changes. In the guinea pig small intestine and canine colon, the nitric oxide (NO) cyclic GMP (cGMP) effector was located by immunochemistry (Shuttleworth et al., 1993, Young et al., 1993). cGMP levels increased in a neuron subpopulation and ICs, indicating active guanylyl cyclase

(the primary cellular receptor for nitrenergic inputs) was expressed in these cells (Shuttleworth et al., 1993). Taken together morphological and molecular experiments confirm that ICs are anatomically and physically close to neurons, both excitatory and inhibitory neurons form close connections with ICs (<20 nm) (Ward et al., 2000a, Sanders et al., 2006, Sanders et al., 2016, Beckett et al., 2005).

### **1.10 IC function in gastrointestinal motility**

Although ICs mainly cKit<sup>+</sup> cells were described as pacemaker cells in 1915, the pacemaker theory only advanced significantly following a publication by Ambache in 1947. Ambache described the regulatory function of electrical slow-waves over intestinal contraction and hypothesized that cKit<sup>+</sup> ICs were the cell type responsible for it (Ambache, 1947). There have been numerous studies on the pacemaker mechanism of cKit<sup>+</sup> ICs in the years following Ambache's observation, and it is now widely accepted that signals are conducted from cKit<sup>+</sup> ICs to SMCs. Therefore, the cells responsible for the generation of gastrointestinal slow waves are, in fact, neither neurons nor fibroblasts.

The essential physiological roles for ICs (cKit<sup>+</sup> and PDGFR $\alpha$ <sup>+</sup> cells) have been hypothesized because of their anatomical locations within the tunica muscularis, their organization into discrete networks, their close morphological proximity to enteric motor nerve fibres, and their gap junction connectivity to SMCs and with each other (Imaizumi and Hama, 1969, Rumessen et al., 1982, Young et al., 1996). This observation has led to increase in studies focusing on the role of both types of Interstitial Cells and spontaneous pacemaker activity

which is generated by cKit<sup>+</sup> ICs, and conducted to adjacent smooth muscle (Sanders et al., 2014, Blair et al., 2014) the detailed mechanism of pacemaking role will be discussed later.

The neurogenic mechanisms responsible for gastrointestinal motility have been investigated by electrophysiological studies in which membrane potential and contraction were simultaneously recorded from smooth muscle and were blocked in the presence of adrenergic and cholinergic antagonists (Keef et al., 1997). Similar studies performed in numerous species including mouse, rabbit, guinea pig and canine established that cKit<sup>+</sup> ICs within the wall of small intestine are intrinsically responsible for generation of electrical slow waves (Keef et al., 1997, Plujà et al., 1999, Huizinga et al., 2011, Costa et al., 2013, Huizinga and Chen, 2014, Berezin et al., 1990, Sanders, 1996).

In controlling the rhythmic peristalsis of the stomach, small intestine and colon, a crucial role was attributed to the ICs. Hara et al (1986) suggested that spontaneous slow waves of small intestine of human and other species are generated in non-neuronal cells located between the LM and CM layers, since intracellular recording in a whole thickness preparation found that the longitudinal muscle cells generated slow waves but in the isolated longitudinal muscle preparation all cells tested were electrically silent. A couple of years later, Langton and colleagues isolated ICs from the canine proximal colon slow-wave pacemaker region, and patch-clamp experiments demonstrated that these cells were excitable and voltage-dependent inward and outward currents were elicited by depolarization. The outward current appears to be, in part, due to Ca<sup>2+</sup> activated K<sup>+</sup> channels commonly expressed by the PDGFR $\alpha$ <sup>+</sup> ICs, ICs

were also spontaneously active, generating electrical depolarizations similar to the slow-wave events of intact colonic muscles (Hara et al., 1986, Langton et al., 1989). In addition to pacemaker role, cKit<sup>+</sup> ICs are implicated in enteric neurotransmission and act as stretch receptors in the gastrointestinal tract, especially in the stomach. By applying an electrode to stretch murine antral muscles while recording intracellular electrical activity, an increase in the length of the muscles by distention of the stomach was found to cause depolarization of the membrane and increased slow-wave frequency. The responses were dependent on the rate of stretch, and neuronal antagonists did not inhibit stretch-dependent responses. Moreover, stretching of *W/W<sup>v</sup>* mice antral muscles, lacking intramuscular cKit<sup>+</sup> ICs affect membrane depolarization or slow-wave frequency (Burns et al., 1996, Ward et al., 2000a, Ward et al., 2000b, Beckett et al., 2002, Suzuki et al., 2003, Torihashi\* et al., Al-Shboul, 2013, Won et al., 2005).

## 1.11 The SIP syncytium

The two types of IC are considered as important mediators of neurotransmission in the gut. Together with ENS they are considered to form a functional syncytium which controls the propulsion activity of the gut. This has come to know as the SMC/ICC/PDGFR $\alpha$  cells (SIP) syncytium (Blair et al., 2014, Blair et al., 2012a).

Physiological evidence and development of numerous theories have demonstrated the complex and intricate network that is the pacemaker system of the gut (Huizinga and Lammers, 2009). Of vital importance is the close connection between SMCs, enteric nerves, cKit $^{+}$  and PDGFR $\alpha^{+}$  ICs and the connectivity that exists between these cells, enabling them to function together as an electrically coupled network, in the other words, as a functional syncytium (Hanani and Freund, 2000b, Sanders et al., 2014, Horiguchi and Komuro, 2000). This connectivity is pivotal for the synchronised contraction and relaxation of the gastrointestinal musculature and normal bowel function where disruption in a cell to cell communication can lead to motility disorders of the GI tract (Sanders et al., 2014).

One of the significant driving forces behind signal transmission across the SIP syncytium and smooth muscle response is through modifications of intracellular Ca $^{2+}$  transients in ICs. This appeared to be the common factor in the different components of this functional syncytium (Koh et al., 2012).

Pacemaker ICs, cKit $^{+}$  ICs and PDGFR $\alpha^{+}$  ICs are found alongside the enteric nerve cells, that help the nerve cells to communicate with each other and with

the muscle layers to perform normal gut motility. Thus the close apposition of neurotransmitter release sites to ICs may limit the post-junctional volume in which sufficient neurotransmitter concentrations are achieved, bridging the gap that would otherwise exist between neurones and smooth muscle (Baker et al., 2015). Spontaneous IC generated pacemaker activity drives electrical slow waves and phasic contraction to SMCs (Blair et al., 2014). Neuronal inputs to ICs can, therefore, be conducted to SMCs and modulate contractile behaviour. In cKit<sup>+</sup> ICs, activation of Ano1 channels by the binding of cholinergic neurotransmitters to the muscarinic receptor expressed by cKit<sup>+</sup> ICs results in spontaneous transient inward currents (STICs) and depolarization of the cKit<sup>+</sup> ICs and electrically coupled SMCs, causing smooth muscle contraction (Zhu et al., 2009), while activation of SK3 channels in PDGFR $\alpha$ <sup>+</sup> ICs causes spontaneous transient outward currents (STOCs) and hyperpolarization of the cells and electrically coupled SMCs, resulting in smooth muscle relaxation (Kim, 2011). These ICs work together in creating the synchronised contraction and relaxation of the musculature (Koh et al., 2012). The major pathway in which these ICs mediate enteric motor neurotransmission is illustrated in **(Figure 1.4)**.

In ICs the main effect of purinergic and cholinergic neurotransmission is to increase intracellular Ca<sup>2+</sup> release from stores via inositol triphosphate (IP<sub>3</sub>) receptors on the ER. This change in the Ca<sup>2+</sup> level intracellularly activates SK3 channels, causing hyperpolarisation and relaxation of electrically coupled SMCs (Ward and Sanders, 2001). These ICs types play a role in the modulation and inhibition of conducted phasic contractions as they are

connected to  $cKit^+$  cells and smooth muscles via gap junctions (Kurahashi et al., 2014, Kurahashi et al., 2013).

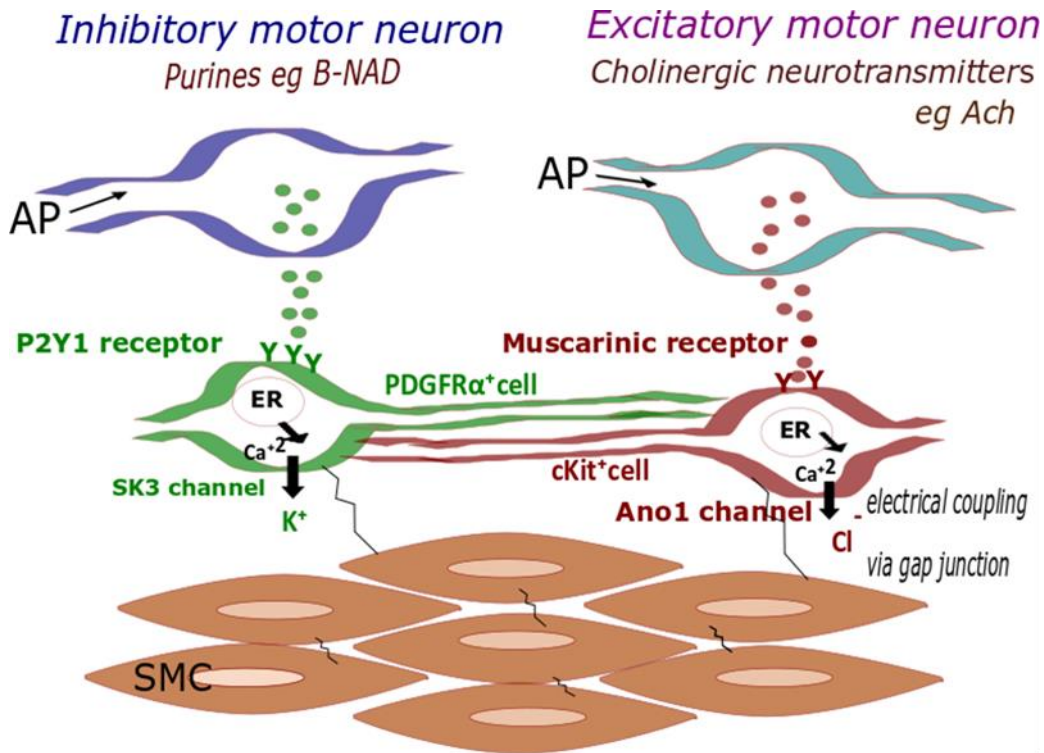


**Figure 1.4 The major pathways of purinergic and cholinergic neurotransmission in ICs.**

Purines bind to P2Y1 receptors on PDGFR $\alpha^+$  cells while cholinergic neurotransmitters acting on muscarinic receptors on cKit<sup>+</sup> cells. Both trigger intracellular Ca<sup>2+</sup> concentration change which affect cellular response. Drawn using Inkscape 0.92.4 software.

### 1.11.1 Glial cells in SIP

The regulation of motor activity through several simultaneously acting mechanisms, along with potential adaptive changes of cells within the gut wall provides a challenge to definitively understanding the role of single cells in the SIP syncytium (Huizinga and Lammers, 2009). For example, a little-studied part

of SIP may be glial cells; a review of recent evidence highlights the multiple emerging roles of these non-neuronal cells (Grubišić and Gulbransen, 2017). Enteric glia is a collection of cells within the intestinal musculature wall and was initially believed to maintain homeostasis and nourish neurons. However, their roles as active regulators of physiological processes such as inflammation and gut motility which were previously thought to be under neuronal control alone are only now being discovered. Evidence suggests that they not only receive neurotransmission but may also communicate with neurons and may even play a role in regulating motility through gliotransmission (Grubišić and Gulbransen, 2017). Enteric glia identified by glial fibrillary acidic protein (GFAP) were found to be excitable. Spread changes in intracellular  $\text{Ca}^{2+}$  transients through the glial networks was proved by using in situ  $\text{Ca}^{2+}$  imaging and immunohistochemistry in a mouse model expressed hM3Dq receptor under the control of the GFAP promoter to selectively trigger glial  $\text{Ca}^{2+}$  signalling (McClain et al., 2014, Zhang et al., 2003, McClain et al., 2015). Disruption of inter- glial cells communication (by genetic ablation of gap junctions in GFAP-positive cells) resulted in a lack of propagation of  $\text{Ca}^{2+}$  signalling through the glial network and consequent constipation (McClain et al., 2014). To rule out the assumption that these  $\text{Ca}^{2+}$  responses in glial cells act only to preserve neural function, one study activated  $\text{Ca}^{2+}$  responses in GFAP positive glial cells alone. It showed that this was adequate by itself for the production of intestinal smooth muscle activity and that glial cells exerted an influence on neuronal cells (McClain et al., 2015). Besides, the role of enteric glia in purinergic neurotransmission has been investigated in guinea pig colon using nerve stimulation and intracellular  $\text{Ca}^{2+}$

imaging. Glia cells were found to respond to purines such as ATP which activated intracellular  $\text{Ca}^{2+}$  release via IP<sub>3</sub> receptors on the ER (Gulbransen and Sharkey, 2009). Thus, glial cells may become to be considered as a part of the functional syncytium once the further understanding of their involvement is achieved.

### **1.12 Mechanism of slow-wave generation in the smooth muscle**

It has been established that slow waves in the smooth muscle have two components, a rapid upstroke depolarization and a plateau phase. The mechanism underlying slow-wave generation has been subject to much discussion over the last decade and has become a topic of significant research interest (Sanders, 1996).

However, recent evidence suggests that the direct innervation of SMCs by acetylcholine does not elicit the adequate response of smooth muscle contraction (Ward et al., 2000b). The proximity of cKit<sup>+</sup> ICs to enteric neurons and SMCs provided the hypothesis that these cells may play a role in neurotransmission as post-junctional receptors (Ward et al., 2000b, Wang et al., 1999). Physiological studies in mice with cKit knockout (Ward et al., 2000b, Klein et al., 2013) have used electrical stimulation to show that a lack of cKit<sup>+</sup> intramuscular (IC-IM) in these mice correlated with a lack of excitatory junction potentials (EJPs) recorded in the muscle compared to wild-type. This reduction in EJPs was not due to decreased sensitivity of SMCs to Ach, nor due to a lack of enteric neurons and reduction in the release of cholinergic neurotransmitters (Sanders et al., 2014). Earlier studies using membrane potential recorded from

gastric antrum circular smooth muscle demonstrated that the smooth muscle from wild-type mice generated a slow-wave that initiated action potentials, while those from IP3 receptor mutant mice showed either quiescent or irregular bursts of the action potential. Also, in the presence of nifedipine ( $\text{Ca}^{2+}$  channel blocker), slow-wave with reduced amplitude in the wild-type mice was generated, and all electrical activity in the mutant mice was abolished (Suzuki et al., 2000).

It was therefore concluded that a loss of IC-IM and hence loss of communication between excitatory neurons and  $\text{cKit}^+$  ICs resulted in the loss of the effects of cholinergic neurotransmission on SMCs. Interestingly, only fast inhibitory junction potentials (FIJP) were observed in these mice (Klein et al., 2013), which recent evidence has shown to be mediated by  $\text{PDGFR}\alpha^+$  ICs (Kurahashi et al., 2014).

## **1.13 Involvement of IC in smooth muscle contractility**

### **1.13.1 Excitatory enteric innervation and smooth muscle contraction in the gut (cholinergic neurotransmission)**

Acetylcholine (ACh) and tachykinins are the two principal neurotransmitters released from excitatory enteric motor neurons. Excitatory motor neurons exert their effect through the release of acetylcholine neurotransmitters (Sternini et al., 1995; Lecci et al., 2002). The cholinergic branch of the excitatory ENS is extensive and is involved in mediating motility and secretion (Cooke, 2000, Harrington et al., 2007b). Functionally, ACh increased the slow-wave frequency in the murine stomach, proved by intracellular electrophysiological recordings, indicating a role for cholinergic neurotransmission in pacemaker activity (Kim et

al., 2003). Cholinergic neurons were previously identified through acetylcholinesterase (AChE), an enzyme involved in Ach breakdown, and choline acetyltransferase (ChAT), an enzyme involved in Ach synthesis (Ward et al., 2000b). However, antibodies targeting vesicular acetylcholine transporter (vAChT) are now the gold standard for identification of cholinergic neurons (Ward et al., 2000b). Immunohistochemical studies using double labelling for vAChT and cKit showed that nerve bundles containing vAChT<sup>+</sup> fibres were closely connected with IC-IM (in mouse fundus) and immunopositive nerve bundles were observed running within the muscle layers (Ward et al., 2000b). Using EM, vAChT<sup>+</sup> nerve fibres and varicosities were found within the CM and LM layers. These fibres were likely enteric motor neurons nerve terminals. Double labelling with antibodies to ICs and vAChT revealed that vAChT positive fibres were closely associated with IC-IM (Ward et al., 2000b).

In the cholinergic ENS, post-synaptic cells and pre-synaptic cells express nicotinic and muscarinic Ach receptors. Nicotinic receptors (nAChRs) are ligand-gated ion channels (Albuquerque et al., 2009). In contrast, the muscarinic receptor (mAChRs) are G-protein coupled receptors (Ishii and Kurachi, 2006). Thus, mAChRs mediate the response to cholinergic signalling by activating second messenger cascades and intracellular signalling pathways (Ishii and Kurachi, 2006). mAChRs divided into five subtypes (M1-M5) (Caulfield and Birdsall, 1998); therefore, cholinergic stimulation is capable of mediating different responses depending upon the receptor subtype that has been bound by Ach.

Experiments using RT-PCR on human tissue and animal models demonstrated expression of M1, M2 and M3 receptor isoforms within nerve fibres from the CM, or myenteric and submucosal ganglia, and on mucosal epithelial cells (Harrington et al., 2007a, Harrington et al., 2007b, Harrington et al., 2008, Harrington et al., 2010a, Harrington et al., 2010b). Based on immunohistochemistry and functional studies, in the murine gastric antrum, nerve stimulation increased the slow-wave frequency and acetylcholine increased pacemaker currents in cKit<sup>+</sup> cells, and both blocked by M3 receptor antagonists (Zhang et al., 2011).

Moreover, while the density of cholinergic nerve bundles within muscles was not significantly different in wild-type and *W/W<sup>v</sup>* mice where ICs-IM are depleted, the cholinergic response was decreased in contrast (Ward et al., 2000a). Animal model studies have shown that cholinergic innervation is compromised in animals lacking IC-IM (Ward et al., 2000b, Forrest et al., 2006). Those studies strongly support the hypothesis that ICs are necessary for the propagation of excitatory enteric neurotransmission. However, arguments are largely centred around the observation that cholinergic neurotransmission is not completely abolished in mouse and rat models in which IC-IM have been depleted (Goyal, 2013). Although Zhang et al. (2011) postulated that cholinergic neurotransmission between nerve varicosities and SMCs is possible via Ach diffusion, they did not wholly reject a role for IC-IM in cholinergic neurotransmission.

#### **1.13.1.1 The role of cKit<sup>+</sup> ICs in mediating cholinergic neurotransmission**

In experiments where LM strips were separated from the MP and CM, rhythmically firing spontaneous depolarization and action potentials were still recorded. Utilizing the sodium channel antagonist tetrodotoxin (TTX) and a muscarinic acetylcholine receptor antagonist, resulted in decreased slow-wave rhythm, leading to the conclusion that the spontaneous pacemaker mechanism in the gut muscles is under cholinergic control (Spencer et al., 2002, Lecci et al., 2002). Ward et al. (2000) identified close contacts between IC-IM and enteric neurons in mouse gastric fundus muscles (Ward et al., 2000a), while studies on guinea-pig small intestine identified both excitatory and inhibitory motor neurons in close contact with ICs (Wang et al., 1999). Taken together, the results of these publications led to the conclusion that ICs play an intermediary role in gut neurotransmission.

### 1.13.1.2 The pacemaker role of cKit<sup>+</sup> ICs

As noted previously, cKit<sup>+</sup> ICs are essential for slow waves generation and propagation in the gut musculature. Research published over the past decade has shown that Ca<sup>2+</sup> activated Cl<sup>-</sup> conductance is responsible for the generation of pacemaker current in ICs (Hwang et al., 2009, Singh et al., 2014). Gomez-Pinilla et al. concluded that Ano1 (anoctamin 1) is the Cl<sup>-</sup> channel responsible for Ca<sup>2+</sup> activated Cl<sup>-</sup> conductance in cKit<sup>+</sup> ICs. Moreover, the authors demonstrate that Ano1 (also known as TMEM16A) is a selective marker of cKit<sup>+</sup> ICs in human and murine gastrointestinal tract since it is not expressed by the mast cells and is expressed by all cKit<sup>+</sup> ICs (Gomez-Pinilla et al., 2009, Sanders et al., 2012b). Research conducted using animals with mutations that render Ano1 non-functional has shown that Ano1 is fundamental for the development of slow waves, which fail to develop in mice that are heterozygous for the mutation (Hwang et al., 2009). Moreover, mice lacking both functional alleles die within short period after birth and slow waves do not develop in organ culture from TMEM16A<sup>-/-</sup> mice (Hwang et al., 2009).

The mechanism of pacemaker currents are initiated through the activation of IP3 receptor on ER and release of Ca<sup>2+</sup> from intracellular store, this activates Ano1 (Chen et al., 2007a), resulting in STICs and subsequent spontaneous transient depolarization (STD) of the cKit<sup>+</sup> cells (Zhu et al., 2015, Koh et al., 2012). When depolarization reaches threshold potential, T-type Ca<sup>2+</sup> channels are activated, further depolarizing the cell and activate Ano1 channels of the cell, resulting in slow-wave production (Zheng et al., 2014). Depolarization

spreads to electrically coupled cKit<sup>+</sup> and SMCs, cause propagation of slow waves along the bowel wall. Ca<sup>2+</sup> stores are restored in the ICs through Ca<sup>2+</sup> reuptake by the ER via sarco-endoplasmic reticulum Ca<sup>2+</sup> ATPase (SERCA) pumps, enabling these cells to regenerate slow waves (Ward et al., 2000a).

The proximity of the ER to the plasma membrane is crucial in the maintenance of Ca<sup>2+</sup> signals within cKit<sup>+</sup> ICs and the generation of the slow waves, which leads to the identification that the ER is essential for the pacemaker function within these cells (Sanders et al., 2014). Disruption in any one component of the pacemaker unit results in disruption of normal bowel motility, where inhibition of IP3 receptors and intracellular Ca<sup>2+</sup> release, along with inhibition of SERA pumps and Ca<sup>2+</sup> re-uptake into the ER, each abolishes slow-wave activity in the GI tract (Ward et al., 2000a).

### **1.13.2 Inhibitory enteric innervation and smooth muscle relaxation in the gut (purinergic neurotransmission)**

The primary inhibitory neurotransmitters in the gut are nitric oxide (NO) and ATP (Saffrey, 2013). NO was first described as a non- adrenergic, non-cholinergic (NANC) inhibitory neurotransmitter (Bult et al., 1990). NO released from inhibitory enteric neurons diffuses to sites of action in adjacent cells.

Several lines of evidence suggest that NO signalling is primarily mediated through ICs. In mouse, IC-IM are closely associated with both NO nerve fibres and SMCs (Burns et al., 1996). In *W/W<sup>v</sup>* mice, loss of ICs produces disruption to nitrergic signalling (Burns et al., 1996, Suzuki et al., 2003). IC-DMP and nitrergic nerve terminals in the DMP of the small intestine are also closely

associated, an interaction that is proposed to mediate nitrergic motor neural input (Ward and Sanders, 2006, Ward and Sanders, 2001).

Burnstock et al. first hypothesized that ATP functioned as an inhibitory neurotransmitter in the gut (Burnstock et al., 1970). A few years later, purinergic receptors, namely P1 purinoceptors (adenosine) and P2 purinoceptors (ATP), were identified by the same author (Burnstock, 1976). Using specific purinergic receptor antagonists, researchers showed that the P<sub>2</sub>Y<sub>1</sub> receptor mediates intestinal SMCs hyperpolarization and relaxation in the gut (Gallego et al., 2006; Auli et al., 2008).

#### **1.13.2.1 The role of PDGFR $\alpha$ <sup>+</sup> IC in mediating purinergic neurotransmission**

FIJPs characterize purinergic neurotransmission and produce the inhibitory response of the gut, ultimately causing smooth muscle relaxation (Hwang et al., 2012). It is controlled by purines such as  $\beta$ -nicotinamide adenine dinucleotide ( $\beta$ -NAD) and adenosine triphosphate (ATP), which are released by inhibitory motor neurons and activate purinergic neurotransmission receptors and effectors, P<sub>2</sub>Y<sub>1</sub> and SK3 respectively (Kurahashi et al., 2014). Studies which isolated PDGFR $\alpha$ <sup>+</sup> ICs from the musculature of mice gut found, using RT-PCR, that both the P<sub>2</sub>Y<sub>1</sub> receptor and SK3 channel were abundantly and almost exclusively expressed by PDGFR $\alpha$ <sup>+</sup> ICs compared to cKit<sup>+</sup> ICs or SMCs (Baker et al., 2013, Peri et al., 2013, Coyle et al., 2015). Stimulation of purinergic neurons while blocking cholinergic neurotransmission in these studies by using Ca<sup>2+</sup> imaging evoked Ca<sup>2+</sup> transient in PDGFR $\alpha$ <sup>+</sup> ICs alone, supporting their role as primary mediators of purinergic neurotransmission. Moreover, Baker et

al. (2015) used electrophysiological experiments to show that PDGFR $\alpha$ <sup>+</sup> ICs were directly innervated by purinergic enteric inhibitory neurons which are mediated by post-junctional P<sub>2</sub>Y<sub>1</sub> receptors in PDGFR $\alpha$ <sup>+</sup> ICs. This purinergic neurotransmission provides a part of the tonic inhibition imposed on colonic muscles to help maintain the phasic nature of contraction (Baker et al., 2015). Evidence that purines act on P<sub>2</sub>Y<sub>1</sub> receptors to activate intracellular Ca<sup>2+</sup> release and the opening of SK3 channels to elicit hyperpolarization of PDGFR $\alpha$ <sup>+</sup> ICs has been demonstrated in numerous studies (Kurahashi et al., 2014, Baker et al., 2013, Kim, 2011, Gallego et al., 2012). Experimental evidence from mice (Kurahashi et al., 2014, Baker et al., 2013) showed that  $\beta$ -NAD, its metabolites and selective P<sub>2</sub>Y<sub>1</sub> agonists, all induced rapid hyperpolarization of PDGFR $\alpha$ <sup>+</sup> ICs and activated Ca<sup>2+</sup> transients. Only minor hyperpolarization was elicited in SMCs, which was not enough to convey the FIJPs and no hyperpolarization was observed in isolated SMCs when stimulated with P<sub>2</sub>Y<sub>1</sub> agonists. The hyperpolarization response was blocked by a P<sub>2</sub>Y<sub>1</sub> antagonist and was absent in *P2Y1*<sup>-/-</sup> mice (Baker et al., 2013), demonstrating the importance of the P<sub>2</sub>Y<sub>1</sub> receptor as part of the purinergic response.

Studies that stimulated the release of neurotransmitters in the presence of apamin, an SK3 channel blocker, showed a reduction in FIJPs and smooth muscle relaxation, indicating the importance of this channel in allowing K<sup>+</sup> efflux from the PDGFR $\alpha$ <sup>+</sup> ICs and its subsequent hyperpolarization (Suzuki et al., 2003, De Man et al., 2003). SK3 channels in PDGFR $\alpha$ <sup>+</sup> ICs were also observed to be activated spontaneously, generating STOCs, and therefore could be used

to regulate the resting membrane potential of PDGFR $\alpha$ <sup>+</sup> IC and SMCs tonic inhibition of the gut (Kurahashi et al., 2012, Sanders et al., 2014). Activation of the SK3 channels, therefore, drives the hyperpolarization phase of PDGFR $\alpha$ <sup>+</sup> ICs, allowing for the inhibitory response to spread to electrically coupled SMCs, decreasing their Ca<sup>2+</sup> influx and causing their relaxation (Baker et al., 2013).

Several studies also investigated the importance of Ca<sup>2+</sup> transient in PDGFR $\alpha$ <sup>+</sup> ICs. Ca<sup>2+</sup> transients were found to be enhanced in the presence of purines and P<sub>2</sub>Y<sub>1</sub> agonists but were disrupted in the presence of antagonists, *P2Y1*<sup>-/-</sup> mice, or through the blockade of Ca<sup>2+</sup> release and reuptake from the ER using IP3 and SERCA pump inhibitors respectively (Baker et al., 2013). Thus, similar to cKit<sup>+</sup> ICs, Ca<sup>2+</sup> transients are pivotal for the normal functioning of PDGFR $\alpha$ <sup>+</sup> ICs.

These studies provide evidence on the crucial role of P<sub>2</sub>Y<sub>1</sub> receptors and SK3 channels in purinergic neurotransmission and the high expression of these proteins in PDGFR $\alpha$ <sup>+</sup> ICs support the hypothesis that this IC is the primary mediator of the gut inhibitory response. Intracellular Ca<sup>2+</sup> imaging was used to provide further evidence on the spread of hyperpolarization from PDGFR $\alpha$ <sup>+</sup> ICs to SMCs (Baker et al., 2015). A short latency was observed between changes in Ca<sup>2+</sup> transients and hyperpolarization of PDGFR $\alpha$ <sup>+</sup> ICs and SMCs which followed. The spread of hyperpolarization to SMCs occurs via gap junctions expressed by PDGFR $\alpha$ <sup>+</sup> ICs (Fujita et al., 2003) and the use of gap junction blockers was shown to inhibit hyperpolarisation of SMCs but not of PDGFR $\alpha$ <sup>+</sup> ICs (Baker et al., 2015). These findings support the conclusion that PDGFR $\alpha$ <sup>+</sup> ICs may be primary mediators of the inhibitory response of the gut.

### 1.14 The role of IC in gastrointestinal disease

Abnormalities in the syncytium cellular component or ENS, disrupting the network, which might, therefore, contribute to motility disorders such as Hirschsprung disease (HD) (Blair et al., 2014). This disruption of the IC network has also been associated with the development of various gastrointestinal disorders, including diarrhoea, slow transit constipation, gastroparesis, infantile hypertrophic pyloric stenosis, achalasia, intestinal pseudo-obstruction and intestinal neuronal dysplasia (Jeng et al., 2000, Rolle et al., 2007, Farrugia, 2008, Chen et al., 2013, Gfroerer and Rolle, 2013) (**Table 1.2**) contains some of the studies performed on ICs using different techniques in different pathological conditions in human.

**Table 1.2 Examples of studies used different ICs identification methods in human tissue in various pathological conditions including HD**

<b>Tissue/Condition</b>	<b>Antibodies used</b>	<b>Method of identification</b>	<b>References</b>
<b>Human colon/ HD</b>	cKit	Immunostaining	(Vanderwind en et al., 1996)
<b>Human colon/ HD</b>	cKit/ AchE	Immunostaining	(Rolle et al., 2002)
<b>Human colon/ HD</b>	SK3/ cKit/ CD34/ 5B5	Immunostaining/ RT-PCR	(Vanderwind en et al., 2002)
<b>Human colon/HD</b>	SK3/ cKit/ PGP9.5	Immunostaining and RT-PCR	(Piotrowska et al., 2003b)
<b>Human colon/ neoplasms</b>	SK3/ PDGFR $\alpha$ /cKit/ PGP9.5/ nNOS	Immunostaining	(Grover et al., 2012)
<b>Human myometrium</b>	cKit/ CD34/ CD31/ SMA	Immunostaining and qRT-PCR	(Rosenbaum et al., 2012)
<b>Human colon/HD</b>	cKit/ Neuroligins	Immunostaining/Western-blot	(Wang et al., 2013a)
<b>Human gut/HD</b>	SK3/Ano1/PDGFR $\alpha$ / PGP9.5	Immunostaining and western blot	(Coyle et al., 2015)
<b>Human colon/ HD</b>	Ano1/ cKit	Immunostaining and Western blot	(Coyle et al., 2016)
<b>Human colon/ HD</b>	SK3	Immunostaining/ qRT-PCR	(O'Donnell et al., 2019b)

### **1.15 Hirschsprung disease**

The ENS, with its neurotransmitters and electrical properties, plays a significant role in the excellent coordination of gastrointestinal tract motor activity.

Abnormalities within the network of neurons or their absence (aganglionosis) can contribute to severe constipation, vomiting, abdominal pain and growth failure in children (Lake and Heuckeroth, 2013, Kenny et al., 2010, Heanue and Pachnis, 2007).

Hirschsprung disease is the most common (1 in 5000 births) (Spouge and Baird, 1985, Sutcliffe et al., 2013) congenital gastrointestinal motility disorder characterised by failure of neuronal-crest derived cells to colonise the distal bowel during embryological development, resulting in the absence of ganglionic cells in the affected segment of the bowel (Lake and Heuckeroth, 2013, Parisi, 2015, Tjaden and Trainor, 2013). This results in aganglionic (distal) bowel that is tonically contracted and unable to relax, causing severe functional obstruction and dilation of proximal bowel (Parisi, 2015, Lake and Heuckeroth, 2013), between the two segments (proximal and distal) lies a transition zone where fewer abnormalities of enteric innervation are apparent (Ghose, 2000). The length of aganglionic (distal) bowel extending proximally from the anus varies with the most common type (80%) affecting the recto-sigmoid area (short-segment disease), 15% extending past the sigmoid flexure (long-segment disease), and total colonic involvement in 5% (total colon aganglionosis). Management of HD remains a challenge with patients requiring surgery to remove the aganglionic (distal) bowel and transitional zone in which some ganglia are present, but ENS abnormalities may still be identified (Lake

and Heuckeroth, 2013). Histologically identified ganglionic (proximal) bowel is then reconnected to the anus (Sutcliffe et al., 2013). Despite advances in surgical techniques, many patients still experience complications such as incontinence and enterocolitis (Sutcliffe et al., 2013) and despite improved post-operative management, up to 10% of patients may die (Prato et al., 2011). For this reason, research surrounding HD has increased in recent years, with the hope that improved therapies can be developed.

An improved understanding of Hirschsprung disease aetiology and the consequence of aganglionosis on the network of cells in the musculature is greatly needed. Researchers have considered whether ICs may play a role in bowel motility disorders and the question may be raised as to whether changes seen in ICs are primary or secondary to pathogenesis (Jain et al., 2003).

### **1.15.1 Distribution of cKit<sup>+</sup> ICs in HD**

The distribution of ICs has been studied in the HD bowel using normal histology sections and whole-mount preparation techniques (Vanderwinden et al., 1996, Rolle et al., 2002, Wang et al., 2009, Yamataka et al., 1995, Solari et al., 2003, Horisawa et al., 1998, Newman et al., 2003). These studies did not only concentrate on the distal portion of the intestine but extended to the proximal HD colon (Horisawa et al., 1998, Nemeth et al., 2000, Newgreen and Young, 2002). Identifying any change in the distribution of ICs from proximal to distal segments of resected bowel may aid our understanding of their role in pathophysiology and be the first step towards inferring the function of these cells in HD. Most of these studies have shown reduced numbers of cKit<sup>+</sup> ICs in the distal bowel in HD patients (Newgreen and Young, 2002; Nemeth et al., 2000). The first study to investigate cKit<sup>+</sup> IC distribution in HD took resected bowel from HD patients and compared immunohistochemical staining to that of bowel taken from age-matched controls patients undergoing stoma closure. Absence of cKit<sup>+</sup> ICs in IM layer and reduction of ICs in MP layer was reported, and the distribution of ICs in the proximal segments of HD bowel was noted to be similar to the distribution seen in control bowel (Yamataka et al., 1995, Yamataka et al., 1997). This provided the opportunity for later studies to use proximal bowel as internal controls. Further research into the distribution of cKit<sup>+</sup> ICs reinforced these initial findings, reporting a markedly reduced distribution of cKit<sup>+</sup> ICs- IM layer and a reduction or disruption in the network of IC-MP in distal bowel in comparison to proximal bowel (Vanderwinden et al.,

1996, Wang et al., 2009). The transitional zone was also investigated by one study which showed a reduction in cKit<sup>+</sup> ICs networks in both IM and MP layers in the distal segments relative to proximal segments of eight patients (Rolle et al., 2002, Anatol et al., 2008). These studies cumulatively showed a greatly reduced expression of cKit<sup>+</sup> IC-IM, the primary mediator of cholinergic neurotransmission, and a decrease in the IC-MP, the primary pacemaker of the gut, in distal bowel in patients with HD. However, the study of Horisawa et al. (Horisawa et al., 1998) opposed these findings and did not reveal a major difference in the distributions of ICs in distal bowel compared to normal controls. They reported that cKit<sup>+</sup> IC distribution is similar all along the resected bowel (Horisawa et al., 1998; Newman et al., 2003). Subsequent studies have agreed with these findings and shown that the distributions of all cKit<sup>+</sup> ICs types are generally normal but are occasionally slightly reduced (Taguchi et al., 2003, Taguchi et al., 2005). However, the specific regions of the bowel under investigation must be delineated because physiological differences in the expression of ICs throughout the normal human colon have been described. However, it is difficult to ascertain whether these cKit<sup>+</sup> ICs detected in the distal segments in these studies have retained their functional properties (Newman et al., 2003).

### **1.15.2 Distribution of PDGFR $\alpha$ <sup>+</sup> ICs in Hirschsprung disease**

The spasticity and tonic contraction of distal bowel in HD may in part be contributed to by a lack of purinergic inhibitory motor neurotransmission in this segment of the gut. This hypothesis is backed by the observation that, electrical stimulation initially induced a relaxation phase in the proximal segment of HD

colon before the transmission of EJPs to SMCs and caused depolarization and contraction (Okasora, 1986). On the other hand, distal segments were only found to have EJPs and SMC contraction (Kubota et al., 1983). These observations support the hypothesis that a lack of functioning PDGFR $\alpha$ <sup>+</sup> ICs in distal segments may be crucial in the pathophysiology of HD. O'Donnell et al. (2016) reported reduced numbers of PDGFR $\alpha$ <sup>+</sup> ICs in distal bowel of 10 HD patients in comparison to controls (O'Donnell et al., 2016).

### 1.15.3 Genetics of Hirschsprung disease

A complete understanding of the genetics of an inherited complex disease is a major challenge. Several studies indicated that genetic factors and their regulatory mechanisms are significant in HD development. Many genes are now known to be involved in HD, those encoding for the proto-oncogene *RET* which is mapped to chromosome 10q11.2, mutation in this gene was identified in a number of HD patients (Romeo et al., 1994, Edery et al., 1994, Kusafuka and Puri, 1997, Amiel et al., 2008, Emison et al., 2010a, Alves et al., 2013). Nevertheless, not all HD cases can be explained by *RET* gene sequence variation. This has led to the discovery of additional genes for HD. Currently, more than 20 genes in the literature are defined as candidate genes in HD development (Fernández et al., 2009, Ruiz-Ferrer et al., 2011, Wang et al., 2011, Tang et al., 2012, Yang et al., 2013a) most known genes which contribute to the development of HD are listed in **(Table 1.3)**.

Glial cell line-derived neurotrophic factor (GDNF) which mapped to chromosome 5p, is the RET receptor ligand (Durbec et al., 1996, Worby et al., 1996, Trupp et al., 1996) and direct genomic sequencing revealed that

mutations in *GDNF/RET* might lead to the development of HD (Ivanchuk et al., 1996). Endothelin B receptor (*EDNRB*) mapped to human chromosome 13q22 was found to have a missense mutation in which Guanine is substituted by Thymine in exon 4 in HD patients (Puffenberger et al., 1994, Tang et al., 2013). *SOX10* gene located on chromosome 22q13 is first expressed during the embryonic stage of cells in the neural crest lineage, thus mutation of *SOX10* results in abnormalities of enteric ganglia (Southard-Smith et al., 1998, Inoue et al., 1999, Bondurand and Sham, 2013). Most of these genes are involved in critical biological processes including migration, differentiation, and development of the ENS (Zhang et al., 2017, Carrasquillo et al., 2002), which means any mutation of these genes can contribute to abnormal gut innervation with motility disorder effects. Many other genes have been implicated in HD, and the list is growing, as recently reviewed in (Heuckeroth, 2018, Parisi and Kapur, 2000, Amiel et al., 2008, Amiel and Lyonnet, 2001). Xiao et al. (2018) used microarray analysis to compare proximal and distal HD segments for variations in gene expression (Shang-jie Xiao, 2018). This study revealed 253 genes that have different expression levels between the two HD segments from these genes, 40 were upregulated, and 213 were downregulated. Most of these genes were involved in the processes of neurone differentiation and development (Shang-jie Xiao, 2018). The genetic causes of HD are complicated, and many gene mutations were identified in HD mouse model (V. Ashley Cantrell et al., 2004) and human HD (Minerva M. Carrasquillo et al., 2002).

**Table 1.3 Genes reported in the literature with an established role in the development of the HD**

<b>Gene</b>	<b>Chromosome</b>	<b>References</b>
<b>RET</b>	10q11.2	(Emison et al., 2005, Emison et al., 2010a)
<b>GDNF</b>	5p12-p13.1	(Salomon et al., 1996)
<b>GFRA1</b>	10q25-q26	(Sánchez-Mejías et al., 2010a)
<b>EDNRB</b>	13q22	(Sanchez-Mejias et al., 2010)
<b>EDN3</b>	20q13.32	(Sánchez-Mejías et al., 2010b)
<b>ECE1</b>	1p36.1	(Hofstra et al., 1999)
<b>PHOX2B</b>	4p13	(Fernández et al., 2013)
<b>SOX10</b>	22q13.1	(Sánchez-Mejías et al., 2010b)

### **1.16 Expression of genes encoding tyrosine kinase protein and ion channels in ICs**

Genes encoding members of tyrosine kinase receptors are abundantly expressed in ICs (cKit<sup>+</sup> ICs and PDGFR $\alpha$ <sup>+</sup> ICs), these cells belong to the same class III receptor tyrosine kinase family and share similar downstream signalling pathway (Chen et al., 2007a). These ICs express receptors that are essential to their role in neuromuscular neurotransmission, mainly excitatory muscarinic cholinergic receptors 2 and 3 (M2, M3) and inhibitory neurotransmitter purinergic receptor P<sub>2</sub>Y in cKit<sup>+</sup> and PDGFR $\alpha$ <sup>+</sup>, respectively (Chen et al., 2007b). Also, genes related to Ca<sup>2+</sup> transport ion channels found to be abundantly expressed in ICs, including Ano1 abundantly expressed by cKit<sup>+</sup> ICs and SK3 highly expressed by PDGFR $\alpha$ <sup>+</sup> ICs (Grover et al., 2012).

In children with HD, functional intestinal obstruction results from the presence of non-relaxing tonically contracted aganglionic segments. While the primary defining abnormality in HD is the absence of ganglion cells for varying extents of the colon, abnormalities in expressing profiles for various neurotransmitters, receptors and other essential proteins involved in inhibitory neurotransmission have been identified by many investigators. P2RY1 and P2RY2, which have been shown to mediate purinergic neurotransmission in the human colon, have been found to be deficient or absent in the MP in the aganglionic segment this suggests that downregulation of the mediators of inhibitory neurotransmission in aganglionic colon leads to unopposed cholinergic activity and a tonic hypercontractile state (Gallego et al., 2006, O'Donnell and Puri, 2008).

Methods for evaluating ICs in HD are confined to imaging. Since the specificity and sensitivity of imaging techniques are limited, there is a need to improve methods for monitoring disease activity (Blay et al., 2007, Hahn et al., 2011, Bauer et al., 2005).

### 1.17 Aims of the study

Previous studies that investigate ICs have often used different techniques making reliable comparison and sharing of data very difficult. Another issue is the insufficient numbers of patients and controls due to variable access to patient tissue in particular control samples.

I intended to create a protocol to identify these cells in human HD and stoma closure samples in a manner that can be replicated in a clinical laboratory. This will require identification of the best method of fixation and immunostaining using more reliable antibodies.

I aimed to develop a reliable method of quantification using more precise techniques, rather than the semi-quantitative quantifications used in most previous studies of ICs.

I also aimed to investigate the viability of the archived tissue of human HD samples for the use in the immunostaining and mRNA using *in situ-hybridisation* techniques to make use of the availability of these samples instead for waiting for fresh samples.

In addition, I aimed to quantify the mRNA expression for specific protein markers using qPCR techniques.

Finally, I used the RNAseq technique on whole HD segments and region-specific tissue layers to get a broad view of the genes changes in HD.

It is imperative that further research is conducted into the mechanisms underlying the pathogenesis of gut motility disorders, perhaps with a focus on the restoration of IC and ENS networks in disrupted animal models.

## **Chapter 2 Optimising Methods of Fixation and Processing for Immunostaining in Fresh Tissue and Evaluating Methods of Quantification**

### **2.1 Introduction**

Histological procedures using microscopic methods remain vital for the diagnosis of gastrointestinal disorders like HD (Szyberg and Marszałek, 2014). The histological analysis of tissue sections can depend on the experience and expertise of the histopathologist, as well as being laborious and difficult to grade in a reproducible manner. There can be substantial intra- and inter-observation variations between experts (Healey et al., 2006). In addition, the application of image analysis methods requires the standardization of histology procedures such as preparation of samples. Similarly, research applying histological procedures to investigate the distribution of particular cell types in healthy and diseased tissue, also require reliable techniques to enable comparisons within and between studies. This chapter will describe experiments designed to optimise the process of fixation, staining and quantification of human and animal colon tissue for the particular aim of examining IC types.

### **2.2 Tissue fixation**

The first critical step for any histological procedure is to achieve proper fixation of the target tissue (He et al., 2012; Leonard et al., 2016). The basis of high-quality histological preparation is the use of proper fixation. The purpose of fixation is to preserve tissue to render the cell and its components resistant to

further autolysis. Fixation also allows the tissue to withstand the adverse effects of subsequent processing reagents. Nevertheless, adequately fixed tissue may still result in altered morphology and affect the staining characteristics of the tissue (He et al., 2012).

Several of fixatives exist, either that have been used for decades (Formaldehyde used over a century) whereas others have only been created in recent years. It is essential to understand that any fixative will initially produce a several tissue changes. These changes include shrinkage, swelling and hardening of multiple tissue components, with tissues also undergoing further changes during the processes following fixation (Eltoum et al., 2001). Selection of proper method of fixation is, therefore, an important consideration.

### **2.2.1 Types of fixation**

Physical or chemical methods could be used to fix tissue. Physical means such as microwave and freezing, as independent procedures, are rarely used for the routine practice of medical pathology. Most fixation procedures used for the preparation of tissue for diagnostic purposes depend on liquid-based chemical fixatives (Carson, 2015; Eltoum et al., 2001). Chemical fixation is best achieved by fully immersing specimen in the fixative solution, which usually involves several different fixing agents in combination.

Fixative can generally be divided into two types: denaturing fixatives and cross-linking fixatives. The most prepared fixative for its mechanism of action is formaldehyde, first found in 1859 and used in a variety of pathological applications. The active ingredient in any formaldehyde solution is methylene glycol, the rate of penetration of formaldehyde and its rate of fixation might be

attributed to the rapid penetration rate of methylene glycol and slow fixation rate of formaldehyde (Prakash and Hussein, 2018, Fox et al., 1985, Helander, 1994). Both conduct their fixative action by developing cross-links between nucleic acids and proteins. The proteins denaturation caused by formaldehyde is partly reversible and may be overcome by using different strategies of antigen retrieval. In practice, it is assumed that these processes require at least one hour per millimetre (mm<sup>2</sup>) of tissue thickness, but fixation for at least 24 hours is routine (Eltoum et al., 2001). Alcohol fixative such as ethanol considered as denaturation fixatives, most commonly this effect is induced by dehydration, these reagents remove and replace the water in cells and tissues and modify the tertiary structure of the proteins and weaken the hydrophobic bonding (Eltoum et al., 2001, Williams et al., 1997). Some ethanol fixatives contain acetic acid that has been incorporated in the fixative solution to prevent nucleic acid loss and also to overcome the shrinkage induced by ethanol (Eltoum et al., 2001). There is a various classification of fixatives based on different criteria. Some of the most commonly accepted classifications are illustrated (**Figure 2.1**).

Due to the variability in staining procedures and the types of antibodies used in immunohistochemistry experiments, it can be challenging to extract the details of fixative quality compared to others when reviewing the literature. In our study, as part of optimising procedures to study tissue from patients with HD, the impact of three different types of fixative on the ability to detect antigens identifying IC in gut tissue were examined.

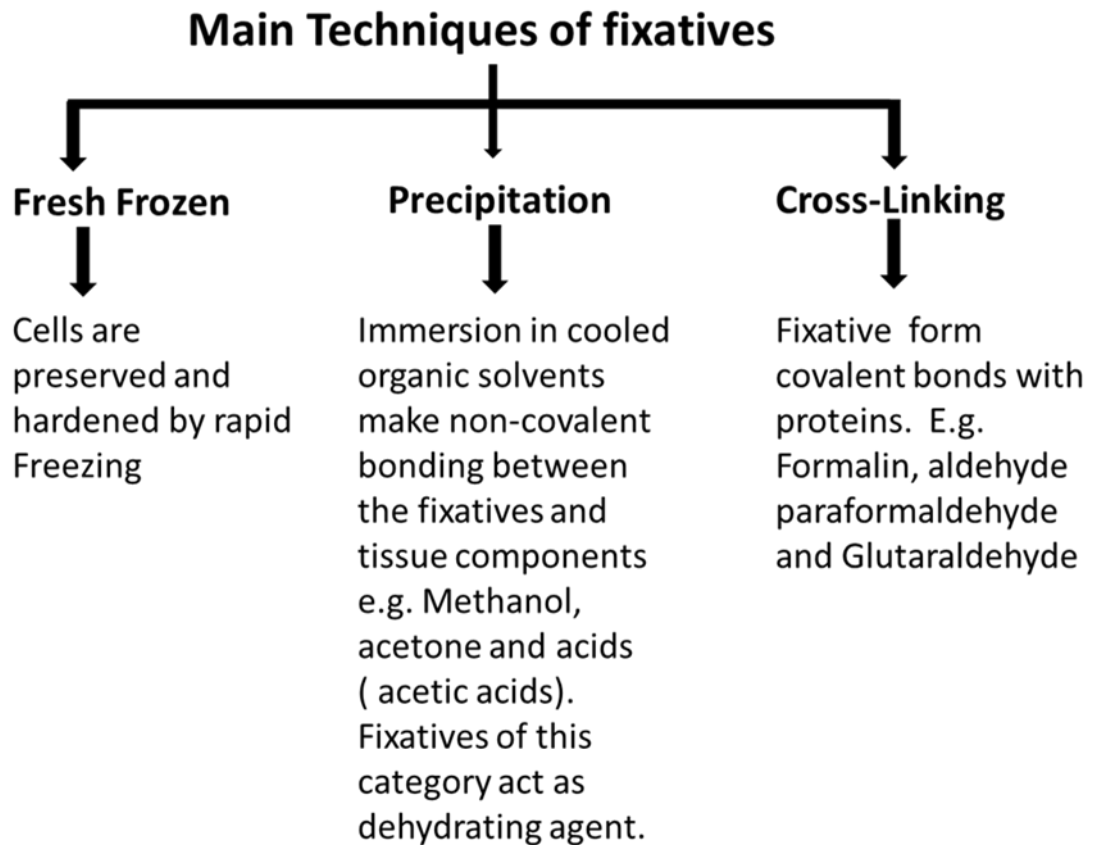


**Figure 2.1** Flow chart illustrating the main techniques of the common fixatives used in histopathological and research. Information extracted from (Alberts et al., 2002, Paavilainen et al., 2010).

### 2.3 Quantification Procedures

Based on the literature reviews, analysis of tissue biopsy continues to play a critical role in classifying ICs and morphology of nerves in HD. In congenital gut motility disorders such as chronic constipation, oesophageal achalasia, HD and chronic intestinal pseudo-obstruction, precise quantification of ICs in both clinical studies (Do et al., 2011a) and experimental models (Davis et al., 2016) has been attempted.

These and similar studies indicate that IC numbers and density, as determined by histological analysis, are useful for evaluation of slow transit constipation

(Wang et al., 2008), congenital intestinal atresia (Wang et al., 2013b), diagnosis of choledochal cysts (Karakuş et al., 2016) and assessing distribution of ICs in colon biopsies (Liu et al., 2012, Lyford et al., 2002). Different types of histological analyses exist (namely stereology, image analysis and morphometry) present with different advantages and disadvantages, in term of precision, accuracy and reproducibility (De Melo Dias et al., 2017).

Morphometry describes the quantitative analysis of the size and shape in 2D data which can be achieved using computer programs (image analysis).

Stereology is morphometry but differs in terms of 3D interpretation of measurements made on the 2D section. Briefly, stereology is a technique based on geometric principles that allow the formation of 3D structures from 2D sections. By stereology methods, three different aspects; the volume, surface and number of the structural features in the tissues can be determined quantitatively (Daunoravicius, 2014). Morphometry has been used in a number of studies (Bassotti et al., 2006, de Lima et al., 2008, Geraldino et al., 2006, Hoshino et al., 2013, Janevska et al., 2015, Karakuş et al., 2016, Park et al., 2005, Villanacci et al., 2008, Wang et al., 2009, Wang et al., 2008, Wang et al., 2013b, Yamashiro et al., 1998), and is a direct 2D quantification of histological sections of images taken with either confocal or electron microscopes by manual counting or digital counters. Some of these studies used a manual grading system based on intensity or density to quantify the target cells (Bassotti et al., 2006, de Lima et al., 2008, Hoshino et al., 2013, Wang et al., 2009), while others used simple counting of tagged cells (Janevska et al., 2015, Yamashiro et al., 1998).

In contrast image analysis, like the approaches reported by (Bernardini et al., 2012, Bettolli et al., 2012, Davis et al., 2016, Lee et al., 2005, Pasternak et al., 2013, Toman et al., 2006, Yang et al., 2013b) utilises specialised analysis software (Northern Eclipse software, Aperio Image Scope, Quantimet, Qwinv 500 plus or Multiscan) to extract information. In studies using image analysis, pixels in the form of density or intensity along a line or outline can be measured and converted to real units such as percentage of positive pixels (PPP) per area (Bettolli et al., 2012) or percentage of the total tissue area examined (Bernardini et al., 2012) after a software calibrations. Like morphometric quantification, image analysis is generally a 2D analysis, which presents with similar limitations.

Image analysis is replacing traditional morphometric analysis, which could be related to the speed and automation capabilities of analysis software. This trend, is however not particularly common for stereology, which is either used independently (Do et al., 2011a, Liu et al., 2012, Lyford et al., 2002) or in combination with either morphometry or image analysis (Popescu et al., 2006). Stereology is more robust and has advantages because it adds a third dimension to the typical 2D histological analysis. Unlike manual counting or measuring pixels, these stereological quantification involves superimposing test systems (such as points, lines, or planes) on physical or optical histological sections to reflect and obtain the 3D information. The ability to account for the structure and 3D nature of tissues offer a stronger statistical foundation to find the differences in samples, as opposed to 2D morphometric analysis or indirect quantification in image analysis.

The accuracy of all quantification methods depends on many factors like sample size and factors unique to the quantification method, like the histology skills of the analyser in morphometry (Mandarim-de-Lacerda, 2003). Moreover, the accuracy of image analysis depends on the assumptions underlying the image software, the digital calibration, and the method of acquiring and editing histological images. The anatomical precision in image analysis often needs extensive editing and masking of image artefacts that are not important for analysis, which can increase the time needed to achieve such precision. Recently, there has been a debate on the best practice for editing scientific images (Graf et al., 2007). Therefore, image analysis reported in several studies present extra bias from editing and the researcher's skills, which the studies hardly described (Bernardini et al., 2012, Bettolli et al., 2012, Davis et al., 2016, Lee et al., 2005, Pasternak et al., 2013, Toman et al., 2006, Yang et al., 2013b). Comparative analysis of the approaches to quantifying cell area, suggest that stereology is faster than image analysis (Glaser and Glaser, 2000; Gundersen et al., 1981). This suggests that time needed to complete analysis of several images often obtained in a research context limits the use of image analysis. While the study by Gundersen et al. (1981) showed that both approaches give almost similar results, pixel counting caused higher variation compared to stereology. This variation, however, can be reduced by putting more effort into outlining the structure that image analysis should focus on. Though similar comparison has not been conducted in the context of HD, the complex structure and morphology of human colon mean that similar issues

could occur in the quantification of ICs using image analysis (Scheppach, 1994, Vanderwinden et al., 1996).

The study by Toman on the relationship between slow transit colon constipation and the number of ICs that used image analysis reported an editing step before image analysis (Toman et al., 2006). Despite the limitations of image analysis and morphometry, they should not be considered incompatible with stereology approaches, but rather complementary, as shown by the study that effectively combined them (Popescu et al., 2006). Image analysis software is of value for a range of diagnostic and research purposes.

## **2.4 Aims and objectives**

Several factors are vital to achieving target precision of quantitative information in the histological analysis of cells in the tissue. These factors include sampling, fixation, processing and analysis. The first aim of the experiments in this chapter is to seek a strong fixative and processing method for staining ICs.

Maintaining the structural and morphological features of a sample is important in the use of image analysis tools. Though the implementation of automated image analysis tools is common in histological evaluation of bowel samples, the quantitative results obtained can differ across different tools. This variability is often associated with the underlying assumptions and mathematical set-up implemented by the developers. Therefore, the second aim was to compare the quantitative results obtained with two image analysis tools, including (IMARIS) and an open-source (Image J), in addition to the semi-quantitative analyses by two observers to measure inter-observers agreeability, these will allow for the selection of the right image analysis for the subsequent analysis of the results of other chapters.

## 2.5 Materials and methods

### 2.5.1 Specimen collection

All experiments using animal tissue were performed according to the regulations of the UK Animal in Scientific Procedures Act, 1986 and under the Home Office License (PID977A177). Young, adult Wistar rats (n=7) and C57/BL6 mice (n=12) were used of both genders. Animals obtained from internal breeding stocks were deeply sedated by intraperitoneal injection of pentobarbitone at 60 mg/kg with sedation confirmed by absence of pedal reflexes before an abdominal incision was made. Colons were freshly dissected from animals and transferred to 0.1M phosphate buffer saline (PBS). The contents were washed out with PBS several times, and the large intestines were transversely cut into smaller segments and transferred into a fixative.

Ethical approval (14/NS/0018, North of Scotland Research Ethics Committee) (**Appendix 1, A**) was secured to obtain human tissue from patients diagnosed with HD (n=14) aged  $10 \pm 3$  months at the time of corrective surgery (Duhamel pull-through) and patients who underwent stoma-closure (DC) aged  $9 \pm 3$  months (n=14) the number of patients used in each experiment is illustrated in (**Appendix 2, Figure A**). Before the surgery, written informed consent was acquired from patients' parents (**Appendix 1, B**). Nine patients (n=9 out of 14), who underwent surgery for recto-sigmoid (short-segment) HD and (n=10) DC samples were used to establish the fixation processes. The length of resection required was confirmed by the identification of enteric ganglia in the proximal resected circumference by histopathologist during the course of the surgery

and prior to full resection of the affected bowel. To minimise ischaemic time, the specimen was obtained from the theatre by opening the resected bowel along the anti-mesenteric edge, and a longitudinal, full-thickness strip was cut from the distal end (aganglionic) to two centimetres distal to the proximal end (ganglionic). This was taken to the laboratory in ice-cold PBS solution while the rest of the bowel was sent to pathology as per routine (**Figure 2.2**).

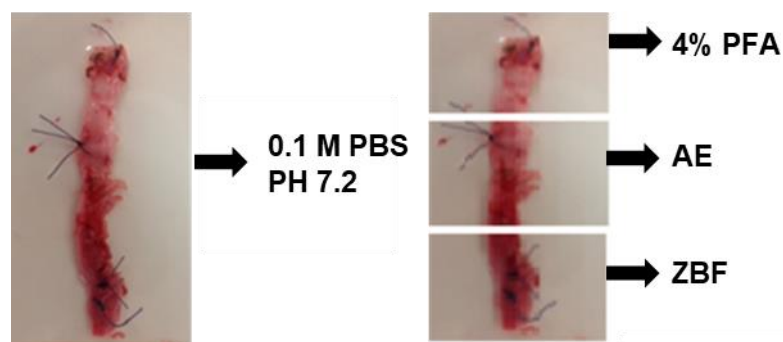


**Figure 2.2 The processing of the human samples for immunohistochemistry workflow.**

PBS-Phosphate buffer saline. PFA-Paraformaldehyde. AE-Acetic ethanol.

ZBF-Zinc based fixative.

### 2.5.2 Fixation and Sectioning

Three different fixatives were used in animal tissue to find the optimum method of fixation for the immunolabelling of gut ICs before the processing of human tissue. Samples were fixed and cryo-protected according to the established laboratory protocols of each fixative, (**Table 2.1**) summarises the temperature and length of time needed for each type of fixative as these are the most important factors required. For acetic ethanol (AE) (25% acetic acid and 75% ethanol), samples were fixed for 10 minutes at room temperature (RT) followed by 0.1M phosphate buffer (PB) wash for 5 minutes. Tissues were then cryo-

protected through incubation in 10% and 20% sucrose for 10 and 30 minutes respectively. Tissues fixed in zinc-based fixative (ZBF) ( $\text{Ca}^{2+}$  acetate 0.5 g,  $\text{Zn}^{2+}$  acetate 5.0 g,  $\text{Zn}^{2+}$  Chloride 5.0 g all in 1000 ml of 0.1 M Tris buffer, pH 6.5) or 4% Paraformaldehyde (PFA) in 0.1 M PB were incubated in their fixative for 24 hours at 4°C, followed by a five-minute wash in 0.1 M PB and cryo-protection in 30% sucrose for 24 hours at 4°C.

Cryo-protected animal colon samples were placed in a cross-sectional orientation into disposable vinyl specimen moulds (Tissue-Tek 4566 Cryomold moulds Intermediate) filled with an optimised cutting temperature compound (OCT; FSC 22 clear frozen section compound, Leica), then sectioned using a Leica CM1850 cryostat set at -20°C. Sections were cut at a thickness of 20  $\mu\text{m}$  to optimise the ability to identify and image networks of ICs by using thicker muscular layers. Sections were transferred directly onto poly-L-lysine coated glass slides (Thermo Scientific).

Longitudinal strips of HD bowel obtained from patients in surgery were cut into two sections (proximal and distal) and some samples were cut into (proximal, distal and transitional) which were divided into three pieces each one incubated and fixed in AE, ZBF and 4% PFA in 0.1 M PB, respectively, to allow for antibody and fixative comparison along the resected bowel. Fixed tissues were washed with PBS and incubated in sucrose then embedded in OCT and cryo-sectioned using the methodology established with animal tissue.

**Table 2.1 Summary of the protocols established for the use of different fixatives and their appropriate method of cryo-protection by incubation in sucrose**

Fixative	Incubation period	Wash in PBS for	Incubation in sucrose
<b>Acetic Ethanol (AE)</b>	10 minutes at RT	five minutes	10% for 10 minutes; 20% for 30 minutes at RT
<b>4% Paraformaldehyde (PFA)</b>	24 hours at 4°C		30% for 24 hours at 4°C
<b>Zinc based Fixative (ZBF)</b>	24 hours at 4°C		30% for 24 hours at 4°C

### 2.5.3 Immunohistochemistry

Slides were washed twice at 5 minutes each in a 0.1 M PBS to remove any residual OCT. The sections were then dried, and an outline was drawn around each section using a Liquid Blocker Super Pap Pen. Sections were first incubated in 10% donkey serum (Sigma, Cat No. d9663) at a dilution of 1:10 in 0.1 M PBS for 20 minutes to minimise non-specific binding of antibodies through the saturation of non-specific endogenous sites. This was followed by another two washes in PBS. Primary antibody solutions were prepared in PBS with 0.1% Triton (PBST) to enable cell membrane permeabilization and antibody binding according to the dilutions shown in **(Table 2.2)**. Then, secondary antibodies were applied (1 in 1000 dilution) one of two ways: direct fluorescence (appropriate Alexa Fluor 488 / 555 were applied to the sections

for 2 hours) or biotinylated secondary (appropriate biotinylated antibodies applied to sections for 2 hours, then streptavidin Alexa Fluor 488/555 applied for 2 hours). The biotin-streptavidin complex was used to amplify and enhance the fluorescence labelling. For double labelling, both primary antibodies (raised in different species) were mixed in a single Eppendorf at the required dilutions before being pipetted onto the sections.

Finally, slides were mounted using a medium containing 4', 6-diamidino-2-phenylindole (DAPI) (Sigma Cat No- SLBT2981) to label the nuclei. In the above procedure, three PBS washes were conducted after each step. Control slides for each antibody were prepared by incubating the sections with secondary antibody but no primary antibody.

**Table 2.2 Properties and manufacturer details of antibodies used**

<b>Antigen</b>	<b>Isotype</b>	<b>Manufacturer</b>	<b>Dilutions</b>	<b>Cat.No.</b>
<b>cKit</b>	Rabbit Polyclonal	Dako (USA)	1 in 200	A4502
<b>PDGFR<math>\alpha</math></b>	Goat Polyclonal	R&D system	1 in 200	AF-307- NA
<b>TMEM-16 (Ano 1)</b>	Rabbit Polyclonal	Abcam(Cambridge, United Kingdome)	1 in 500	Ab5321 2
<b>SK3</b>	Rabbit Polyclonal	Alomone labs(Israel)	1 in 200	APC- 025
<b>SV2</b>	Mouse monoclonal	DSHB	1 in 500	
<b>Secondary antibodies</b>		<b>Manufacturer</b>		
<b>Alexa fluor 488 Donkey anti- Goat</b>		Invitrogen		
<b>Alexa fluor 555 Donkey anti- Rabbit</b>		Invitrogen		
<b>Biotin-conjugate anti- Rabbit</b>	<b>Donkey</b>	Novex life technologies		
<b>Biotin-conjugate anti- Goat</b>	<b>Donkey</b>	Novex life technologies		
<b>Extra- Avidin peroxidase</b>		Sigma		
<b>Streptavidin 555</b>		Life technologies		

## 2.5.4 Imaging and quantification analysis

All sections were visualised and analysed with a Nikon E600 microscope and images were taken using a laser LSM 880 upright confocal microscope (Zeiss MicroImaging, Germany). Z-stacks at a magnification of x 20 at an interval of 0.7  $\mu\text{m}$  were constructed to capture high quality, full-section thickness image of a wide region of the colon section to fully appreciate the networks of ICs.

## 2.5.5 Quantification Methods

### 2.5.5.1 Semi-quantitative analysis

Interstitial Cells were identified according to immunopositive labelling intensity for cKit, Ano1, PDGFR $\alpha$  or SK3 around a DAPI<sup>+</sup> nucleus and long cell processes. Stoma-closure samples (n=10) stained with four different antibodies (total 40 sections) were used to establish this kind of quantification analysis by two observers to assess the quality of ICs labelling for each antibody. A scoring system was created from 0 -10 (0- indicates no staining and 10 reflects intense staining) and two observers examined the confocal z-stack sections and the maximum intensity projection for each section, considering the area around the MP. The scoring system was then converted into a subjective plus system where a score from 1-3 given one plus, from 4-6 given two pluses and from 7-10 were given three pluses (**Table 2.3**). The inter-observer agreeability was then calculated using Kappa statistical testing aiming at measuring the agreement between the observers due to chance or an actual agreement due to real observation. The analysis of the sections was repeated after two weeks by a single researcher to compare any differences in subjective measures.

## **2.5.6 Quantification using automated software**

### **2.5.6.1 Quantification using IMARIS**

First, the performance of IMARIS, a commercial image analysis tool available for histological evaluations, was explored. This IMARIS section was part of collaborative work with a private Bioimaging facility (BITPLANE, Oxford Instruments Company). Three randomly selected slides from three different DC samples were imaged using a confocal microscope and sent to the facility for analysis using IMARIS software. Filament count, morphological characteristics and analysis mark-up were obtained from the facility and used for comparative analysis with ImageJ, which is described below. IMARIS uses a proprietary surface rendering technology to create filament traces on digital images, a process that has been used in various life sciences contexts, including neurology, vascular biology and cancer biology.

### **2.5.6.2 Quantification using Image J**

The randomly selected images of the DC sample sent for IMARIS analysis were further analysed with ImageJ. ImageJ is a widely-used open-source software (<https://imagej.nih.gov/ij/>) with a wide range of plugins available for process tracking. Initially, immunofluorescence images were opened on the software and converted to the 8-bit format. The cell counter plugin was then used to identify and count the filament outlines. To ensure consistency, every section was converted and counted ten times and the average count used for statistical analysis.

## **2.6 Statistical analysis**

The results are displayed as the mean  $\pm$  SD of the mean. The differences between the analysis tools were assessed using Unpaired t-test, with the significance set at a  $p$ -value of  $<0.05$ . GraphPad (GraphPad Software Inc 7.03) was used to perform the statistical analysis and create graphs.

## 2.7 Results

### 2.7.1 Labelling of ICs in fresh tissue is fixative dependent

Interstitial Cells were labelled by both cKit and Ano1 and by PDGFR $\alpha$  and SK3 immunomarkers. Immunopositive labelling was seen in all animal tissues as well as human tissue to different degrees, according to their method of fixation, with proper labelling of dense networks of cell bodies and processes seen in the MP region and smooth muscle layers, CM and LM (**Figure 2.3**). Staining using each fixative was compared using a semi-qualitative analysis (**Table 2.3**).

**Table 2.3 Semi- qualitative patterns of staining of different protein markers according to the method of fixation**

Antibody	AE	PFA	ZBF
cKit	+++	++	+
PDGFR $\alpha$	+++	++	+
Ano1	+++	-	++
SK3	+++	+	-

- indicates no staining, + few, ++ moderate, +++ extensive

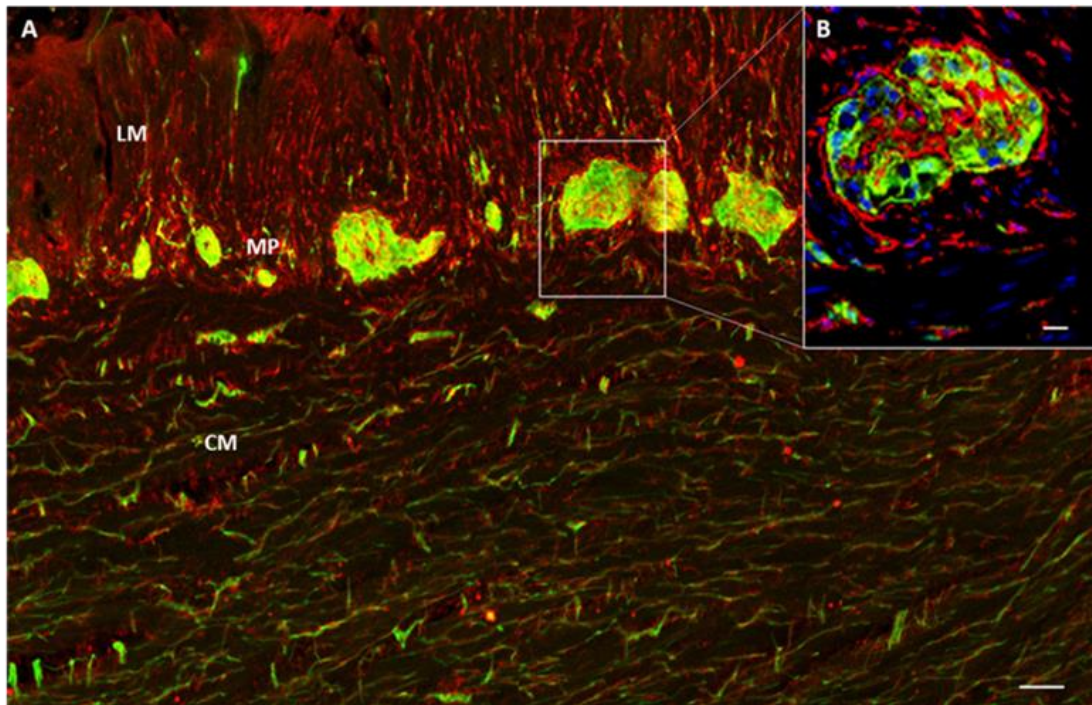


**Figure 2.3 Confocal image of the disease control sample (stoma-closure).**

(A) Showing the PDGFR $\alpha$ <sup>+</sup> ICs (red) in longitudinal muscle (LM) and circular muscle (CM) and SV2 (green) staining the enteric ganglion in the region of myenteric plexus (MP) scale bar 100  $\mu$ m. (B) Magnified area shows the enteric ganglion and the PDGFR $\alpha$ <sup>+</sup> ICs run in close contact to it, scale bar 10  $\mu$ m.

Gut tissue fixed with zinc-based fixative (ZBF) showed fewer labelled cKit<sup>+</sup> ICs despite the labelling of cKit<sup>+</sup> mast cells, which act as an internal positive control for the antibody (in the gut musculature, cKit<sup>+</sup> ICs and mast cells are the only cells that have prominent cKit receptor expression (Streutker et al., 2007, Pieri et al., 2008)). There was some labelling of cKit<sup>+</sup> cells in ZBF fixed gut tissue. However, clear cells were hard to identify. With PDGFR $\alpha$ , the labelling of the innermost mucosa acted as an internal control (similar to mast cells for cKit) where PDGFR $\alpha$  is expressed along the villi due to their role in driving their

embryological development (Andrae et al., 2008). Ano1 and SK3 both showed moderate labelling of cells, yet the connectivity of the networks was not well observed. Tissue fixed in AE showed better labelling of all ICs protein markers in comparison to tissue fixed in PFA. PFA- fixed tissue showed proper labelling of cell bodies, particularly for PDGFR $\alpha$ <sup>+</sup> ICs. However, these were fewer in comparison to cells identified in AE fixed tissue which also labelled more cell processes, particularly for cKit<sup>+</sup> IC networks (**Figure 2.4**).

Tissue fixed in AE also allowed for the visualisation of Ano1 channels. Ano1 was immunopositive along the processes of cKit<sup>+</sup> ICs and around the DAPI<sup>+</sup> nuclei, as seen by double labelling (**Figure 2.5**). Immunofluorescence showed complex networks of cells expressing this functional marker that was not observed in PFA fixed tissue. In contrast, AE and ZBF show positive immunostaining for Ano1 however, the cell processes were more distinct in AE compared to ZBF (**Figure 2.6**).

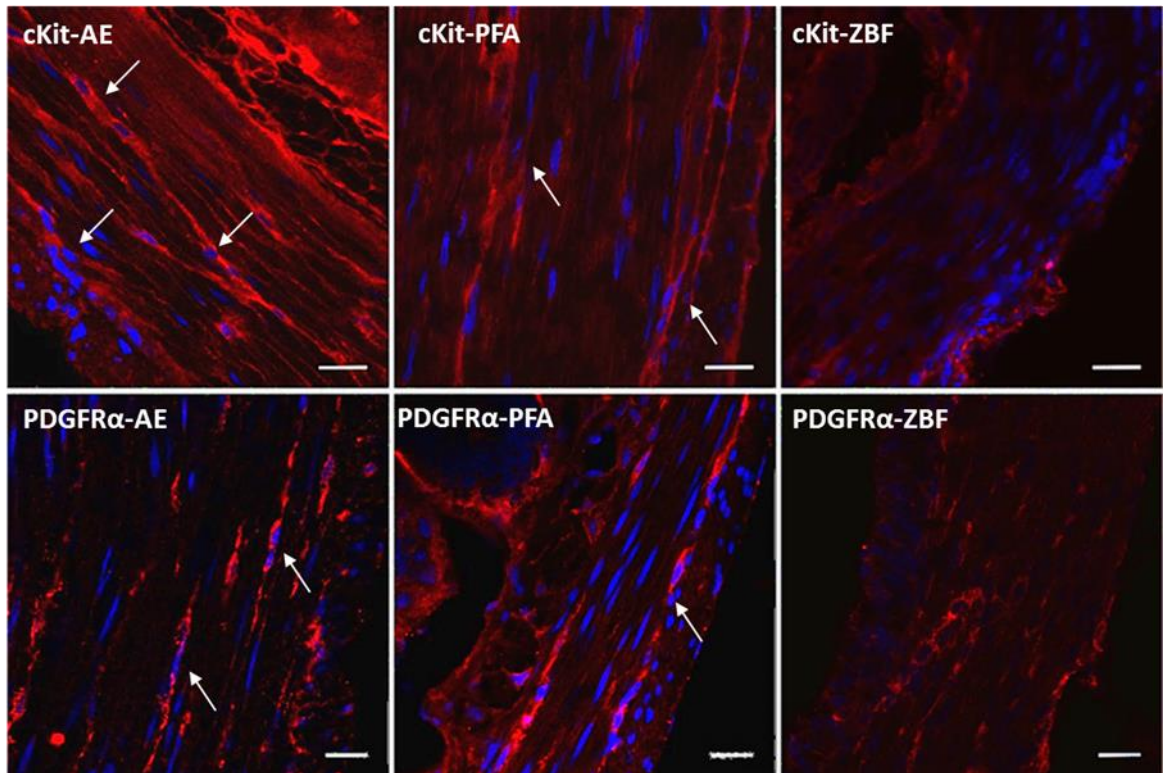


**Figure 2.4 Confocal images of cKit and PDGFR $\alpha$  immunoreactivity in rat colon fixed in different fixation.**

cKit<sup>+</sup> and PDGFR $\alpha$ <sup>+</sup> ICs fluorescence staining shows better cell marking with distinct processes and cell bodies (arrows indicate positive cells with DAPI (blue) nuclei. Scale bars 20  $\mu$ m for cKit and 10  $\mu$ m for PDGFR $\alpha$ . AE- Acetic Ethanol (+++), PFA- 4% Paraformaldehyde (++) , ZBF- Zinc based fixative (+), the plus sign (+) represents the semi quantification method of analysis of staining intensity according to **(Table 2.3)**.

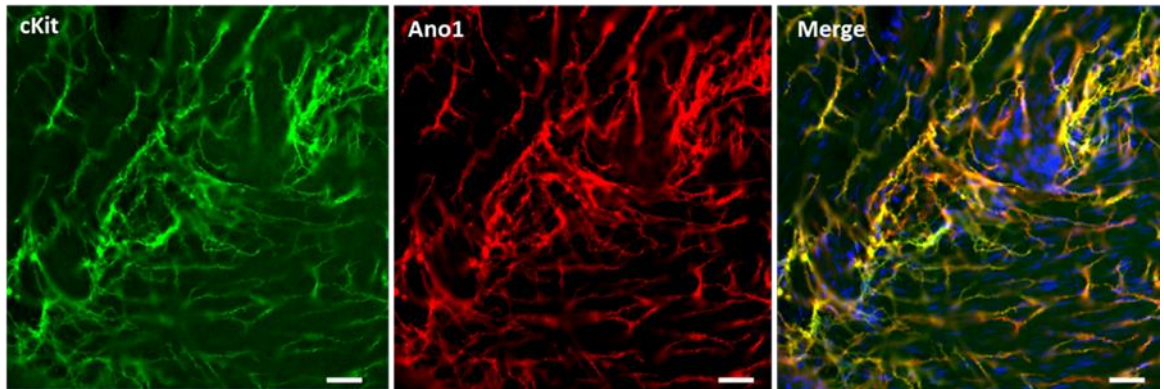


**Figure 2.5 Human colon tissue fixed in AE and stained with cKit and Ano1.**

The staining shows complete co-localisation of these markers in the MP indicating that these proteins are expressed by the same interstitial cell. Scale bar 20  $\mu\text{m}$ .

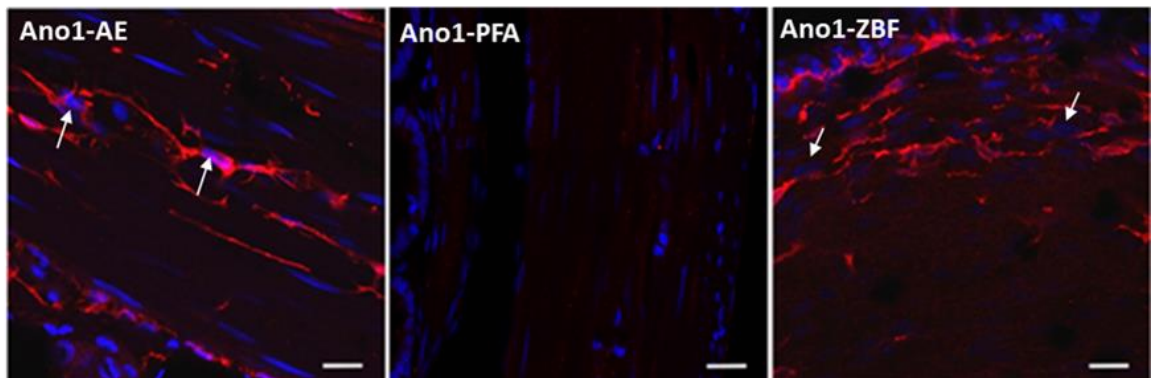


**Figure 2.6 Confocal images of rat colon show the difference in the immunostaining intensity of Ano1 protein marker in different fixatives.**

The fluorescence staining showed ICs networks in AE and ZBF but not PFA. Scale bar 20  $\mu\text{m}$ . Ano1-  $\text{Ca}^{2+}$  activated chloride channels, AE-acetic ethanol, PFA- 4% paraformaldehyde, ZBF-zinc based fixative.

Similarly, SK3 channels were preferentially identified in AE fixed rather than PFA, and ZBF fixed gut. There was some labelling of the cell processes in addition to somatic labelling similar to PDGFR $\alpha$ . However, the integrity of the cells was more preserved in PFA fixed tissue in comparison to zinc fixed tissue (**Figure 2.7**). The co-localisation of the SK3 channel with the PDGFR $\alpha$  receptor was further established by double labelling (**Figure 2.8**).

The use of 0.2% tween for the permeabilization of cell membranes was less effective than the use of 0.1% triton, as the expanses of the networks and their connectivity were less visible (**Figure 2.9**).

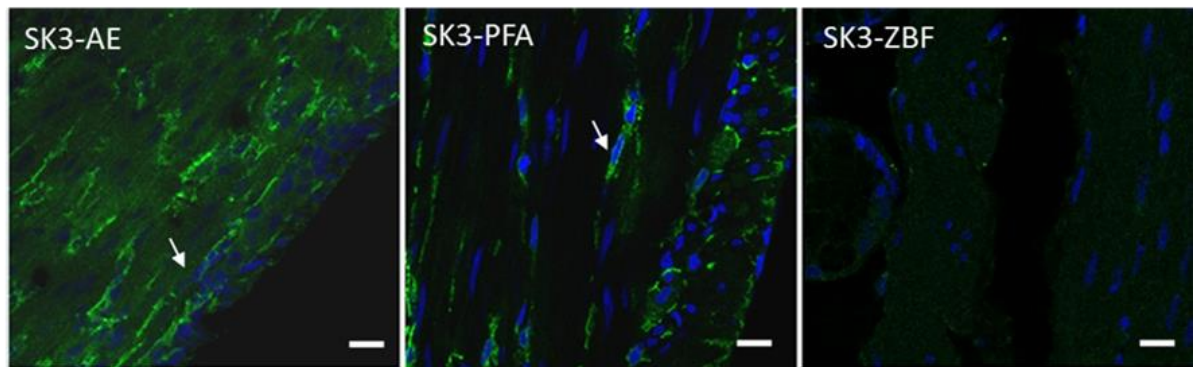


**Figure 2.7** Rat fixed colon shows immunoreactivity of the SK3 antibody in three different fixatives.

Both AE and PFA show positive fluorescent staining as compared to ZBF where no staining was detected. scale bar 20  $\mu\text{m}$ . SK3- Ca<sup>2+</sup> activated K<sup>+</sup> channel protein, AE- acetic ethanol, PFA- 4% paraformaldehyde, ZBF- zinc based fixative.

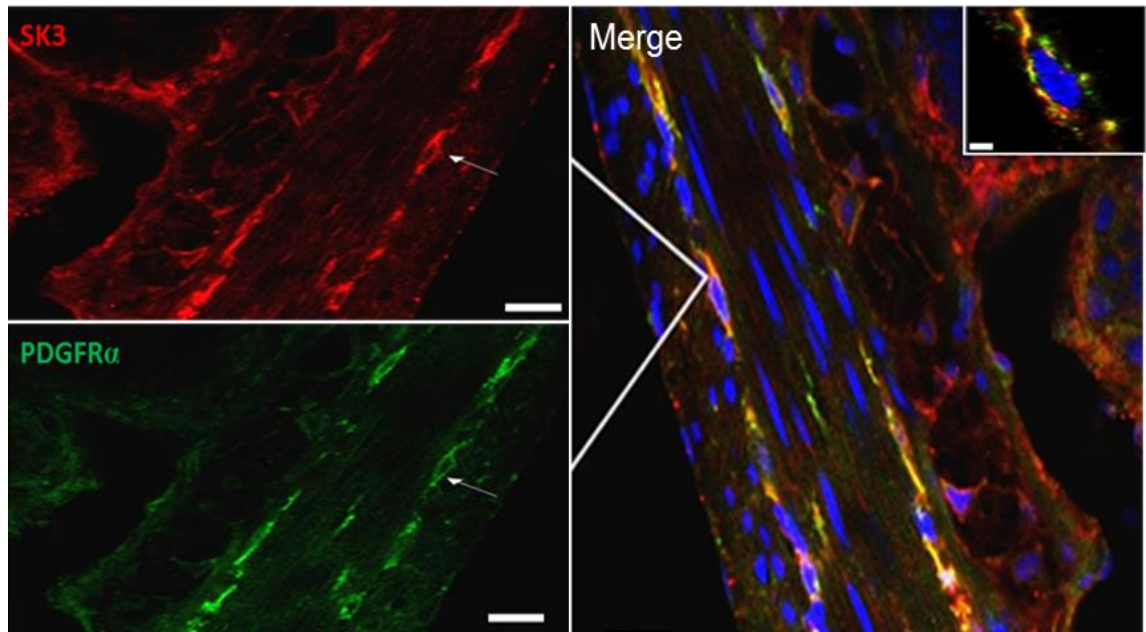


**Figure 2.8** Confocal images show a split view of a AE fixed mouse colon section.

Double-labelled with SK3 (red) and PDGFR $\alpha$  (green), scale bars 20  $\mu$ m. Merged section Scale bars 10  $\mu$ m and 5  $\mu$ m.

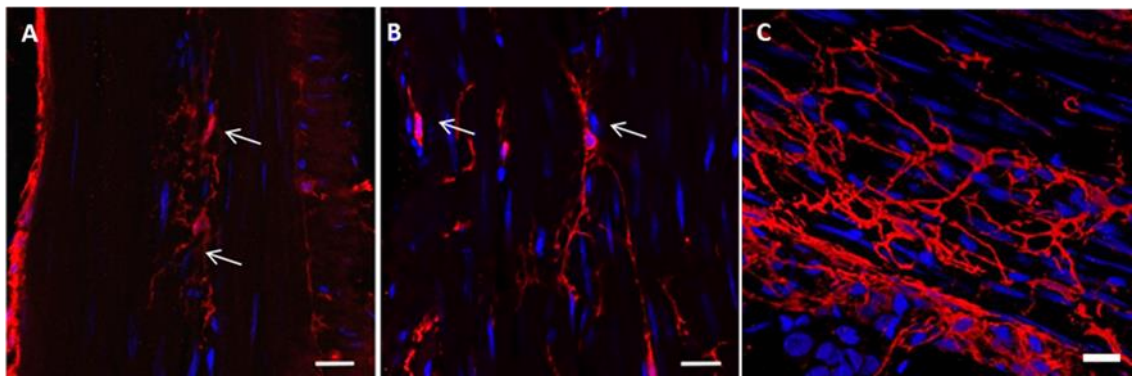


**Figure 2.9** Ano1 networks in rat colon tissues AE fixed and treated with 0.2% tween 20 (A) and 0.1% triton (B).

Arrows indicate examples of cells with extending processes. Scale bars 20 $\mu$ m. (C) A compressed z-stack showing the network of Ano1<sup>+</sup> cells throughout the section thickness.

These findings were further emphasised by using human colon tissue fixed in the three different fixatives, the intensity of staining for all antibodies was vigorous in AE fixed tissue as compared to the other two fixatives as shown in **(Figure 2.10)** cKit antibody staining was more prominent in AE than that of PFA and ZBF.

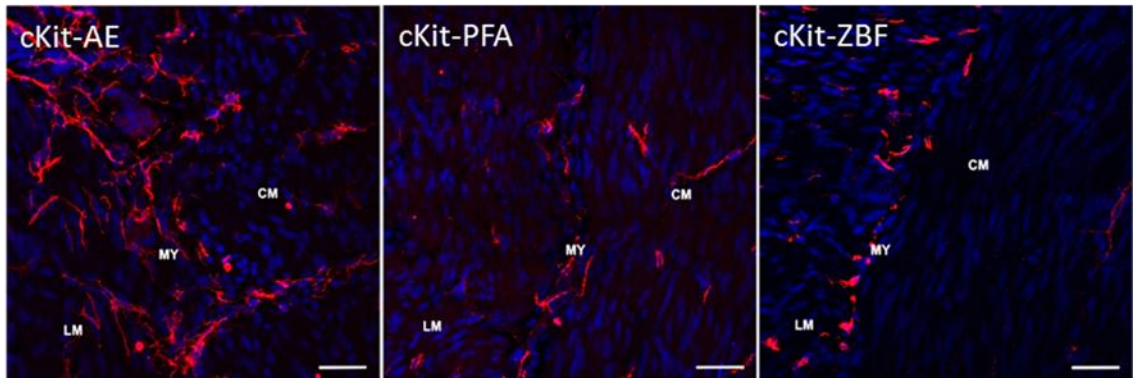


**Figure 2.10 Immunofluorescence of cKit<sup>+</sup> ICs in human colon fixed in AE, PFA or ZBF from a stoma-closure sample patient.**

Network of cKit<sup>+</sup> cells seen in the AE fixed sample is more distinct than the PFA and ZBF fixed samples. Scale bar 50  $\mu$ m. AE- Acetic Ethanol, PFA- Paraformaldehyde, ZBF- Zinc based fixative.

## 2.8 Quantification Results

The optimal immunofluorescence labelling of the networks of these two different ICs (cKit<sup>+</sup> and PDGFR $\alpha$ <sup>+</sup>) in animal and human tissue was established and used in human tissue from HD and stoma-closure as disease control samples. These tissues were used to test different methods of quantification to establish the best protocol for subsequent studies.

### 2.8.1 Semi-quantification method

Ten stoma closure samples that were stained with the four different protein markers have been assessed. Two observers analysed the same slides independently considering fluorescent intensity of ICs around MP. The frequency of agreement between the two observers are shown along the diagonal seen in (**Table 2.4, Figure 2.11, Figure 2.12**).

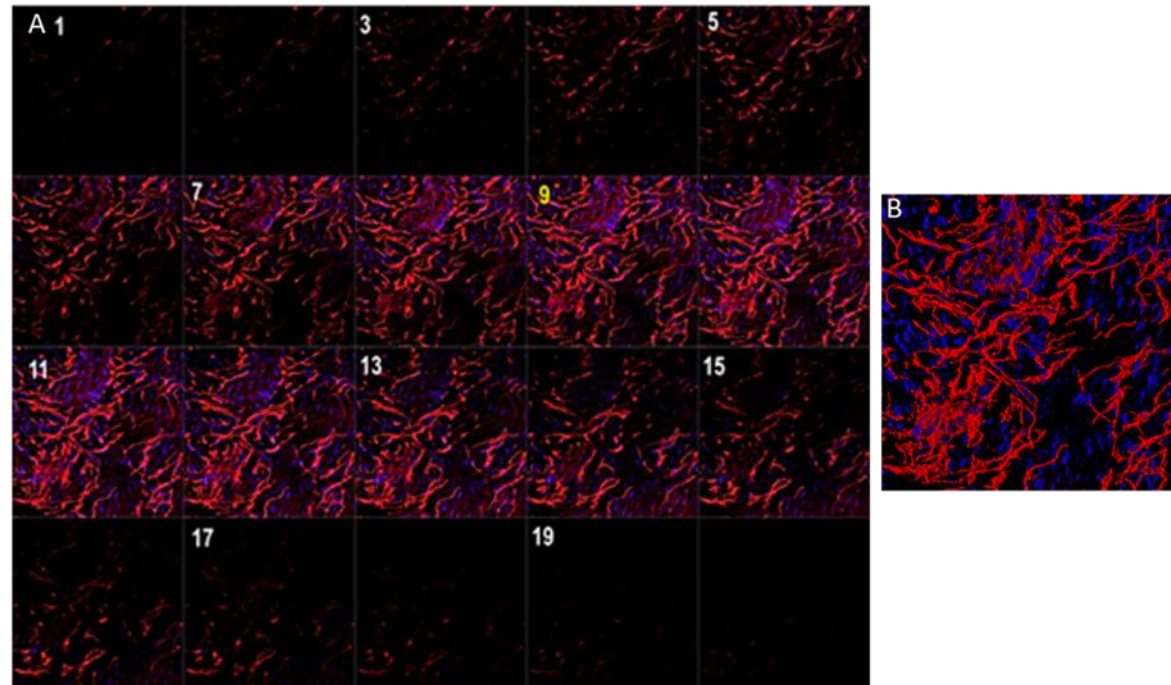


**Figure 2.11 Semi-quantitative analysis of z-stack confocal images compared to maximum intensity projection image.**

z-stack of cKit stained ICs (A), maximum intensity projection of compressed z-stack (B). The analyses performed by two different observers and inter-observer agreement quantified using Kappa statistics (0.8) (n=40).

Table 2.4 Frequency of agreement between the two observers

		Observer 2		
		Yes	NO	Total
Observer 1	Yes	19	3	22
	No	1	17	18
Total		20	20	40

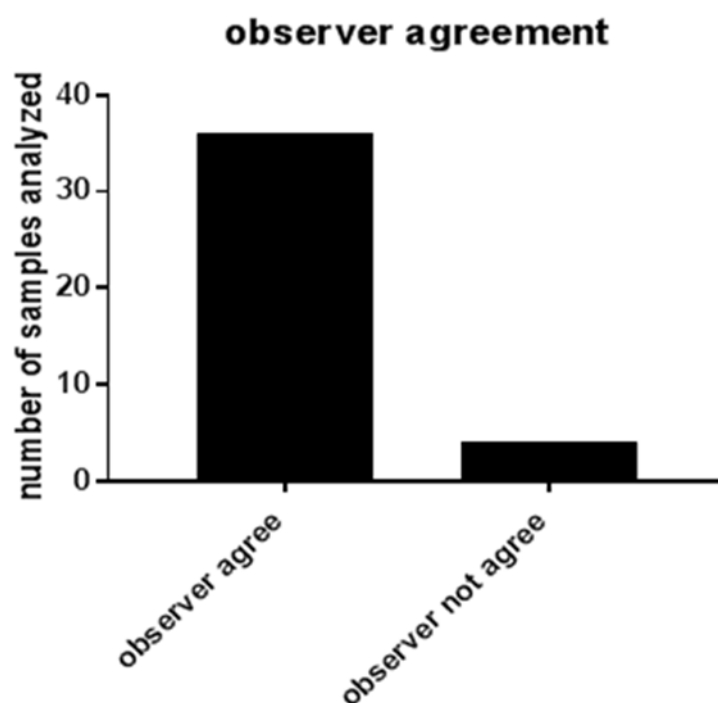


**Figure 2.12 Graph illustrating observer agreement according to the number of cases analysed.**

The corresponding frequencies *expected* ( $P_e$ ) if the assumption were made randomly, can be calculated, each of the relevant row total divided by overall total is multiplied by the relevant column total divided by the overall total.

Whereas the actual or observed agreement ( $P_o$ ) can be calculated by adding the highlighted values and divided by the overall total. The degree of agreement is then measured using Cohen's Kappa ( $K$ ),

<https://www.graphpad.com/quickcalcs/kappa1/>, which is given by the following equations:

$$K = \frac{P_o - P_e}{1 - P_e}$$

$K$  = is the Kappa coefficient.

$P_o$  = observed agreement (represent the actual agreement).

$P_e$  = expected agreement (due to chance).

Perfect agreement is evident when  $K$  equals 1; a value of  $K$  equals to zero indicates no agreement. The following levels of agreement are often considered appropriate for judging the extent of agreement (McHugh ML, 2012):

The level of agreement is:

No or poor if  $K < 0,001$

Slight if  $K$  is 0.01 to 0.20

Fair if  $K$  is 0.40 to 0.60

Good if  $K$  0.61 to 0.80

Almost perfect if  $K > 0.80$

According to these measurements, the results of the two observer agreeability were good as  $K = 0.8$ . The conclusion was, therefore, that semi-quantitative scoring could be used as a potential method for some immunomarkers.

### 2.8.2 Computational quantification of stained disease control samples

Tissue was processed as described in (section 2.5.3) and stained with either cKit<sup>+</sup> and Ano1<sup>+</sup> or cKit<sup>+</sup> and PDGFR $\alpha$ <sup>+</sup>. Immunofluorescent images were captured and analysed with ImageJ or IMARIS.

Initially, the differences in the number of filaments obtained by applying both tools on confocal images of cKit<sup>+</sup> and Ano1<sup>+</sup> stained slides was investigated. The results showed that both IMARIS and ImageJ generated a similar number of filaments stained with cKit or Ano1 in the samples. IMARIS analysis obtained 218 cKit<sup>+</sup> filaments and 145 Ano1<sup>+</sup> filaments. Further ImageJ analysis to confirm consistency in the results obtained with the IMARIS analysis showed relatively similar results, with 210 filaments showing positive staining for cKit and 139 filaments for Ano1. There was no statistical difference in the number of filaments counted by each method in using the unpaired t-test. This result suggests that either of the tools could be used in the analysis of cKit and Ano1 stained IC processes (**Figure 2.13**).

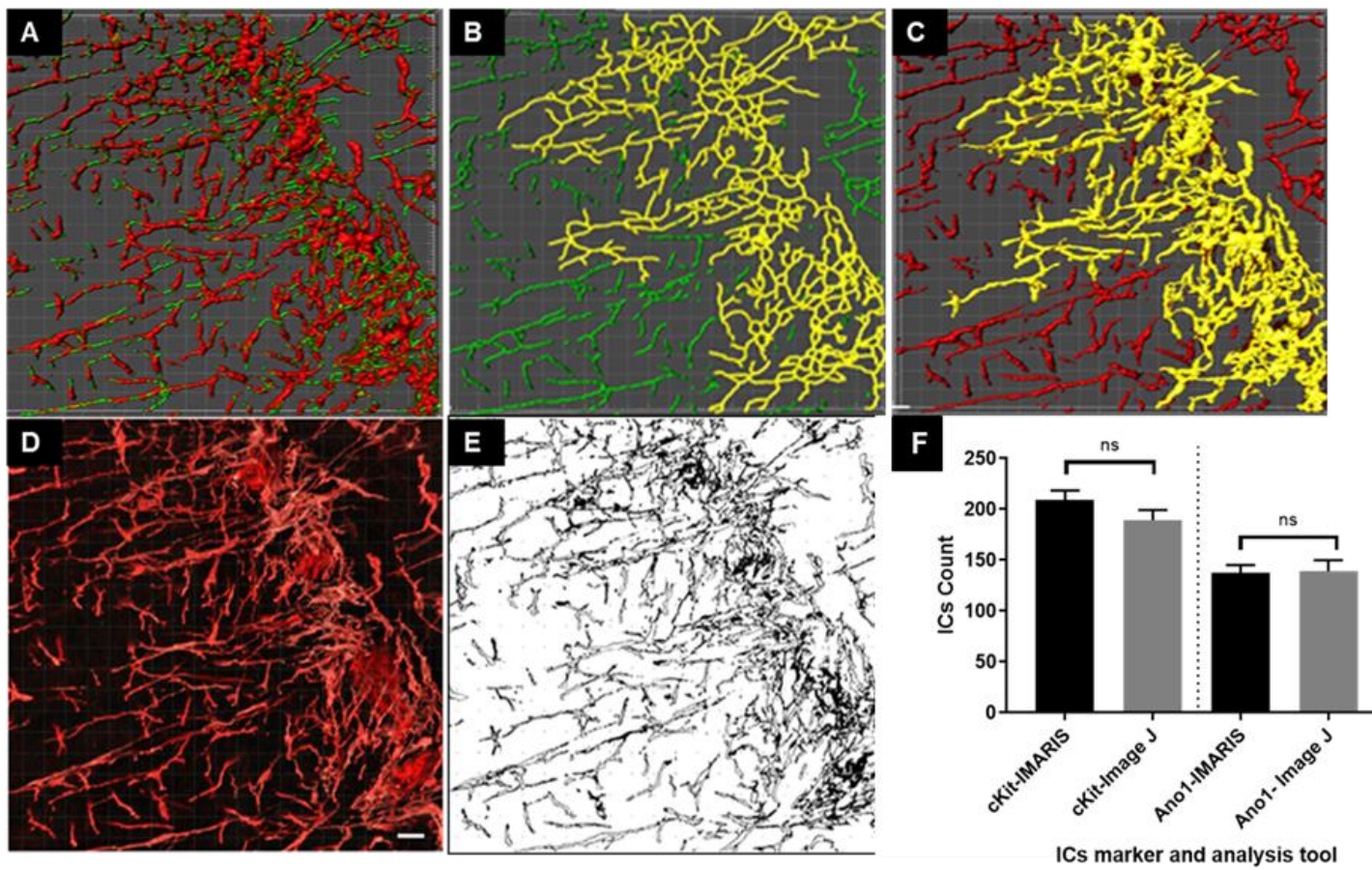


**Figure 2.13 ImageJ and IMARIS analyses of cKit<sup>+</sup> ICs and Ano1<sup>+</sup> ICs stained disease control samples show similar positive filament counts.**

(A-C) Representative image of filament trace using IMARIS, (D-E) Representative image of process trace using ImageJ (F) Graph for quantification of cKit and Ano1 positive filaments shows no statistical difference between the two tools using unpaired t-test,  $p > 0.05$ . Results expressed as mean  $\pm$  SD,  $n=3$ .

Following the observation that both tools produce the same filament counts for samples stained with cKit and Ano1, the differences in other combination of IC markers were compared. Here, the ability to use either ImageJ or IMARIS for the analysis of cKit and PDGFR $\alpha$  stained filaments were investigated. ImageJ and IMARIS generated a similar number of filaments stained with cKit or PDGFR $\alpha$  (**Figure 2.14**). IMARIS analysis obtained 374 cKit<sup>+</sup> filaments and 590 PDGFR $\alpha$ <sup>+</sup> filaments. Correspondingly, ImageJ analysis showed consistent results with IMARIS, where 361 stained filaments were obtained for cKit, while 575 stained filaments were measured for PDGFR $\alpha$ . Unlike the cKit and Ano1 combination, the cKit and PDGFR $\alpha$  combination revealed a slightly higher variation of about 15. The analysis also showed that the implementation of the tools in co-localised staining compared to no localised had similar outcomes. This analysis was necessary because of the potential overestimation or underestimation of stained filaments due to staining overlap when using both markers. Therefore, the result suggests that either of the tools could also be used independently in the analysis of combined cKit and PDGFR $\alpha$  stained ICs slides (**Figure 2.15**).

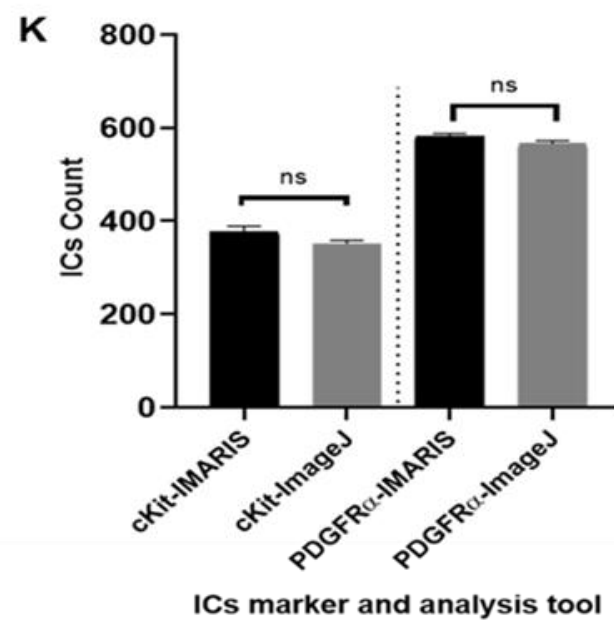
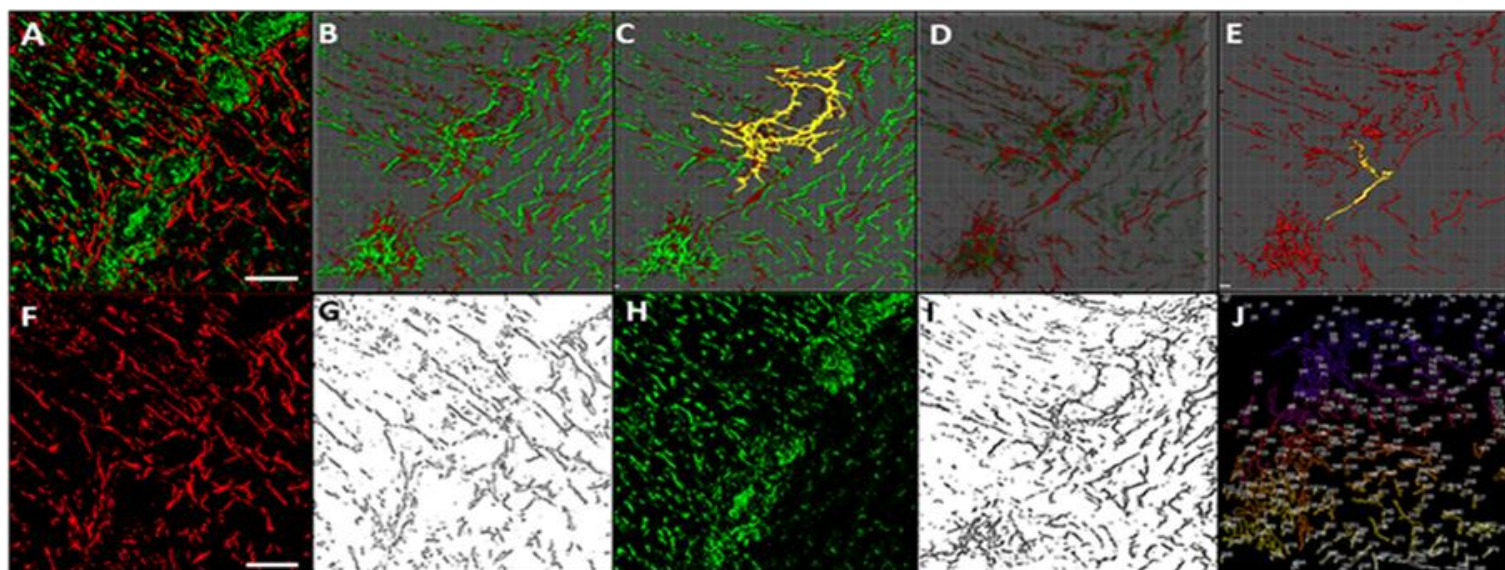


**Figure 2.14 IMARIS and ImageJ analyses of cKit and PDGFR $\alpha$  stained disease control samples.**

(A) confocal image of cKit<sup>+</sup> IC (red) and PDGFR $\alpha$ <sup>+</sup> IC (green). (B-E) represent image of filament trace using IMARIS for both ICs types. (F-G) Represent cKit<sup>+</sup> IC processes traced using ImageJ. (H-J) Represent PDGFR $\alpha$ <sup>+</sup> IC processes traced using ImageJ. (K) Graph for quantification results of cKit<sup>+</sup> and PDGFR $\alpha$ <sup>+</sup> shows no statistical difference between the two tools using unpaired t-test,  $p > 0.05$ . Results expressed as mean  $\pm$  SD,  $n=3$ .

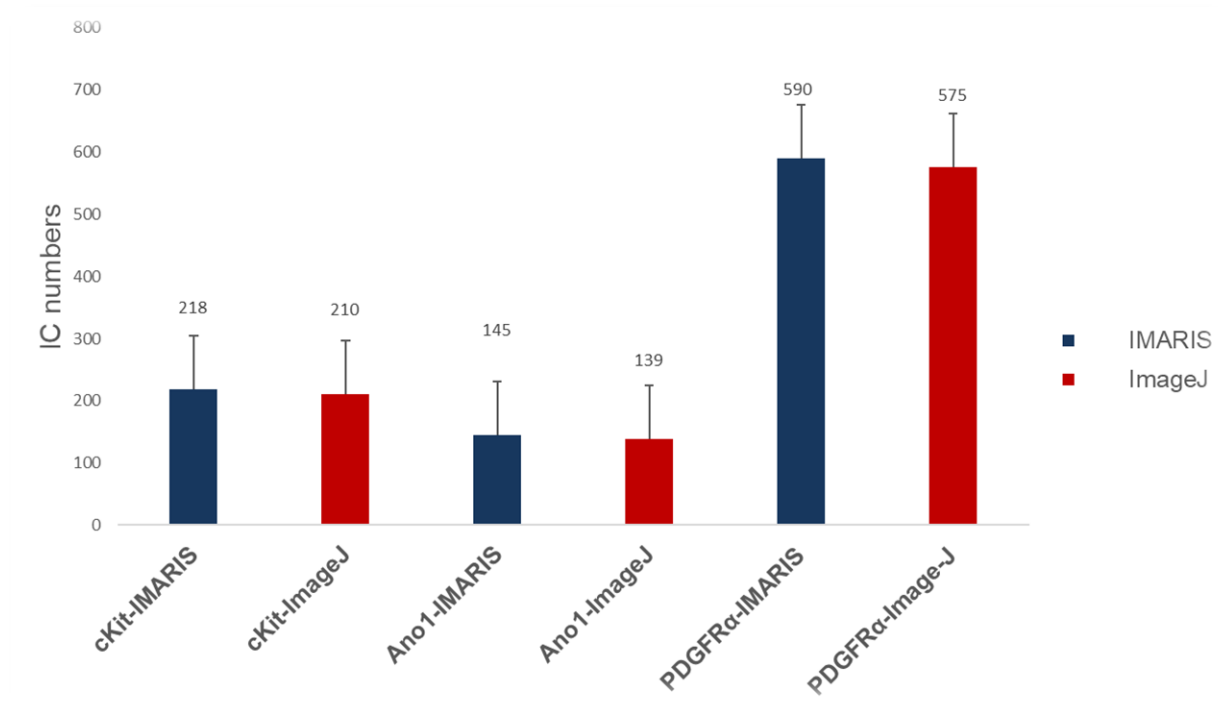
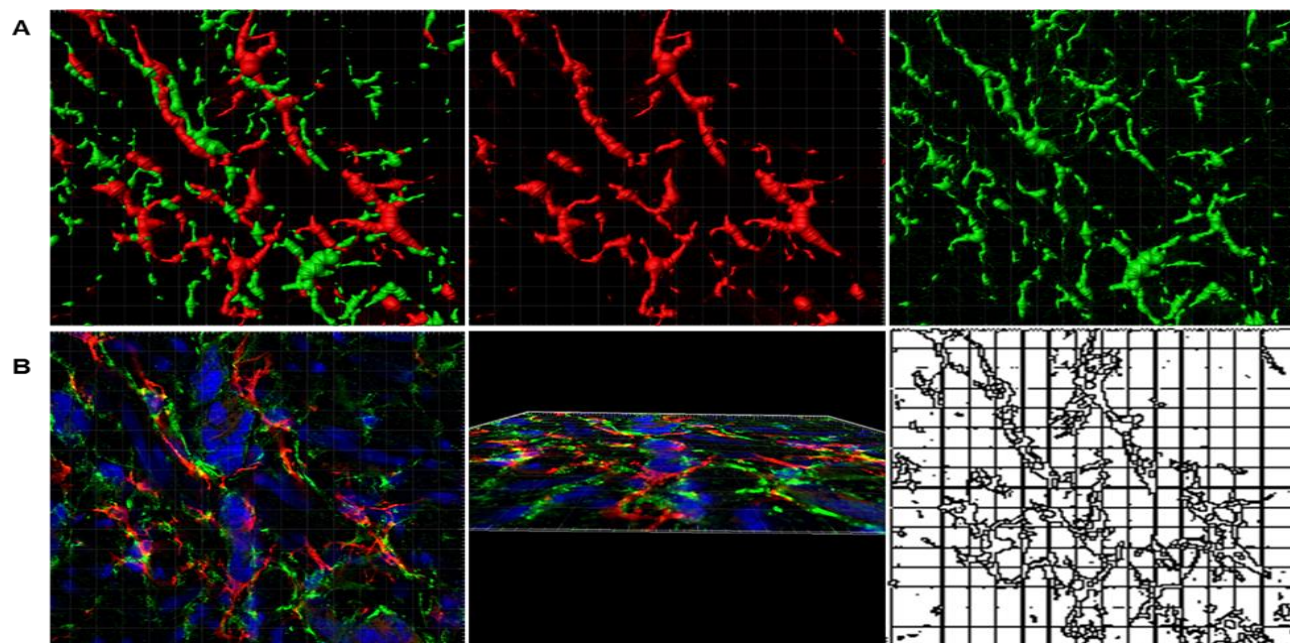


**Figure 2.15** IMARIS and Image J show no significant differences between the two tools used to analysis the tested sections.

Finally, the performances of the tools when using 3D rendering of images were explored. As described in the methods section, multiple 2D images of the same section were used to create a 3D volume before the analysis of the filament staining. Like the 2D images analysed before, the 3D analyses showed that both ImageJ and IMARIS generated a similar number of filaments for cKit or PDGFR $\alpha$  staining. IMARIS analysis obtained 235 cKit<sup>+</sup> filaments and 390 PDGFR $\alpha$ <sup>+</sup> filaments. Correspondingly, ImageJ analysis showed consistent results with IMARIS. In this analysis, 230 stained filaments were obtained for cKit, while 373 stained filaments were obtained for PDGFR $\alpha$  (**Figure 2.16**). In

contrast to the difference of 5 filaments seen for cKit<sup>+</sup> filament identification between the two tools, PDGFR $\alpha$ <sup>+</sup> filament identification with IMARIS was a count for 17 filaments higher than that obtained with ImageJ. However, this was not a statistically significant difference and suggested that creating 3D volume may affect the results generated with ImageJ, indicating a need for further optimisation of 3D images analyses by ImageJ.



**C**

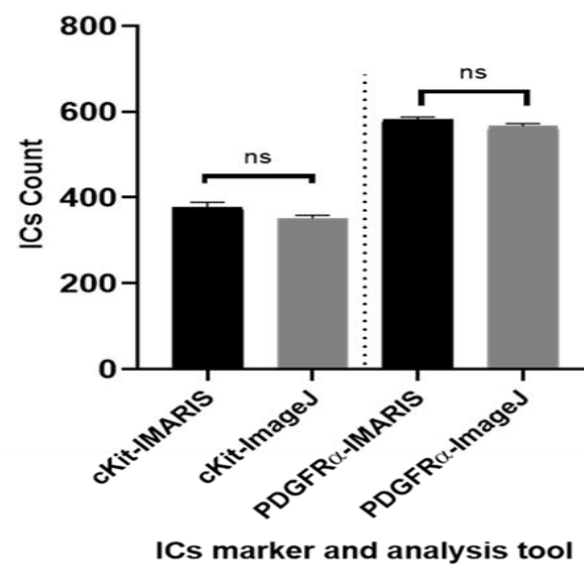


**Figure 2.16 Creation of 3D images has no effect on the consistency and reproducibility of ImageJ and IMARIS analysis of cKit and PDGFR $\alpha$  stained filament.**

(A) Representative created 3D image and filament trace for cKit+ (red) and PDGFR $\alpha$ + (green) using IMARIS, (B) Representative 3D image and process trace for the same section using ImageJ (C) Quantification of cKit and PDGFR $\alpha$  positive filaments from 3D images show no statistical difference using unpaired t-test,  $p > 0.05$ . Data shown are mean  $\pm$  SD, n=3 independent control samples.

## **2.9 Discussion**

Current approaches for investigating IC utilise various techniques. This limits comparability across studies. The work in this chapter attempted to generate an accessible, easily applied, inexpensive 'fit for purpose' practice for visualisation and quantification of ICs including, cKit<sup>+</sup>/Ano1<sup>+</sup> ICs and PDGFR $\alpha$ <sup>+</sup>/SK3<sup>+</sup> ICs in the bowel. This chapter describes methods for obtaining high-quality histological images of currently known IC networks using three methods of fixation and comparing the staining intensity of all four antibodies, which had not been considered previously. The resulting method for detection and analysis established in this chapter allows IC networks to be visualised throughout the sections of resected bowel enabling improved definition of what is the 'normal' distribution and function of these pacemaker ICs may then be more reliable.

### **2.9.1 Optimized methodology of labelling and assessing IC networks**

Previous studies looking at cKit<sup>+</sup> and PDGFR $\alpha$ <sup>+</sup> ICs in the gut of animals and humans have shown immunostaining images (Newman et al., 2003, Coyle et al., 2016, Vanderwinden et al., 2002) with more limited visibility of networks in comparison to those seen in this study. Those that have attempted to show higher degrees of cell processes have utilised whole-mount preparations, with varying degrees of success (Iino et al., 2009, Kurahashi et al., 2012, Horisawa et al., 1998). Whole-mount preparation is seen as an effective method of looking at the 3 D structure of the network of ICs compared to the previously

used thin histological sections (Gfroerer and Rolle, 2013). However, it requires expert skills due to the need to sharp-dissect the submucosal layer away from the muscular wall and the circular layer away from the longitudinal layer and mount and stretches the tissue before fixing (Kurahashi et al., 2012, Gfroerer and Rolle, 2013, Iino et al., 2008).

The methodology established here is quicker and more straightforward, allowing the networks to be visualised through the depth of the muscle section, either by fluorescence microscopy or imaging techniques using a confocal microscope to create 3 D representations. A further consideration is that these techniques could apply to the future assessment of these cells in HD in clinical histopathology laboratories. Furthermore, the different types of quantification techniques tested in this chapter had not been carried out in previous studies investigating ICs in HD. The development of a numeric grading system and method of adjusting for the subjectivity of the researcher's analysis was recently investigated and established as an efficient process of accurately analysing immunofluorescence (de Lima et al., 2008). Moreover, the numeric grading carried out in this study allowed for the range of labelling in the MP layers to be more fully appreciated and represented.

If the identification of ICs in clinical practice would appear to be beneficial in the future, the improved labelling of cKit, Ano1, PDGFR $\alpha$  and SK3 in AE fixed tissue identified in this chapter may aid towards doing so. Acetic ethanol fixed tissue required two days less time for processing in preparation for cryo-sectioning in comparison to PFA and ZBF due to its quick penetration and shorter fixation time. The degree of fixation of AE is due to the effect of acetic

acid in the mixture which counteracts the shrinkage effects of ethanol and produces tissue fixation by making hydrogen bonds between tissue constituents. This differs with PFA, which has limitations of cross-linking interactions that harm protein antigen resolution (Howat and Wilson, 2014). In addition, the process here eliminated the need for antigen retrieval which may be required for tissue fixed to a higher degree such as formalin-fixed and paraffin-embedded (FFPE) samples (Chen et al., 2014). The development of a protocol in which bowel could be taken straight from theatre meant that the study was not restricted to FFPE tissue, the current method of processing tissue in pathology. Further investigation into techniques to analyse ICs in such tissue is required to be able to investigate archived tissue processed in this way; details will be considered in the next chapter.

The performance of two image analysis software packages widely used in the field of life science was compared. The ability to use automated process tracker in the analysis of histological samples presents an opportunity for effective diagnosis and research quantification, but the reproducibility and consistency of any given tool present technical challenges. Mainly, the computational processes integrated into the different software packages are variable, which reduces the ability to compare results from different laboratories and studies. Commercial software like the IMARIS investigated in this project may provide more information on morphological features of cells and processes (although Image J performed well in these samples). However, the high cost of installing them could limit their uptake across many labs and so hinder comparability. Alternatively, open-source software like ImageJ can eliminate this challenge.

The availability of a wide range of user-generated plugins for ImageJ makes it an essential tool for analysing biological images. Interestingly, we showed that IMARIS and ImageJ produce consistently similar results and that ImageJ could, therefore, be used for the remaining parts of this project.

Developing a reliable computational work-flow to quantify IC filaments would substantially increase the speed of obtaining relevant information from achieved tissue sections. Beyond HD, computational histological evaluation of the gastrointestinal structure and the corresponding cell populations is essential in a range of diagnostic and research purpose (Lee et al., 2005, Toman et al., 2006, Bernardini et al., 2012, Bettolli et al., 2012, Pasternak et al., 2013, Yang et al., 2013b, Davis et al., 2016). These studies have applied similar analyses of pixels in the form of density or intensity along a line or outline to obtain filament counts (Bettolli et al., 2012), which is consistent with this being an approach suitable to widespread practice. It is important to note that like morphometric quantification, image analysis is a 2D analysis, which presents with unique disadvantages. The accuracy of the results obtained with either IMARIS or ImageJ depends on the sample size and computational skills (Mandarim-de-Lacerda, 2003). However, the negative impact of these factors on accuracy is limited by using automated approaches like the one implemented in the IMARIS or ImageJ analysis. Indeed, the similarity between the Image J and IMARIS results in this chapter is consistent with user-related errors being reduced via automation. Likewise, the accuracy of individual image analysis software depends on the assumptions underlying the image software, the digital calibration, and the implemented editing steps. Though intellectual

property rights protect the assumptions of the IMARIS software, the observation that it yielded similar results to those of ImageJ suggests that appropriate consideration of the array of factors affecting histological evaluation before image analysis could help eliminate inconsistencies. Factors such as sampling, fixation and processing are crucial to achieving a precision of the quantitative information. Interestingly, this chapter described a robust optimisation protocol for obtaining and analysing quality immunofluorescent digital images.

Firstly, a systematic selection was deemed appropriate to compare the tissue area and analysed slides. Both random and systematic sampling is important in the quantitative histological analysis because they give each filament equal sampling chance (Cruz-Orive and Weibel, 1990). In this comparative analysis, we used a systematic selection for both the tissue area and the analysed slides. This approach is consistent with the approaches reported by other studies that used image analysis tools (Gardi et al., 2008; Boyce et al., 2010). Moreover, the volume of intestinal biopsy needs to be estimated and used calculate filament counts per biopsy effectively. However, the current approach focused on filament counts per slides due to the robust sampling method used.

Secondly, the importance of fixation and processing varies according to the target cells and analysis. For example, the length of fixation may produce staining artefacts, which in turn will have a negative impact on the accuracy of the analysis (Wisse et al., 2010). However, earlier in this chapter, optimisation of fixation method was addressed, and it is unlikely this affects the results obtained here. It is important to note that the results from different fixation times

were not compared due to time limitations. Another critical issue related to fixation is shrinkage, which can affect computational identification and quantification of cell processes. However, manual observation of the immunofluorescent images suggests that tissue integrity was maintained.

## **2.10 Conclusion**

This chapter addressed the need to reliably identify and stain IC to assess their distribution in resected HD bowel. This study was the first to label for both types of IC networks and compare the effect of different fixatives on their localisation. Building an understanding of the distribution and protein expression of cKit<sup>+</sup> and PDGFR $\alpha$ <sup>+</sup> ICs within each layer of the musculature wall may open doors for the future identification and development of ways to manipulate the activity of these cells in motility disorders such as HD.

Further, this chapter showed that both IMARIS and ImageJ evaluation of stained ICs obtained similar results, a degree of consistency potentially due to our optimised fixation and staining protocol. Therefore, the results presented in this chapter allow us to use ImageJ for subsequent analyses of tissue samples in this study. In addition, the morphological information will inform further studies of cell isolation and RNA analyses.

## **Chapter 3 Testing Immunohistochemical and *In Situ* hybridisation protocols in human archived formalin-fixed paraffin-embedded Hirschsprung disease tissue samples**

### **3.1 Introduction**

The availability of fresh human disease specimens is often a limiting step in experimental research. Formalin-Fixed Paraffin-Embedded (FFPE) tissue is widely available for pathological analysis in hospitals and stored in a pathology archive in the pathology department (Liu and Pollard, 2015). The ability to use FFPE archival tissues would significantly enhance the pool of material for research.

In FFPE tissue processing, the formalin inhibits cell metabolism. It preserves the cellular structure and tissue morphology by introducing inter and intramolecular cross-links between side chains of amino acids (Srinivasan et al., 2002), thereby maintaining secondary and tertiary structures of proteins (Rait et al., 2004a, Rait et al., 2004b). However, by doing so, the fixatives chemically modify the proteins, and such modification may mask the antigen proteins so that the primary antibodies cannot detect and bind to them (Scalia et al., 2017, Otali et al., 2009) (**Figure 3.1**). The role of paraffin is to seal the tissue and reduce the rates of oxidation (Liu and Pollard, 2015).

Fifty years ago, fresh frozen tissue was considered essential for preserving antigenicity for Immunohistochemical staining (PK Nakane, 1966). Within the following 10 years, however, modifications of the immunostaining methods (Taylor and Burns, 1974), with or without the use of antigen retrieval (AR)

techniques (Shi et al., 2011), rendered FFPE tissue suitable for detecting a wide variety of intracellular and surface antigens by immunohistochemistry for diagnostic pathology practice, research and validation of biomarkers (Gaffney et al., 2018).

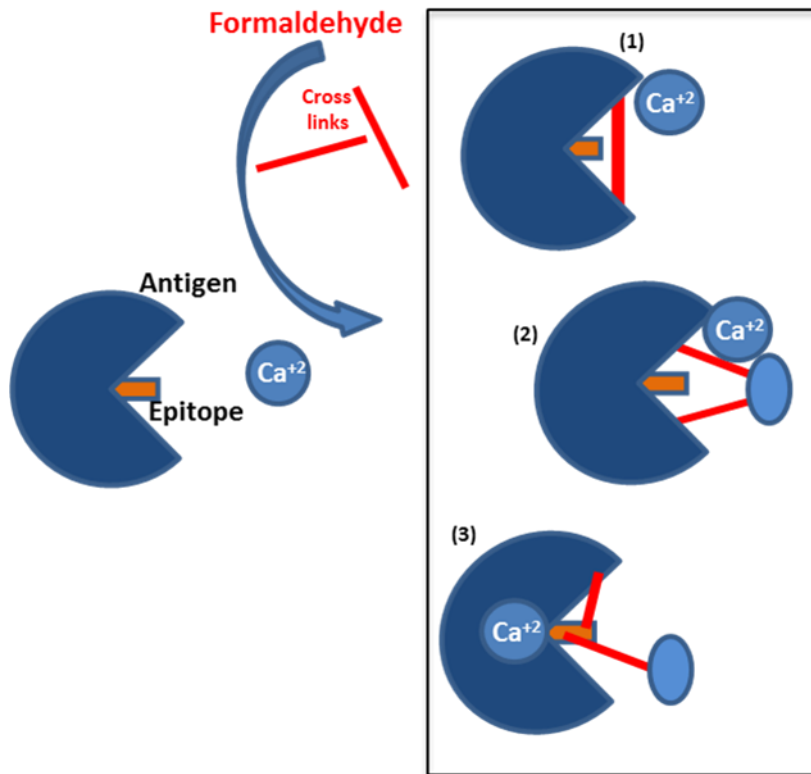


**Figure 3.1 Mechanism of Formaldehyde fixation**

Formaldehyde introduces cross-links between proteins. These cross-links reduce the access of antibodies to the epitope. Cross-links may be formed between two parts of the antigen (1), between two or more different molecules (2), or affect the epitope itself (3). Redrawn from (Werner et al., 2000).

### 3.2 Fresh Frozen vs FFPE tissue samples

Fresh frozen (FF) tissue sections have been considered as standard for immunofluorescence and Immunohistochemical analysis from the establishment of these methods in the mid-20<sup>th</sup> century. However, an evaluation of Immunohistochemical results of 26 antibodies in OCT frozen sections with various fixative conditions and FFPE sections, concluded that FFPE tissue sections might serve as a useful tool for immunostaining for a variety of antigens (Shi et al., 2008). A summary of the main concepts of differences between FF and FFPE specimens is shown in **(Table 3.1)**.

Subsequently, with the advent of immunoperoxidase labelled antibodies, there was a growing focus on the application of Immunohistochemical analysis to archival FFPE tissue sections in practice (Shi et al., 2008).

**Table 3.1 The main difference considered between fresh frozen (FF) and formalin fixed paraffin embedded (FFPE) samples**

	<b>FF</b>	<b>FFPE</b>
<b>General comparison</b>	<ul style="list-style-type: none"> <li>• Consuming less time and effort when considering sample preparation.</li> <li>• Rapidly deteriorates once it is at room temperature as it requires to be frozen as soon as possible.</li> <li>• Dedicated freezer space is required which increases the space and cost to store these specimens.</li> </ul>	<ul style="list-style-type: none"> <li>• Time consuming as formalin fixation and paraffin embedding take longer time.</li> <li>• Cost effective as these samples are able to be stored at room temperature.</li> </ul>
<b>Molecular analysis</b>	<ul style="list-style-type: none"> <li>• Gold standard for most molecular assays e.g mass spectrometry, qRT-PCR, next generation sequencing and Western blotting.</li> </ul>	<ul style="list-style-type: none"> <li>• The non-standardized protocols in the preparation of these specimens are likely to affect molecular data e.g DNA, RNA, post translational modification.</li> <li>• Can leads to false results when comes to sequencing experiments.</li> <li>• However, FFPE blocks could make valuable resources if an optimized extraction kit can be used especially when FF samples are not available.</li> </ul>
<b>Morphology</b>	<ul style="list-style-type: none"> <li>• Have poor quality in histomorphology.</li> </ul>	<ul style="list-style-type: none"> <li>• Considered as best in morphological preservation.</li> </ul>
<b>Immunostaining</b>	<ul style="list-style-type: none"> <li>• More preferred over the FFPE</li> </ul>	<ul style="list-style-type: none"> <li>• Can be used if much more standardized methods is applied.</li> </ul>

Information extracted from (Lüder Ripoli et al., 2016, Geneticist, 2018).

### **3.3 Issues of standardisation and the use of antigen retrieval**

The standardisation of immunohistochemistry is essential to allow comparison between studies through the application of the same protocol over time and different laboratories. It includes several variables, antibodies and reagents, technical processes and interpretation (Burry, 2011; Ramos-Vara, 2005).

Perhaps the most challenging issue is the unknown adverse influence of fixation and processing of the paraffin-embedded tissue. Formalin fixation influences tissue antigenicity, which is dependent on the total time of fixation (Werner et al., 2000). It is usually hard to standardize the immunostaining process; the antigen retrieval (AR) technique can be used to help standardize immunohistochemistry on archival FFPE tissue sections (Shi et al., 2007). AR, by definition, is a process used to retrieve the antigenicity of tissue sections that were obscured by formalin fixation (Shan-Rong Shi, 2001).

Immunohistochemical methods with AR are now applied to FFPE tissue for almost all diagnostic work in pathology and many research studies (Shi et al., 1997; Gown, 2004; Taylor, 2006).

Many variables contribute to the effect of AR on diagnostic pathology (Shi et al., 2007). First, AR critically facilitated immunohistochemistry use of FFPE tissue, maintaining the use of current morphological criteria. Secondly, the value of archival FFPE blocks of tissue has been increased, offering resources for clinical and basic research (Shi et al., 2011). Third, AR is a secure, cheap, and efficient method that results in satisfying immunostaining (Yamashita, 2007). AR has, therefore facilitated the use of FFPE tissues. A standard AR method is the application of heat to tissues, the use of heat to reverse changes

produced by formalin on protein structure has revolutionized immunohistochemistry and dramatically increase the number of antibodies used in FFPE tissues (Ramos-Vara and Beissenherz, 2000). Probably the primary impact of heat is the disruption of protein-protein cross-links (McNicol and Richmond, 1998). In addition, tissue-bound calcium ions and other divalent cations may also be chelated or precipitated using heat and a buffer in the AR solution (Morgan et al., 1994). Different heating devices have been used, including pressure cookers, microwave ovens, steamers and water baths (Taylor et al., 1996). These different heating methods produce similar results provided that optimal incubation time in the heated solution is used (Taylor et al., 1996). However, for specific antigens, heat treatment does not improve but may even reduce their detection (Syrbu and Cohen, 2011). A study by Ramos et al. (2000), using different AR methods on various human tissues with 63 antibodies concluded that many antibodies benefit from the use of AR. It was evident that consideration of the sources (supplier and type) of antibodies was important as different sources of antibodies might change the conditions of optimal AR for several reasons (Ramos-Vara and Beissenherz, 2000).

### **3.4 Analysis of genetic material**

Genetic diagnosis methods, including fluorescence *in situ hybridization* (ISH), are essential for routine pathological examination as gene abnormalities could be observed in the affected patients (Ikeda, 2018). Traditional RNA *in situ hybridization* is not commonly used because of the high technical complexity (Cassidy and Jones, 2014), the RNAscope method instead, is a significant

advancement in RNA ISH technology that addresses the challenges of traditional RNA ISH (Wang et al., 2014a, Wang et al., 2014b, Wang et al., 2012) (**Figure 3.2**) shows the principles of the RNAscope technique, and protocol. This method makes a unique signal amplification approach that enables the visualization of target RNAs as dots, where each dot represents an individual RNA molecule. Previous studies have shown that nucleic acids can be extracted from FFPE components (Hewitt et al., 2008), although, the genetic material isolated from these FFPE blocks is generally of low quality because considerable RNA degradation can occur before the formalin fixation process is completed (Specht et al., 2001, Doleshal et al., 2008). However, the development of RNA-based assays from FFPE tissue is practicable and could be considered as an alternative to immunostaining for FFPE. More considerable attention to tissue handling and processing is essential to improve the quality of bio-specimens for the development of robust RNA-based assays which requires intensive testing of alternative protocols to ensure that these assays function as designed (Lim et al., 2010).

Since HD fresh tissue samples are not readily available, the ability to use archived tissue could be of significant benefit.

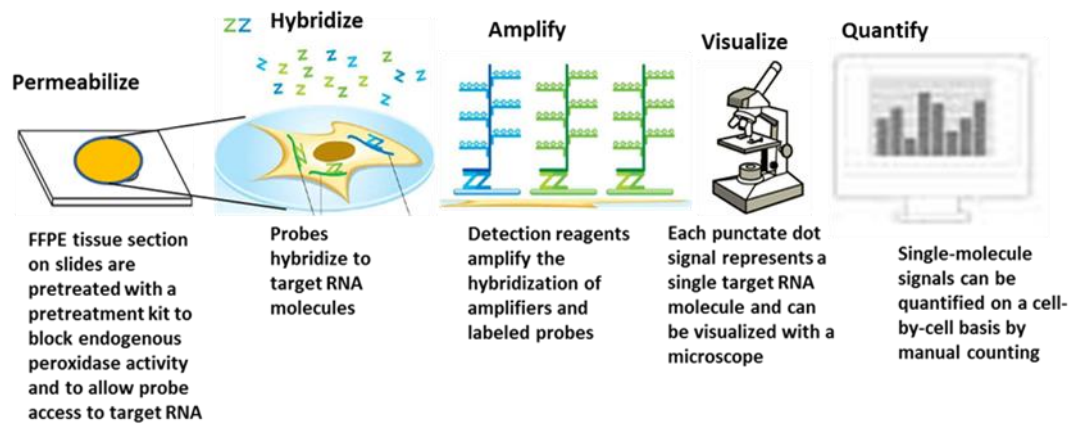


**Figure 3.2** The main steps of the RNAscope protocol.

### 3.5 Aims and objectives

The purpose of this study was to explore a method by which immunofluorescent staining for IC could be applied to FFPE sections from HD to demonstrate cellular or tissue-specific antigens that mark ICs. To unmask the immunoreactive sites of antigens, different antigen retrieval methods were tested. In addition this study, sought to obtain the best result for a specific antigen. Further, the use of *in situ hybridisation* to localise mRNA encoding HD relevant proteins was tested in FFPE tissue.

## **3.6 Material and methods**

### **3.6.1 Formalin-fixed paraffin-embedded (FFPE) archived samples**

Human archived tissues from patients diagnosed with HD (n=15) were obtained from the histopathology department at St James NHS hospital with ethical approval (14/NS/0018, NHS/HSC). Archived FFPE samples were collected and processed from patients aged 6 weeks to 1 year. Tissue blocks were sectioned at 5-20  $\mu\text{m}$  thickness using a microtome (Leica RM 2155) and placed in a 40°C water bath before mounting on poly-L-lysine coated slides and drying overnight.

### **3.6.2 Preparing FFPE sections for immunostaining**

The staining obtained with four antibodies, cKit, Ano1, PDGFR $\alpha$  and SK3 details in (**Table 2.2, Chapter 2**) were compared in fresh and archived HD samples. For the FF samples, the protocol for fixation and processing was established in the previous chapter, in brief, fresh tissue was collected from the theatre in PBS, fixed for 10 minutes in AE, washed in PBS then incubated in the 10% and 20% sucrose for 10 and 30 minutes respectively. FFPE slides were deparaffinised in two fresh xylene washes of 5 minutes each. After that, sections were rehydrated by double incubation in 100% ethanol for 10 minutes each, followed by double incubation in 95% ethanol for 10 minutes each. Finally, slides were incubated twice in dH<sub>2</sub>O for 5 minutes each. Before antibody staining, three different AR solutions were tested by applying them to the different sections to determine the most effective antigen retrieval solution in FFPE samples for the target antigens. For citrate-based AR, samples were boiled in 10 mM sodium citrate buffer (pH 6.0) and maintained at just below boiling temperature (90°C) for at least 20 minutes, then cooled at room

temperature (RT) for 30 minutes. For Ethylene Diamine Tetra Acetic acid (EDTA) solution, slides were incubated in 1 mM EDTA (pH 8.0) at boiling temperature for 20 minutes. For sodium borohydrate, the sections were incubated in 0.1% sodium borohydride for 10 minutes at RT, after AR incubations the sections were washed twice in 0.1M PBS for 5 minutes each.

### **3.6.3 Immunofluorescent staining**

Similar steps were used for immunofluorescent staining of both fresh and archived tissue samples, except for antibody dilutions as described below.

Generally, the FFPE sections used more concentrated primary antibody (1:50) compared to the fresh sections (1:200). The sections were incubated in donkey serum (1:10 PBS) for 20 minutes at RT to block non-specific antibody binding, then washed twice with 0.1 M PBS for 5 minutes. Primary antibodies were diluted in 0.1 M PBS containing 0.1% Triton (PBST) and incubated overnight at RT. Sections were then washed three times for 10 minutes each in 0.1 M PBS and incubated at RT for 2 hours with secondary antibodies. Sections were washed three times for 10 minutes in 0.1 M PBS and mounted in Vectashield Mounting Medium with DAPI (Vector Labs, UK).

### **3.6.4 Chromogenic DiaminoBenzidine (DAB) staining**

Archived FFPE sections were stained using DAB for the PDGFR $\alpha$ , SK3 and SV2 antigens. After deparaffinization and AR steps, sections were incubated in 3% hydrogen peroxide (H<sub>2</sub>O<sub>2</sub>) for 10 minutes, to block endogenous peroxidase activity. Thereafter, sections were washed in 0.1 M PBS for 5 minutes and incubated with donkey serum for 20 minutes at RT. Primary antibodies were diluted and incubated overnight at RT in a humidified chamber and washed in

in 0.1 M PBS three times for 5 minutes each. Then sections were incubated with the biotinylated secondary antibody (1:500) for 2 hours at RT and washed with 0.1M PBS and incubate with extra-avidin (1:1000) overnight. After incubation, slides were washed twice with 0.1 M PBS buffer for 5 minutes each before incubation with DAB which was monitored 1-10 minutes generally 3 minutes. Sequentially, sections were washed for 5 minutes with 0.1 M PBS buffer, counterstained for 30 seconds with hematoxylin and washed for 5 minutes with running water. Finally, the sections were dehydrated in 95% ethanol for 3 minutes, followed by three wash in 100% ethanol for 3 minutes and two wash in xylene for 5 minutes. Sections were mounted using DPX under glass coverslips, workflow for FFPE immunostaining is summarized in **(Figure 3.3)**.

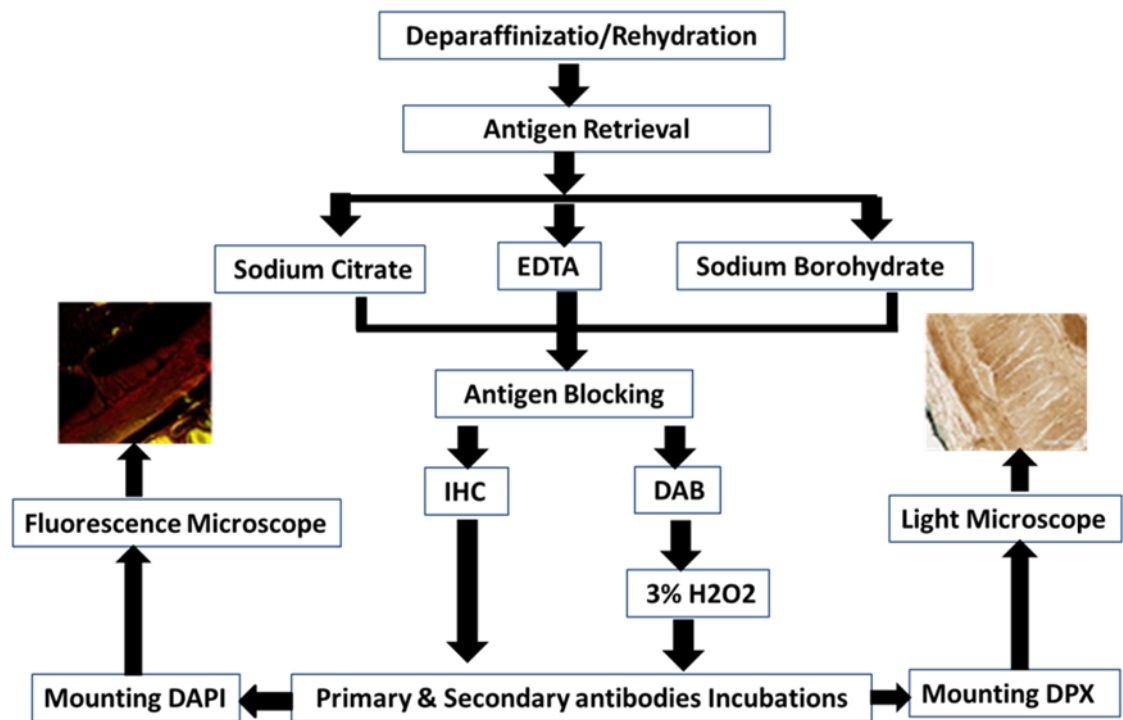


**Figure 3.3** Flow chart of the work flow of the immunostaining steps using FFPE samples.

Quantitative evaluation of ICs were performed using ImageJ software as described in the previous chapter, images were taken by Zeiss LSM 880 confocal microscope (Zeiss Micro Imaging, Germany) using 40 x objective. The chromogenic immunostained slides were scanned with the virtual pathology scanning system in the histopathology department. Results of quantification were expressed as mean  $\pm$  SD.

### **3.6.5 *In Situ Hybridisation (ISH) using RNAscope technique***

Archived FFPE tissue sections were deparaffinised in fresh xylene twice for 5 minutes each, then in 100% ethanol twice for 1 minute each and dried for 5 minutes at RT. For pre-treatments, sections were incubated in H<sub>2</sub>O<sub>2</sub> for 10 minutes at RT and washed in dH<sub>2</sub>O for 15 seconds. Next, sections were incubated in the target retrieval solution (supplied by the ACD Company) for 15 minutes at boiling temperature and washed with dH<sub>2</sub>O for 5 seconds. Sections were incubated with 100% ethanol for 5 seconds and air-dried. Finally, sections were incubated with protease plus for 30 minutes at 40°C, washed with dH<sub>2</sub>O and air-dried before hybridisation. For hybridisation stage, the sections were incubated with the target probe for 2 hours at 40°C followed by washing twice for 2 minutes with buffer (supplied by the ACD Company). In the amplification stage amplifier solutions (amp1-amp6) were used for different times and temperatures. In-between these steps, the sections were washed twice with washing buffer for 2 minutes. Finally, the mRNA signal was detected by fast red chromogenic staining and visualized by light microscope and quantified according to manufacturer scoring system, **(Figure3.4)** shows the workflow steps of RNAscope.

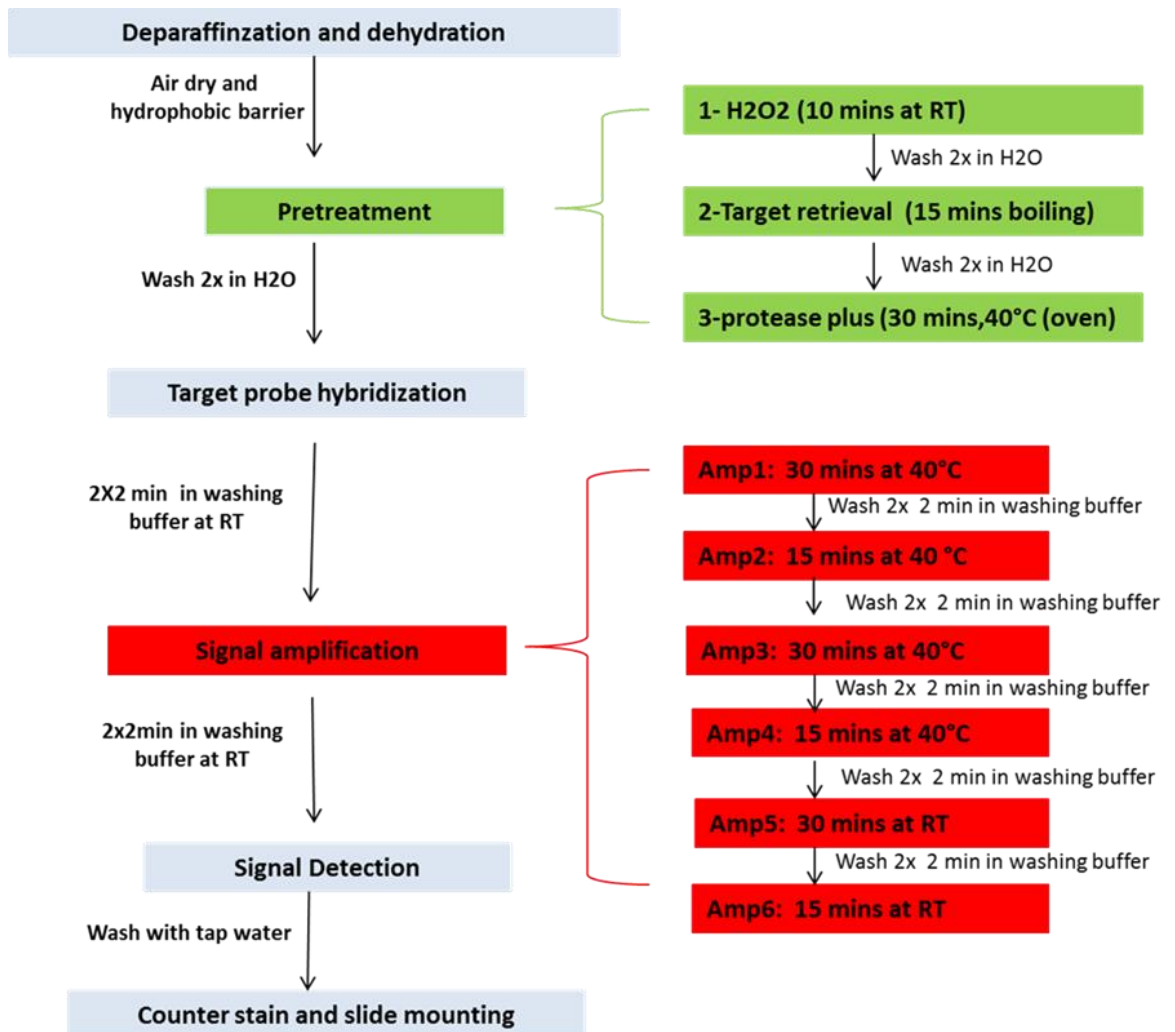


**Figure 3.4 Flow chart of the main working steps of the RNAscope.**

The steps include the deparaffinization, pre-treatment steps which involve 3 sub-steps, target probe hybridization, signal amplification steps include 6 steps of amplifiers which used a series of oligonucleotide probes to amplify the target signals, the detection of the signal by using fast red reagent for 10 minutes at RT and finally the counter stain step with 50% Haematoxylin for 2 minutes at RT and mount the section with mounting media. The whole experiment took approximately 6 hours to finish.

### 3.6.6 Quantification of the RNA expression

The RNAscope assay can enhance the *in situ hybridization* outcomes by allowing a semi-quantitative scoring guideline based on the estimated amount of dots present within each cell (**Table 3.2**).

**Table 3.2 Semi-quantitative assessment of RNAscope staining**

Staining Score	Microscope Objective Scoring
0	No staining
1	1-3 dots /cell
2	4-10 dots/cell
3	>10 dots/cell

## 3.7 Results and conclusion

### 3.7.1 Antigen Retrieval and immunostaining of FFPE

The intensity of the immunostaining of specific IC protein markers was evaluated in HD archived FFPE tissue under the influence of three different types of AR, namely, citrate, EDTA and borohydrate, including different temperatures. In general, without AR, there was no distinct cell labelling in the wall of the colon along the whole section, even though ganglia were present (**Figure 3.5 C**). By contrast, with the use of water-bath heating buffers (sodium citrate, EDTA) some IC processes were visible running around the MP in case of citrate-based buffer (**Figure 3.5 D**) and in between the smooth muscle cells of the colon wall musculature for EDTA (**Figure 3.5 E**). Labelling was most visible in citrate-based AR, but least apparent in the EDTA approach. Borohydrate AR methods, on the other hand, which does not involve heating,

gave less immunostaining intensity (**Figure 3.5 F**). Immunolabelling was enhanced by heating. However, higher temperatures sometimes results in tissue destruction, and many times the tissue fell off the slides. Heating was therefore applied for less than 30 minutes.

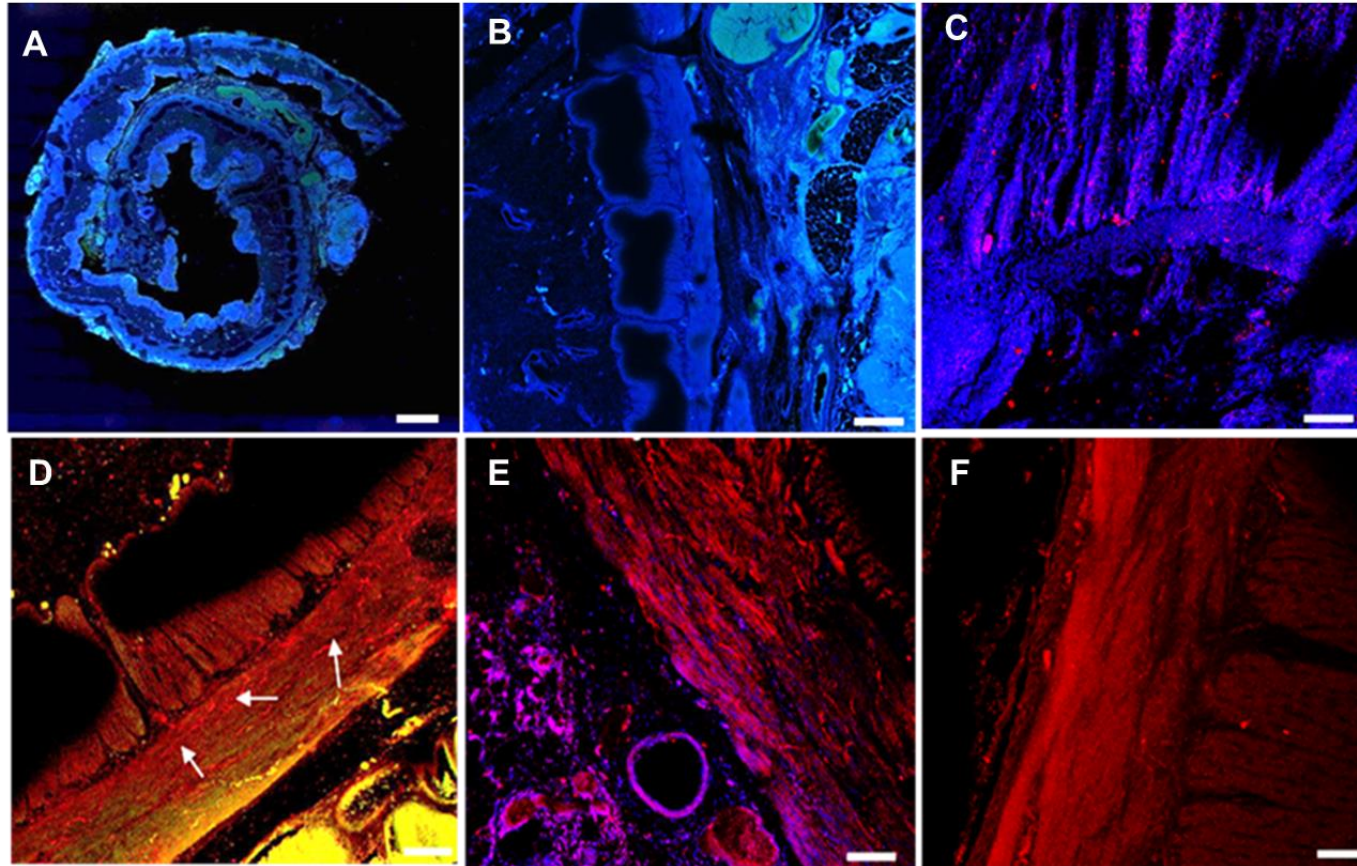


**Figure 3.5 Immunofluorescence staining for cKit in FFPE using different antigen retrieval solutions.**

The whole section of FFPE samples scale bar 7mm (**A**). Control section with no primary antibody (**B**). Section stained with primary antibody but not antigen retrieval (**C**). Citrate based antigen retrieval, arrows indicate cKit+ ICs in between the smooth muscle cell layer (**D**). EDTA antigen retrieval (**E**). Borohydrate antigen retrieval (**F**). Scale bar 20  $\mu\text{m}$ .

### 3.7.2 Immunoperoxidase chromogenic immunostaining

Immunoperoxidase immunostaining was performed on FFPE based on the standard Avidin-Biotin complex (**Figure 3.6**), showed positive immunoreactivity of the antibodies tested against PDGFR $\alpha$  and SV2 (synaptic vesicle protein marker), illustrating the viability of archived FFPE tissue samples to the chromogenic immunostaining as well as the fluorescence immunostaining.

When comparing FFPE with fresh tissue for which the protocol was established in the previous chapter, the concentration of the primary antibodies regularly employed in our laboratory was changed as the working concentrations for the FFPE frequently were more concentrated than the dilution supplied by the manufacturer.

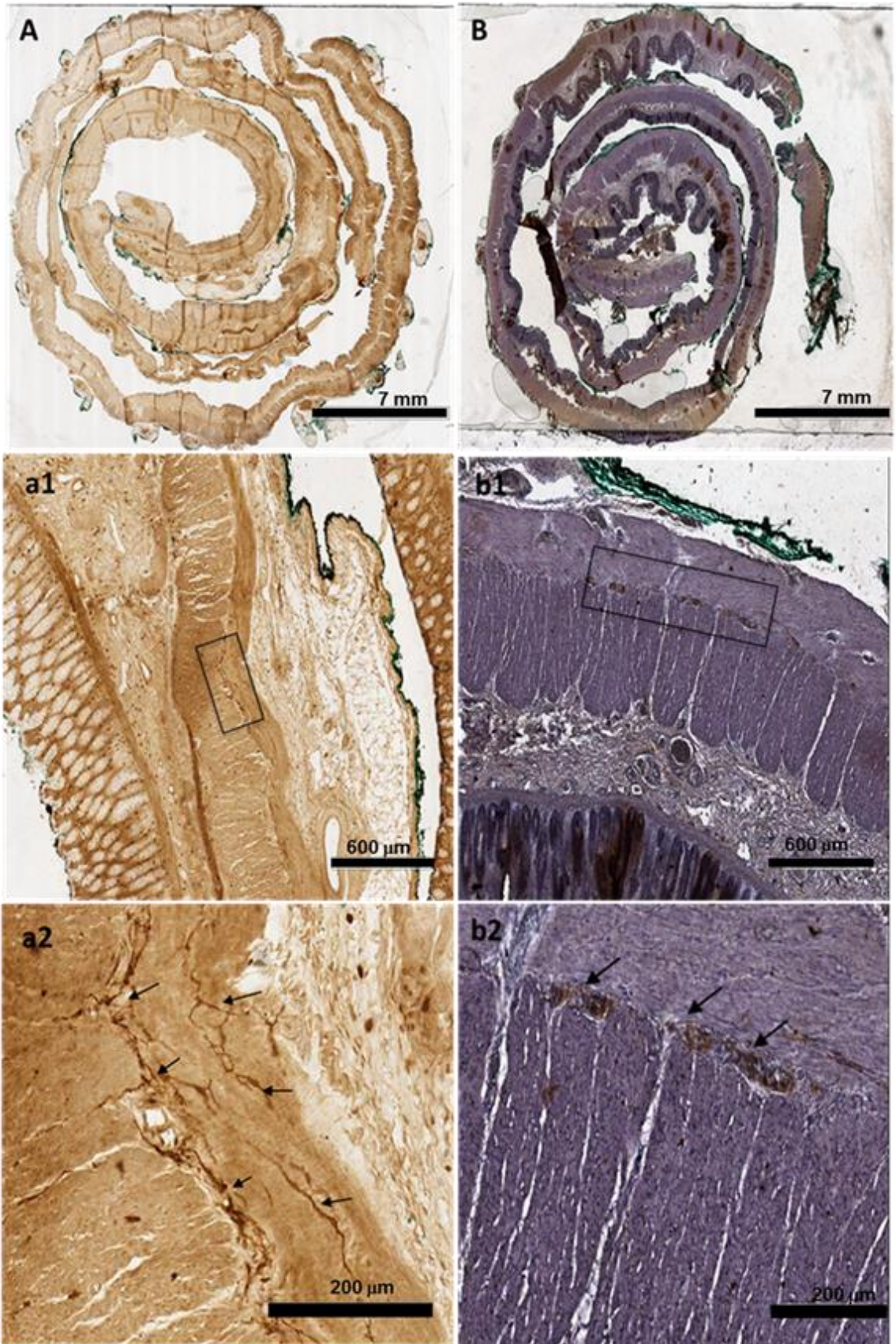


**Figure 3.6 Chromogenic immunostaining of FFPE sections.**

Immuno-peroxidase technique used to stain PDGFR $\alpha$  (A) and SV2 (B). Scale bars for the whole sections 7mm, for the magnified sections 600  $\mu\text{m}$  (a1,b1). Arrows indicate PDGFR $\alpha$ <sup>+</sup> cells (a2), ganglion between the circular muscle (CM) layer and longitudinal muscle (LM) layer (b2), scale bar 200  $\mu\text{m}$ . Sections were scanned with virtual pathology scanning system in the histopathology department facilities.

The difference in the immunofluorescence between the two tissues was statistically significant when quantifying using image J counting cells per unit area ( $\text{mm}^2$ ) and analysed using GraphPad prism two-way ANOVA, numbers expressed as mean  $\pm$  SD) (FF  $170 \pm 10$ , FFPE  $105 \pm 2$ ) (**Figure 3.7**) (**Figure 3.8**). However, in FFPE, the immunofluorescence staining of the IC did not clearly outline the cell morphology i.e. the cell body and the processes as compared with the fresh tissue in which the cells were more distinct.

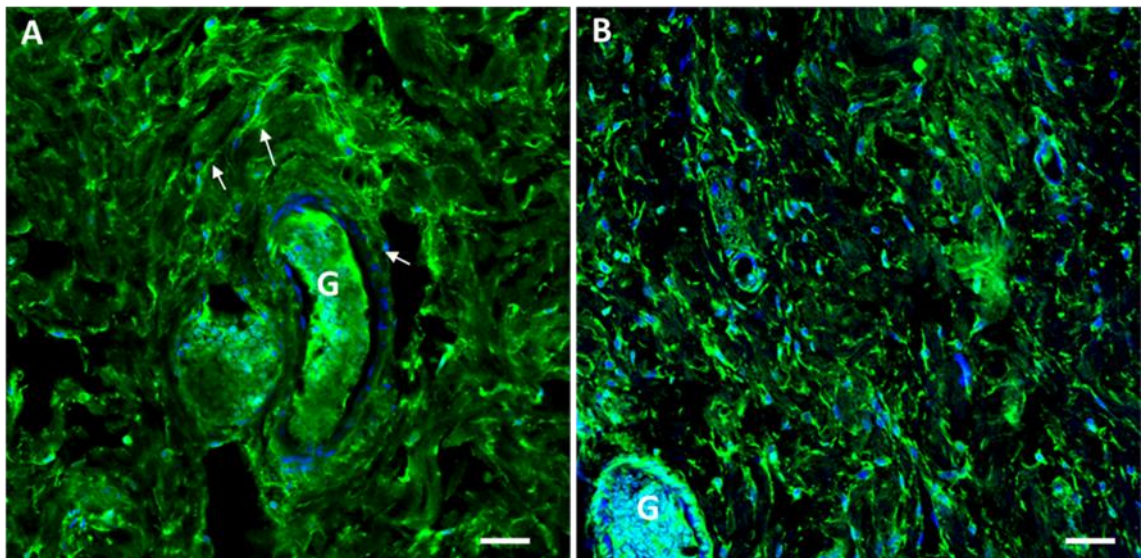


**Figure 3.7 Confocal images of PDGFR $\alpha$ <sup>+</sup> cells in fresh fixed tissue and FFPE tissue.**

Acetic ethanol fixed tissue (A) and FFPE tissue from patient with Hirschsprung Disease (B). Arrows indicate positive ICs with processes around the ganglion (G) Scale bar 20  $\mu\text{m}$ .

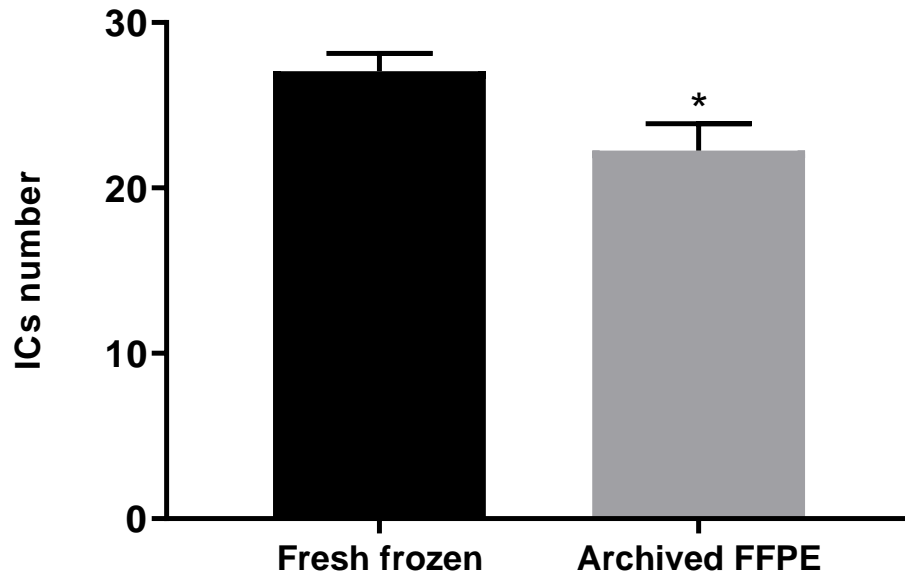


**Figure 3.8** The statistical difference in the numbers of ICs in two different tissue types,\* P=0.013.

### **3.7.3 RNAscope *In Situ* Hybridisation (ISH)**

In situ hybridisation using RNAscope technique was performed on FFPE tissue.

The stained slides were visualised under a standard bright-field microscope (with chromogenic labels); the slides were scanned using virtual pathology scanning services at St. James's University Hospital / UK. The results showed score 3 according to ACD scoring system (**Table 3.2**) (**Figure 3.9**).

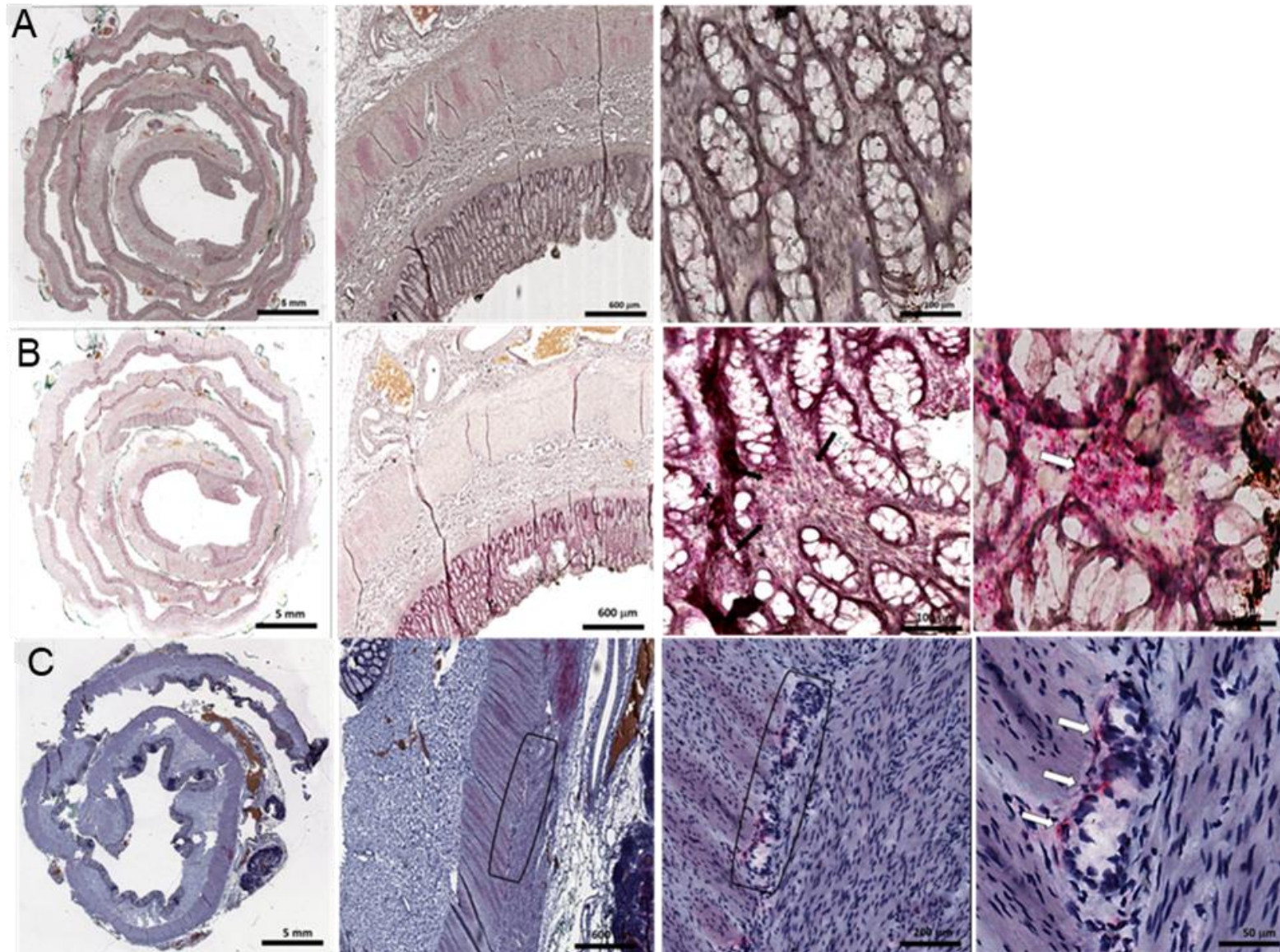


**Figure 3.9 RNAscope detection of mRNA for Kit gene in FFPE Hirschsprung disease samples.**

Negative control probe (bacterial gene *dapB*) shows no staining (**A**) top row scale bars (5 mm, 600  $\mu\text{m}$  and 100  $\mu\text{m}$ ). The positive control probe PPIB (peptidylprolyl isomerase B) shows a considerable number of red dots scattered in the epithelial layer (**B**) middle row scale bars (5 mm, 600  $\mu\text{m}$ , 100  $\mu\text{m}$  and 50  $\mu\text{m}$ ) which represent the amount of mRNA for PPIB gene. Target probe for cKit showed score 3 stainings scattered around the myenteric plexus selected area (**C**) bottom row scale bars (5 mm, 600  $\mu\text{m}$ , 100  $\mu\text{m}$  and 50  $\mu\text{m}$ ). Arrows indicate the positive dots staining reflecting mRNA. The images were taken using virtual pathology scanning software.

### **3.8 Discussion**

The use of archived tissue could have a significant impact on the current investigations into the numbers and distributions of ICs in HD human samples. The objective of this research was, therefore, to examine whether FFPE human colon samples from HD patients are appropriate for precise identification and reliable counting of immunolabeled ICs or even RNA around the MP region in the colon wall. While detection of protein and RNA was possible in FFPE tissues, it was not sufficiently robust for current investigations.

#### **3.8.1 Immunostaining of FFPE archived HD samples**

The ability to analyse archived FFPE tissue presents a valuable opportunity for research but has significant technical challenges including formalin fixation which form cross-linking between proteins, duration of tissue fixation, age and storage condition of the FFPE blocks (Kresse, 2018) all these could lead to issues with further applications. Although some success was found in our study, including the first localisation of RNA for cKit in FFPE human colon. However, we did not overcome the challenges sufficiently, to enable the use of FFPE tissue in research laboratory the protocols for immunostaining of FFPE must efficiently be designed and use proper antigen retrieval solutions with the right concentrations of primary antibodies.

Indeed, the mechanisms that influence antigenicity preservation and loss have not been well characterized and remained unclear (Xie et al., 2011). Many different possibilities could vary to enhance this staining. Several factors could affect the suitability of FFPE tissues for immunostaining; these include, tissue

fixation time, processing steps of deparaffinization and the storage conditions as the temperatures and humidity of the environments in addition to the application of immunostaining (Otali et al., 2009, Engel and Moore, 2011). Furthermore, a few studies observed that long term storage of FFPE do not affect the immunostaining properties and the mRNA levels, most studies reported that immunostaining was affected by the storage periods of the FFPE blocks (Wester et al., 2000). However, these studies are contradictory regarding the time of storage, a significant reduction in estrogen receptor immunostaining after only few weeks of storage (Bromley et al., 1994), whereas other studies reported that immunostaining was only affected after several months (Bertheau et al., 1998) or even years of storage (Shin et al., 1997). The main goal of this study was to find an approach for using the archived tissue regardless of storage time, so we did not test for the effect of varying duration of fixation or of storage.

Since different antigens may require specific adjustments to AR protocols (Pileri et al., 1997), several approaches were investigated. Widely established AR techniques that are currently employed by pathologists worldwide were tested, including different buffer solutions such as citrate and EDTA. For example, Long and Buggs (2008) tested three different buffer solutions for AR with heating in a microwave oven these buffers namely (100 mM Tris, pH 10, 0.05% citraconic anhydride, 10 mM citrate with 2 mM EDTA and 0.05% Tween 20 pH 6.2) and attained adequate immunostaining outcomes for all three AR solutions (Long and Buggs, 2008). Jiao et al. (1999) successfully tested multiple immunostainings in FFPE tissue sections by using 10 -50 mM sodium

citrate buffer at pH 8.5 -9.0, heating at 80°C in a water bath for 40 minutes (Jiao et al., 1999).

The current research provides further support for the usefulness of citrate-based AR solution by demonstrating significant exposure of many relevant antigens. Our results with citrate-based AR in FFPE samples parallel that previously reported in the literature (Chargin et al., 2016; Delcambre et al., 2016; Grafen et al., 2017). The study by Ippolito et al. (2009) concluded that FFPE human gut samples could be regarded as valid samples to estimate the numbers and proportions of neurons and glial cells within MP area, they used microwave heating citrate solution as AR method (Ippolito et al., 2009). From a practical point of view, one of the most difficult issues in the optimization of immunostaining in FFPE tissues is the effect of formalin fixation on immunostaining, however, to minimize the variation of immunostaining in FFPE tissue samples AR protocols should be optimal. (Shi et al., 2007). In addition, many studies revealed comparable immunostaining results between frozen and FFPE tissue sections following AR (Shi et al., 2008).

### **3.8.2 Detection of RNA in FFPE tissue**

In addition to immunohistochemistry, RNA *in situ hybridization* is widely used in clinical settings to assess mRNA biomarkers. However, RNA analysis remains limited due to the high degree of clinical complexity of current RNA *in situ hybridization* techniques. To date, the use of RNA *in situ hybridization* in clinical diagnostics has been limited to highly expressed genes and certain medical conditions (Gulley, 2001, Ambinder and Mann, 1994, Mahmood and Mason, 2008). Here, the use of RNAscope was described, a novel RNA *in situ*

*hybridization* targeting cKit mRNA in Hirschsprung disease FFPE archival tissue from tissue bank in histopathology department stored for several years, this new RNAscope in situ hybridization technique could sensitively detect the target RNA, to the best of our knowledge this is the first approach toward the use of this advanced method in FFPE from HD archived tissue. While cKit mRNA could be detected, it was not sufficiently robust to allow comparison across tissues because cKit labelling was present only in patches and at low levels. However, the presence of RNA does offer some hope that ICs could be extracted from the archived tissue, for example using laser capture microdissection (Coudry et al., 2007), and subjected to sensitive approaches such as RNAseq. The methods are emerging in application of FFPE tissue (Chan et al., 2013; Hedegaard et al., 2014). However, further development will be required for RNAscope to be applied as a quantitative marker for ICs as required for this study.

### **3.9 Conclusion**

Archived FFPE tissue did not provide sufficiently robust immunolabelling or mRNA detection for comparison across laboratories. This is the basis for further development since there were some antibody labelling and hints of success with RNAscope. However, FF tissue provides far superior labelling and should, therefore, remain the choice approach to investigate IC morphologically.

## Chapter 4 cKit<sup>+</sup> and PDGFR $\alpha$ <sup>+</sup> Interstitial Cells in Hirschsprung Disease

### 4.1 Introduction

Intestinal motility has both central and enteric nervous system controls that overlap and interact with each other but are not directly controlled by the central nervous system (Olsson and Holmgren, 2001). The normal peristaltic and segmental motor activity requires co-operation between the musculature, ENS and ICs (Huizinga, 1999, Huizinga et al., 2001). Gastrointestinal motility, therefore, depends on more than just intact ganglionated nerve networks, it also requires IC networks (**Figure 4.1**).

The Interstitial Cells are pacemaker cells organized in networks located in all layers of the colon wall (**Figure 1.3, Chapter1**). Both networks of ICs and ENS control the movements of the colon and generate the motility patterns, commonly known as peristalsis (Zhu et al., 2014). This in turn moves the intestinal content toward the end of the colon through the contraction of the intestine in the proximal section and relaxation in the distal portion of the given segment of the colon located around the bolus (Kumral and Zfass, 2018).

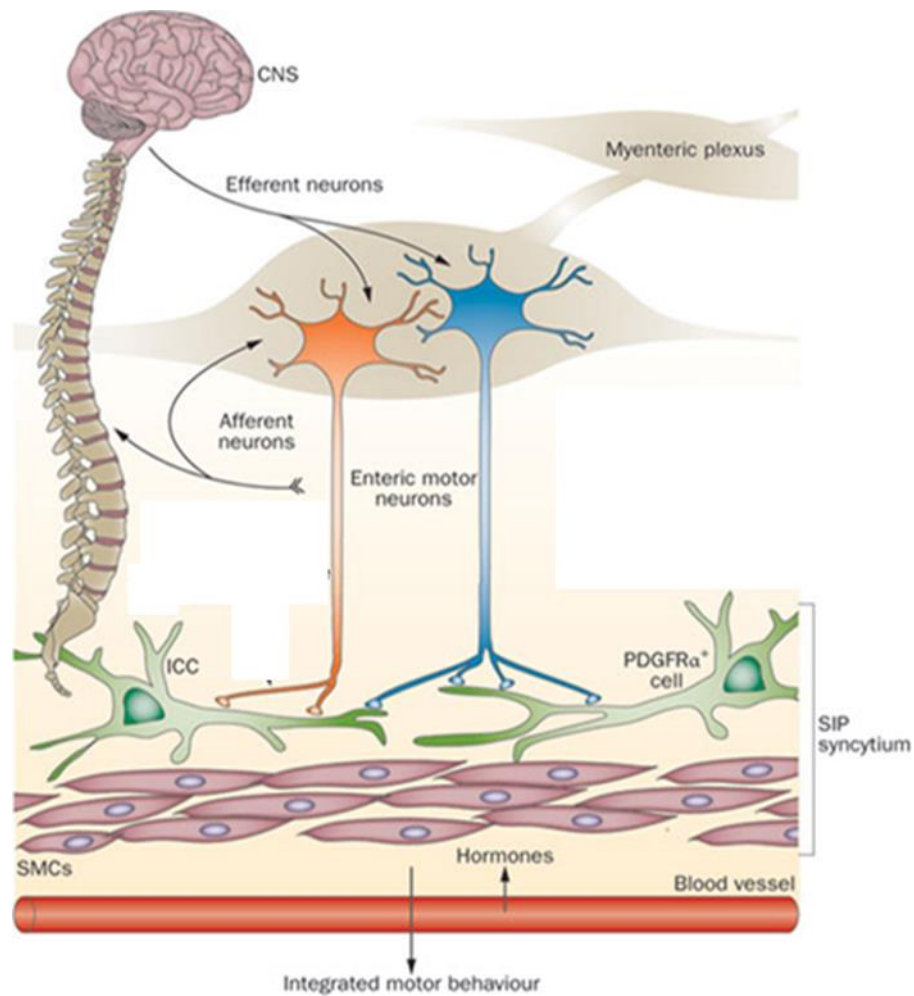


**Figure 4.1 Regulation of gut motility, schematic drawing shows the interaction between the CNS and the ENS with the ICs (Sanders et al., 2012a)**

Contractions of the muscle layers of the intestine have two distinct sources; myogenic and neurogenic. The myogenic smooth muscle contraction is driven primarily by the ICs in close interaction with SMCs (Der-Silaphet et al., 1998), the neurogenic control comes from the vagus nerve (Travagli et al., 2006), and the neurons located at the MP (Mao et al., 2006).

In the MP, there are three types of neurons classified on the bases of their function and electrical behavior. The first type is the sensory neurons and are thought to be responsible for the initiation of peristaltic reflex (Furness, 2012,

Furness et al., 2013). The second type is the motor neurons which are directly responsible for the contraction (excitatory motor neurons) or relaxation (inhibitory motor neurons) of the smooth muscle layers. The third type of neurons are located mainly within the ganglia and are the interneurons which mediate the communication between sensory and motor neurons (Costa et al., 2000), however any myenteric neurons will be considered and not specific neuron subpopulations, as this is beyond the purpose of this study and will not be used.

In research using mechanical stimulation of the gut lumen, electrical responses were detected in MP neurons; the idea is that the initiation of the peristaltic reflex is caused by luminal distention and sensed by MP neurons. Mao and his group recorded from MP neurons using a mouse longitudinal muscle preparation with patch-clamp and sharp intracellular electrodes; all neurons possessed a hyperpolarization-activated current that was blocked by extracellular cesium (a blocker of the hyperpolarization-activated cationic current) (Mao et al., 2006). Nevertheless, motor patterns in the gut can be observed in the presence of neuronal action blockers like Tetrodotoxin (TTX), and these patterns can be modified using drugs targeting SMCs and ICs (Huizinga et al., 2011). This research demonstrates that gut motility can be controlled by overlapping neurogenic and myogenic processes of contraction (Zhu et al., 2014; Huizinga and Lammers, 2009).

The contractions of the smooth muscle in the gut wall are driven by oscillatory changes in membrane potential known as slow waves; this spontaneous activity is myogenic in origin because the neural blocker TTX does not block

them. Confirmation was obtained in canine colonic circular muscle strips where intracellular microelectrode recording revealed a characteristic slow-wave activity in cells identified as IC by morphological appearance (Barajas-Lopez et al., 1989).

The anatomical relationship between cKit<sup>+</sup> ICs, PDGFR $\alpha$ <sup>+</sup> ICs located close to the MP and SMCs (functional syncytium unit SIP), is believed to be participating in the generation of slow waves through a mechanism involving distinct ion channels generating rhythmic membrane potential (Parsons et al., 2011). These membrane potentials in ICs evoked Ca<sup>2+</sup> changes in the SMCs through gap junctions (**Chapter 1, Section 1.11**). The role of cKit<sup>+</sup> ICs is to depolarize the smooth muscle syncytium increasing the opening of the voltage-dependent ion channels, which are abundantly expressed in the SMCs. The increase of intracellular Ca<sup>2+</sup> activates Cl<sup>-</sup> channels in the cKit<sup>+</sup> ICs to give STICs which lead to the formation of STD resulting in the slow waves of membrane depolarization. The current flows through the gap junctions to the neighbouring SMCs to activate contraction (**Figure 4.2**) (Berridge, 2008).

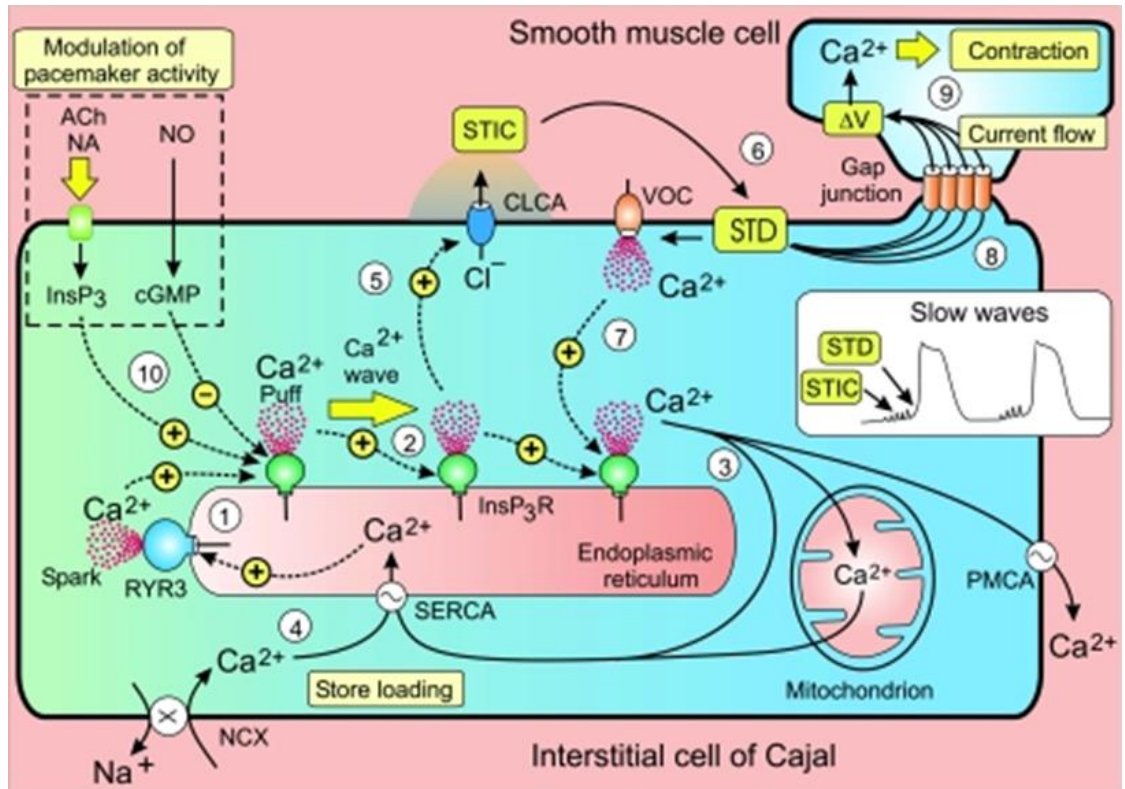


Figure 4.2 The changes in intracellular Ca<sup>2+</sup> levels responsible for pacemaker activity in cKit<sup>+</sup> ICs (Berridge, 2008).

cKit<sup>+</sup> ICs give pulses of Ca<sup>2+</sup> that form Ca<sup>2+</sup> waves. The release of Ca<sup>2+</sup> from the intracellular store (endoplasmic reticulum) through RYR3 and InsP3R (labelled 1, 2 in Figure) leads to an increase in the intracellular Ca<sup>2+</sup> levels. To maintain the normal Ca<sup>2+</sup> homeostasis, the extra Ca<sup>2+</sup> will be taken by the mitochondria or released out of the cells through the PMCA plasma membrane transporter or reuptake by SERCA pump to the endoplasmic reticulum (labelled 3). Ca<sup>2+</sup> exchanged with Na<sup>+</sup> through NCX could also contribute to the increase of the intracellular Ca<sup>2+</sup> levels (labelled 4). This Ca<sup>2+</sup> gives the STIC which leads to STD (labelled 5, 6), and will cause more Ca<sup>2+</sup> to be entered through VOC which causes more Ca<sup>2+</sup> to be released from the intracellular store (labelled 7). The STD transmitted to the adjacent SMCs through gap junctions (labelled 8) and cause smooth muscle depolarization and muscle contraction (labelled 9). The modulation of pacemaker activity through stimulatory (Ach and NA) by InsP3 pathway or inhibitory (NO) by cGMP pathway control the intracellular Ca<sup>2+</sup> homeostasis (labelled 10). CLCA- Ca<sup>2+</sup> activated Cl<sup>-</sup> channels, RYR3- Ryanodine receptor 3, InsP3R- Inositol trisphosphate receptor, PMCA - plasma membrane Ca<sup>2+</sup> ATPase, SERCA - sarco/endoplasmic reticulum Ca<sup>2+</sup>-ATPase, NCX - sodium-calcium exchanger, STIC - spontaneous transient inward currents, STD- spontaneous transient depolarization, VOC–voltage operated Ca<sup>2+</sup> channel, Ach – acetylcholine, NA- norepinephrine, NO- Nitric oxide, cGMP - Cyclic guanosine monophosphate (Berridge, 2008).

The presence of neurotransmitter receptors in ICs raise the possibility for them to be regulated by neuronal stimulation, as indicated above. In the colon, IC-MP generates rhythmic transient depolarizations that can be related to propulsive patterns in the colonic smooth muscle (Yoneda et al., 2004). The neuronal activation of peristaltic reflex in the colon could therefore, be due to activation of the IC through excitatory neurotransmitters (Costa et al., 2013). Experimentally the effect IC-MP on the peristaltic reflex of the colon was tested by using acetylcholine receptor agonist (carbachol) in the presence of TTX. This revealed that carbachol actively promotes rhythmic activity in cKit<sup>+</sup> ICs (Huizinga et al., 2011). Carbachol stimulates ICs through the downstream activation of Ano1 channels expressed by cKit<sup>+</sup> ICs, and the inactivation of K<sup>+</sup> channels in the plasma membrane of PDGFR $\alpha$ <sup>+</sup> ICs (SK3) these roles modulating the upstroke potential of slow waves and the recovery to resting potential of ICs (Zhu et al., 2011). From this point of view, ICs are considered as an important part of the mechanism of controlling gut motility. The close relationship between ENS and the two different types of ICs (cKit<sup>+</sup> and PDGFR $\alpha$ <sup>+</sup> ICs) raise the possibility that ICs could be involved in the neurotransmission process (Epperson et al., 2000). The present study will provide evidence for histological- relationship to what is called functional syncytium by using double and triple immunolabelling.

Numerous studies report loss or damage to ICs networks in a variety of motility disorders. Altered distribution of ICs have been examined in human intestinal motility disorder due to HD (Vanderwinden et al., 1996, Rolle et al., 2002), with reduced number of ICs consistently detected in the distal (aganglionic)

compared to the proximal (ganglionic) segment of the sample (Barshack et al., 2004). Aganglionosis and severe hypoganglionosis can be due to an abnormality of the ENS (Zhi-Wen Pan, 2012, Toshihide Iwashita et al., 2003). Additionally, the ICs also contribute to the functional disorder of the gut motility.

## **4.2 Aims**

The objective of this research is to assess the anatomical relationship between the two different types of ICs and the enteric neurons in the MP region. A further aim is to compare the distribution of cKit<sup>+</sup> / Ano1<sup>+</sup> ICs, PDGFR $\alpha$ <sup>+</sup> / SK3<sup>+</sup> ICs in HD proximal and distal parts with disease control samples from stoma closure.

### **4.3 Material and Methods**

Ethical approval for the use of human tissue samples was obtained (14/NS/0018, North of Scotland Research Ethics Committee). HD samples (9/14) and stoma closure samples (10/14) were immediately fixed after surgical resection, following the protocols developed in Chapter 2.

#### **4.3.1 Tissue processing for Hematoxylin and Eosin staining**

The specimens were fixed in AE for 10 minutes at RT and rinsed in PBS. Specimen were then incubated in 10% and 20% sucrose solution for 10 and 30 minutes respectively. The samples were subsequently frozen in OCT (FSC 22 clear frozen section compound, Leica) using dry ice. The OCT-embedded specimens were sectioned into 20  $\mu$ m using cryostat (Leica CM1850). Sections were dried for 5 minutes at RT to remove the moisture; the sections were dipped in 0.1% Mayers Hematoxylin (Sigma; MHS-16) for 10 minutes in 50 ml conical tube. The slides were rinsed in cool running dH<sub>2</sub>O for 5 minutes. The sections were dipped in 0.5% Eosin (1.5 g dissolved in 300 ml of 95% ethanol) 12 times, washing performed in dH<sub>2</sub>O till eosin stop streaking. Then a series of ethanol concentration was used 50% 10 times, 70% 10 times, 95% for 30 seconds and 100% for 1 minute finally dipped in xylene (clearing agent; Sigma) several times and mounted using DPX (Thermo-scientific), Sections were visualized using light microscope and imaged using the virtual pathology scanning system and processed by Image Scope software.

### **4.3.2 Immunohistochemical staining**

#### **4.3.2.1 cKit<sup>+</sup> and PDGFR<sup>+</sup> ICs close proximity**

For immunostaining to demonstrate the close anatomical relationship between cKit<sup>+</sup> ICs and PDGFR $\alpha$ <sup>+</sup> ICs sections were washed in PBS, and double-labeled with cKit primary antibody (rabbit polyclonal, Dako 1:200) and PDGFR $\alpha$  primary antibody (goat polyclonal; R&D system; 1:200) overnight at RT after which the secondary Alexa flour donkey anti-rabbit (555, Invitrogen) and donkey anti-goat (488, Invitrogen) was applied for 2 hours at RT, sections were then mounted with mounting media with DAPI and visualized using fluorescence microscopy (Nikon E600). Double staining was also performed between cKit (mouse FITC; Sigma, 1:500) and Ano1 (rabbit polyclonal; Abcam, 1:100), and PDGFR $\alpha$  (goat polyclonal; R & D system; 1:200) and SK3 (rabbit polyclonal; APC-025; Alomone Lab; 1:100) following the same steps of immunostaining mentioned above.

#### **4.3.2.2 cKit<sup>+</sup>, PDGFR<sup>+</sup> ICs and enteric ganglion proximity**

For identifying the functional unit, triple immunostaining was performed for cKit, PDGFR $\alpha$ , with S100 $\beta$  (rabbit monoclonal, Abcam; 1:200) to label ganglia, TuJ1 (rabbit polyclonal, protein tech; 1:500) to label neurons and SV2 (mouse, DSHB; 1:500) to visualize synaptic terminals were tried to see the best staining for the ganglion and neurons of the enteric nervous system and their relationship to the two different types of ICs. Secondary antibodies conjugated to Alexa Flour 555, 488 and 647 were used specifically to the animal in which the primary antibodies were raised.

### **4.3.3 Protein receptor markers of ICs colocalization with the functional ion channels expressed by ICs**

HD samples were stained for cKit, Ano1, PDGFR $\alpha$  and SK3 markers for ICs, staining was performed in the distal part of the sample and compared with the proximal part of the same sample, HD samples were also compared with the DC samples in the three different histological layers namely CM, MP and LM. All images were taken using laser LSM 880 upright confocal microscope (Zeiss Micro-Imaging, Germany). Image analysis and IC quantification were performed using Image J software method explained in details in **(Chapter 2)**.

### **4.3.4 Statistics**

The results are displayed as the mean  $\pm$  SD of the mean. The differences between the IC numbers in different layers were assessed using Unpaired t-test and ANOVA, with the significance set at a p-value of  $<0.05$ . GraphPad (GraphPad Software Inc 7.03) was used to perform the statistical analysis and create graphs.

## **4.4 Results**

### **4.4.1 Hirschsprung disease histopathology confirmation**

The presence and absence of ganglia in the proximal and distal segments of HD colon were tested by the histopathologist using the H & E staining.

Hematoxylin-eosin stained the ganglionic area surrounding the MP between the two smooth muscle layers CM and LM in the proximal part of the HD samples which indicate the presence of MP neurons and considered as normal gut compared to the distal part of the specimen where typical features of

aganglionic bowel in all HD patients show absence of ganglia in MP (**Figure 4.3**).

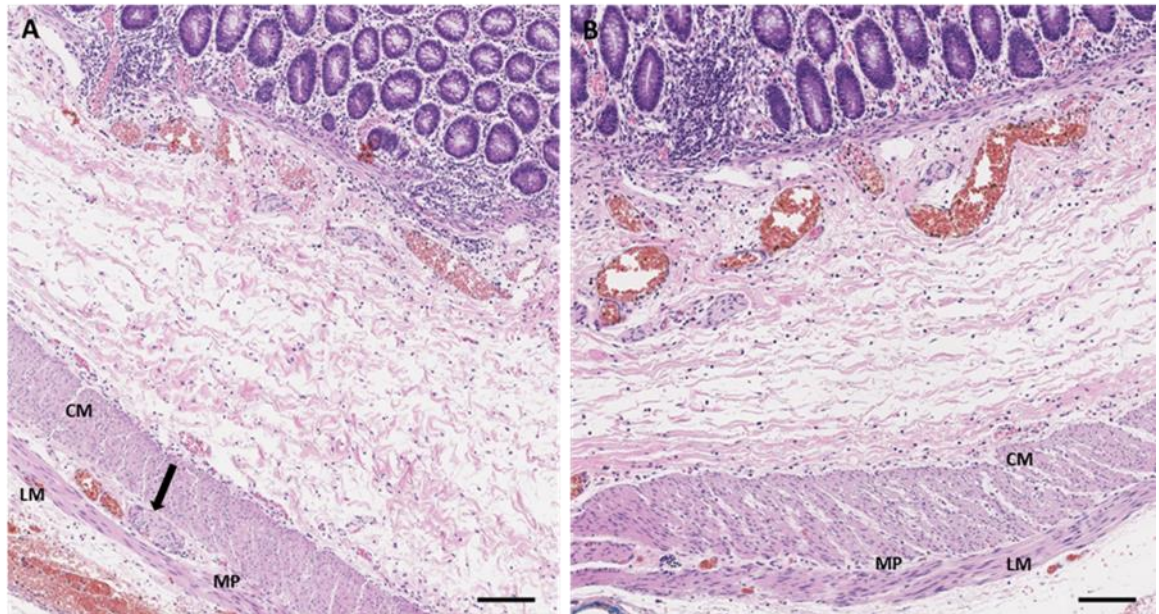


**Figure 4.3 Haematoxylin-Eosin staining of the proximal (A) and distal (B) parts of HD sample.**

In (A) the arrow indicates the ganglionic area in the MP between CM and LM in the proximal part. (B) The complete absence of ganglionic area in the distal part of the sample, which is consistent with the HD diagnosis (aganglionosis). MP-myenteric plexus, CM- circular muscle, LM- longitudinal muscle, scale bar 100  $\mu$ m.

#### 4.4.2 Immunohistochemical staining

Double labelling of cKit<sup>+</sup> ICs and PDGFR $\alpha$ <sup>+</sup> ICs was performed to illustrate the anatomical relationship between the two different classes of ICs. These cells exhibited the morphology of ICs, appearing mainly as thin bipolar cells and forming a network closely related to enteric neurons (**Figure 4.4, Figure 4.5**), as well as being positive for the protein markers cKit and Ano1, PDGFR $\alpha$  and SK3 (**Figure 4.6**). These two different sub-types of IC were seen close to each other (**Figure 4.7**), and to the myenteric plexus (**Figure 4.8**). They were

scattered around the MP and ran in-between the smooth muscle layers, both circular and longitudinal (**Figure 4.9**).

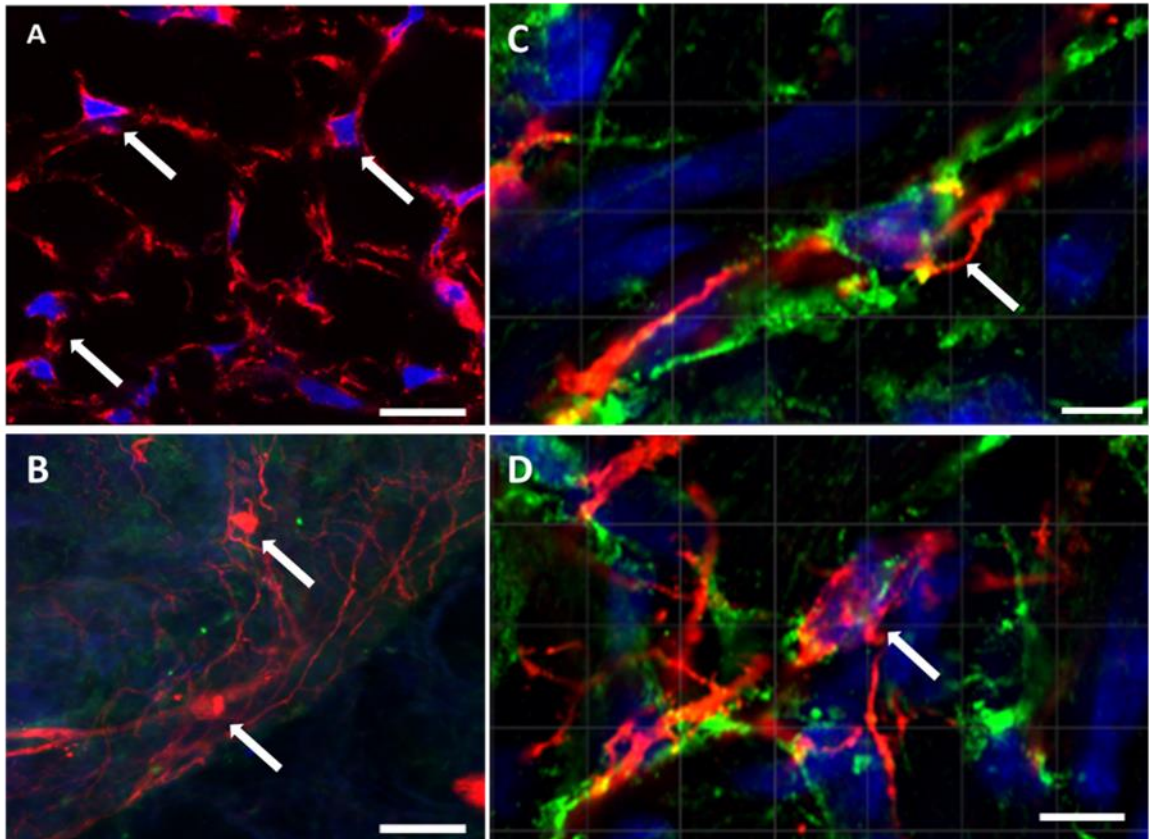


**Figure 4.4 Confocal images of ICs showing the morphological feature of these cells.**

(A) cKit<sup>+</sup> ICs (red) arrows are indicating the cell bodies (DAPI stained) and the intercalated processes that form the network, scale bar 10  $\mu$ m. (B) the highly complicated network formed by the cKit<sup>+</sup> ICs processes in the wall of the colon, scale bar 20  $\mu$ m. (C and D) a closer view shows how ICs (cKit<sup>+</sup> ICs – red, PDGFR $\alpha$ <sup>+</sup> ICs- green) are adjacent and overlap, scale bar 5  $\mu$ m.

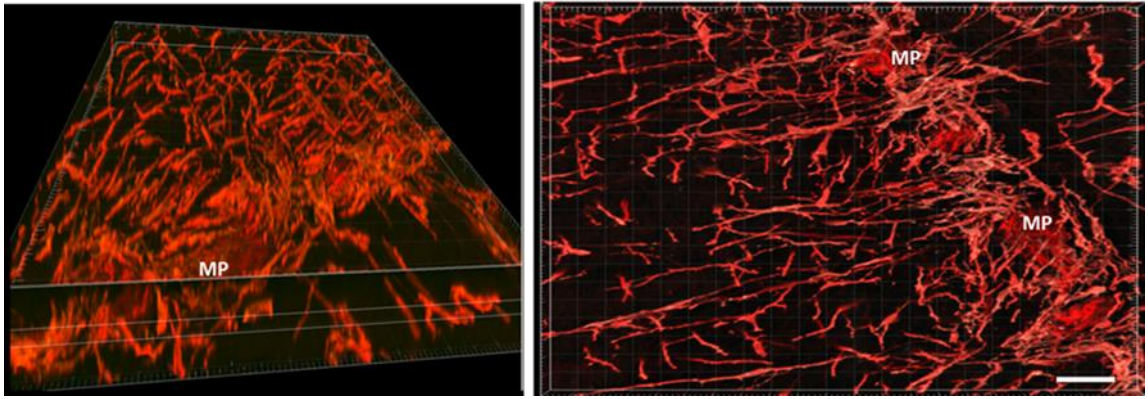


**Figure 4.5** 3D images of cKit<sup>+</sup> ICs show complex networks around the myenteric plexus area (MP), scale bar 50  $\mu$ m

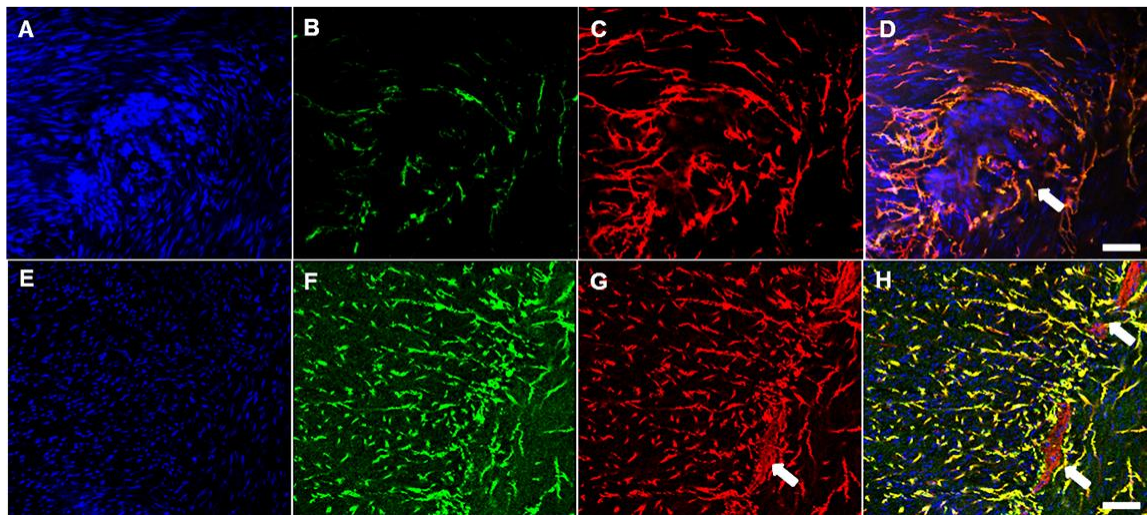


**Figure 4.6** Confocal images show the complete co-localization of the two types of ICs with their functional ion channels.

The top row shows the cKit (B) and Ano1 (C) with their merged image (D), which indicate that these two proteins are expressed by the same ICs, scale bar 20  $\mu$ m. The bottom row illustrates the co-localization between PDGFR $\alpha$  (F) with the SK3 (G), and their merge (H) scale bar 50  $\mu$ m. (A and E) Shows the control section without primary antibodies only nuclear staining with DAPI. Arrows indicate the myenteric ganglion.

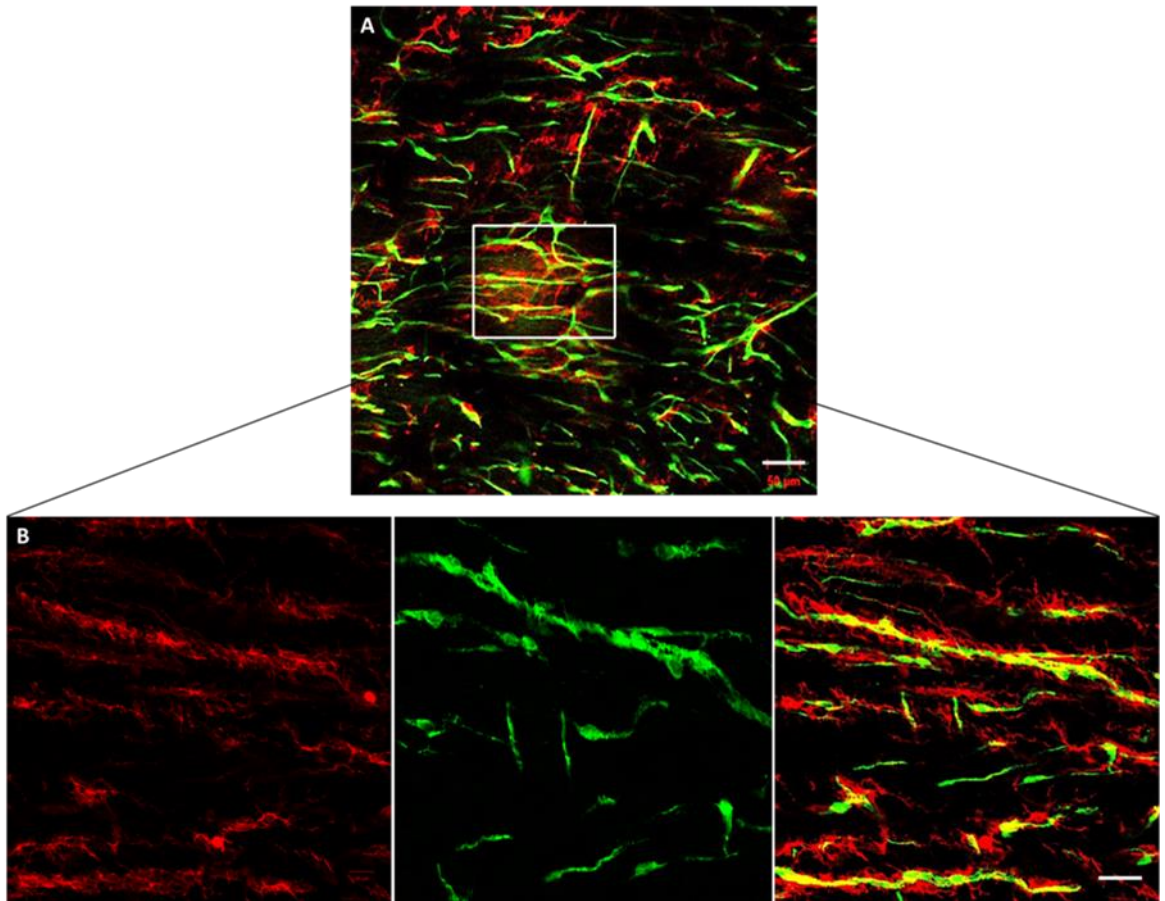


**Figure 4.7 Confocal images show the complex network formed by the two different types of ICs**

(A) cKit<sup>+</sup> ICs (red) and PDGFR $\alpha$ <sup>+</sup> ICs (green), scale bar 50  $\mu$ m. The two cells are not co-localized but rather run close to each other (B), scale bar 20  $\mu$ m.

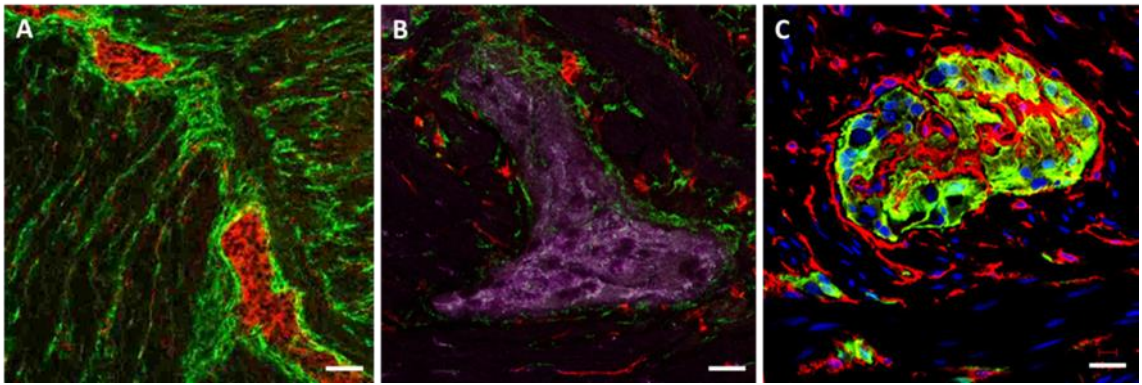


**Figure 4.8** Confocal images for ICs in the MP area show the close apposition of these cells and the enteric neurons and ganglion.

(A) Double labelling of cKit (green) with S100B (red), scale bar 50 μm. (B) Triple labelling of cKit (FITC-green), PDGFRα (red) and Tuj 1 (magenta), scale bar 20 μm. (C) Double labelling of PDGFRα (red) and SV2 (green), scale bar 10 μm.

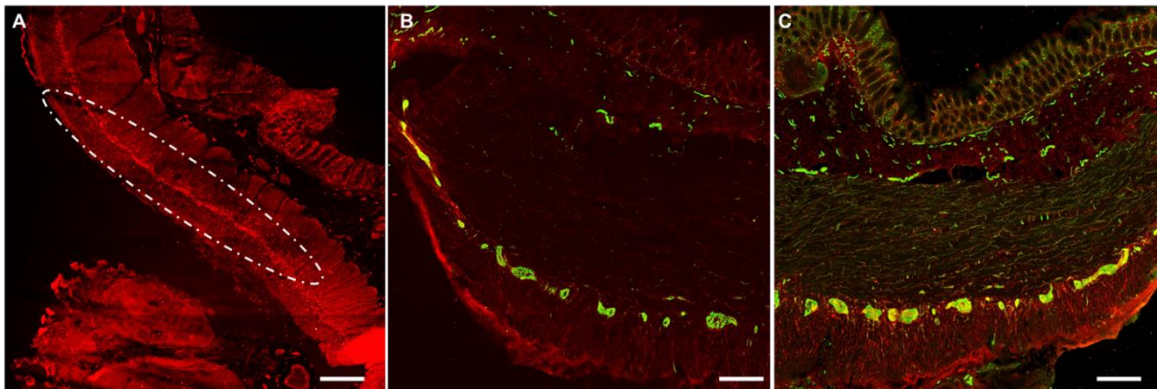


**Figure 4.9** Confocal tile scans of the human colon sample show the distribution of the PDGFRα<sup>+</sup> ICs around the MP.

(A) Selected area MP, scale bar 200 μm. (B) The MP and SMP stained with SV2, scale bar 100 μm. (C) The PDGFRα<sup>+</sup> ICs (red) with the MP (green), scale bar 100 μm.

#### 4.4.3 Distribution of cKit<sup>+</sup> and Ano1<sup>+</sup> ICs in HD

Immunoreactivity to cKit stained two types of cells, ICs identified as oval DAPI<sup>+</sup> nuclei with extending processes, and rounded mast cells which are abundantly found in the mucosa and submucosa. ICs were labelled with cKit and Ano1, which was mainly well defined around the DAPI<sup>+</sup> nuclei as well as labelling the cell processes which formed dense networks (**Figure 4.10**). Regions of MP and intramuscular layers of DC samples from stoma closure as well as the proximal part (ganglionic) of the HD were abundantly labelled with cKit<sup>+</sup> and Ano1<sup>+</sup> ICs. The labelling of ICs was particularly well concentrated around the ganglia in the MP with the extension of networks seen into the muscle layers on either side. However, there were significantly fewer cells in the proximal part of the HD sample, particularly in the MP area, compared to DC tissue, with cell count expressed in means  $\pm$  SD for DC cKit<sup>+</sup> ICs (MP  $117 \pm 3$ ) (CM  $62 \pm 4$ ) and (LM  $45 \pm 2$ ) for the proximal part of HD cKit<sup>+</sup> ICs counts (MP  $86 \pm 3$ ), (CM  $55 \pm 3$ ) and (LM  $44 \pm 2$ ). The number of cKit<sup>+</sup> ICs was markedly decreased in the distal part (aganglionic) of the HD, compared to the proximal segment, in the (MP  $5 \pm 1$ ), (CM  $8 \pm 1$ ) and (LM  $5 \pm 1$ ) (**Figure 4.11**). Similarly, the number of Ano1<sup>+</sup> ICs in each area of the tested bowel gave similar trends to cKit, where there was a significant reduction in the number of ICs in the distal part of the HD as compared to the proximal part of HD and the DC control samples, Ano1<sup>+</sup> ICs counts in DC (MP  $101 \pm 1$ ), (CM  $55 \pm 2$ ) and (LM  $46 \pm 4$ ) for the proximal part of HD Ano1<sup>+</sup> ICs count (MP  $79 \pm 4$ ), (CM  $48 \pm 1$ ) and (LM  $40 \pm 1$ ). The number of cells in the distal part of HD was markedly decreased, (MP  $4 \pm 1$ ), (CM  $6 \pm 1$ ) and (LM  $4 \pm 1$ ) (**Figure 4.12**).

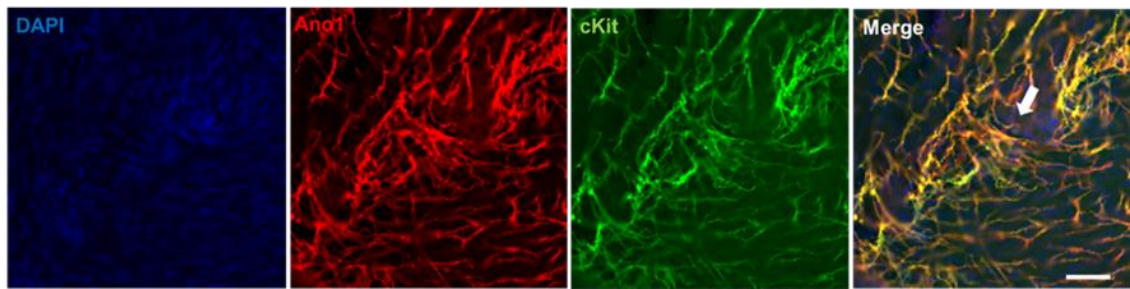


**Figure 4.10** Confocal images of the cKit and Ano1 immunostaining show complete co-localization of these two protein markers and the network around the ganglionic area (arrow), scale bar 20  $\mu\text{m}$ .

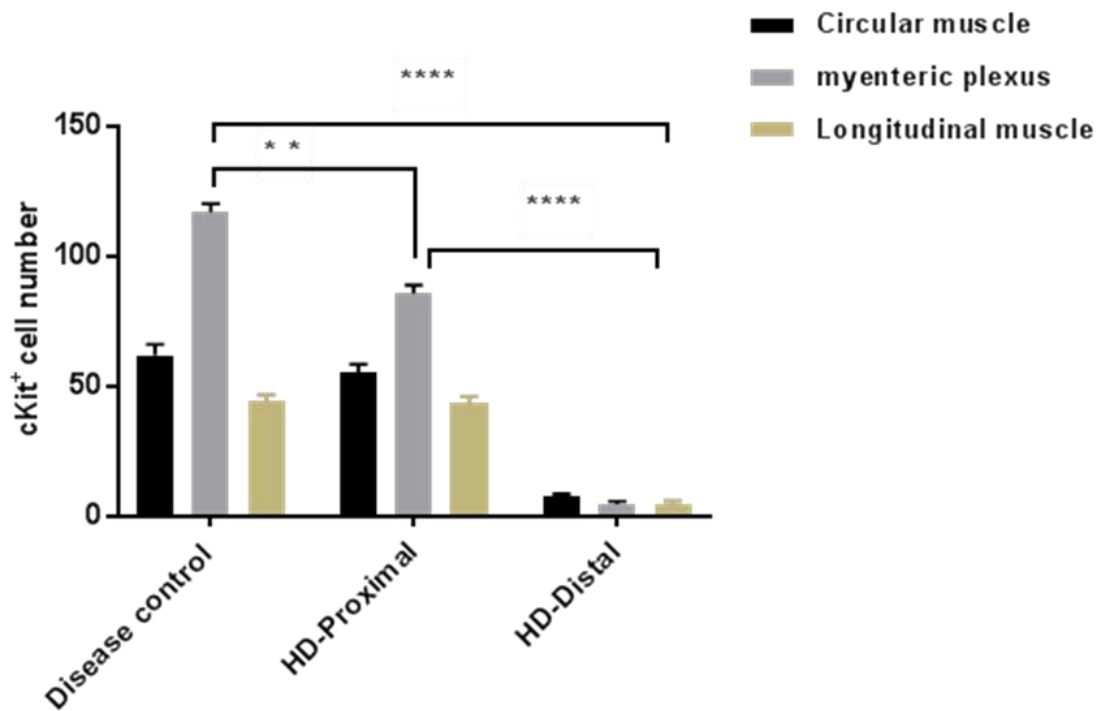


**Figure 4.11** The number of cKit<sup>+</sup> ICs in the three different histological layers of the colon of HD and DC samples.

The cell count per unit area ( $\text{mm}^2$ ) in the distal part of the HD sample was significantly decreased compared to the proximal part of HD ( $p < 0.0001$ ) and the DC samples ( $p < 0.0001$ ). The myenteric plexus of the proximal part of HD cKit cell count was significantly reduced compared to DC ( $p < 0.001$ ).

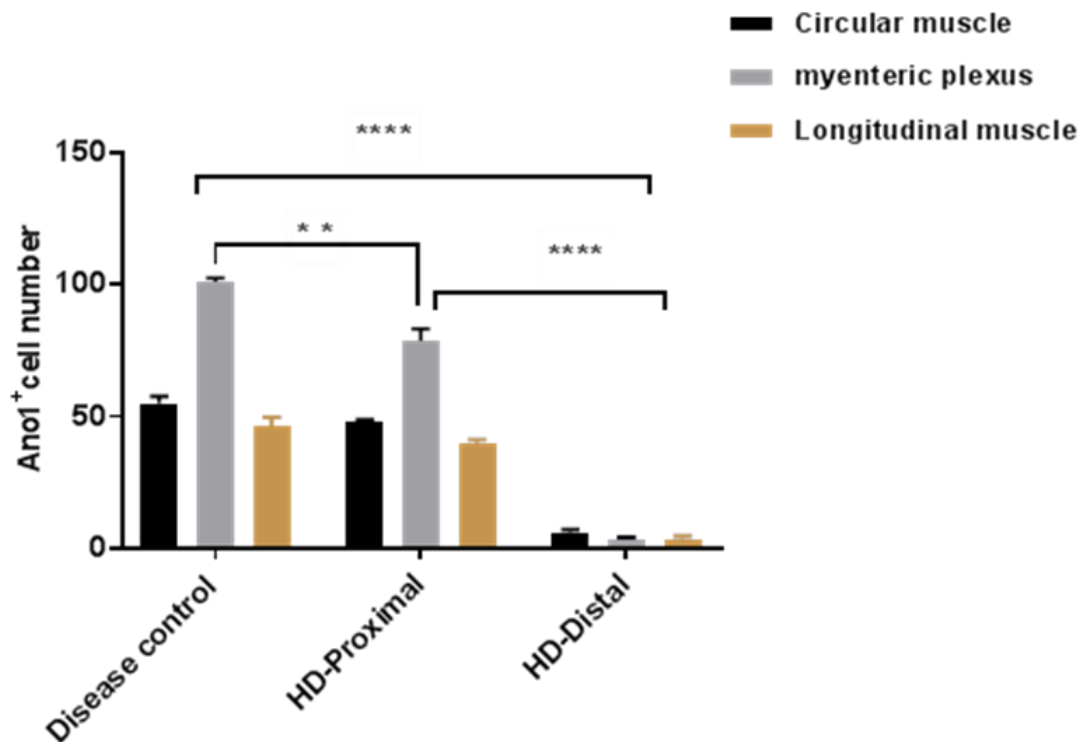


**Figure 4.12** The number of Ano1<sup>+</sup> ICs in the three different histological layers of the colon of HD and DC samples.

The cell count per unit area (mm<sup>2</sup>) in the distal part of the HD sample was significantly decreased as compared to the proximal part of HD ( $p < 0.0001$ ) and the DC samples ( $p < 0.0001$ ). The myenteric plexus of the proximal part of HD Ano1 cell count was significantly reduced compared to DC ( $p < 0.01$ ).

#### 4.4.4 Distribution of PDGFR $\alpha$ <sup>+</sup> and SK3<sup>+</sup> ICs in HD

Immunofluorescence with an antibody against PDGFR $\alpha$  labelled the intramuscular layers, and MP. Broad networks of PDGFR $\alpha$ <sup>+</sup> ICs were seen throughout the bowel muscular layers. PDGFR $\alpha$ <sup>+</sup> ICs formed extensive networks and were abundantly labelled in the region of MP concentrating around the ganglia in the DC samples and the proximal part of the HD samples. The networks consisted of cells with multiple extending processes creating meshes that sometimes covered the ganglia in the MP. In the distal part of HD, the networks were found to be significantly decreased compared with the proximal part and the DC samples (**Figure 4.13, Figure 4.14**). Again like cKit and Ano1, the number of PDGFR $\alpha$  and SK3 cells was significantly reduced in the proximal part of the HD as compared with the DC samples. For PDGFR $\alpha$ <sup>+</sup> ICs cell counts in DC samples was (MP 131  $\pm$  1), (CM 64 $\pm$  4) and (LM 56  $\pm$  3), for the proximal part of HD the cell count was (MP 81  $\pm$  2), (CM 58  $\pm$  1) and (LM 37 $\pm$  2). The number was significantly reduced in the distal part of HD with cell counts (MP 4 $\pm$  1), (CM 5 $\pm$  1) and (LM 4  $\pm$  1) (**Figure 4.15**). Again SK3<sup>+</sup> ICs showed reduced number of cells in the distal part of HD being (MP 4 $\pm$  0.5), (CM 4  $\pm$  1) and (LM 4 $\pm$  1) as compared to the proximal part of HD (MP 74 $\pm$  3), (CM 48  $\pm$  1) and (LM 38  $\pm$  4). Both proximal and distal showed a significant reduced in the cell count around the MP when compared to DC samples (MP 102  $\pm$  2), (CM 58  $\pm$  2) and (LM 66  $\pm$  3) (**Figure 4.16**) cell numbers in HD and DC shown in (**Table 4.1**) with their ratio shown in (**Figure 4.17**).

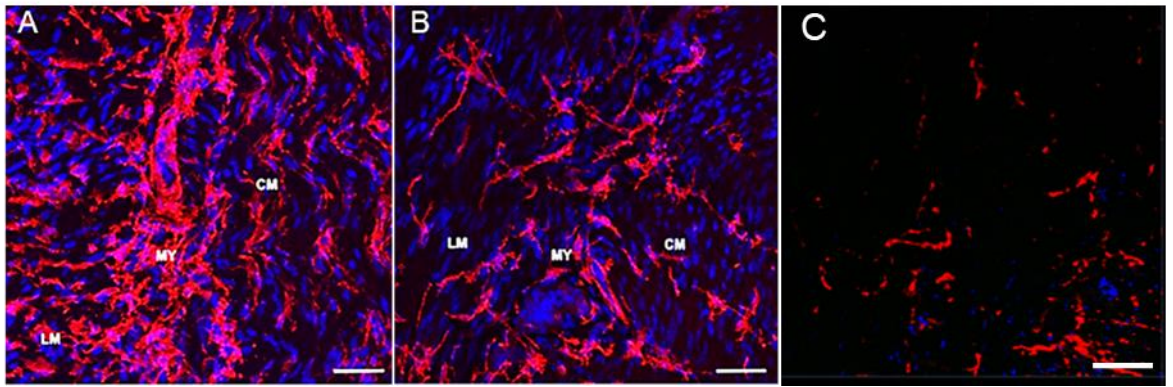


**Figure 4.13 Confocal images of PDGFR $\alpha$  immunostaining.**

(A) disease control (DC) sample from stoma closure shows the dense staining around the MP, as well as in the CM and LM. (B and C) Reduced levels of immunostaining in the proximal part of the HD sample (B) and distal HD sample (C). LM, longitudinal muscle. CM, circular muscle, MP, myenteric plexuses. Scale bar 50  $\mu$ m.

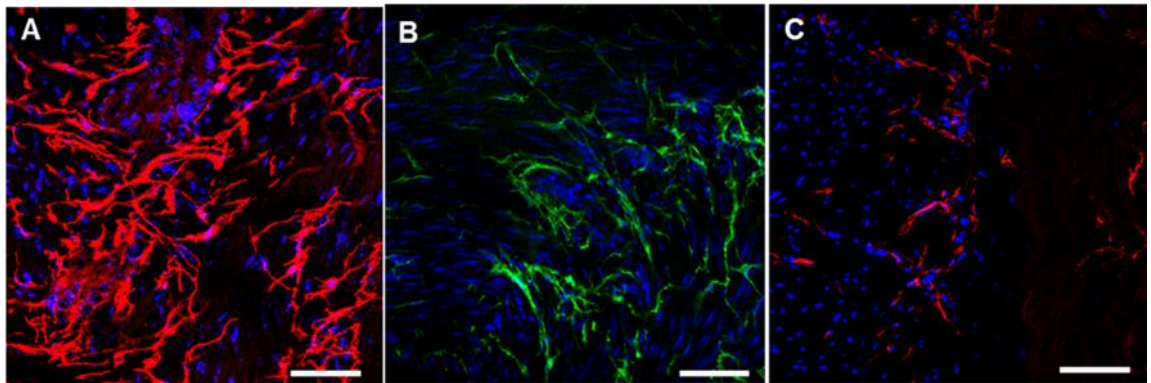


**Figure 4.14 Confocal images show the immunolabelling of SK3.**

The density of the immunofluorescence in the distal part of the HD (C) is markedly reduced compared to the proximal HD sample (B) and disease control sample (A). Scale bars 20  $\mu$ m (A,B), 50  $\mu$ m (C).

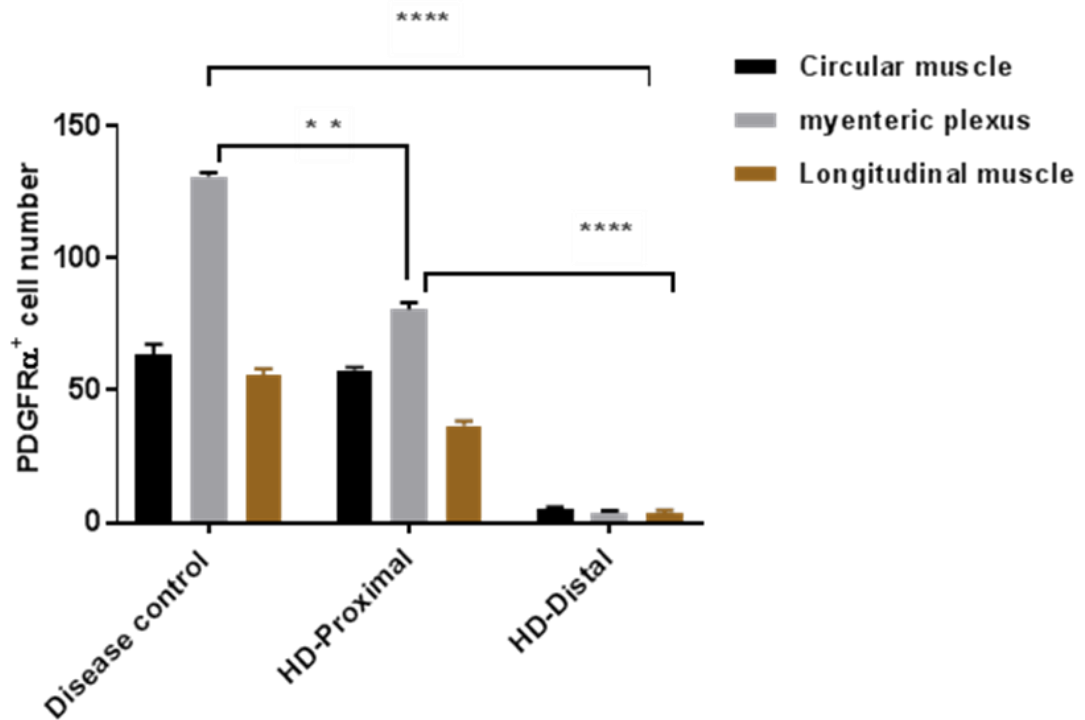


**Figure 4.15** The number of PDGFR $\alpha$ <sup>+</sup> ICs in the three different histological layers of the colon of HD and DC samples.

The number of cells per unit area (mm<sup>2</sup>) in the distal part of HD colon was significantly decreased compared to the proximal part of HD colon ( $p < 0.0001$ ) and the DC colon sample ( $p < 0.0001$ ). The PDGFR $\alpha$ <sup>+</sup> cell count in the myenteric plexus and the longitudinal muscle layers were significantly reduced in the proximal part of the HD compared to DC ( $p < 0.001$ ).

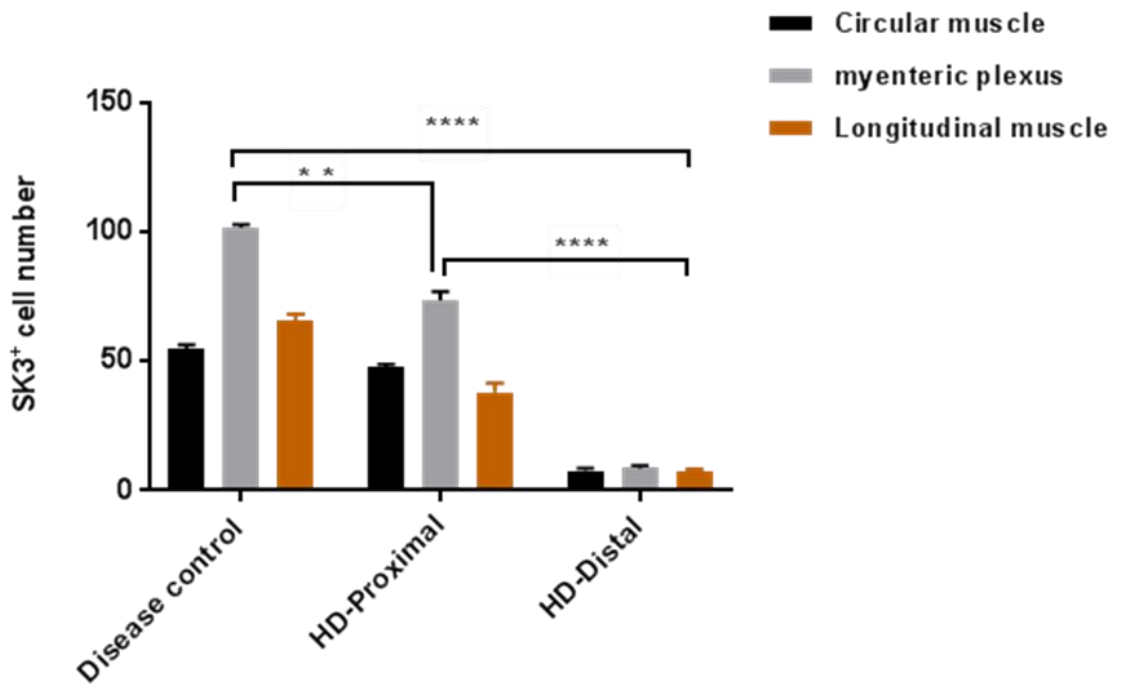


**Figure 4.16** The number of SK3<sup>+</sup> ICs in the three different histological layers of the colon of HD and DC samples.

The number of cells per unit area (mm<sup>2</sup>) in the distal part of HD colon was significantly decreased compared to proximal part of HD colon ( $p < 0.0001$ ) and the DC colon sample ( $p < 0.0001$ ). The SK3<sup>+</sup> cell count in the myenteric plexus and the longitudinal muscle layers were significantly reduced in the proximal part of the HD compared to DC ( $p < 0.001$ ).

**Table 4.1 IC numbers for the four different protein markers in the same ROI (mm<sup>2</sup>) area performed using Image J software, numbers expressed in mean  $\pm$  SD**

	cKit			Ano1			PDGFR $\alpha$			SK3		
	CM	MP	LM	CM	MP	LM	CM	MP	LM	CM	MP	LM
<b>DC</b>	62 $\pm$ 4	117 $\pm$ 3	45 $\pm$ 2	55 $\pm$ 2	101 $\pm$ 1	46 $\pm$ 4	63 $\pm$ 4	131 $\pm$ 1	56 $\pm$ 3	58 $\pm$ 2	102 $\pm$ 2	66 $\pm$ 3
<b>HD-Proximal</b>	55 $\pm$ 3	86 $\pm$ 3	44 $\pm$ 2	48 $\pm$ 1	79 $\pm$ 4	40 $\pm$ 1	58 $\pm$ 1	81 $\pm$ 2	37 $\pm$ 2	48 $\pm$ 1	74 $\pm$ 3	38 $\pm$ 4
<b>HD- Distal</b>	8 $\pm$ 1	5 $\pm$ 1	5 $\pm$ 1	6 $\pm$ 1	4 $\pm$ 1	4 $\pm$ 1	5 $\pm$ 1	4 $\pm$ 1	4 $\pm$ 1	4 $\pm$ 1	4 $\pm$ 0.5	4 $\pm$ 1

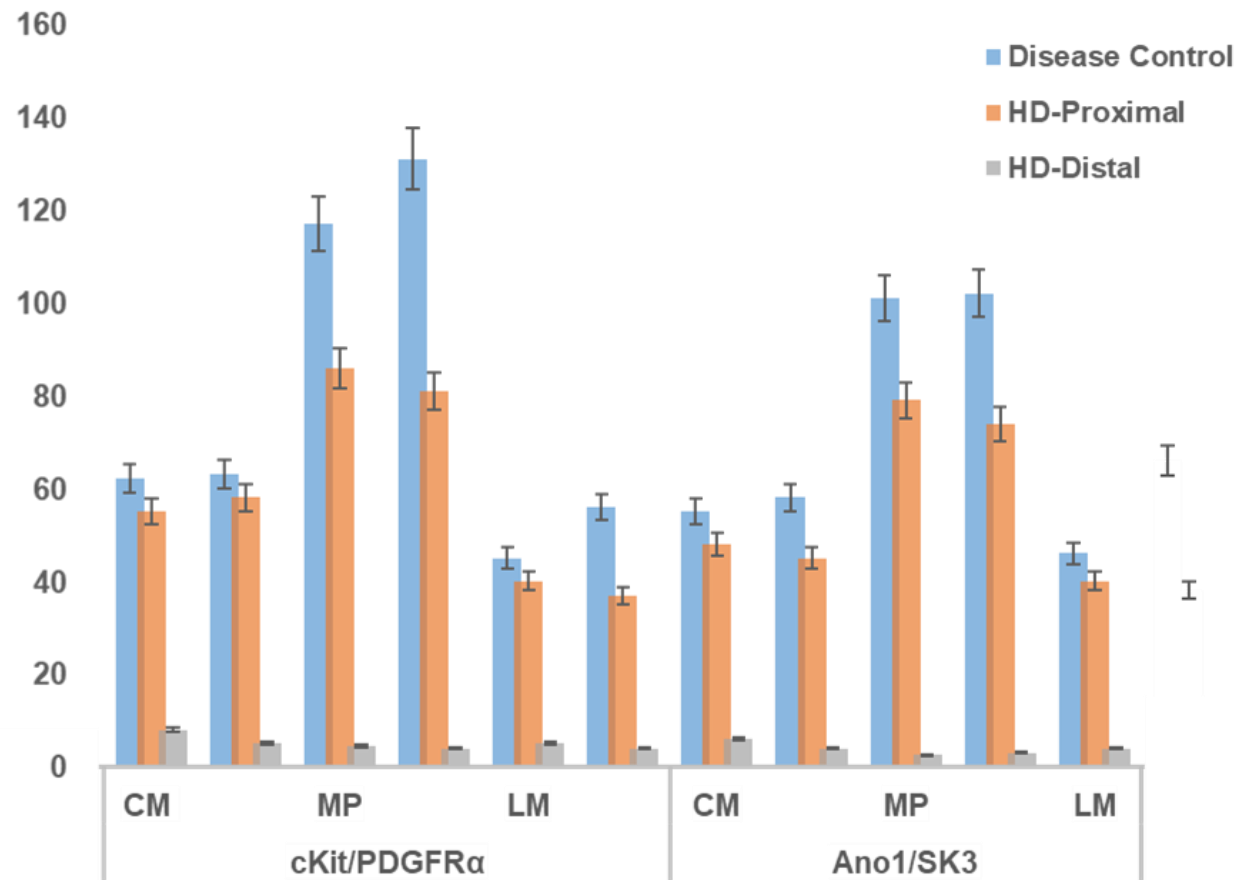


Figure 4.17 Ratio between the two IC subtypes as expressed by their specific markers and the functional protein markers.

## **4.5 Discussion**

This chapter made use of the improved method of detection established in the previous work to show that the PDGFR $\alpha$ <sup>+</sup> and cKit<sup>+</sup> cells are located in the longitudinal and circular muscle layers, but are mainly concentrated around the myenteric ganglia. In the HD tissue, both cell types are reduced in number in the distal versus proximal portions of the samples. Interestingly even in the HD proximal portions, the IC number was significantly lower in the HD tissue compared to DC. Finally, of potential significance for function, the ratio of cKit<sup>+</sup>: PDGFR $\alpha$ <sup>+</sup> cells varied along with the diseased samples as more distal portions had more cKit<sup>+</sup>: PDGFR $\alpha$ <sup>+</sup> cells than proximal portions. To the best of our knowledge, this study is the first that show the four IC markers together and compare them in different human colon samples.

### **4.5.1 Distribution of Interstitial Cells as compared to other studies in HD**

Since loss or disruption of ICs has been involved in a variety of gut motility disorders, ranging from minor illness such as diarrhoea and constipation to severe diseases such as HD, studies have demonstrated the importance of cKit signaling in the development of cKit<sup>+</sup> ICs, in which the disruption of these signalling results in reduced numbers of pacemaking cells and disrupted signalling networks which lead to the motility disorder of the gut wall (Maeda et al., 1992, Torihashi et al., 1995, Torihashi et al., 1999a).

The finding in this study supports previous observations regarding the reduction of the Ano1<sup>+</sup> ICs number in the distal part of HD colon (Coyle et al., 2016). This

suggests a loss of electrical coupling and gives support to the lack of spontaneous slow waves in the distal part of HD samples. Throughout this research, the first study looking at the distribution of PDGFR $\alpha$ <sup>+</sup> ICs in HD reported a reduced distribution of these ICs in aganglionic bowel indicated in this study as distal part in samples taken from 10 patients (O'Donnell et al., 2016). This was found to be in comparison to 10 control bowel specimens taken from age-matched patients undergoing surgery for colostomy closure following surgical correction of the imperforated anus. Our results were similar to their finding as both demonstrated reduction in the number of this type of ICs in both proximal and distal parts of the diseased specimen as compared to the control samples. However, O'Donnell and her colleagues did not indicate how this was quantified and the only general statement was made with no reference to individual layers within the bowel wall, as demonstrated in this study. The same group confirmed that SK3 channel expression is decreased in HD by using immunofluorescence and western blot protein quantification analysis (Coyle et al., 2015), which again is consistent with our immunofluorescent results for SK3 in HD and the qPCR results which will be considered in the next chapter.

In our present research, we confirmed that the number of ICs is decreased in the human colon with HD in the distal part as compared to the proximal part, however, comparing the proximal part of the disease to the control samples revealed decrease in the number of cells which could explain the post-operative symptoms in many cases.

The results of our study have revealed a significant decrease in the four antibodies markers in distal and proximal parts of the HD compared to disease control colon. The marked decrease in PDGFR $\alpha$ <sup>+</sup> ICs suggests a deficiency in inhibitory neurotransmission in the HD bowel and may improve our knowledge of the mechanism by which the distal portion of the HD intestine continues in a tonic contraction. Future studies may explore function more precisely by performing an electrophysiology study in which these cells are stimulated or inhibited and the response in the smooth muscle cells is recorded, this research might be carried on genetically modified mice gut tissue in which these cell express gene that is sensitive to light and when stimulated they might trigger the intracellular changes that are responsible for the smooth muscle action.

The location of two distinct ICs close to each other conducting antagonizing action as indicated by the functional ion channels expressed by each type of ICs, and also being alongside the enteric nerves and nerve varicosities, in addition to the fact that they are combined with gap junctions to SMCs highly indicate a function for these cells in enteric neurotransmission (Cobine et al., 2011, Kurahashi et al., 2011, Baker et al., 2013). In addition to being enteric pacemaker cells, cKit<sup>+</sup> ICs also act as mediators of neurotransmission and are essential regulators of gut motility (Hirst and Edwards, 2004). cKit<sup>+</sup> ICs are structurally similar to PDGFR $\alpha$ <sup>+</sup> ICs, but they express different protein receptors related to tyrosine kinases (discussed in details in Chapter1) and perform different functions. Iino et al (2009) were the first who examine PDGFR $\alpha$ <sup>+</sup> ICs in the murine gut, according to their observation these cells were

present in musculature throughout gut tissue and closely associated with cKit<sup>+</sup> ICs and enteric nerve fibres (Iino et al., 2009), similar to our study these cells were seen to form a cellular network with their processes overlapping around the ganglion in the MP region. Cobine et al (2011) examined the distribution of both ICs types and nitric-oxide synthase positive (NOS<sup>+</sup>) neurons in the internal anal sphincter of both wild type and cKit mutant mice in which cKit<sup>+</sup> ICs were significantly reduced, their findings were a reduction in PDGFR $\alpha$ <sup>+</sup> ICs. They also observed a close relationship between inhibitory motor neurons and the two different types of ICs which suggest a functional interaction between these cells (Cobine et al., 2011).

A group of researchers confirmed a functional role of PDGFR $\alpha$ <sup>+</sup> ICs in the gut smooth muscle by using transgenic mice which expressing enhanced green fluorescent protein (eGFP) in PDGFR $\alpha$ <sup>+</sup> ICs that enable the researcher to isolate and study the function of these cells. They found that PDGFR $\alpha$ <sup>+</sup> ICs express receptors that receive and transduce purinergic neural signals (Kurahashi et al., 2011). The same group found that PDGFR $\alpha$ <sup>+</sup> ICs express SK3, which mediate purinergic neural regulation of colonic muscles contraction (Kurahashi et al., 2012).

#### **4.5.2 Hirschsprung Disease and Disease Control samples difference**

We identified ICs by immunostaining technique in HD samples (proximal and distal part of the colon) and compared them to a disease control samples from stoma closure. Perhaps not surprisingly, in addition to the differences between proximal and distal parts of the HD colons, there was an apparent reduction in

IC numbers in the distal HD colon compared to the DC tissue. Similar findings have been reported by others, revealing a reduced number of cKit (Rolle et al., 2002), SK3 (Coyle et al., 2015, O'Donnell et al., 2019b) and PDGFR $\alpha$  ICs (Coyle et al., 2015) in HD tissue compared to stoma closure disease control tissue. This study indicates that Ano1 is also reduced in HD distal colon compared to disease control. This loss of two markers of IC is consistent with cell numbers being reduced, rather than loss of immunoreactivity being due to a reduction in expression of proteins in the cells.

An important finding here was the number of cKit<sup>+</sup>, and PDGFR $\alpha$ <sup>+</sup> cells were reduced in even the proximal portion of the HD compared to the DC tissue. The reduction in cell numbers possibly indicates improper colon function even at the proximal level and why some HD cases exhibit GI symptoms such as constipation following surgery, as has been highlighted by several previous studies (Meinds et al., 2019). A question, therefore, remains at what point, if at all, does IC number and colon function return to control levels in HD colons? This would require anatomical examination of potentially entire colon from HD patients, along with some functional studies if possible. Such information could be valuable for patient care, being able to determine precisely where the function would be optimally retained, could enhance targeting of resection. However, since the availability of such tissue is likely to be a post-mortem, it is difficult to determine how realistic it could be to obtain such information. Alternatively, a successful animal model of HD is required.

### **4.5.3 Ratio of different types of IC target PDGFR $\alpha$ <sup>+</sup> cells**

Our observation that the ratio of cKit<sup>+</sup>: PDGFR $\alpha$ <sup>+</sup> cells increased the more distal the diseased colon region may have significant consequences for potential treatment consideration. For example, it seems appropriate to consider boosting the numbers and/or function of the PDGFR $\alpha$ <sup>+</sup> cells in the distal portions, perhaps by selective applications of drugs working on either PDGFR $\alpha$  or the SK3 ion channel, indeed, both activators and inhibitors of SK3 like CyPPA (Hougaard et al., 2007) and Apamin (Van der Staay et al., 1999) respectively, are available at least for basic research, and so this approach could be tested in a gut bath approach with samples of HD colon.

## **4.6 Conclusion**

The results of our study have revealed a significant decrease in the four protein markers expressed by ICs in distal and proximal parts of the HD compared to healthy control colon. The marked reduction in PDGFR $\alpha$ <sup>+</sup> ICs indicates a deficiency in the inhibitory neurotransmission in HD bowel and may enhance our understanding of the mechanism by which the distal part of HD bowel remains in a tonic contraction. Future studies may explore the function more precisely by performing an electrophysiology study in which these cells are stimulated or inhibited, and the response in the SMCs is recorded, this work might be carried on genetically modified mice gut tissue using an optogenetic technique.

## Chapter 5 Gene expression in Hirschsprung Disease

### 5.1 Introduction

Hirschsprung Disease also known as aganglionosis, is a congenital disease in which ganglion cells are absent from a part or a whole colon. It has been known that the obstructive symptoms in HD are due to abnormal motility of the distal narrow aganglionic segment; however, a full understanding of the occurrence of the spastic diseased segment is not yet known (Puri and Friedmacher, 2018). The normal intestinal motility requires the coordinated interaction of ENS, SMC, cKit<sup>+</sup> IC and PDGFR $\alpha$ <sup>+</sup> ICs. The interaction between these cells propagates the regular pattern of peristaltic movement seen in healthy human colon (Blair et al., 2014) as detailed in (Chapters 1 and 4).

The genetic fingerprint of ICs is established during embryonic development. Staining for cKit and markers of smooth muscle cells and neurons revealed that the IC-MP and longitudinal SMCs developed from common precursors, but that separate identities were established at the early postnatal stage (Torihashi et al., 1997). However, Torihashi and his group relied on cKit to identify IC, and no other gene expression was examined; therefore, the PDGFR $\alpha$ <sup>+</sup> / SK3<sup>+</sup> cells were not considered. To date, most published data regarding gene expression of these cells has been done in animal models; however, fewer studies focused on the expression of these genes in the human colon although not altogether in one study.

Due to the complex inheritance pattern of HD (Borrego et al., 2013), it is unclear how many genetic disorders are associated with HD disease. This has led to increasing interest in studies on genetic factors regarding the pathogenesis of HD (Heuckeroth and Schäfer, 2016, Torroglosa et al., 2016), HD genetic contribution reviewed in details in (Chapter 1 section 1.15.3 and Table 1.3).

As genome expression data offers essential clues in cellular functions and biological processes, a step toward the analysis of IC genome began recently. In 2017 a group of researchers developed the first online resources which provide a library of all recognized genetic transcripts expressed in cKit<sup>+</sup> ICs. Using flow cytometry to isolate the population of ICs and RNAseq techniques to sequence the transcriptomes of cKit<sup>+</sup> ICs isolated from the jejunum and colon Kit<sup>+/copGFP</sup> mice, by analyzing the transcriptome, they were able to identify new selective markers of cKit<sup>+</sup> ICs namely: *Thbs4* and *Hcn4*, in addition to several additional ion channels and transporter isoforms (*Cacng6*, *Cacng8*, *Cacnb4*, *Kcng3*, *Abcc8*, *Kcnkj2*, *Kcnmb2*, and *Slc4a4*) which were characteristic of cKit<sup>+</sup> ICs identity and function (Lee et al., 2017). The same group of researchers also confirmed that *Ano1* was the most highly and specifically expressed ion channel gene in cKit<sup>+</sup> ICs (Lee et al., 2017).

PDGFR $\alpha$ <sup>+</sup> ICs directly interact with cKit<sup>+</sup> ICs and SMCs in the gut tissue. These cells form part of an electrical syncytium (SIP syncytium) thus the electrophysiological events in one SIP cell can affect the excitability of the other cells in the syncytium detailed in (Chapter 1), which helps in the regulation of normal gut motility (Sanders et al., 2012a). A similar study was performed to

analyze the transcriptomes of the PDGFR $\alpha$ <sup>+</sup> ICs and SMCs aiming at completing the SIP cell transcriptome. FACS isolated PDGFR $\alpha$ <sup>+</sup> ICs from *Pdgfra*<sup>eGFP/+</sup> and *Pdgfra*<sup>eGFP/+;Myh11</sup><sup>Cre-ERT2/+</sup>; *Rosa26*<sup>LacZ/+</sup> mice and RNAseq libraries were created, the researcher group were able to identify voltage-dependent Ca<sup>2+</sup> channels, *Cacna1g* and *Cacna1h* (T-type, *Cav3.1* and *Cav3.2*), *Cacna1d* (L-type, *Cav1.2*), and Ca<sup>2+</sup> channel regulators including *Gas6* and *Jph2* as being abundantly expressed by PDGFR $\alpha$ <sup>+</sup> ICs, among them *Cacna1g* appeared to be the most specific to PDGFR $\alpha$ <sup>+</sup> ICs (Ha et al., 2017). PDGFR $\alpha$ <sup>+</sup> ICs were found to express as many as 92 K<sup>+</sup> channel subunits, among them SK3 (*KCNN3*) was the most abundant and most specific gene, this gene is related to the purinergic neurotransmission function of PDGFR $\alpha$ <sup>+</sup> ICs other genes related to purinergic signalling, including *P2ry1*, *Adora1*, and *P2rx7*, all were abundantly expressed in PDGFR $\alpha$ <sup>+</sup> ICs (Ha et al., 2017). From the SIP transcriptome analysis, they found that all the cellular component of SIP have similar transcriptomes up to 93% similar genes were found, this similarity in the expression profile supports the concept that all the SIP cells share a common developmental lineage (Ha et al., 2017). Torihashi et al. (1999) demonstrated cKit<sup>+</sup> ICs plasticity in which MP cKit<sup>+</sup> ICs turned into SMC phenotypes when cKit receptors were blocked (Torihashi et al., 1999). However, despite this shared gene expression, there were approximately 1500 genes that are specific to each type of SIP cell which reflects their phenotypical differentiation and functional roles (Ha et al., 2017).

Understanding expression profiles of individual IC will be of importance for a complete understanding of their function in normal and HD tissue. However, it

is also important to consider changes in gene expression across the tissue, since normal function relies on the coordinated action of different cell types. Several studies have completed whole human genome sequencing which resulted in important scientific finding and new insights into human genetic variations in HD (Levy et al., 2007, Wheeler et al., 2008, McKernan et al., 2009, Pushkarev et al., 2009). Analysis of gene expression changes between proximal and distal portions of human HD tissue has been reported. Xiao and his colleagues (2018), used raw microarray data from 8 HD patients, a total of 253 genes were identified to be differentially expressed between the distal and proximal bowel segments of HD samples. Forty genes were upregulated, and 213 genes were downregulated (Shang-jie Xiao, 2018). Elucidating gene changes in HD tissue cells could add a significant understanding of the motility function and mechanism of disorders and help provide potential targets for therapy development.

## **5.2 Aims of the study**

We designed this study to test the hypothesis that the expression of cKit, Ano1, PDGFR $\alpha$  and SK3 are altered in the distal (aganglionic) colon of patients with HD. To accomplish this goal, quantitative polymerase chain reaction (qPCR) was used to compare the expression levels of the four ICs markers used throughout this thesis to the levels from the control samples considering the proximal and distal of HD samples. An attempt was carried to isolate single IC using different methods, namely Fluorescence-Activated Cell Sorting (FACS) and manual microelectrode cell isolation. In addition, to understand changes in gene expression in the proximal and distal portion of HD tissue that may contribute to dysfunction, RNAseq analysis was performed to identify the differences in gene expression between various segments of HD sample considering different histological layers in the colon wall of HD.

## **5.3 Material and methods:**

### **5.3.1 Sample collection**

Tissue samples from 4 HD patients and 4 matched controls of colonic samples taken from patients undergoing colostomy closure following surgery for imperforate anus were obtained under informed ethical consent (14/NS/0018, North of Scotland Research Ethics Committee). HD specimens were further divided into proximal (ganglionic) and distal (aganglionic) samples.

### **5.3.2 RNA extraction, reverse transcription and quantitative polymerase chain reaction (qPCR)**

#### **5.3.2.1 Design and synthesis of primers**

The gene encoding human *GAPDH* was used as an internal control. First, searches for candidate gene (*Kit*, *Ano1*, *PDGFR $\alpha$*  and *SK3*) sequence transcripts using (<http://www.ensembl.org/index.html>) were performed. Gene lists and transcripts accession numbers used to design the primers presented in (**Appendix 4**), then primers designed using primer3 (<http://primer3.ut.ee/>), after which primer properties were checked using IDT Oligo analyser (<https://eu.idtdna.com/calc/analyser>). Primer pairs for *cKit*, *Ano1*, *PDGFR $\alpha$*  and *SK3* were synthesized and purified by Sigma-Aldrich. Primer design was performed with the consideration of general guidelines: melting temperatures of all primers were set between 58°C and 60°C; the length of the primers was approximately 30 nucleotides; GC contents were in the range of 40-60%. The primers pairs are listed in (**Table 5.1**).

**Table 5.1 Human Interstitial Cell primer pairs sequences.**

<b>Oligo Name</b>	<b>Sequence (5`-3`)</b>
<b>human GAPDH-F</b>	5'GTCAAGGCTGAGAACGGGAA3'
<b>human GAPDH-R</b>	5'AAATGAGCCCCAGCCTTCTC3'
<b>human cKit-F</b>	5'AGGAAACGCTCGACTACCTG3'
<b>human cKit-R</b>	5'CATTCCAGGATAGGGGCTGC3'
<b>human PDGFR<math>\alpha</math>-F</b>	5'CGGAGGAGAAGTTTCCCAGAG3'
<b>human PDGFR<math>\alpha</math>-R</b>	5'CTGCTCACTTCCAAGACCGT3'
<b>human Ano1 –F</b>	5'ACGGGCTTTGAAGAGGAAGA3'
<b>human Ano1 –R</b>	5'TAGATGATGACGCCGAGGAC3'
<b>human KCNN3-F</b>	5'CTTCAACACCCGCTTTGTCA3'
<b>human KCNN3-R</b>	5'GGCAGCAATGATCCACAGAG3'

### 5.3.2.2 RNA isolation from colon specimens

Total RNA extraction using TRIzol (Direct-Zol™ RNA Microprep, Zymo research, cat No: R2060) was performed according to the manufacturer's instructions. Colon tissue < 5 mg (strips of 10 mm width) were suspended in 300  $\mu$ l of TRI Reagent (guanidium thiocyanate/phenol) to homogenize the sample. To remove the particulate debris from homogenized tissue samples, they were centrifuged for 1 minute at 14,000 x g. The supernatant was then transferred into RNase free tube. The tissue lysate was mixed thoroughly by pipetting with 100% (v/v) (300  $\mu$ l) ethanol. The mix was transferred into a Zymo- spin IC column (Zymo Research) housed in a 2 ml collection tube and centrifuged for 30 seconds at 13,000 x g. The flow-through was discarded, and the column was transferred into a new collection tube. 400  $\mu$ l of RNA wash buffer was used once to wash RNA bound to the silica membrane for 30 seconds at 13,000 x g and a mixture of 5  $\mu$ l DNase1 (6 U/ $\mu$ l) with 35  $\mu$ l DNA

Digestion Buffer was added to column and incubated at RT for 15 minutes to remove DNA and purify the RNA sample. 400 µl Direct-zol RNA prewash buffer was added to the column and centrifuged for 30 seconds at 13,000 x g; this step was used twice (30 seconds each). 700 µl of RNA wash buffer was added to the column and centrifuged for 2 minutes at 13,000 x g, to ensure complete removal of the residual washing buffer. After washing steps, the column was placed in a new 1.5 ml RNase free collection tube. To elute RNA, 15 µl of DNase/ RNase free water was added to the column and centrifuged for 30 seconds at 13,000 x g, the centrifugation repeated in order to maximize RNA yield. The harvested RNA concentration was measured using a Nanodrop spectrophotometer (ThermoFisher) (**Appendix 2, Figure B**) to show the purity of RNA extracted from the samples. Samples were immediately stored at -80°C. The 260 /280 OD ratio typically ranges from 1.8 to 2.0, indicating high RNA purity.

### **5.3.2.3 Reverse transcription and cDNA synthesis**

Complementary DNA (cDNA) was synthesized using qScript cDNA synthesis kit consist of qScript Reaction Mix (5x), qScript Reverse transcriptase and nuclease-free water (Quanta bio 95047-025). 1 µg of RNA was needed to start the reaction, which was run in 0.2 ml thin-walled PCR tube (**Table 5.2**) shows the amount needed from each reagent. To make 20 µl final reaction volume, the tube was vortexed gently to mix reagents and centrifuged for 10 seconds. The thermal cycler was used to perform the cDNA synthesis, programmed as follows: 1 cycle of 22° C for 5 minutes; 1 cycle of 42° C for 30 minutes; 1 cycle of 85° C for 5 minutes; then the sample was held at 4° C and the reaction

product stored at  $-20^{\circ}\text{C}$  until ready to proceed with qPCR. In addition, cDNA quality was verified using 4% agarose gel electrophoresis of the reaction products. The gel was prepared by mixing agarose powder (Sigma, A5304) and TBE buffer (Sigma T4415) and the mixture heated using a microwave until the agarose was dissolved completely. Ethidium bromide (Sigma, E1385) was used to stain cDNA and illumination with a UV light source to visualize the cDNA banding pattern, DNA ladder (ThermoFisher, SM1332) was used to compare the cDNA, and then visualized by ChemiDoc Bio-Rad (Cat: 17001401).

**Table 5.2 The volumes to make 20  $\mu\text{l}$  per reaction for cDNA synthesis**

<b>nuclease free water</b>	Add to make final volume of 20 $\mu\text{l}$
<b>qscript reaction mix 5x</b>	4 $\mu\text{l}$
<b>RNA 10 <math>\mu\text{g}</math> to 1 <math>\mu\text{g}</math> total RNA</b>	Depend on RNA concentration
<b>qscript RT</b>	1 $\mu\text{l}$

#### **5.3.2.4 Quantitative Polymerase Chain Reaction (qPCR)**

Quantitative PCR is a simple, rapid, specific and efficient method based on the detection and quantification of a fluorescent reporter to monitor the fluorescence emitted during each PCR cycle, which increased in direct proportion to the amount of PCR products, the reaction reviewed in (Smith and Osborn, 2009). For each reaction, the following components (master mix) were added: 10  $\mu\text{l}$  Power-up (Syber Green solution) (Thermo Fisher Cat No A25741) which contains (buffer, dNTPs, DNA polymerase and Sybr green), 1.2  $\mu\text{l}$  forward and 1.2  $\mu\text{l}$  reverse primers, 5.6  $\mu\text{l}$  nuclease-free water to make 18  $\mu\text{l}$

volume in total, these volumes were multiplied to the number of samples to make the master mix stock solution, 2  $\mu$ l of the cDNA samples was then added to the 18  $\mu$ l master mix to make a final 20  $\mu$ l reaction volume. All PCR reactions were carried in a triplet. The control samples included one without template and one without reverse transcriptase (both were in a triplet). All reactions were done in 96-well plates (ThermoFisher, Cat No AB-2396/B) in 20  $\mu$ l volumes, and the plate was sealed before being centrifuged for 4 minutes at 800 rpm. Thermal cycler conditions were as follows: 50° C for 2 minutes, 95° C for 2 minutes, 95° C for 3 seconds, 60° C for 30 seconds, the third and fourth cycles repeated for 39 times and the annealing temperatures were dependent on the  $T_m$  for each pair of primers and range from 50° C to 60° C. The resultant samples were run in gel electrophoresis to verify the quality of the qPCR results for the different primers. The results were plotted using Bio-Rad CFX software; each gene was quantified relative to GAPDH, the workflow steps of qPCR experiments are shown in **(Figure 5.1)**.

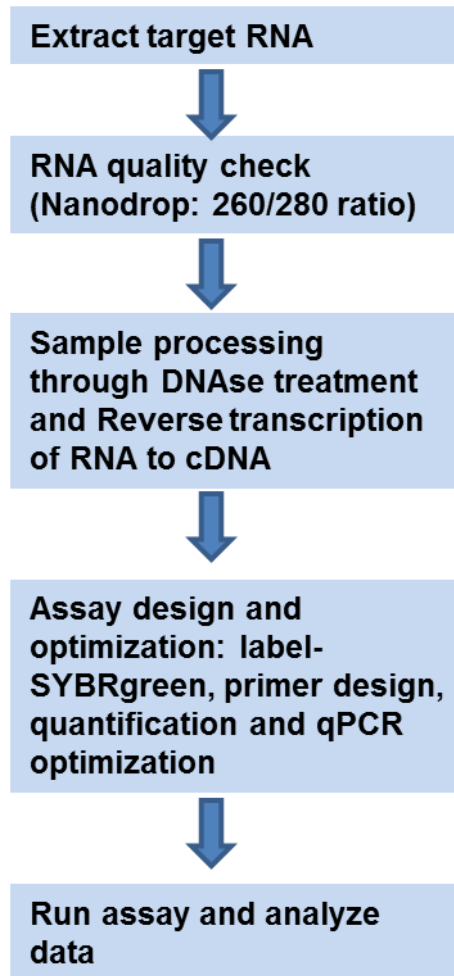


**Figure 5.1 Sample preparation and workflow of qPCR experiments**

### **5.3.3 Interstitial Cell isolation using Fluorescence-Activated Cell Sorting (FACS)**

Full-thickness colonic specimens from HD patient (n=1) were used to sort out single cKit<sup>+</sup> ICs and single PDGFR $\alpha$ <sup>+</sup> ICs. The tissue was processed within 3 hours. The sample was rinsed by manually shaking for 10 seconds in sterile Hanks' Balanced Salt Solution (HBSS 1 x) (Life Technologies) solution in 50 ml centrifuge tube (Thermo Fisher). The tissue was minced with scissors into small pieces and suspended in HBSS solution. The tissue pieces were then transferred carefully into a centrifuge tube containing 1ml of 0.1% trypsin

(Thermo Scientific 90057). The tissue suspension was transferred in a well plate and put on a shaker at 4° C for 30 minutes. After the incubation period, the tissue was transferred from trypsin to 3 ml RPMI medium (1 x) (Life Technologies) and incubated in a water bath at 37° C for 15 minutes. The tissue was then transferred using forceps into a tube containing 3 ml HBSS and shook gently. This washing step was performed twice before the tissue was incubated in 1 ml of 0.1% collagenase type I (Life Technologies 17100-017) at 37° C for 45 minutes. Tissue was then transferred into 1 ml of RPMI pre-warmed in a water bath at 37° C.

Tissue was triturated using a glass pipette until the tissue was dissociated entirely and then homogenized with RPMI. The homogenate was separated by centrifugation at 4° C at 150 x g for 5 minutes. The supernatant was removed, and the cell pellet was re-suspended into fresh RPMI. The cell suspension was passed through a Falcon 70 µm single-cell strainer (Life Sciences, 352350) harvested cells washed with ice-cold FACS buffer (PBS, 10% BSA and 1% sodium azide) and centrifuged at 150 x g for 10 minutes. The remaining fragments were incubated in fresh collagenase solution for 20 minutes, after which the remaining cell suspension was filtered through Falcon 70 µm single-cell strainer. The filtered cell suspensions were collected and rinsed with ice-cold FACS buffer solution and centrifuged at 150 x g for 5 minutes (**Figure 5.2**) summarize the work-flow of tissue dissociation.

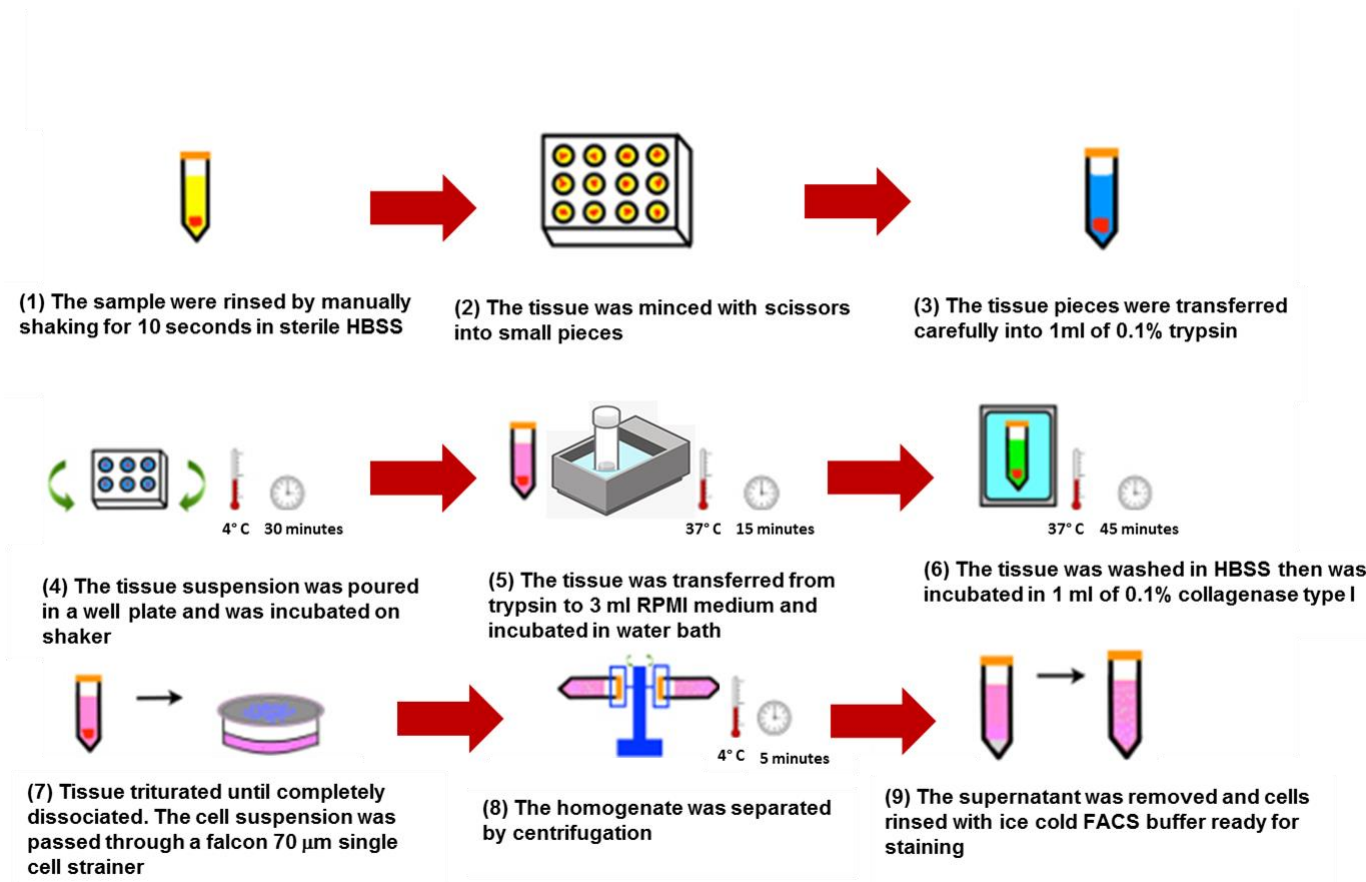


**Figure 5.2 Work-flow for the human colon tissue cell enzymatic dissociation**

Counting was performed using a C-chip disposable hemocytometer (Labtech), and cell counts adjusted to a concentration of  $1 \times 10^6$  cell/ml in ice-cold (FACS buffer). Cells were stained immediately with antibodies diluted with ice-cold FACS buffer solution (CD140a-FITC (PDGFR $\alpha$ ), CD117-PE (cKit), anti-fibroblast (vioblue) (for fibroblast cells) and CD45-vioblue (for mast cells)) all anti-human for 30 minutes at 4° C in falcon tubes to identify ICs and differentiate between them and other cells expressing same markers. After staining, the cells were washed with PBS and resuspended in FACS buffer and kept in the dark on ice until analysis. ICs from the sample were sorted from the cell suspension by BD FACS Melody Cell Sorter (BD Life Sciences, Cat No 95131).

Using a 488 nm excitation laser and a 527/32 nm emission filter, sorting was performed using a 100  $\mu$ m nozzle, with live cells were gated according to their fluorescence intensity. Isolated ICs were collected in 96 well plates filled with 0.5  $\mu$ l RNA-free water (**Appendix 2, Figure B**).

#### **5.3.4 Manual isolation of ICs using microelectrode techniques**

These experiments were conducted to determine if a single IC could be isolated from frozen sections of HD colon for subsequent RNAseq. Colon sample from HD patient (n=1) was collected immediately after dissection in ice-cold Krebs solution prepared fresh in 500 ml dH<sub>2</sub>O (3.51 g NaCl, 0.65 g NaHCO<sub>3</sub>, 1.04 g glucose, 219.78 g KCl, 138.73 g CaCl<sub>2</sub>, 71.98 g NaH<sub>2</sub>PO<sub>4</sub> and 57.13 g MgCl<sub>2</sub>) and was kept oxygenated until the time of collection. The tissue was then embedded in OCT and snap-frozen using dry ice, sectioned using cryostat at different thicknesses (20, 40 and 60  $\mu$ m) mounted on poly-lysine

coated slides and kept at  $-80^{\circ}\text{C}$ . The slide box was then carried in dry ice to perform the microelectrode cell aspiration. The sections were washed in artificial cerebrospinal fluid (ACSF) used for brain slice experiment (NaCl 7.245 g,  $\text{NaHCO}_3$  2.184 g, KCl 0.2237 g,  $\text{MgSO}_4 \cdot 7\text{H}_2\text{O}$  0.4933 g,  $\text{NaH}_2\text{PO}_4$  0.39 g, glucose 1.8 g and 2 ml  $\text{CaCl}_2$  in 1 litre  $\text{dH}_2\text{O}$ ) and a barrier around the sections were made using ImmEdge™ pen (Vector 94010). A microscope (Nikon Eclipse E600FN) combined with a micropipette mounted on a manipulator was used to target individual cells for photography using QCapture computer software Pro 6.0. The micropipette was advanced under visual guidance to cells considered to be IC based on morphological features until indentations in the membrane were observed. Negative pressure was applied through the micro-pipette so that the cell of interest could be aspirated into the pipette **(Figure 5.3)**, then incubated in 3  $\mu\text{l}$  RNase free water for further RNA analysis. Several attempts were tried from different thickness sections; in addition, different concentration of collagenase and elastase were used for different incubation times but were unsuccessful.

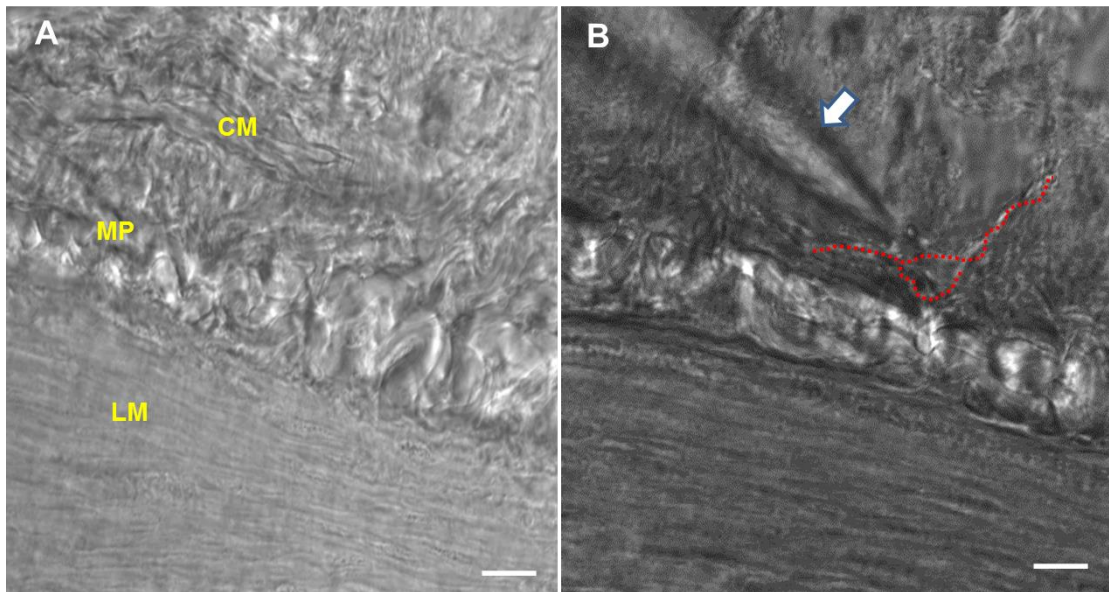


**Figure 5.3 Microelectrode IC aspiration.**

(A) Shows the distinct histological layers of the colon wall. (B) The probe (arrow) approaching the target IC (red) around the MP region. CM-circular muscle, MP- myenteric plexus, LM- longitudinal muscle. Scale bar 50  $\mu\text{m}$ .

### 5.3.5 Targeted RNA sequencing of specific colon wall layers

Since amounts of RNA were obtained from either FACS or manual isolation of ICs were insufficient to carry out the scRNAseq experiments, workflow outlined in (Figure 5.4), another approach using more significant amounts of tissue to provide sufficient RNA was performed. The aim was to target the collection of tissue to specific regions of the colon (e.g. CM, MP, LM). Fresh HD sample proximal and distal parts (n=1) were collected in ice-cold ACSF.

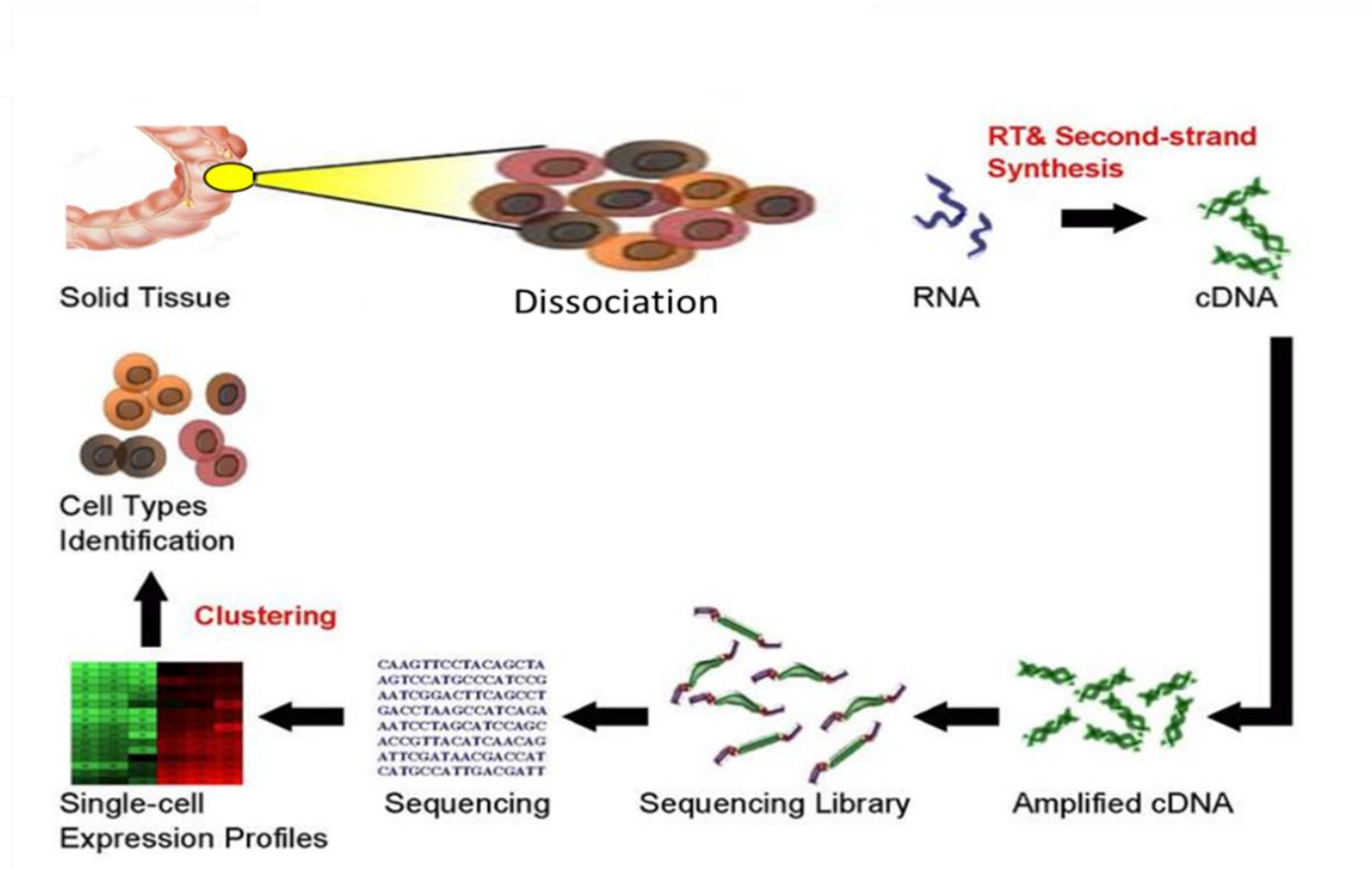


Figure 5.4 RNA Sequencing Workflow.

The proximal, transitional zone (TZ) and distal samples were divided into two sections, one used for the Direct Zol RNA kit (described previously) to extract RNA from the entire tissue specimen. The second part was embedded in OCT and sectioned at 60  $\mu\text{m}$  using cryostat. By using a magnifying microscope and micropipette specific regions were removed from tissue sections. The different layers of the colon wall (CM, MP, LM) were collected in 300  $\mu\text{l}$  Trizol in RNase-free Eppendorf tubes, and the same steps for RNA extraction followed (described earlier in this chapter). The RNA obtained from this step was then diluted to 10 ng/ $\mu\text{l}$  to run it through the SMART-Seq v4 Ultra low Input RNA kit for sequencing (Takara Bio, 634889).

### 5.3.6 cDNA synthesis

Starting with RNA concentration of 10 ng/ $\mu$ l purified in nuclease-free water, the first-strand cDNA synthesis was primed by the 3' SMART-seq CDS Primer II A and use the SMART-Seq v4 Oligonucleotide for template at 5' end of the transcript (both primer and oligonucleotide are included in the SMART-Seq kit). The reactions were done in 0.2 ml RNase free PCR tube a total volume of 10.5  $\mu$ l were formed by adding 8.5  $\mu$ l Nuclease free water, 1  $\mu$ l RNA sample and 1  $\mu$ l of 10X Reaction Buffer (prepared by adding 19  $\mu$ l 10X Lysis Buffer and 1  $\mu$ l RNase inhibitor) the sample then was incubated for 5 minutes at room temperature and then kept in ice. 2  $\mu$ l of 3' SMART-Seq CDS Primer II A (12  $\mu$ M) was added and gently vortexed and then spun down briefly to collect the contents at the bottom of the tube, the tubes were then incubated at 72° C in a pre-heated thermal cycler for 3 minutes and immediately placed in ice for 2 minutes, meanwhile the master mix solution was prepared as follows: 4  $\mu$ l of 5 X Ultra Low First-Strand Buffer, 1  $\mu$ l SMART-Seq v4 Oligonucleotide and 0.5  $\mu$ l RNase Inhibitor, total volume of 5.5  $\mu$ l was needed per reaction, just prior to the use of master mix, a 2  $\mu$ l of SMART Scribe Reverse Transcriptase was added and gently mixed to form a total volume of 7.5  $\mu$ l per sample. The total volume of master mix was then added to the sample tube and placed in the thermal cycler preheated to 42° C and run the following program: 42° C for 90 minutes, 70° C for 10 minutes and kept at 4°C at which point the sample could be stored for later use.

### **5.3.7 cDNA amplification by PCR**

A PCR master mix was prepared by combining the following reagents: 25  $\mu$ l 2 X SeqAmp PCR Buffer, 1  $\mu$ l PCR Primer II A (12  $\mu$ M) 3  $\mu$ l nuclease-free water and 1  $\mu$ l SeqAmp DNA Polymerase a total volume of 30  $\mu$ l per reaction which was added to the 20  $\mu$ l of the first-strand cDNA product in the previous step.

The tubes were incubated in a preheated thermal cycler for the following program: 95° C for 1 minute the 8 X cycles of 98° C for 10 seconds, 65° C for 30 seconds and 68° C for 3 minutes, then at 72° C for 10 minutes and the sample was kept at 4° C.

### **5.3.8 Purification of amplified cDNA**

The PCR- amplified cDNA was purified using Agencourt AMPure XP Kit, where cDNA was immobilized on AMPure XP beads, the beads washed with 80% ethanol and cDNA was eluted in 17  $\mu$ l elution buffer. 1  $\mu$ l of 10 X Lysis Buffer was added to the PCR product followed by 50  $\mu$ l of AMPure XP beads and mixing by pipetting up and down 10 times and the samples incubated at room temperature for 8 minutes. The samples then placed in a magnetic separation device for 5 minutes, while still in the magnetic device the supernatant was removed and discarded. 200  $\mu$ l of 80% ethanol was then added to remove the contaminants and after 30 seconds ethanol was removed and repeat the same washing step. Samples were then dried at room temperature for 2.5 minutes, after which 17  $\mu$ l of Elution Buffer was added to the bead pellet and removed from the magnetic separation device and rehydrated at room temperature for 2 minutes. Samples were placed back in the magnetic separation device for 1 minute until completely clear supernatant containing purified cDNA was formed.

The supernatant was then transferred into a nuclease free tube and stored at -20° C, then validated using Agilent 2100 Bioanalyzer to verify whether the samples were suitable for further processing.

## 5.4 Statistical analysis

All numerical data obtained from Bio-Rad are presented as the mean  $\pm$  standard error of the mean (SEM). One-way ANOVA was used for evaluation of differences between the distal, proximal of HD samples and DC specimens and unpaired t-test to determine the significance between two groups of data with  $p$ -value  $<0.05$  considered as significant.

## 5.5 Results

### 5.5.1 Cell isolation using Fluorescence-Activated Cell Sorting

The aim of this experiment was to determine gene expression within individual IC types. Isolation of different IC types was tried using FACS (**Appendix 2, Figure B**). To isolate PDGFR $\alpha$ <sup>+</sup> IC, all PDGFR $\alpha$  expressing cells were labelled with anti-CD140a-FITC (anti PDGFR $\alpha$ ), but since fibroblasts may also express PDGFR $\alpha$ , they were identified for elimination through sorting by also tagging them with an anti-fibroblast antibody. Similarly, CD 45 antibodies (anti mast cell) and CD117-PE (anti-cKit antibodies) used before FACS cell sorting to isolate only cKit<sup>+</sup> ICs. After sorting, the ICs were processed through the RNA extraction and analysis. Unfortunately, RNA concentration from these single cells was very low as measured by the Qubit 4 Fluorometer.

### 5.5.2 Quantitative Polymerase Chain Reaction (qPCR)

A sufficient amount of RNA for the following experiments was obtained from HD samples (n=4), and DC (n=4), OD 260 /280 ratio of all samples was more than 1.8 as shown in (**Appendix 2, Figure C**); therefore all samples were considered to be of high purity. Furthermore, the quality of the cDNA created from the RNA was determined by gel electrophoresis. Gene expression was normalized against expression of GAPDH, expression of all genes of interest was significantly reduced in the distal part of the HD samples relative to both proximal (**Figure 5.5**) and DC specimens (**Figure 5.6**) with ( $p < 0.05$  considered as significant). cKit gene expression in the distal part of HD was 31.1% of that in the proximal part (P  $0.4 \pm 0.02$ , D  $0.13 \pm 0.01$ ), and proximal part of the HD sample was 48% of the disease control samples (P  $0.4 \pm 0.02$ , DC  $0.83 \pm 0.3$ ). Ano1 gene expression in the distal part was 22.7% of the proximal HD samples (P  $0.61 \pm 0.03$ , D  $0.14 \pm 0.01$ ) and the proximal make 63% of DC samples (P  $0.61 \pm 0.03$ , DC  $0.96 \pm 0.02$ ). For PDGFR $\alpha$  the distal was 30% of the proximal HD parts (P  $0.43 \pm 0.03$ , D  $0.13 \pm 0.01$ ) while the proximal make 51% of DC (P  $0.43 \pm 0.03$ , DC  $0.83 \pm 0.03$ ). SK3 showed a difference between the distal and proximal parts of HD samples of 21% (P  $0.6 \pm 0.02$ , D  $0.13 \pm 0.01$ ) and between the proximal and disease control of 71.8% (P  $0.6 \pm 0.02$ , DC  $0.8 \pm 0.2$ ).

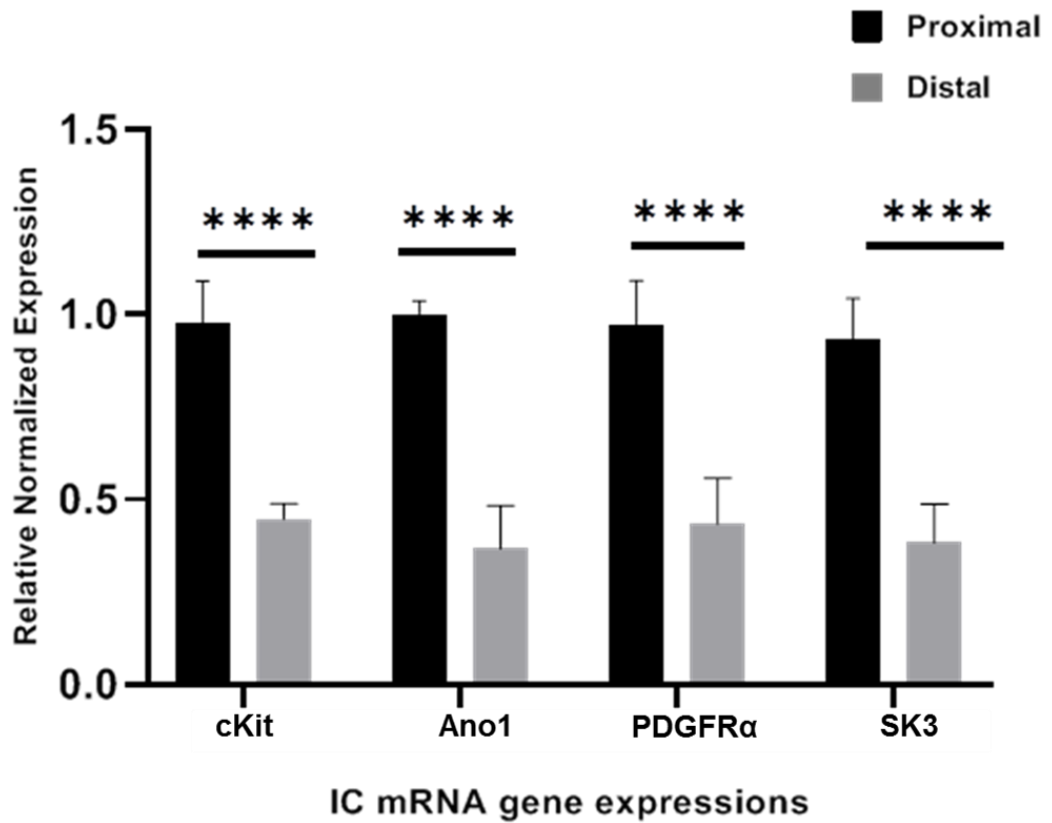


**Figure 5.5 qPCR revealed significantly decreased relative mRNA expression levels of ICs marker genes ( $p < 0.0001$ ) in the proximal HD specimen compared to the distal specimen, results are presented as mean  $\pm$  SEM,  $n=4$ .**

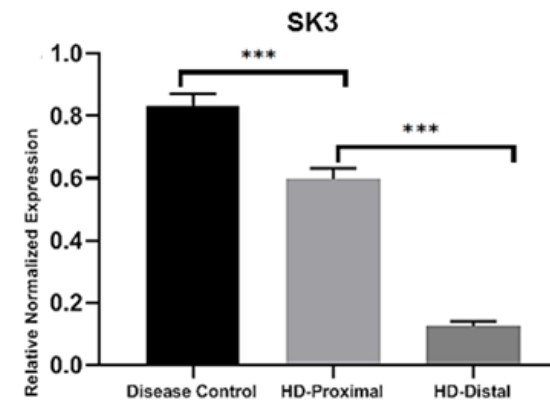
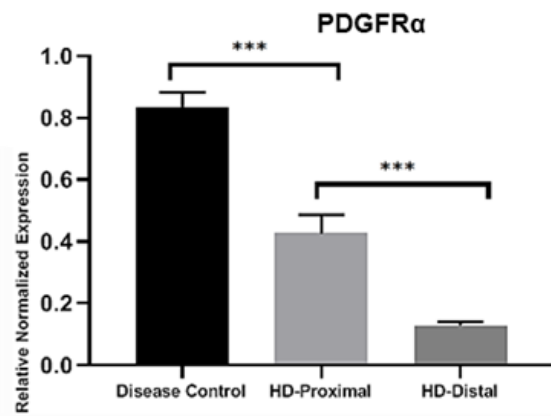
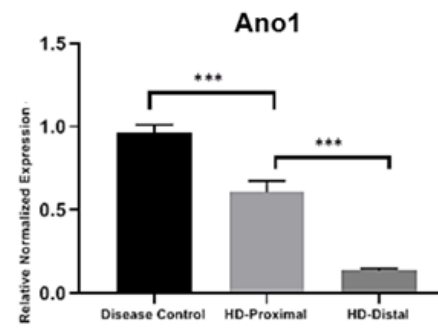
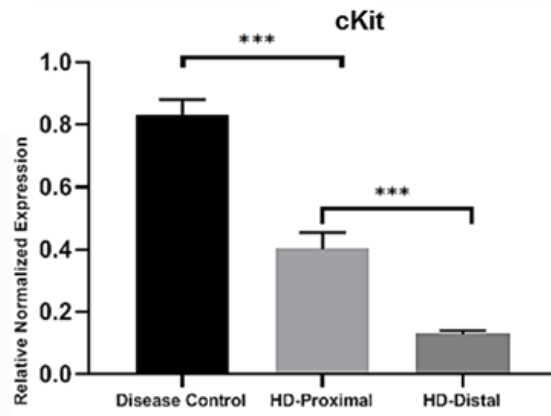


**Figure 5.6 Relative normalized IC genes expression in the two different parts of HD as compared to the DC samples. IC- Interstitial Cells, HD- Hirschsprung Disease, DC- disease control (\*\* $p < 0.001$ )**

### 5.5.3 RNAseq: Validation of cDNA from targeted RNA using Agilent 2100 Bioanalyzer

The quality of the cDNA samples created from RNA extracted from the tissue microdissection using a manual technique was analyzed using Bioanalyzer. No product was detected with the negative control supplied in the SMART-Seq v4 Ultra low Input RNA kit (**Figure 5.7 A**). A distinct peak was present in the positive control (**Figure 5.7 B**). An example of the HD positive sample cDNA analysis of the HD sample is shown in (**Figure 5.7 C**), which yielding approximately 159.22 pg / $\mu$ l of cDNA. The data is also displayed as a gel-like image (**Figure 5.7 D**).

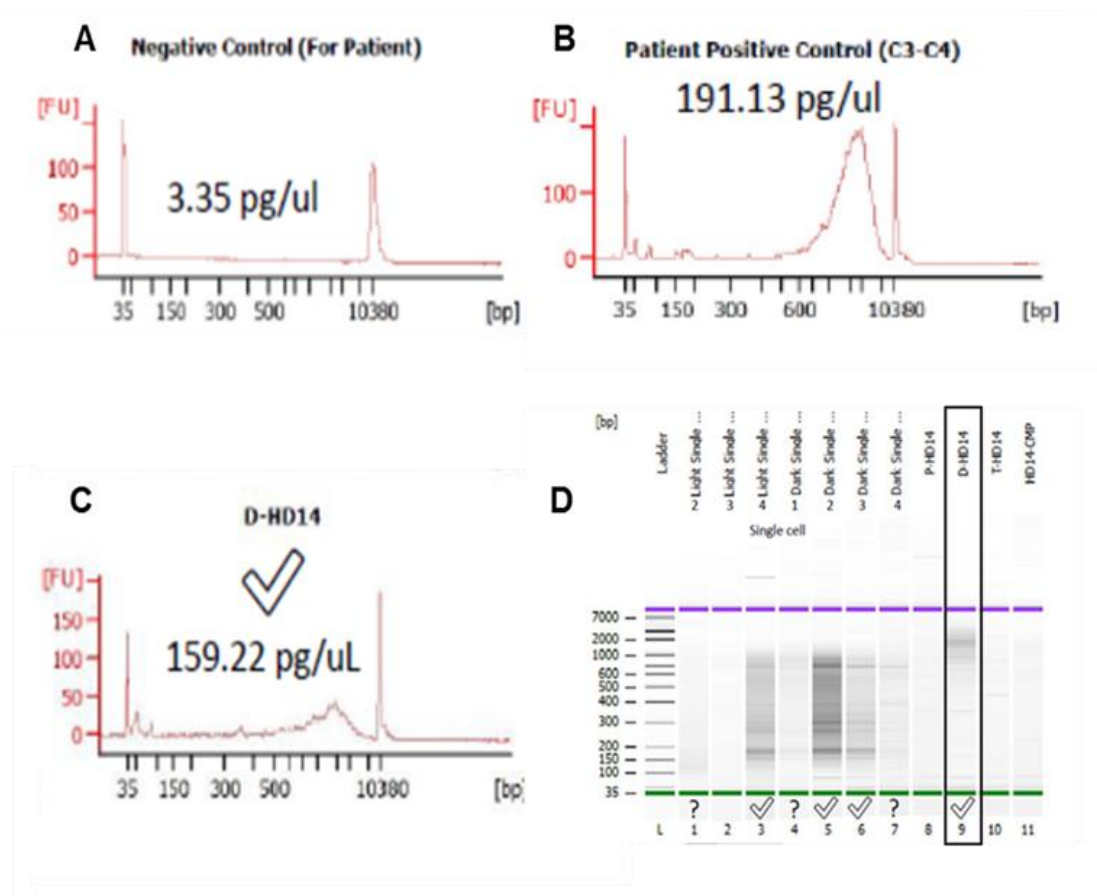


**Figure 5.7 Agilent 2100 bioanalyzer results of the HD sample.**

Data are displayed as electropherograms (**A-C**). (**A**) Negative control no product was detected. (**B**) Positive control a concentration of 191.13 pg/ $\mu$ l was detected. (**C**) HD sample cDNA concentration of 159.22 pg/ $\mu$ l. (**D**) Gel-like image for the sample.

#### 5.5.4 Library preparation for sequencing

Library preparation was carried out at St James Next-Generation Sequencing (NGS) Facility (<http://dna.leeds.ac.uk/genomics/>). The cDNA output of the SMART-Seq v4 Ultra Low Input RNA kit for sequencing was processed with Nextera XT DNA Library Preparation Kits (Illumina, Cat. No: FC-131-1024 and FC-131-1096), the work-flow of the RNAseq process is summarized in **(Figure 5.8)**, and the main steps are illustrated in **(Figure 5.9)**.

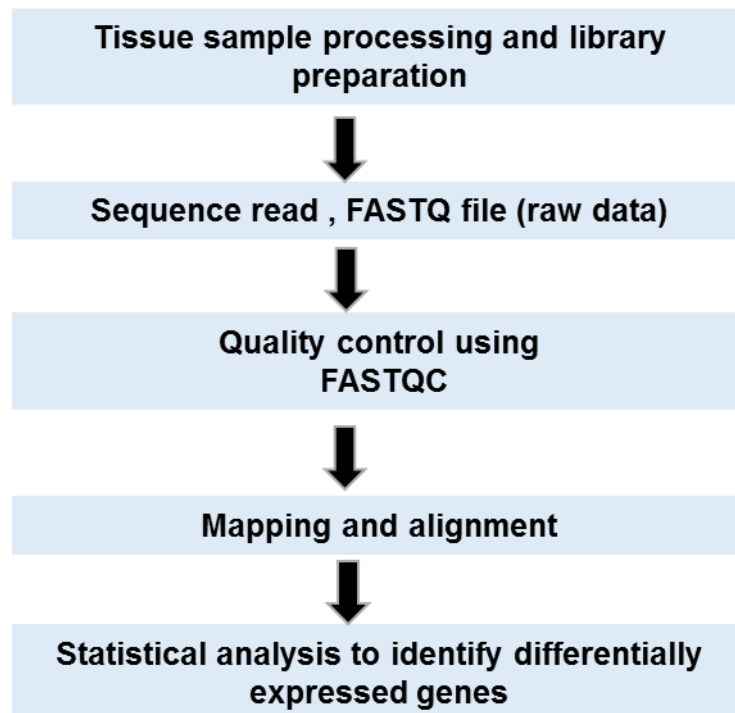


**Figure 5.8** The work-flow of RNAseq experiment

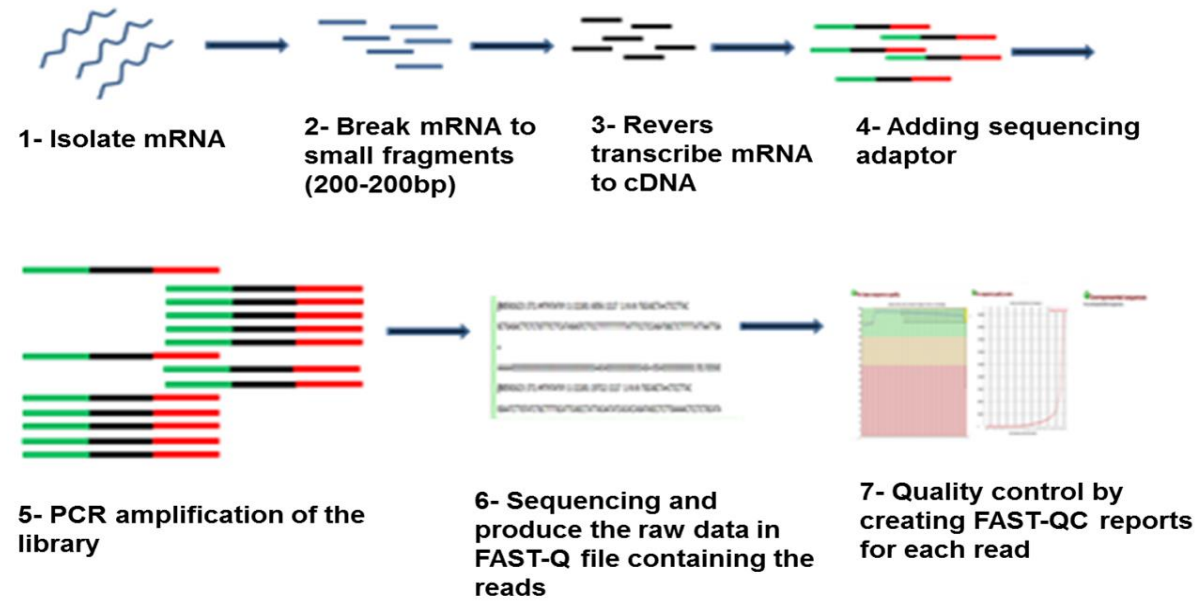


Figure 5.9 Summary of RNAseq experiment steps

### 5.5.5 Unmapped read data (FASTQ)

The RNAseq raw data were received from the St James NGS Facility in FASTQ file format and contains paired-end sequencing reads. This file contains the nucleotide sequence of each read and a quality score at each position. An example of the FASTQ file of HD samples with paired-ended reads R1 and R2 are shown in **(Appendix 2, Figure D)**.

### 5.5.6 Assessing quality using FAST-QC

FAST-QC provide a simple way to run some quality control (QC) checks on the raw sequence data in the FASTQ files by using the RiboGalaxy (<https://ribogalaxy.ucc.ie/>). The main aims of FAST-QC are: import the raw data in the form of FASTQ files, provide a quick overview of the raw data, provide summary graphs and tables to quickly assess our data **(Appendix 2, Figure E)** shows examples of the graphs provided by the FAST-QC report. The QC for sequencing data includes the number of raw reads produced by the sequencing machine, the number of cleaned reads, the percentage of reads passing the sequencing score filter, and the percentage of uniquely mapped reads **(Table 5.3)**.

These data were analyzed in the Bioinformatics data analysis department at the University of Leeds. The clean reads were aligned to the reference genome; the reads of this experiment were aligned to Human (hg 38) reference genome using the STAR read aligner. The expression levels of transcripts with RPKM (number of Reads Per Kilo-bases of the transcript, per Million of

mapped reads) values were  $\geq 1$ . The cut-off FC  $> 2$  considered upregulated, whereas FC  $< 0.5$  is for downregulated genes.

Table 5.3 Summary of the quality control for sequencing data

Sample	The number of raw reads	The number of Clean reads	Percentage	STAR uniquely mapped Reads rate
R_CM_D	5124170	5116034	99.84%	84.99%
R_CM_P	4517138	4510877	99.86%	86.13%
R_LM_D	4707158	4700530	99.86%	83.90%
R_LM_P	4521923	4513533	99.81%	81.08%
R_MP_D	3969843	3964388	99.86%	86.36%
R_MP_P	3486630	3478375	99.76%	73.68%
R_Proximal	5235760	5226023	99.81%	72.72%
R_Transitional	5422784	5406167	99.69%	67.29%
R_Distal	4147454	4141747	99.86%	86.31%

CM- Circular Muscle, D- Distal, LM- Longitudinal Muscle, MP- Myenteric Plexuses, P- Proximal, R- Read

### 5.5.7 Calculating expression levels

The calculation of gene expression level (RPKM) is based on the reads aligned to the genome. The RPKM value is calculated for each gene, and the overall similarity between the samples was assessed and plotted using a principal components plot (**Figure 5.10**).

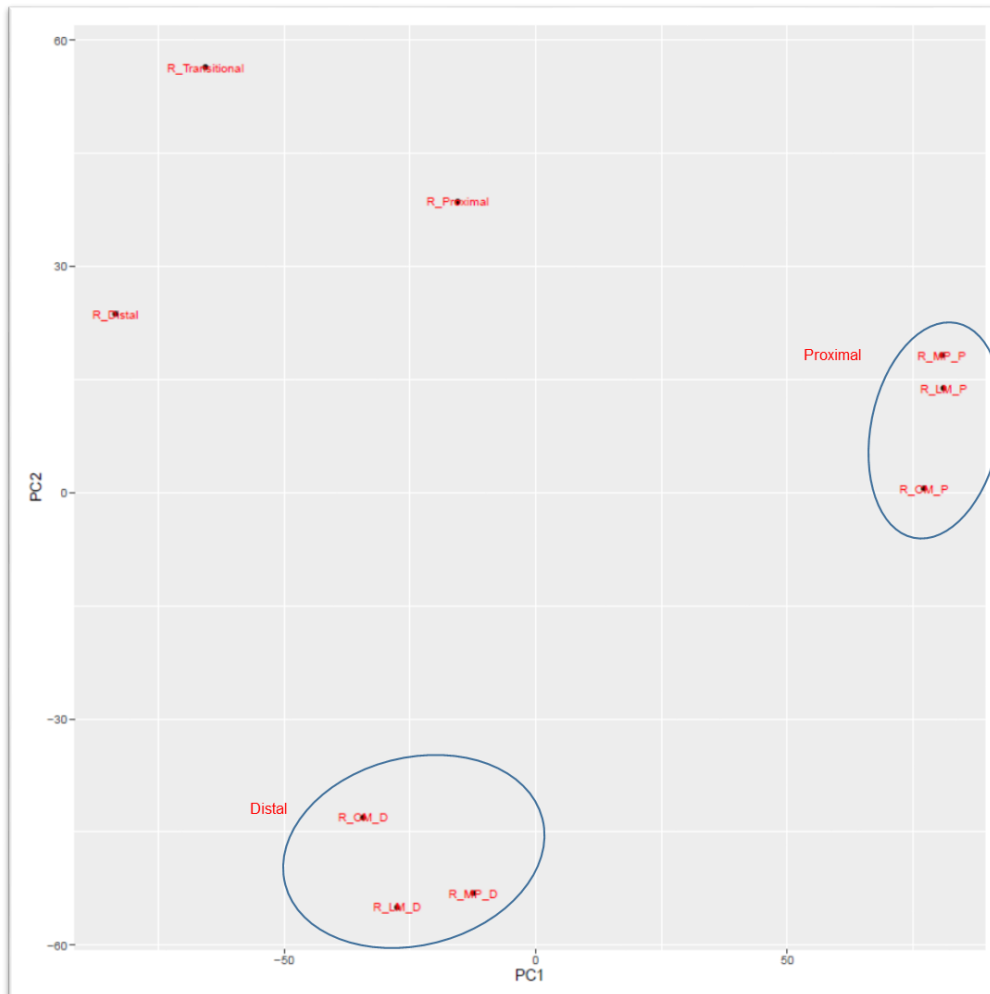


**Figure 5.10 Principal component (PC) analysis plot describes the similarities between gene expression values of Hirschsprung disease samples.**

The proximal samples are clustered together as well as the distal samples show similarities between the gene expression values, whereas the differences are apparent between the proximal, transitional and distal samples. MP-Myenteric Plexus, CM- Circular Muscle, LM- Longitudinal Muscle, D-Distal, P-Proximal.

### 5.5.8 Visualizing gene expression

We selected 54 genes most of them popular are known to contribute to HD development, some ion channel encoding genes were also selected to create a big heat map and visualize gene expression in the different experimental samples in which expression of each gene is scaled (**Figure 5.11 A**). From the figures, a difference in the gene expression between the samples can be seen, with the distal diseased segment being the one with the most down-regulated genes (**Figure 5.11 B**). The up-regulated genes and down-regulated genes are illustrated with different colour annotations.

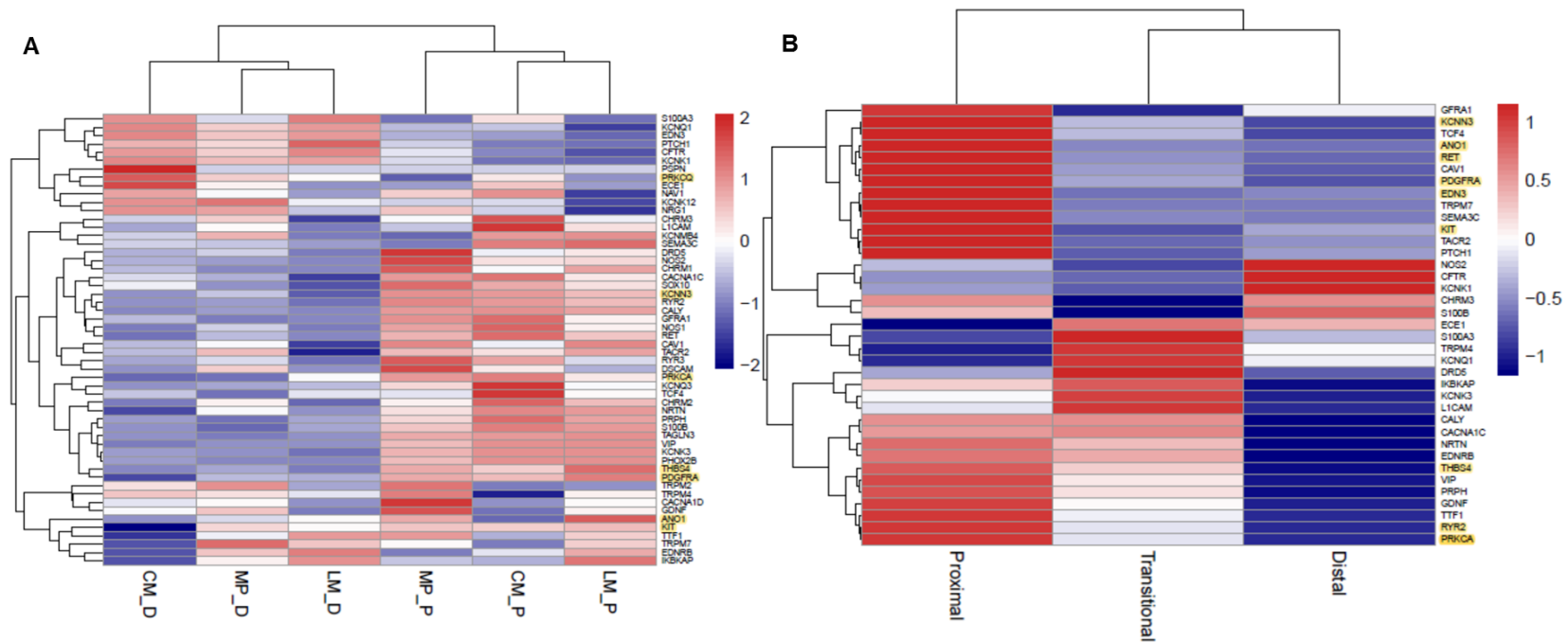


**Figure 5.11** Heat map of 9 samples from HD for the selected genes.

The samples were clustered based on the similarity of gene expression. **(A)** Illustrates the differentially expressed genes in different histological layers of HD colon sample. **(B)** Shows the differentially expressed gene between the three segments of HD colon. The colour bar on the right side demonstrates the  $\log_2$  fold change from comparisons of distal to proximal segments. Red and blue represent genes upregulated and downregulated.

### **5.5.9 Functional analysis of differentially expressed genes (DEG) and identifying the most up-regulated and down-regulated genes**

To identify functional groups of DEGs, gene ontology (GO) was applied to characterize the RNAseq data. Separate GO term analysis using WEB-based Gene Set Analysis Toolkit (<http://www.webgestalt.org/>) for the whole list of raw data genes were carried out. From (15247) total number of genes, (7629) were downregulated genes and (6309) were upregulated genes. Additional GO term analysis was performed for down-regulated and up-regulated genes. Furthermore, they were grouped into different functional groups according to the GO term analysis for biological process, cellular component and molecular functions (**Appendix 2, Figures F1, F2, F3**) represents these functional groups in different HD samples in addition to the number of the genes in each category. The top 20 GO terms of downregulated DEGs and top 20 GO terms of upregulated DEGs involved in biological process functions were chosen according to  $\log_2$  fold change  $< -1$  and  $\log_2$  fold change  $> 1$  respectively (**Figures 5.12, Figures 5.13**) (**Appendix 3, Table 1, Table 2**). Interestingly, the most significantly upregulated DEGs were involved in the GO terms related to immune activation and processing, such as leukocyte activation, immune system process, immune responses and cell activation.

In contrast, the most significantly downregulated DEGs were related to metabolism, mainly involved in the nucleic acid metabolism process, cellular metabolic process, cellular nitrogen compound metabolic process and RNA

metabolic process. Among all GO terms the most significant upregulated genes were *PNP*, *CXCL8*, *CXCL13* and *CD22* and among the most significant downregulated genes were *HRAS*, *HOXD9*, *HOXA3*, *HOXB5* and *SOX6*.

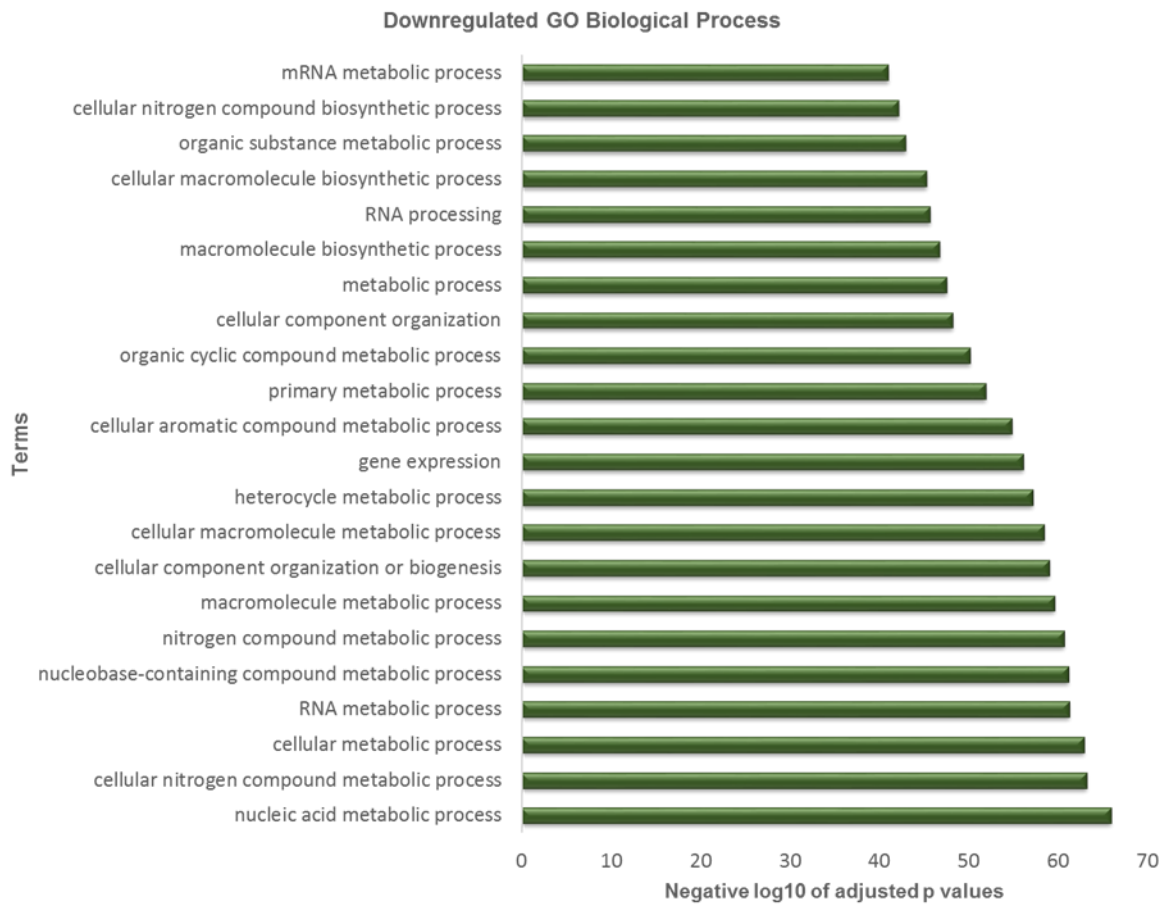


**Figure 5.12 The Gene Ontology term analysis of biological process for the top 20 most down-regulated genes between the distal and proximal HD segments.**

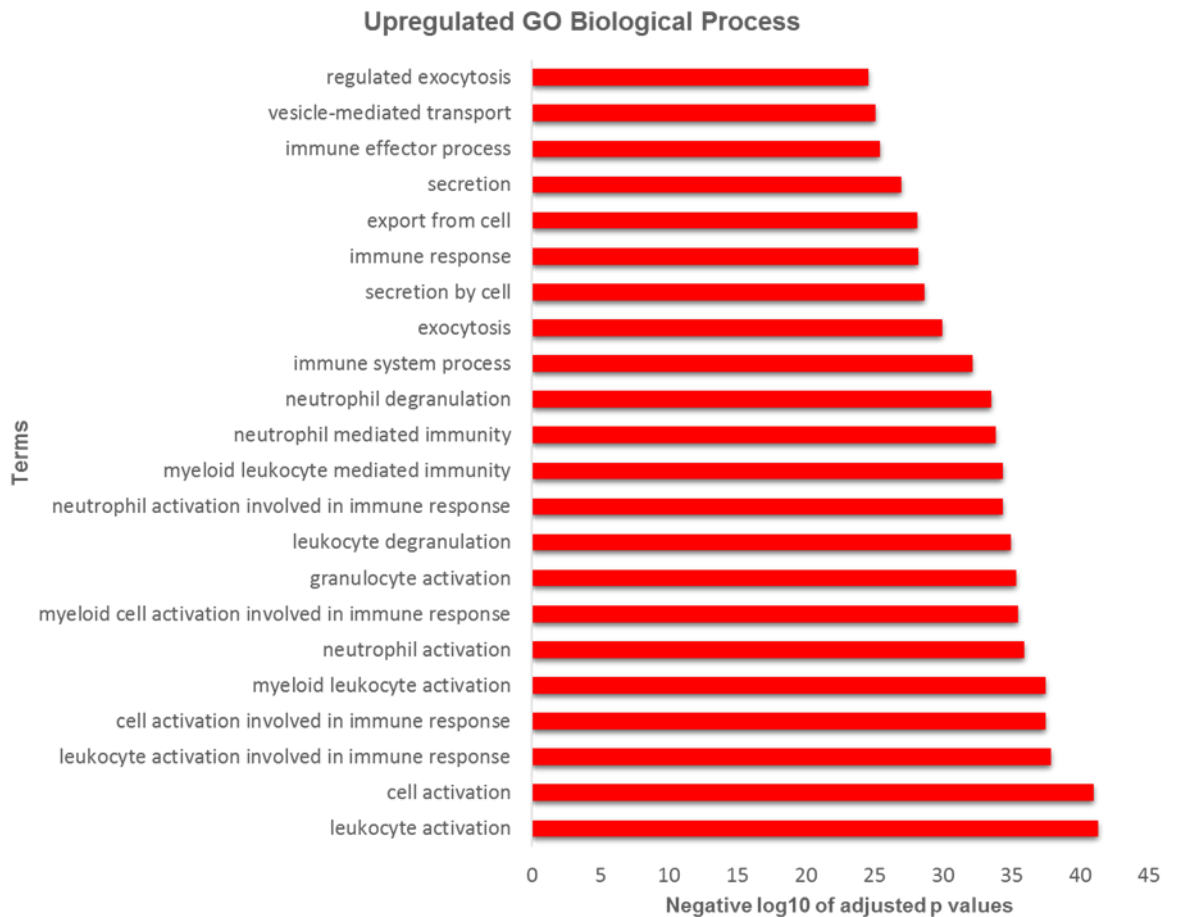


**Figure 5.13 The Gene Ontology term analysis of biological process for the top 20 most up-regulated genes between the distal and proximal HD segments.**

### **5.5.10 Kyoto Encyclopedia of Genes and Genomes (KEGG) pathway analysis**

The gene list was mapped to the KEGG pathway. In general, genes were mapped into 11 KEGG pathways for the downregulated genes and 45 KEGG pathways for the up-regulated genes of the distal vs proximal HD segments.

The top 13 upregulated KEGG pathways and top 11 downregulated KEGG pathways are shown in **(Figure 5.14)**, and results are illustrated in **(Appendix 3, Table 3 and Table 4)**. The genes were grouped in various pathways such as the metabolic pathway and apoptosis for the upregulated genes, on the other

hand for the downregulated genes the KEGG pathways were mainly involved in RNA transport and RNA degradations. Among all KEGG pathway, up-regulated genes were *HLA-DOB*, *SOCS3*, while the down-regulated genes involved in the KEGG pathway were *EXOSC6*, *EXOSC8*, *SRSF1* and *HRAS*. These GO terms and KEGG pathways are of significant importance as they could help to understand the role these DEGs played in HD.

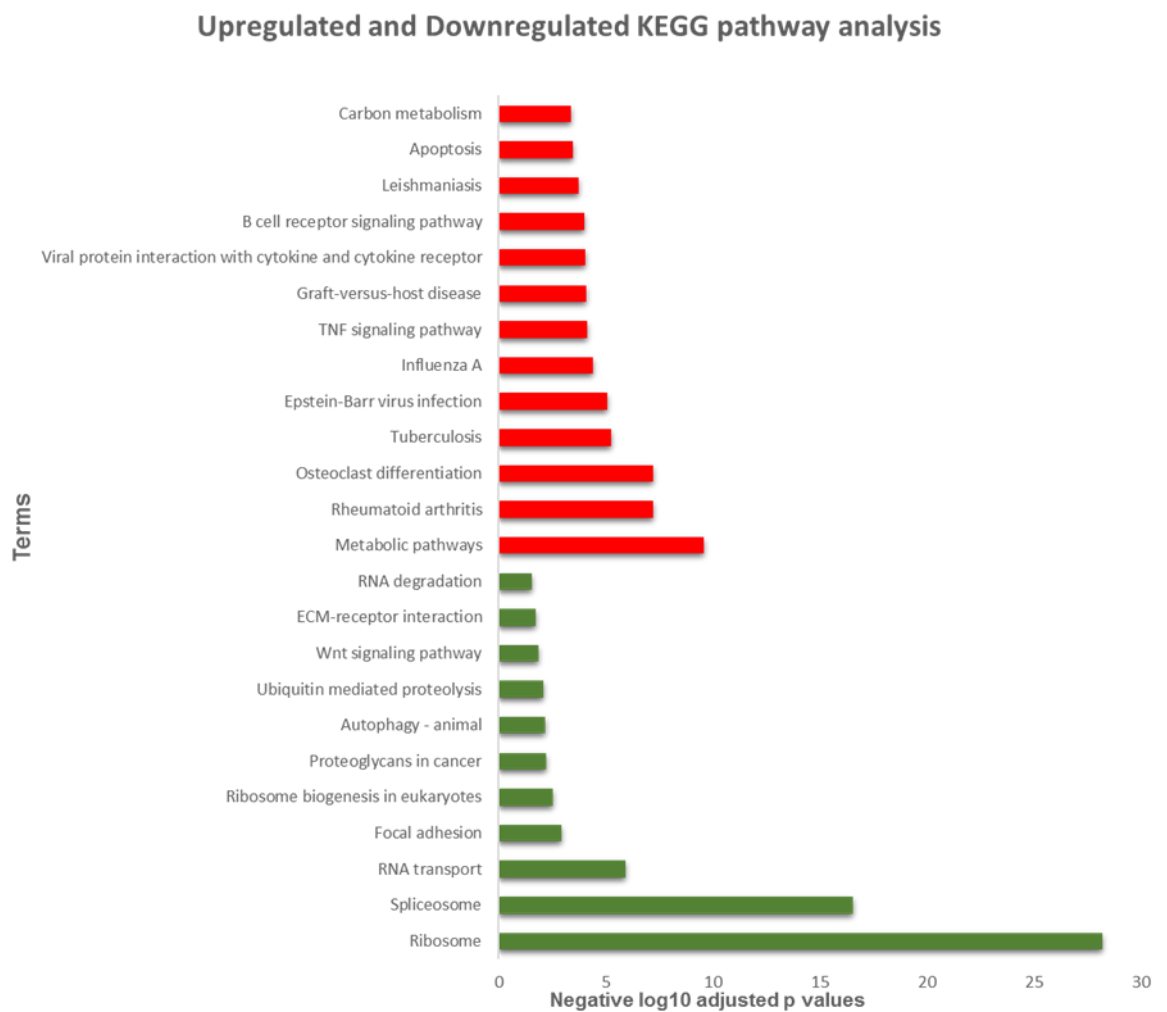


**Figure 5.14 The Kyoto Encyclopaedia of Genes and Genomes pathway analysis for the up-regulated (red) and down-regulated (green) genes of the distal vs proximal HD segments.**

### 5.5.11 Known genes contributing to HD development

Genes collected from previous research that is known to have a role in the development of HD pathology (**Chapter 1, Table 1.3**) were selected in this experiment for comparison. Those genes namely: *RET*, *GDNF*, *GFRA1*, *EDNRB*, *EDN3*, *ECE1*, *PHOX2B* and *SOX10*. However in our experiment the comparisons of those genes was widely considered in which different HD segments were involved (Proximal, Transitional and Distal) (**Figure 5.15**) the gene expression levels shown as RPKM values revealed that the levels of expression were reduced in the HD samples especially the distal segment as for the *SOX10* gene the level of expression was absent in the three segments, whereas *PHOX2B*, *RET* and *GDNF* expression levels were absent from the distal segment. In contrast, for the *EDN3* in which the expression levels in the transitional and distal segments was not much reduced as compared to the proximal segment. For *ECE1* the expression levels in the transitional and distal segments were even higher than that of the proximal segments, however, being only one HD sample that is used in this experiments these finding needs to be validated by using large sample numbers.

Furthermore, the expression of these genes was also compared in the different histological layers of HD sample proximal and distal (CM, MP, LM) (**Figure 5.16**) (**Figure 5.17**). The expression levels of *RET*, *SOX10* and *PHOX2B* were absent in the distal layers as compared to the proximal layers. Again these findings need further validation due to the sample number.

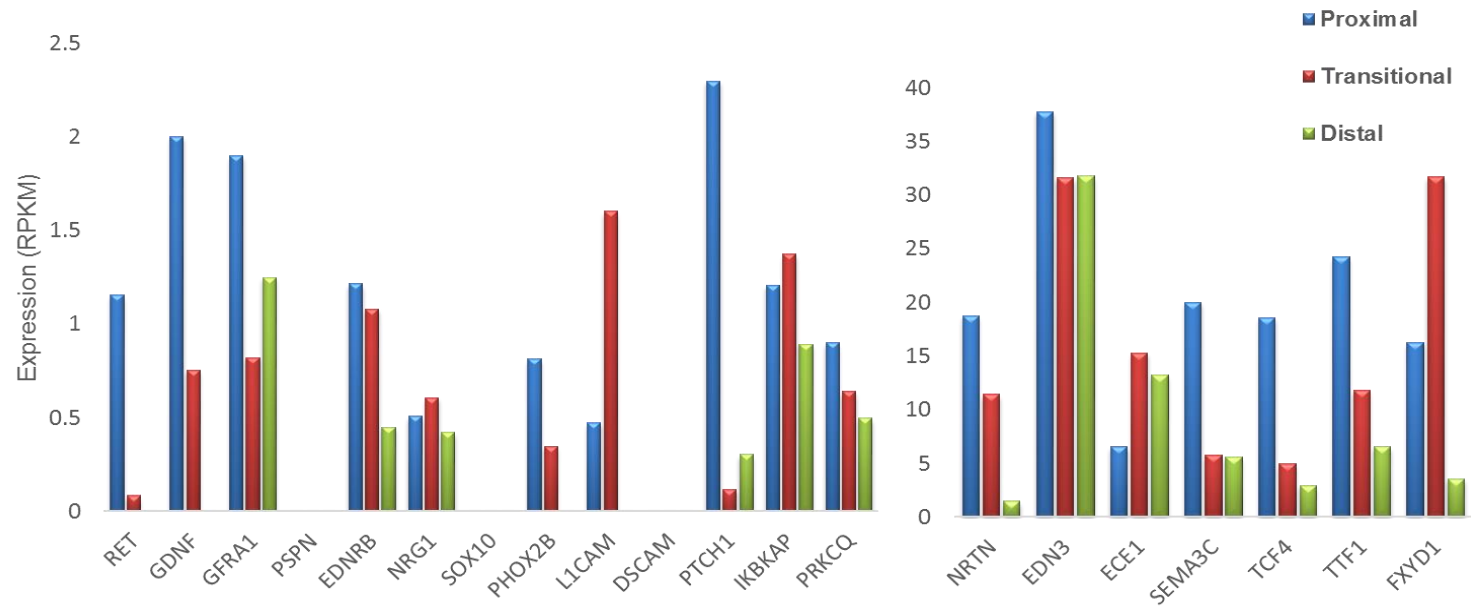


**Figure 5.15 The RPKM for the genes known to contribute to the HD development in the proximal, transitional and distal segments of HD.**

Apart from *EDN3* and *ECE1* genes all other genes show considerable reduction or absence in the distal segment of HD, these genes were also reduced in the transitional segments. *SOX10*, *PHOX2B*, *RET* and *GDNF* were all downregulated in the distal segment of HD colon.

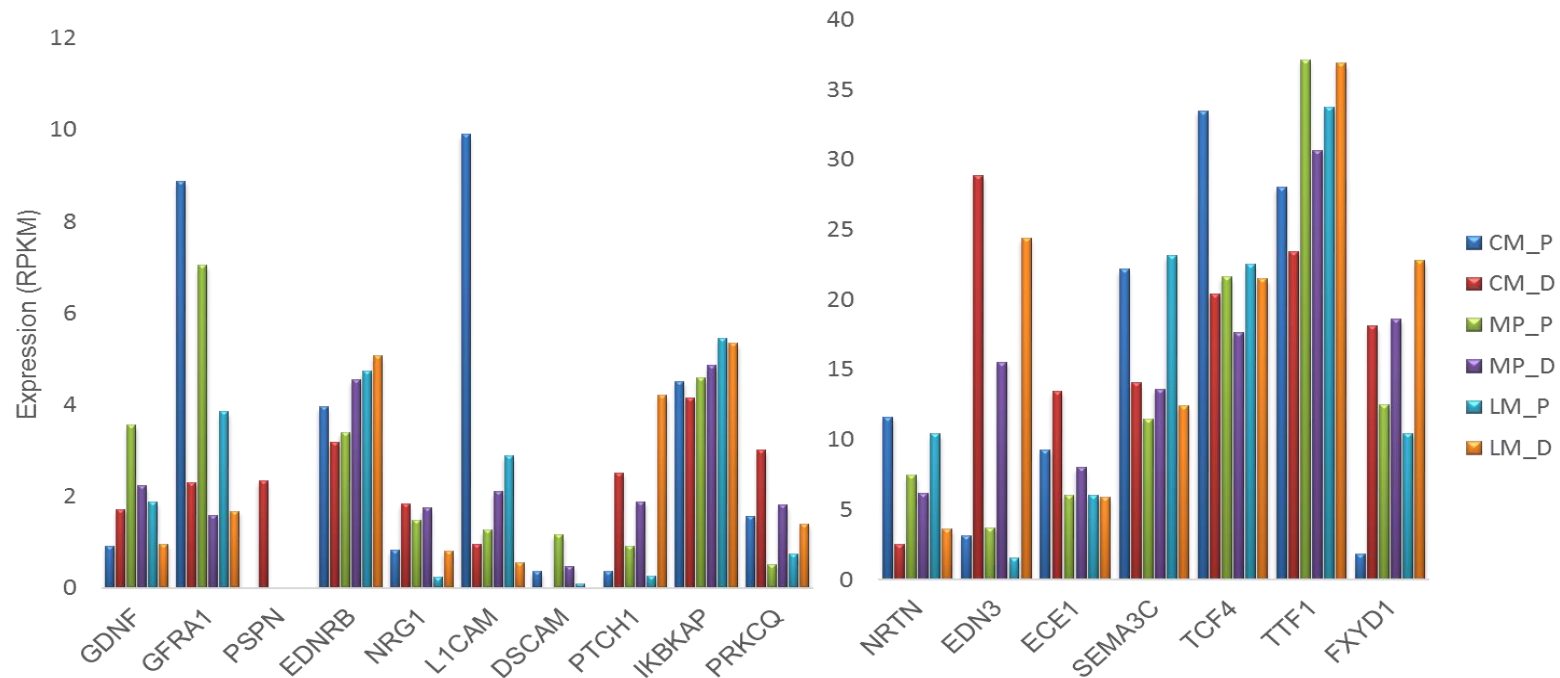


**Figure 5.16 The RPKM for the genes known to contribute to the HD development in the distal compared to the proximal different histological layers of HD colon.**

Huge variation was observed of the expression levels of some genes that are known to contribute to the development of HD. CM- Circular Muscle, LM-Longitudinal Muscle, MP-Myenteric Plexuses, D-Distal, P-Proximal.

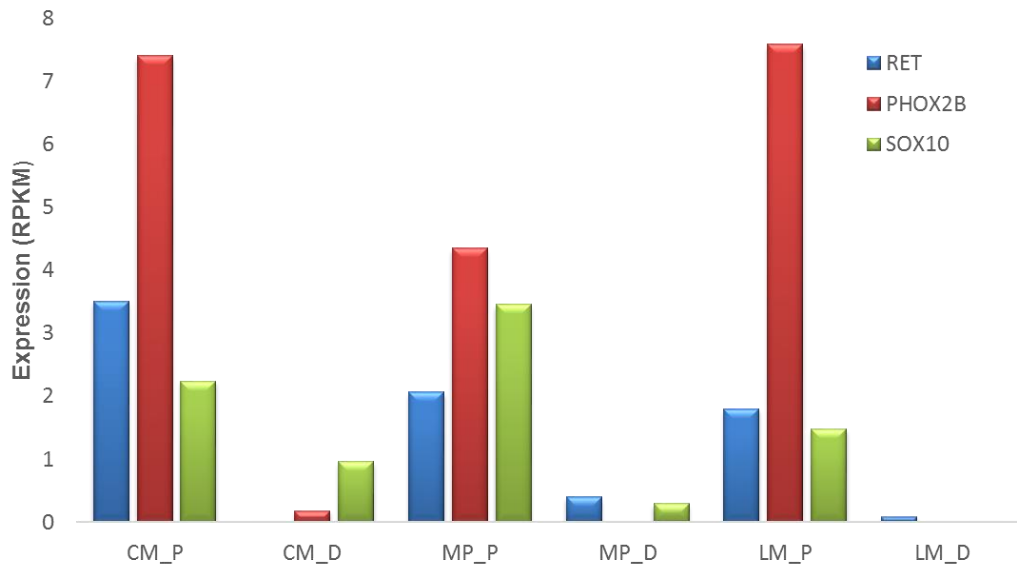


**Figure 5.17** The RPKM for the genes known to contribute to the HD development in the different histological layers of the wall of the colon of HD.

The expression of *RET*, *SOX10* and *PHOX2B* were much reduced in the distal segment as compared to the proximal segment.

### 5.5.12 Genes expressed in the ICs

Genes which are highly expressed in ICs (*KIT*, *PDGFRA*, *ANO1* and *KCNN3*), that were tested using qPCR technique were also selected to validate our qPCR results by measuring the RPKM values in the different HD segments (proximal, transitional and distal) and different histological layers (CM, MP, LM) (**Figure 5.18**) (**Figure 5.19**). Specific genes for cKit<sup>+</sup> ICs that were identified by Lee Moon and his colleague using mice colon tissue namely *PRKCQ*, *PRKCA* and *THBS4* (Lee et al., 2017), were chosen in our human HD colon samples. The protein encoded by *PRKCQ* is protein kinase C (PKC), which is required for the activation of specific transcription factors. Lee et al. (2017) by analyzing the transcriptome of copGFP-labeled mice cKit<sup>+</sup> ICs from colon tissue revealed

that cKit<sup>+</sup> ICs were enriched in *Ano1*, *Kit* and *PRKCQ* genes which were considered as a known cKit<sup>+</sup> ICs markers (Lee et al., 2017).

*THBS4* involved in cell to cell interactions (Human-NCBI), was found to be a new gene expressed by cKit<sup>+</sup> ICs. Interestingly, these genes were found to be down-regulated in HD distal segment as well as in the MP-D layer in our experiment.

The proteins encoding by *PRKCA* gene encodes protein kinase C (PKC) which required for different cellular functions, including regulation of cardiac myocytes contractility by controlling Ca<sup>2+</sup> levels in myocytes (Braz et al., 2004). This gene expression was compared in the distal vs proximal samples, and it was found to be downregulated in the distal segments compared to the proximal (**Figure 5.20**) which might reflect a similar mechanism of smooth muscle cell contraction in the colon musculature resembling that of the cardiac myocytes.

The RPKM values for these genes were all reduced in the distal layers compared to the proximal layers, which were consistence with our qPCR results. However, the RPKM values of *PDGFRA* gene were higher in the different layers of the distal part of HD as compared to the RPKM values of the other genes in the layers of the distal segments (**Figure 5.19**), which might reflect a compensatory mechanism of the constricted SMCs of HD distal colon to relax.

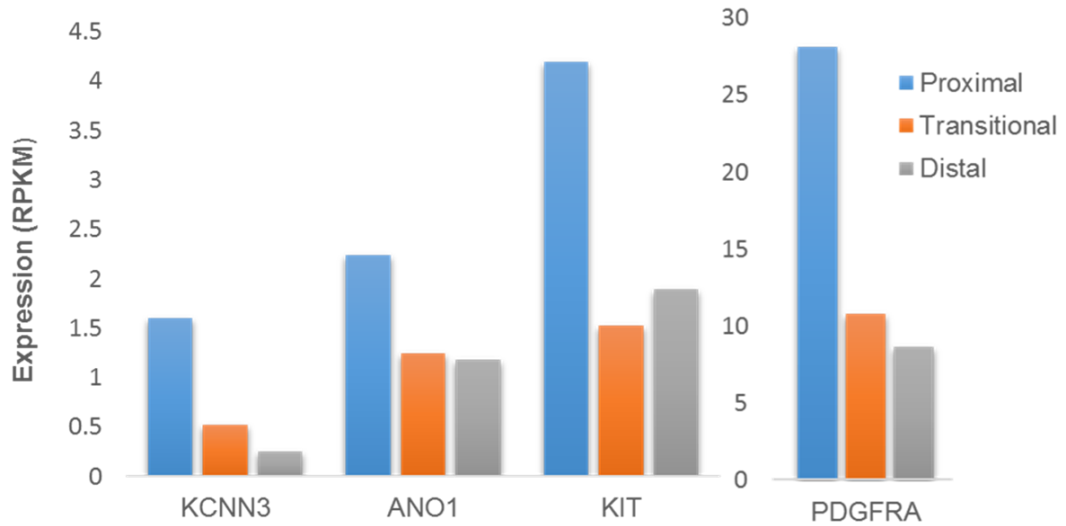


**Figure 5.18** The RPKM for the genes highly expressed in the ICs.

All gene expressions were reduced in the distal segment of HD sample as compared to the proximal sample.

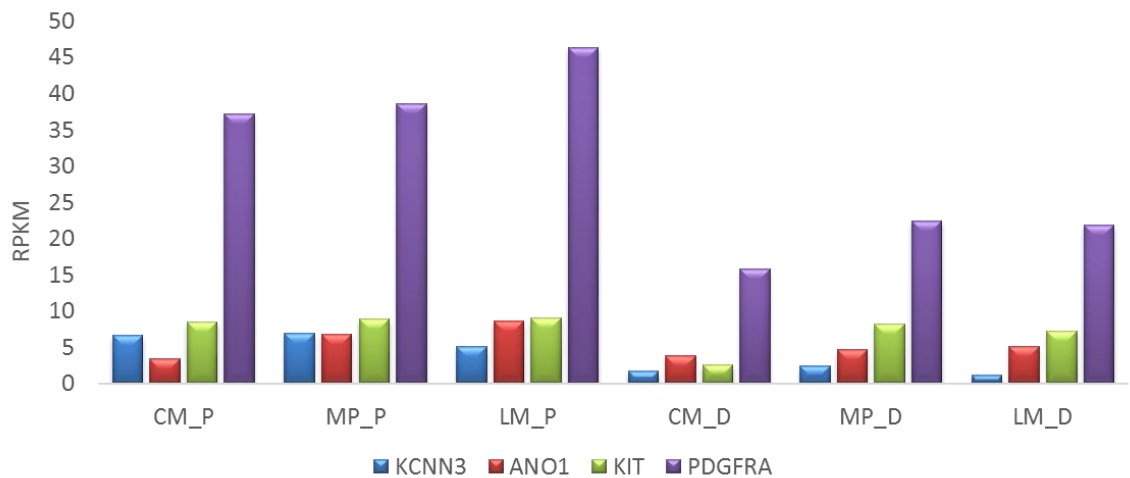


**Figure 5.19** The RPKM for the genes highly expressed in the ICs.

All gene expressions were reduced in the different histological layers in the distal segment of HD sample as compared to the layers in the proximal sample.

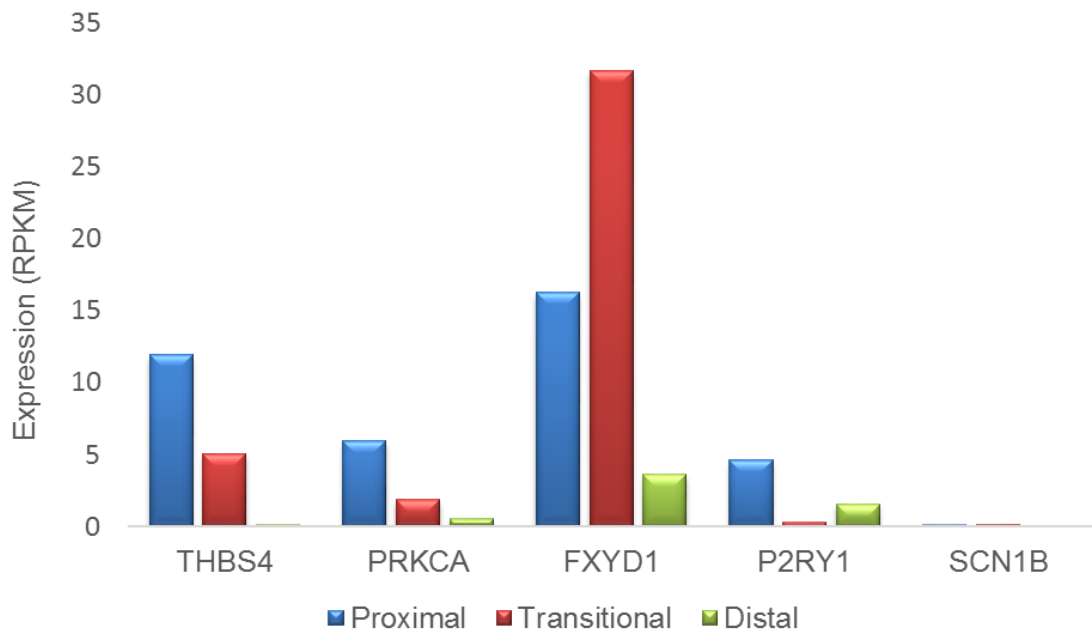


**Figure 5.20 RPKM values of genes that are exclusively expressed by ICs.**

### 5.5.13 Genes related to Ion channels proteins

Specific genes which express functional proteins that influence cell excitability such as neurotransmitter receptors proteins (muscarinic receptors, purinergic receptors and nitrenergic receptors) or ion channels proteins were selected to measure the RPKM values in HD samples. Those genes are *P2RY1*, *RYR2*, *RYR3*, *CAV1*, *NAV1*, *CFTR*, *KCNQ1*, *CACNA1C*, *TRPM2*, *TRPM4*, *TRPM7*, *NOS1*, *CHRM1*, *CHRM2*, *CHRM3*, *TACR2* and *S100B* illustrated in heat- map **(Figure 5.11 A and B)**. The levels of gene expression were measured in HD (proximal and distal) segments, the log<sub>2</sub> fold changes of distal vs proximal segments shown in **(Figure 5.21)**. The same list of genes was compared in the distal myenteric region vs the proximal myenteric region, and the log<sub>2</sub> fold change is shown in **(Figure 5.22)**. Genes encoding ryanodine protein receptor

(*RYR2*, *RYR3*) an ion channel proteins that regulate  $\text{Ca}^{2+}$  influx thus influence cellular activity (Nakamura and Puri, 2019), and genes express muscarinic protein receptors (*CHRM1*, *CHRM2*, *CHRM3*) for acetylcholine neurotransmitter, which are involved in the role of ICs were investigated. These genes were downregulated in the distal diseased segment of the HD colon as compared to the proximal part. Additionally, the inhibitory nitroergic neurotransmission belongs to nitric oxide synthase enzyme encoded by *NOS1* gene was found to be downregulated in the distal part compared to the proximal part, as shown in **(Figures 5.11)**. This finding was reinforced by the GO term analysis, which showed that some of the downregulated genes were related to cellular nitrogen compound biosynthetic process and nitrogen compound metabolic process.

These significantly differentially expressed genes could be a focus of further researches as these genes are highly contributing to the cellular function and could be a good therapeutic target for HD.

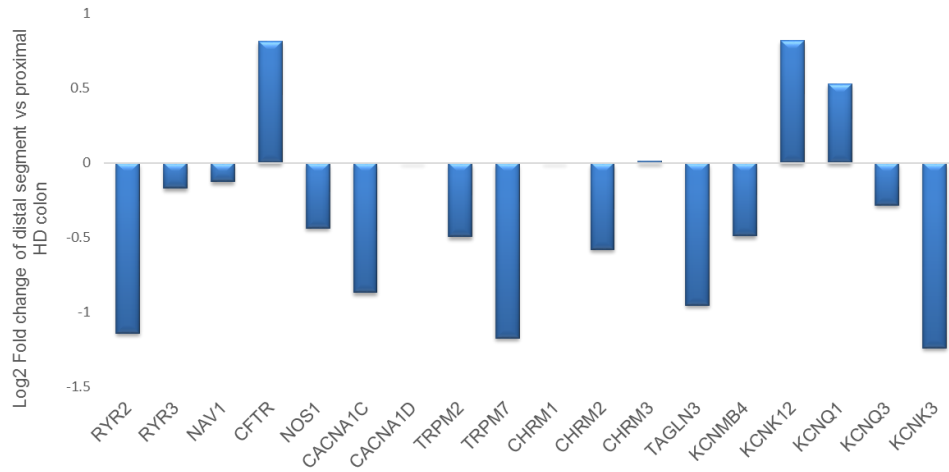


**Figure 5.21 The log<sub>2</sub> fold change of certain functional genes in the distal vs proximal segments of HD colon.**

The expression of certain genes (*RYR2*, *RYR3*, *CACNA1D*, *NOS1*, *NOS2*, and *CHRM2*) were down regulated in the distal part of HD colon sample relative to proximal part. These include of ryanodine, muscarinic and the nitrenergic genes.

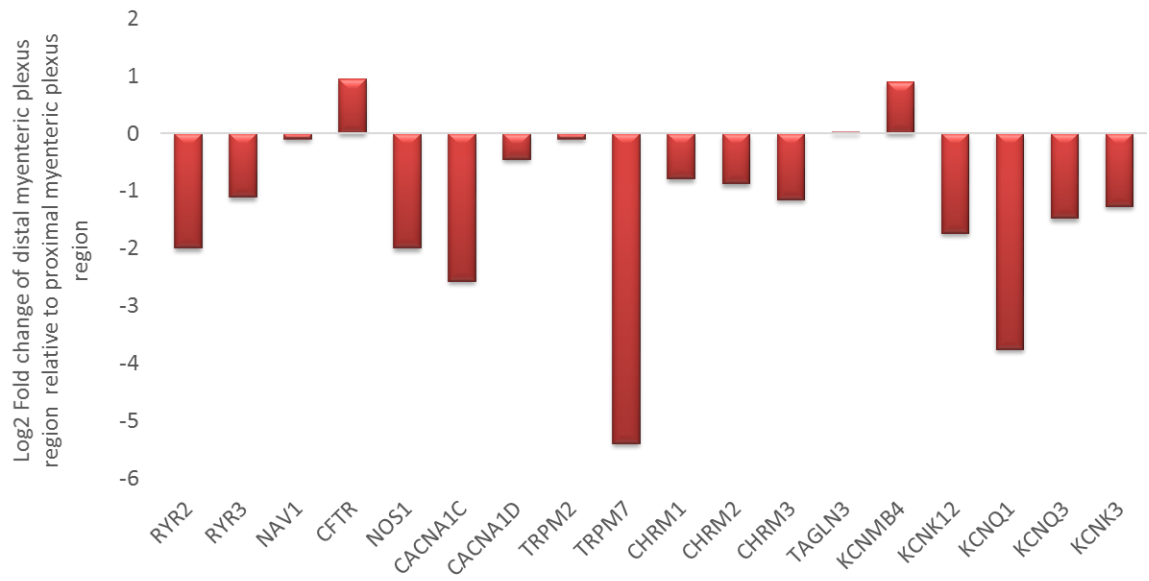


**Figure 5.22 The log<sub>2</sub> fold change of certain functional genes in the distal myenteric plexus vs proximal myenteric plexus of HD colon.**

The expression of *CACNA1D*, *CACNA1C*, and *KCNQ1,3* were down regulated in the distal MP region of HD colon sample relative to proximal MP. The expression of ryanodine (*RYR2* and *RYR3*), muscarinic (*CHRM1*, *CHRM2*, *CHRM3*) and the nitrenergic (*NOS1*) genes were all downregulated.

## 5.6 Discussion

Experiments in this chapter revealed the levels of gene expression of the four mRNA expressing IC protein markers (cKit, Ano1, PDGFR $\alpha$  and SK3) obtained from qPCR were significantly reduced as in the distal compared to the proximal part of the HD segments.

These findings were further emphasized by the RNAseq gene expression analysis represented by the RPKM value, which showed clear down-regulated levels of expression of genes of IC markers with progression from proximal to distal HD colon. Moreover, RNAseq analysis of tissue from HD colon revealed changes in expression of many other classes of the gene (although it should be noted that this is from a single sample).

Both qPCR and RNAseq revealed that cKit, Ano1, PDGFR $\alpha$  and SK3 were downregulated in the distal segment compared to proximal HD colon which is consistent with previous reports that these proteins levels are reduced in HD (**Chapter 4**). The ability to examine these four genes in a single sample could enable rapid quantification of expression levels and help determine if sufficient colon has been resected, even whilst the patient is on the operating table. The current procedure for confirmation of the level of sample dissection is to examine for presence (or absence) of ganglia in the most proximal segment, but quantification of expression could be correlated with long term outcomes to determine appropriate levels.

RNAseq data results confirm the reduction in gene expression seen in earlier qPCR experiments. However, this powerful method enabled an analysis of all

genes which expression levels changed in different segments of the HD colon, as well as considering differences between different layers mainly CM, MP and LM in the distal and proximal part.

From a list of raw gene data containing (15247) gene names, we were able to select specific genes were known by previous studies to contribute to the development of HD and other genes were selected based on their functional role as ion channels or neurotransmitter protein receptors. Our results revealed many genes and pathways in HD, however, is only one sample used in this experiment and the lack of technical replicate made the statistical analysis inappropriate.

Nonetheless, since this is the only sample examined to date to our knowledge, examination of further specimens is required. Among the top 20 terms of upregulated genes (GO term analysis) large numbers of genes were related to immune system processes and the immune response in the distal diseased segment of HD as compared to the proximal by using log<sub>2</sub> fold change >1. Some of the genes found in most of the GO terms namely, *PNP*, *CXCL13*, *CXCL8*, *CEACAM1*, *TMBIM1* and *ADAM8*. These genes mainly encode proteins that are related directly to cell activation and immune response.

Previous studies revealed that immunological activity associated with the development of enterocolitis in HD (Moore et al., 2000; Frykman et al., 2015). Furthermore, in Moore et al. (2000) experiment, the expression of major histocompatibility complex antigen was found to be high in the distal part of 23 samples of HD without any evidence of enterocolitis. This immunological response in HD led to the hypothesis that the immune system might contribute

to the pathogenesis of HD (Moore et al., 2000). Furthermore, a study done on *EdnrB*<sup>NCC<sup>-/-</sup></sup> mice to determine the gut cellular immune defects related to the development of enterocolitis in HD. The study demonstrated that increased levels of mature B-lymphocytes even before the development of enterocolitis (Gosain et al., 2015). Similar immune gene responses have been detected in colon samples from patients with ulcerative colitis (UC) (Christophi et al., 2012). In particular, *ADAM8*, which encodes a protease involved in cell adhesion, was identified as a novel gene up-regulated in UC, and we report that it is also up-regulated in HD. The alterations in the immune system which may predispose to enterocolitis in HD, therefore, need further investigation as therapeutic agents might target it and reduce the after surgery complications and improve the outcome of the HD patients.

In other hand, the GO term analysis for the downregulated genes revealed the association of many metabolic process with the HD where the distal part of HD showed reduced expression levels of genes such as *HRAS* which encodes proteins play an important role in cell division and differentiation in addition to apoptosis, *HOXD9*, *HOXA3*, and *HOXB5* are related to gene family encodes Hox proteins which are type of transcription factors and *SOX6* encodes transcription factor that is involved in developmental process and neurogenesis. In general, many of the downregulated genes encode proteins important in developmental processes.

The *RET* receptor tyrosine kinase gene was the first which identified as a major HD susceptibility gene (Edery et al., 1994, Romeo et al., 1994, Geneste et al., 1999, Iwashita et al., 2001), and mutation of this gene is responsible for the

majority of the HD cases (Seri et al., 1997). *RET* protein receptor and its *GDNF* ligand interaction are important for the migration and differentiation of enteric neurons from neural crest cells (Taraviras et al., 1999), our RNAseq results revealed significant downregulation of both *RET* and *GDNF* genes in the distal part of the HD samples when compared to the proximal part.

Other cases of HD was found to be caused by mutations in *EDNRB* or *EDN3* genes (Parisi and Kapur, 2000, Edery et al., 1996), our experimental results showed reduced expression of these genes in the distal part of HD samples when compared to the proximal segment. *PHOX2B* gene (Zhao et al., 2019), *SOX10* gene (Falah et al., 2017) both associated with the development of HD, the expression levels of these genes were significantly low in the HD distal part compared to the proximal in our experiment.

Studies have demonstrated *Scn1b* and *Fxyd1* as genes most predominantly expressed by ICs both (cKit<sup>+</sup> and PDGFR $\alpha$ <sup>+</sup>) in the murine colon (Lee et al., 2017, Ha et al., 2017). These findings suggest the critical role for these genes in the functioning of the SIP syncytium as *Scn1b* gene encodes proteins that are involved in the modulation of sodium channel gating and voltage dependence (Yao et al., 2018). *Fxyd1* produces chloride-activated currents and shown by immunoreactivity to be co-localize with Na/Ca exchanger, which indicate a direct interaction between the two proteins (Geering, 2005). Using immunohistochemistry and qRT-PCR O'Donnell et al found that both genes and their protein expression were significantly reduced in proximal and distal parts of the HD as compared to the control samples (O'Donnell et al., 2019a).

The RNAseq data here is consistent, with *Fxyd1* and *Scn1b* being down-regulated; however, more samples are required.

As mentioned earlier, gut motility is controlled by four different groups of cells, ENS, SMC, cKit<sup>+</sup> and PDGFR $\alpha$ <sup>+</sup> ICs, The communication between these cells is the key for intestinal peristalsis. Our results regarding the levels of SK3 expression were consistent with previous studies where a marked decrease in the SK3 expression in the distal part of HD specimens by using RT-PCR, western blot and immunoreactivity experiments were reported (Piotrowska et al., 2003b, Coyle et al., 2015, O'Donnell et al., 2019b, Gunadi et al., 2018). Furthermore, another study by O'Donnell et al. (2016) using Western blot experiments revealed a significant reduction in PDGFR $\alpha$ <sup>+</sup> protein expression in both proximal and distal parts of HD samples compared to control sample (O'Donnell et al., 2016). This decrease in the expression of PDGFR $\alpha$  along with their ion channel functional unit indicate a deficiency in inhibitory neurotransmission in HD bowel and may explain the tonic contraction of the distal part of the HD samples.

As shown on our previous chapters that Ano1 is co-labelling with cKit antibodies which are expressed by cKit<sup>+</sup> ICs this data was consistent with many studies (Chen et al., 2007b, West et al., 2004, Espinosa et al., 2008). Being not expressed by cKit<sup>+</sup> mast cells Ano1 considered as a more reliable marker of cKit<sup>+</sup> ICs in the gut tissue (Gomez-Pinilla et al., 2009, Coyle et al., 2016). Coyle et al. (2016), used immunohistochemistry and Western blot analysis for Ano1 and cKit<sup>+</sup> ICs revealed a reduction of the protein expression in the distal part of HD colon compared to healthy control (Coyle et al., 2016). To the best of our

knowledge, our study is the first that performed qPCR analysis on both cKit and *Ano1* gene expression in proximal and distal HD samples and comparing them to disease control specimens. Our finding was a significant reduction in the expression of these two genes in the distal (aganglionic) part compared to the proximal (ganglionic) segments; moreover, the proximal part showed a significant decrease in the levels of gene expression of these two marker genes of ICs as compared to DC samples. Low IC numbers in proximal regions may explain the poor outcome of some patients following a correction operation as the proximal part even though containing the ganglionic structure still dysfunction in most cases due to the fact that the ICs in this part is still reduced. Potentially, examining expression levels in the proximal part may help inform exactly to what level should the dissection be performed for best outcomes.

The limitation of this experimental study was the shortage in the number of samples; however, we compare a relative number of gene expression in the different HD segments as well as different histological layers related to one patient sample. The preliminary finding was the reduction of the levels of expression of genes related to ryanodine receptor and nitrenergic inhibitory neurotransmitter receptors (*RYR2*, *RYR3* and *NOS1*) in HD distal segments explain the failure of the SMCs to relax. The results of the gene expression related to ICs reinforced our immune-finding, and qPCR results performed earlier in this project in which genes encoding the protein markers of cKit, *Ano1*, *PDGFR $\alpha$*  and *SK3* were downregulated in the distal part of the HD compared to the proximal part especially in the MP where enteric

neurotransmitter are most concentrated. To the best of our knowledge this study is the first that highlighted the variations in the gene expression between the different layers (CM, MP, and LM) in human HD colon sample. However, further studies are needed to understand the functional role of these genes and a detailed different expression profiles of each cell type of the SIP syncytium because each cell type may have very specific roles in controlling the smooth muscle contractility.

In conclusion, this study demonstrated that the ICs marker protein gene expression is markedly decreased in the diseased distal part of HD compared to the proximal part of the HD specimen (qPCR and RNAseq), furthermore, the proximal part gene expression of the ion channels (SK3 and Ano1) were significantly reduced compared to the disease control samples (qPCR). This study could add to our understanding of the biological basis of HD and gut motility disorder in general. Further, our understanding if bowel is adequate to pull through and potentially lead to the development of novel therapeutic agents to treat patients with gastrointestinal dysmotility conditions.

## Chapter 6 General Discussion and Future perspectives

### 6.1 General Discussion

This thesis reports the outcomes of different approaches to studying IC in HD. To identify and count IC using Immunohistochemical techniques, the best approach appeared to utilise acetic ethanol fixation with frozen sections. Should quantification of IC (or indeed other cell types) be required,, image analysis presented a semi-automated approach that could be used in other labs to reduce experimenter bias. In comparison, while immunolabelling of archived FFPE tissue did provide some staining with antigen retrieval protocols, the quality of staining was more variable than fresh-frozen sections. Whilst RNAscope also revealed some labelling, this too was not as effective to reveal IC as immunofluorescence on fresh frozen sections. The use of archived tissue would greatly expand the pool of tissue available. Although these first steps towards the routine use of archived tissue for HD research displayed some potential, further use will require refinement, validation and technical development.

Examining RNA from fresh tissue using qPCR revealed expression of IC markers was decreased in HD distal segments compared to proximal, consistent with the immunolabelling. Whilst time constraints limited RNAseq to a single sample, this has revealed some impressive outcomes, with the expression of genes indicating inflammation significantly increased in distal compared to proximal HD colon which explains the association of enterocolitis with HD. Genes and processes identified as disrupted can, therefore, be

analyzed using the immunostaining protocol developed in this thesis in future investigations.

Using immunostaining technique our research emphasizes, as others have also stated, that ICs significantly decreased in the distal aganglionic portion of HD relative to proximal ganglionic (Yamataka et al., 1995, Vanderwinden et al., 1996, Rolle et al., 2002, Anatol et al., 2008, Do et al., 2011b).

Moreover, the difference in ICs numbers between the proximal ganglionic segments of HD samples was significantly reduced compared with the disease control samples, which is consistent with previous studies (Taguchi et al., 2005). Such IC reductions may contribute to the poor outcome that some patients have after surgery, suggesting that the surgeon may usefully be able to predict the outcome of HD patients by testing the number of ICs in the proximal ganglionic segment. Since there is no study has established the standard IC numbers in the colon's wall, no one can predict how many ICs should be in the colon to perform an adequate function.

Disruption of neural crest cell migration during the early embryonic stages is the main reason behind the development of HD (Amiel et al., 2008). In addition to the lack of ganglia, several studies have shown reductions in the number of different types of ICs. Significant advances have been made regarding the distribution of these cells in HD (Yamataka et al., 1997, Horisawa et al., 1998, Nemeth et al., 2000, Newgreen and Young, 2002, Coyle et al., 2016, O'Donnell et al., 2016). Most of these studies used Immunohistochemical methods to detect ICs in the proximal and distal part in HD by using histological sections and whole-mount tissue. Their finding was similar to our immunostaining results

in the different parts of the HD specimens where the numbers of ICs were reduced in the diseased part of HD compared to the normal ganglionic segments (Yamataka et al., 1995, Vanderwinden et al., 1996, Yamataka et al., 1997, Nemeth et al., 2000, Rolle et al., 2002, Piotrowska et al., 2003a).

The reduction in the number of ICs appears critical for function. This is likely because cKit<sup>+</sup> ICs act as pacemakers due to their intrinsic slow waves of depolarization and hyperpolarization which are transmitted to the SMCs via gap junctions and so lead to contraction and relaxation of the gut musculature (Epperson et al., 2000, Ward and Sanders, 2001, Sanders et al., 2016).

These functional roles of cKit<sup>+</sup> ICs have been confirmed by using cKit mutant animals or animals treated with cKit neutralizing antibodies (Ward et al., 1994b, Hulzinga et al., 1995, Torihashi et al., 1995). Additionally, isolated cKit<sup>+</sup> ICs display autorhythmicity consistent with the slow-wave recorded in the intact SMCs as seen with patch-clamp experiments and pharmacological agents (Langton et al., 1989, Hirst et al., 2002, Hwang et al., 2009, Hwang et al., 2012, Zhu et al., 2009). All these findings make ICs a good therapeutic target for pharmacological, intervention in many gut motility disorders such as HD. Nevertheless, extensive research is needed regarding this point, starting with establishing a method for fixation as well as identifying these cells with immune-markers which could be used in this research area. This could make the comparison between these studies more reliable and make more benefits to the current status of our knowledge of the morphological and physiological features of the different types of ICs.

Considerable data has demonstrated that coordination between ENS and ICs networks in the gut wall is necessary for normal intestinal motility (Yadak et al., 2019). However, these interconnections make the cause and effect in many gut motility disorder difficult to distinguish. Whether the ICs loss in HD is the primary cause or occurs secondary to loss of functional obstruction in the contracted colon of HD is not yet known.

Most research on human gut motility disorders based primarily on immunostaining and TEM; however, understanding gene expression provides important indications of both reasons and implications for disrupted HD intestinal function. In this study, a collection of transcriptomes were identified in human HD colon using RNAseq. Our results were consistent with previous findings demonstrating downregulation of genes contributing to HD developing namely, *RET* (Emison et al., 2010b, Chatterjee et al., 2019), *PHOX2B* (Zanni et al., 2017) and *SOX10* (Chatterjee et al., 2016). It is perhaps not a surprise that these genes were found to be downregulated in the distal diseased part of HD compared to the proximal part as they are involved in generation and maintenance of neurons and glial cells, all markedly reduced in number in distal segments (Tam and Garcia-Barceló, 2009). Furthermore, investigating the expression in the LM, CM and MP of the distal segment revealed for the first time using human colon tissue of downregulation of such genes.

However, in future, it will be of interest to undertake scRNAseq for each cell type in the SIP syncytium, hopefully also helping to define the exact role of these cells in controlling normal gut motility. Such experiments could be considered in subsequent research.

Our preliminary RNAseq data highlighted, for the first time, that the most upregulated genes (according to GO term analysis) were genes belonging to the activation of immune response and immune system process. This upregulation may explain the reason behind the development of inflammation of the colon tissue in HD patients, the most significant genes that we noticed in most of the GO terms were: *PNP*, *CXCL8*, *ADAM8* and *CXCL13*. These findings need further investigation to broaden our understanding of how the immune system and ENS are integrated and why inflammation of the colon occurs in patients with HD. In contrast, the downregulated genes mostly encoded transcription factors, for example, *HOX* and *SOX* families.

To conclude, if this experiment were to be repeated using a more significant number of samples, it could provide a dataset resource of use in the study and understanding of HD pathology. In addition, single-cell genome analysis for ICs should be considered to improve our understanding of their role in the gut motility disorder.

## **6.2 Future perspectives**

### **6.2.1 How can these findings help future HD patients?**

In the longer term, it is possible that the approaches and methods established in this thesis could be applied to benefit HD patients. For example, future research could include immunostaining for IC markers and assessment of ganglia alongside quantifying RNA levels for these cell markers in proximal and distal segments. The next stage could involve correlating these values with patient outcomes which could help determine if the resection has been at the

appropriate level for a good prognosis. The immunostaining could be rapidly performed whilst qPCR can be conducted even in the theatre using mobile PCR machines (King et al., 2008, Ozanich et al., 2017) or digital PCR (Baume et al., 2019).

To better understand HD pathophysiology more RNAseq experiments need to be performed which could add a better knowledge of what is changed in the distal diseased part as compared to the proximal part which could provide a chance of better treatment options.

### **6.2.2 Can IC and neurons be replaced as a future treatment**

There are other exciting areas of research where the possibility of using stem cells as a source of enteric neural crest cells transplantation, could serve as a promising therapy for HD (Almond et al., 2007, Cheng 2015). In addition, induced pluripotent stem cells (Frank, 2017), can be used to model HD and to test for therapeutic medication that can enhance the motility of the gut (Miguel and Chen, 2017). Another option to be considered is the use of an artificial colon (organoid) to be engrafted into the HD colon (Christopher, 2017).

However, a current limitation of stem cell transplant therapy is limited differentiation. This could be overcome by, for example, co-application of growth factors. To improve the survival and differentiation Liu et al (2018) found that engrafted ENSc expressing Insulin Growth Factor-1 (IGF-1) to aganglionic mice colon increase differentiation and improve colonic motility (Liu et al., 2018), the reason behind this effect is that IGF-1 influences the SCF/cKit signalling which is vital for the development and maintaining of cKit<sup>+</sup> ICs

(Horváth et al., 2006, Lin et al., 2009). Neurogenesis of transplanted neural stem cells in postnatal, and adult mouse colon has been shown by different studies (Cooper et al., 2017, McCann et al., 2017). Furthermore, transplantation of ENSc into a mouse model of human motility gut disorders enhance GIT motility by restoring the numbers of ICs which were reduced in these animal models (McCann et al., 2017).

As an alternative to transplantation, endogenous neurogenesis could be targeted. For example, Kulkarni et al. (2017) concluded that enteric neurogenesis in adult gut tissue maintains homeostasis where there is a high rate of neuronal death, however, the number of neuronal cells remains stable, these new neurons formed from dividing precursor cells that are located within the MP (Kulkarni et al., 2017). This evidence has a potentially huge clinical benefit, where induction of neuronal cells in the distal aganglionic HD segment might lead to novel therapies for HD.

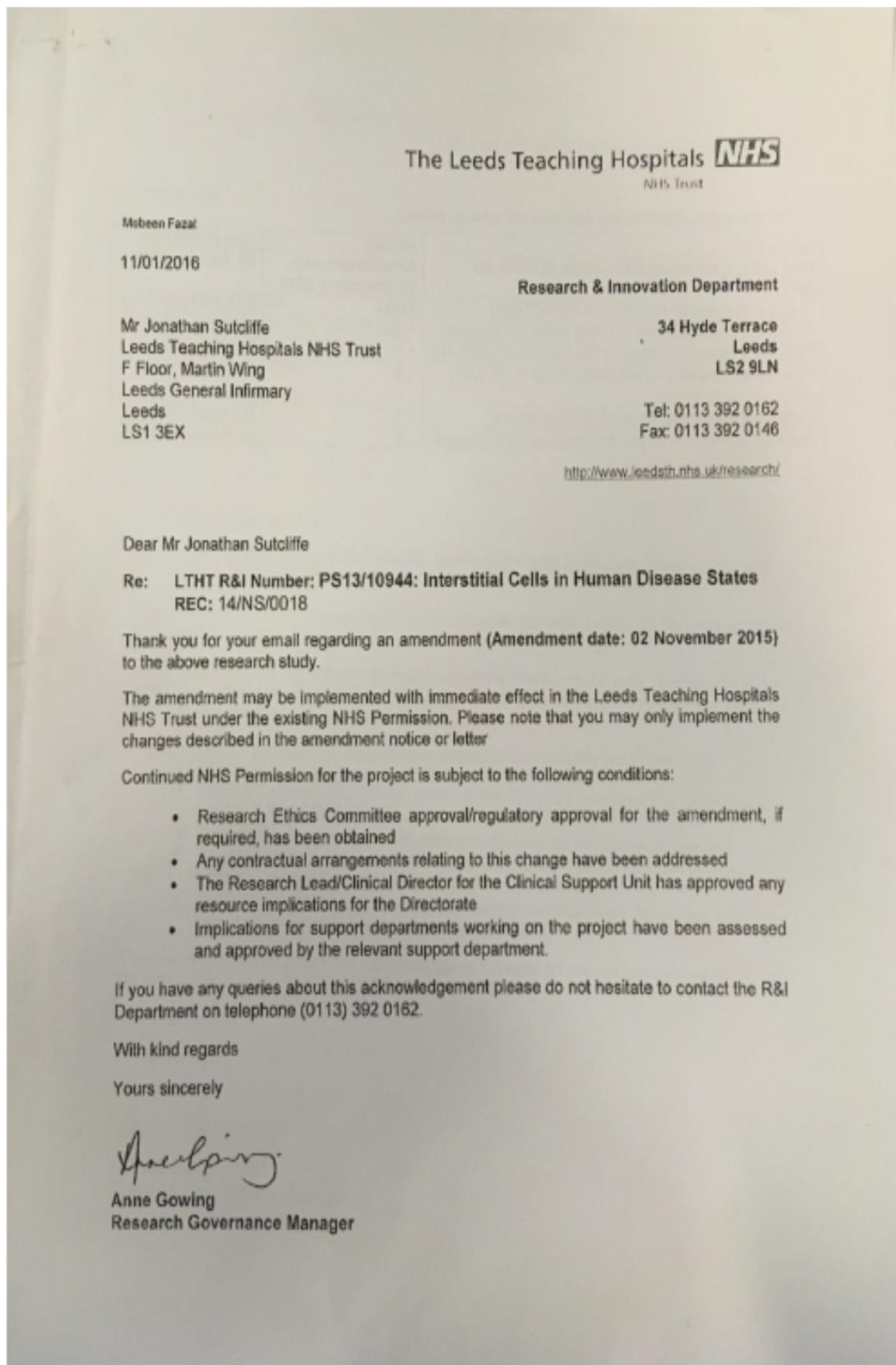
McCann et al. (2013), demonstrated that transplanting cKit<sup>+</sup> ICs into MP of cKit mutant mice intestine, resulted in the development of distinct cKit<sup>+</sup> ICs network in the MP with the restoration of pacemaker activity into mice devoid of IC-MP and slow waves (McCann et al., 2013). This suggests that transplanting ICs, or inducing their endogenous production, could provide promise towards a cure for HD patients.

### **6.3 General Conclusion**

This study provided a set of techniques to investigate ICs in HD. These approaches could provide foundations for future research. Adopting reliable method of staining and using appropriate markers for these cells in addition to semi-automated quantification methods such as used in this thesis would enhance IC research. Following the same ICs protocol could make comparable analysis across different research more convenient. Highlights of the genetic properties of HD different segments could usefully add to our knowledge regarding the disease pathology mechanism.

## **Chapter 7 Appendix**

## **7.1 Appendix (1): Ethical Approval and Consent Forms**

**(A) Ethics Approval**

**(B) consent forms (1)****Patient Information Sheet for IC Project****Child 6-10 years old**

**This sheet belongs to.....**

I am Jonathan Sutcliffe and I am a Doctor at the Hospital. My friend is Jim Deuchars - he is a scientist. We work together. We have a question about something called IC.

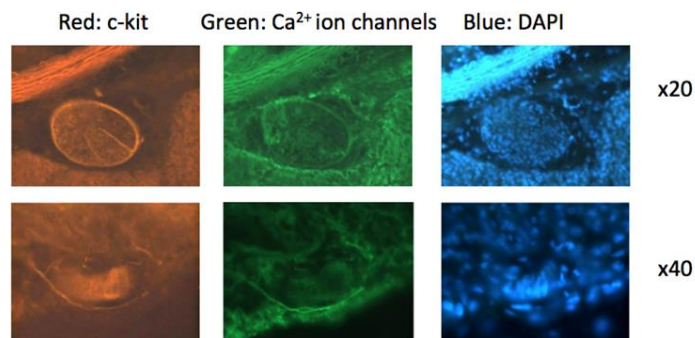
We think IC might help your body to work. They are cells – the building blocks of your body. IC are very small and nobody can see them with just their eyes. They are even hard to see when scientists use a special machine called a microscope. And nobody knows what they really do – they are still a mystery.

If we can find out how to see them then we can find out if they are important. We might even be able to help other children or grownups get better.

Because you are having an operation, we want to see if we can find any IC in your body. When the doctor fixes your problem, they might have to take the bit that's caused the problem away – we want to look at this bit when it's gone. It won't make the operation bother you more and it won't be dangerous for you. But we want to make sure you are ok with this.

We will talk to your Mum or Dad to see if they want to ask anything of if you want to know anything. It would be great if you would help but if you say no, it's really ok.

If you want to see a picture of an IC, take a look!



The orange picture in the top row shows a big round blob. There is an IC giving a big round blob a hug – it's the thin white line around the edge. Can you see it? Can you see the two pointy things going into the middle of the blob? We reckon they might be like telephone wires.

Can you see an IC in the orange picture on the bottom row? It's a thin white line again.

You might be able to see ICs in the green pictures too, but only just. Can you see them?

IC should have gone in the blue picture – can you see them, or are they hiding? If your Mum or Dad would like more information about the study the person to contact is :

**Name: Jonathan Sutcliffe**

**Consultant Pediatric Surgeon/ F Floor/ Martin Wing Leeds General Infirmary Great George Street**

**Leeds- LS1 3EX**

**Contact telephone: 011339231**

**Consent form (2)****Patient Information Sheet for IC Project****Child 11-15 years old****What is this form for?**

When Doctors need to do research they want to make sure that their patients understand what it's about. As well as talking to your Mum and Dad, we want to check that you understand and see if you have questions.

**What is the Research Project about?**

Many parts of your body need a special type of muscle. This is called smooth muscle. Smooth muscle just seems to work all by itself without us having to worry about it. A good example of this is your belly – when you have had your food, your body can take the goodness out of it and then pass the waste out when you go to the toilet - you don't need to really do anything because your body just does it. It's the same with your wee with drink, and your heart with blood- the blood just moves around your body without you having to think about it.

We don't know enough about how all of this happens and how your body controls it. As you might know, your body is made of building blocks called cells. There are many types of cells. We used to think that the smooth muscle is controlled by nerve cells that link to a part of your brain. Whilst this is partly true, there aren't enough nerves for this to be the whole story. So we have been examining a different group of cells, called IC.

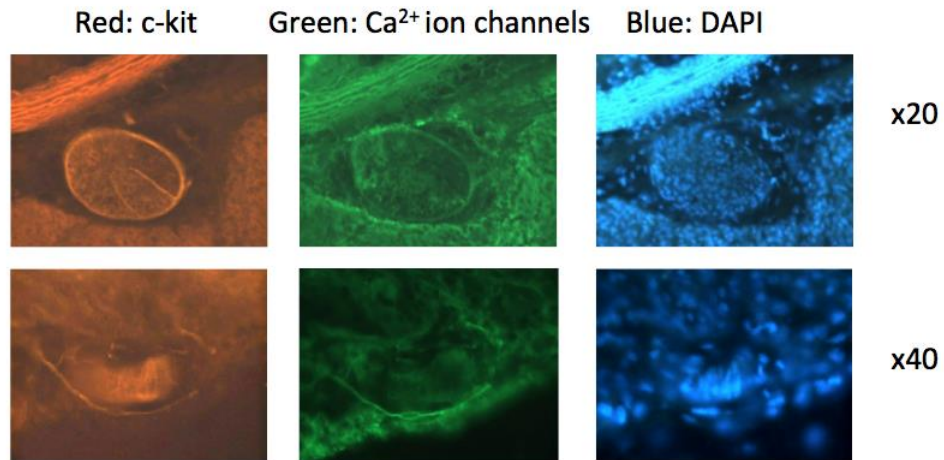
IC have been known about for nearly 150 years. They are very hard to see, even with powerful microscopes. Because of this nobody has been able to study them properly until recently. Someone found a marker for them which allows them to stand out from the cells around them. Since then we have found that the number of cells does not seem to be normal in patients with problems with their smooth muscle.

The problem is that the marker we have might not quite be good enough – it seems to show some of the cells, but probably not all. It is really important to be able to show as many of the cells as possible otherwise you'll never know if the cells are there or not in patients with problems. You will also not know how many cells there are supposed to be in people with normal smooth muscle. Once we figure out whether they're there or not, we can then see if they are working properly and what it is exactly that they do.

We want to ask you if you would be happy to take part in this study because you are due to have an operation. If the surgeon removes any smooth muscle as part of your operation, they will always send it to the laboratory for one of the scientists there to examine it. They will look at most of the tissue to get a diagnosis, but there is often something left over that wouldn't be used for anything else. We want to be able to look at that bit. So we don't want to take any extra tissue for this part of our study.

Part of this study is for us to understand about IC in blood vessels. It's important because we can then learn more about how adults develop heart disease, and how some babies have abnormal blood vessels that then need operations. It's very hard to get access to blood vessels to study though. When the surgeon does an operation on an abdomen they will have to divide something that used to be a blood vessel before

you were born. It isn't of any use once you are born and it isn't dangerous to divide. We want to be able to examine a small piece of this tissue. If you want to see a picture of an IC, take a look!



The orange picture in the top row shows a big round blob. This is a nerve. There is an IC wrapped around the nerve – it's the thin white line around the right hand side edge. Can you see the two spikes going into the middle of the nerve? We believe that the IC have a role in communicating with the nerves and that the spikes are there to do the communicating.

There is an IC in the orange picture on the bottom row. It's a thin white line again going from left to right below the smudge.

You might be able to see ICs in the green pictures too, but only just. On the bottom green picture, you can see the IC again going from left to right.

IC should have gone in the blue picture. We use different chemicals to stain different cells. This allows us to see how the cells differ.

#### **Who are the Researchers?**

The research team is led by Mr Jonathan Sutcliffe (Consultant Paediatric Surgeon at the Leeds General Infirmary) and Professor Jim Deuchars (University of Leeds)

#### **Why am I being asked to be in this research project?**

We are asking you to take part in this project because you are due to have an operation in which tissue will be removed that would be of use to study.

#### **What are the alternatives to participating in this project?**

If you choose not to take part in this study, your treatment will not change in any way.

#### **What do I need to do to be in this research project?**

We are asking you and your Mum or Dad to consent to the use of your tissue samples and to allow us to find out about the operation and your symptoms from your medical notes. You will not need to give any important tissue because we will be able to learn by examining the tissue that your Doctor is already planning to remove. The only exception to this is where we hope to examine blood vessels that lie in your tummy wall behind your tummy button. As stated above, these vessels no longer carry blood or have any other function once a baby is born and are routinely divided when carrying out the operation. There are no consequences to the removal of this tissue.

**Is there likely to be a benefit to me?**

You are unlikely to benefit except by you/your family knowing you are taking part in a study aiming to help patients in the future.

**Is there likely to be a benefit to other people in the future?**

If we can work out what parts of the control mechanism for muscle go wrong, we would be more likely to be able to find a better treatment for our patients in the future.

**What are the possible risks and/or side-effects?**

As with any operation, there may be additional unforeseen or unknown risks. However, since all we want to do is examine tissue that was already being removed and read the medical notes, the risk of anything serious happening is low. If you are a patient in whom we hope to examine a section of the umbilical vein or artery (the blood vessels used before birth but no longer required after birth), there are no additional risks as the vessels are no longer required.

**What are the possible discomforts and/or inconveniences?**

There are unlikely to be any discomforts or inconveniences. If you feel worried or concerned about your involvement in the project or what we have found, you can contact us. Our contact details are below at the end of this document.

**What will be done to make sure the information is confidential?**

Any information we collect in connection with the project that can identify you will remain confidential, except as required by law. Names will be removed and study numbers will be used. This means that if we need to, we will be able to find out your name from the study number.

The type of information we will collect include date of birth, diagnosis, date of operation, symptoms and reason for operation.

When our findings are published in medical journals, or presented at conferences, it will not be possible to identify you.

**Who has reviewed the study?**

All research in the NHS is looked at by an independent group of people, called a Research Ethics Committee, to protect your interests. This study has been given the go ahead by the North of Scotland Research Ethics Committee.

**Will I be informed of the results when the research project is finished?**

If you wish to know the results of the experiments, please ask and we can find out. It may be that it is not until we have finished looking at all the results that we can give you the results. Please contact us by post at the LGI or by telephone (contact details below)

You can decide whether or not to take part in this research project. You can decide whether or not you would like to withdraw at any time without explanation.

You may like to discuss participation in this research project with your family and with your doctor. You can ask for further information before deciding to take part.

If your Mum or Dad would like more information about the study the person to contact is :

**Name:** Jonathan Sutcliffe

Consultant Paediatric Surgeon F Floor Martin Wing Leeds General Infirmary Great George Street Leeds, LS1 3EX **Contact telephone:** 01133923156

**Consent form (3)****PARENT/GUARDIAN INFORMATION STATEMENT AND CONSENT FORM FOR RESEARCH INVOLVING TISSUE SAMPLES****Title of Project: Interstitial Cells In Human Paediatric Colon Of Hirschsprung Disease**

Principal Investigators: Mr Jonathan Sutcliffe and Professor J Deuchars

Thank you for taking the time to read this Information Statement.

This information statement and Consent is 5 pages long. Please make sure you have all the pages.

For people who speak languages other than English:

If you would also like information about the research and the Consent Form in your language, please ask the person explaining this project to you. We will talk to you through an interpreter.

You are invited to participate in a Research Project that is explained below.

**What is an Information Statement?**

These pages contain information about a research project we are inviting your child to take part in. One of us will have spoken to you and your child already. The purpose of this information statement is to explain to you clearly and openly all the steps and procedures of this project. The information is to help you to decide whether or not you would like to take part in the research.

Please read this information carefully. You can ask us questions about anything in it. You may also wish to talk about the project with your parents or guardians, friends or health care worker. Once you have understood the information, if you wish to take part please sign the consent form at the end of this information statement. You will be given a copy of this information and consent form to keep.

**What is the Research Project about?**

Many tissues need co-ordination of muscle activity to function properly. The type of muscle involved is "smooth muscle". There are many conditions caused by abnormal control of smooth muscle. We do not fully understand this abnormal control. Treatments are therefore less effective and some conditions can produce severe symptoms that respond poorly to treatment.

One of the cell types that help to control smooth muscle are Interstitial Cells (ICs). We know that in experiments they play a very important role in many tissues, but we don't yet know enough about how they work in humans. This is because they can't be identified using normal techniques and are therefore hard to test.

Special methods in the laboratory have now been developed to stain the cells so they can be seen. Unfortunately no one method has been shown to be the best and a number of different techniques exist. This makes it hard to compare results.

We wish to learn more about these cells by working out the best way to stain them. We also want to know what exactly it is that they do to control the smooth muscle and we can find this out by looking at the proteins in these cells. We hope this will help us understand their role in normal people and in patients with symptoms potentially related to IC abnormalities. Finally we hope that we can build links with other centres to be able to compare results meaningfully.

In order to learn more about these cells, we hope to be able to examine smooth muscle removed from patients having surgery to remove relevant tissue. Mostly this will be from tissue that was being resected anyway.

There are some small blood vessels close to the umbilicus (tummy button) which were useful before you were born to carry blood (umbilical vein and arteries) but which are not used at all following birth. Examining these vessels would be a very useful way to learn more about IC in blood vessels. Because the vessels lie under the abdominal wall, they are routinely encountered and divided when doing many operations. Removing a small segment (approximately 2cm) will cause no problems for any patient. Our research team will say if we hope to obtain some of this tissue.

If you join the study, some parts of your child's medical records and the data collected for the study will be looked at by authorised persons from the Leeds Teaching Hospitals NHS Trust. They may also be looked at by authorised people to check that the study is being carried out correctly. All will have a duty of confidentiality to your child as a research participant and we will do our best to meet this duty.

### **Who are the Researchers?**

The research team is led by Mr Jonathan Sutcliffe (Consultant Paediatric Surgeon at the Leeds General Infirmary) and Professor Jim Deuchars (University of Leeds)

### **Why is my child being asked to be in this research project?**

We are asking your child to take part in this project because they are due to have an operation in which tissue will be removed that would be of use to study.

What are the alternatives to participating in this project?

If you choose for your child not to take part in this study, your child's treatment will not change in any way.

### **What do I need to do to be in this research project?**

We are asking you to consent to the use of your child's tissue samples and to allow us to find out about the operation and your child's symptoms from their medical notes. Your child will NOT need to give any tissue in addition to the normal treatment they receive. The only exception to this is where we hope to examine a small section of blood vessels from behind the tummy button. As stated above, these vessels no longer carry blood or have any other function once a baby is born and are routinely divided when carrying out the operation. There are no consequences to the removal of this tissue.

### **Is there likely to be a benefit to me?**

Your child is unlikely to benefit except by them/your family knowing they are taking part in a study aiming to help patients in the future.

### **Is there likely to be a benefit to other people in the future?**

If we can work out what parts of the control mechanism for muscle go wrong, we would be more likely to be able to find a better treatment for our patients in the future.

### **What are the possible risks and/or side-effects?**

As with any operation, there may be additional unforeseen or unknown risks. However, since all we want to do is examine tissue that was already being removed and read the medical notes, the risk of anything serious happening is low. If your child is a patient in whom we hope to examine a section of the umbilical vein or artery (the blood vessels

used before birth but no longer required after birth), there are no additional risks as the vessels are no longer required by patients.

In the event that something does go wrong and your child is harmed during the research and this is due to someone's negligence then you may have grounds for a legal action for compensation against the Leeds General Infirmary but you may have to pay your legal costs. The normal National Health Service complaints mechanisms will still be available to you (if appropriate).

**What are the possible discomforts and/or inconveniences?**

There are unlikely to be any discomforts or inconveniences. If you feel worried or concerned about your child's involvement in the project or what we have found, you can contact us any time. Our contact details are below at the end of this document.

**What will be done to make sure the information is confidential?**

Any information we collect in connection with the project that can identify your child will remain confidential, except as required by law. Names will be removed and study numbers will be used. This means that if we need to, we will be able to find out your child's name from the study number.

The type of information we will collect include date of birth, diagnosis, date of operation, symptoms and reason for operation.

Information will be stored on a secure database. It will be deleted at the end of the study. The information will be password protected and only members of the research team will be able to access it.

When our findings are published in medical journals, or presented at conferences, it will not be possible to identify your child.

**Who has reviewed the study?**

All research in the NHS is looked at by an independent group of people, called a Research Ethics Committee, to protect your interests. This study has been reviewed and given favourable opinion by the North of Scotland Research Ethics Committee.

**Will I be informed of the results when the research project is finished?**

If you wish to know the results of the experiments, please ask and we can find out. It may be that it is not until we have finished looking at all the results that we can give you the results. Please contact us by post at the LGI or by telephone (contact details below)

You can decide whether or not your child takes part in this research project. You can decide whether or not you would like your child to withdraw at any time without explanation.

You may like to discuss participation in this research project with your family and with your doctor. You can ask for further information before deciding to take part.

If you would like more information about the study or if you need to contact a study representative, the person to contact is :

Name: Jonathan Sutcliffe

Consultant Paediatric Surgeon

F Floor Martin Wing, Leeds General Infirmary,

Great George Street , Leeds

LS1 3EX

Contact telephone: 01133923156

**What are your child's/your rights as a participant?**

1. I am informed that except where stated above, no information regarding my medical history will be released.
2. I am informed that the results of any tests involving my child will not be published so as to reveal their identity.
3. It has also been explained that my child's involvement in the research may not be of any benefit to them personally. I understand that the purpose of this research project is to improve the quality of medical care in the future.
4. I understand that this research project has been approved by the North of Scotland Research Ethics Committee.
5. I have received a copy of this document.

**Title of Project: Interstitial Cells In Human Paediatric Colon Of Hirschsprung Disease**

Participant ID \_\_\_\_\_

Principal Investigator(s): Mr Jonathan Sutcliffe and Professor J Deuchars

- I have received an Information Statement to keep and I believe I understand the purpose, extent and possible effects of my involvement
- I have had an opportunity to ask questions and I am satisfied with the answers I have received
- I understand that the researcher has agreed not to reveal results of any information involving me, subject to legal requirements
- If information about this project is published or presented in any public form, I understand that the researcher will not reveal my child's identity
- I understand that if I refuse to consent, or if I withdraw from the study at any time without explanation, this will not affect my access to the best available treatment options and care
- I understand I will receive a copy of this consent form.

Please tick one box below regarding the use of this tissue for the future:

The taking of a tissue sample for use in this research project and future ethically approved research projects. I understand that I WILL be contacted and asked whether I consent before my tissue sample can be used for any future research.

The taking of a blood/tissue sample for use in this research project and future ethically approved research projects. I understand that I WILL NOT be contacted when my tissue sample is used in future research and that by consenting now, I consent to all future uses of my tissue sample.

I \_\_\_\_\_ voluntarily consent

PARENT'S/GUARDIAN'S SIGNATURE-----Date-----

I would like to be sent information describing the results of the study Yes/No (Please circle)

I have explained the study to the participant who has signed above, and believe that they understand the purpose, extent and possible effects of their involvement in this study.

RESEARCHER'S SIGNATURE

Date-----

1 Copy for notes, 1 Copy for Study File, 1 Copy for Participant

## 7.2 Appendix (2): Supplementary Figures

**Figure (A): Hirschsprung's disease and Disease Control samples used in this project**

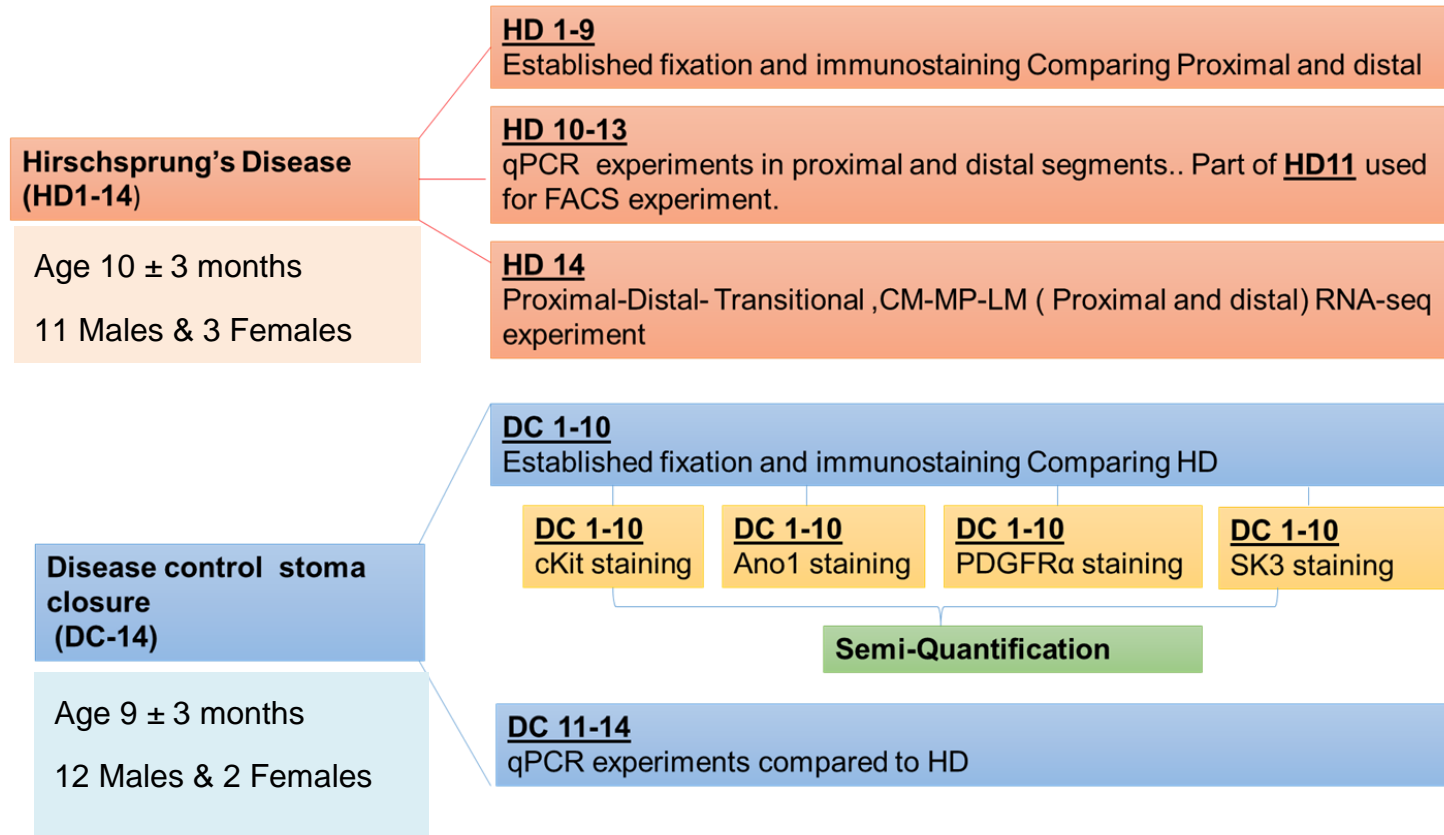


**Figure (B):** Flow cytometry detection of ICs isolation from human colon of HD shows a representative expression of CD140a-FITC ( PDGFR $\alpha$  cell marker), CD117-PE (cKit cell marker) and ant fibroblast and CD45 (mast cell) markers.

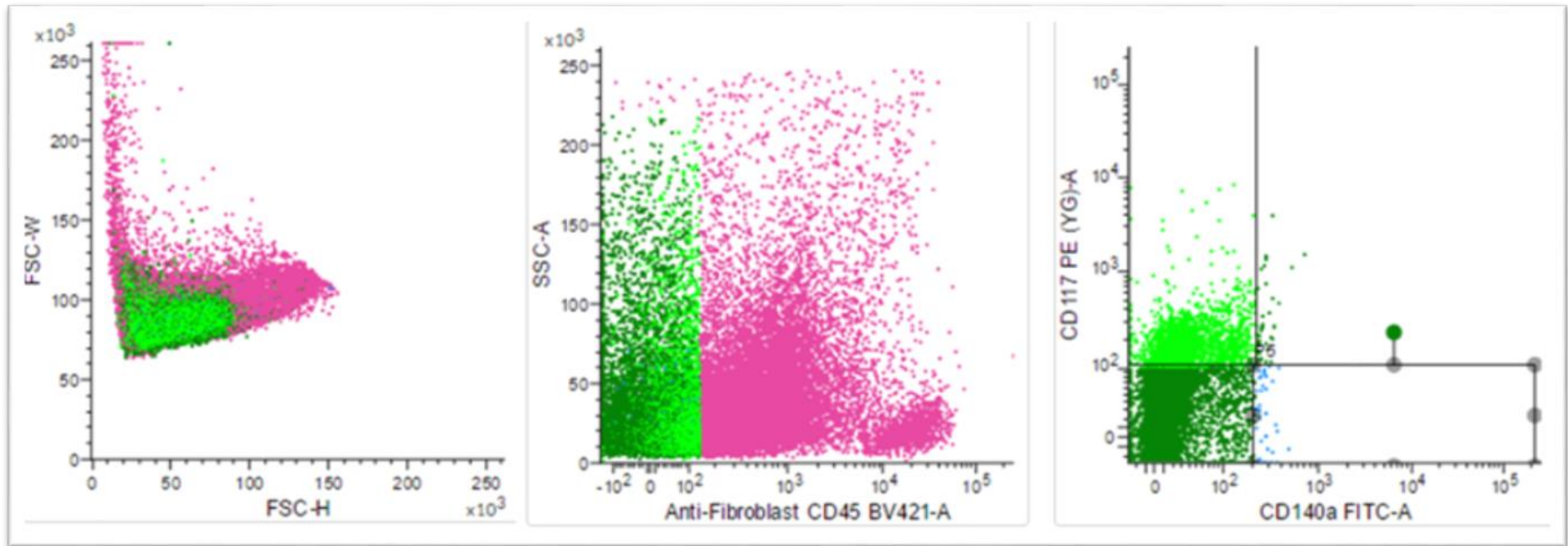


Figure (C): Example of Nanodrop reading of the 260 / 280 OD ratio for some samples.

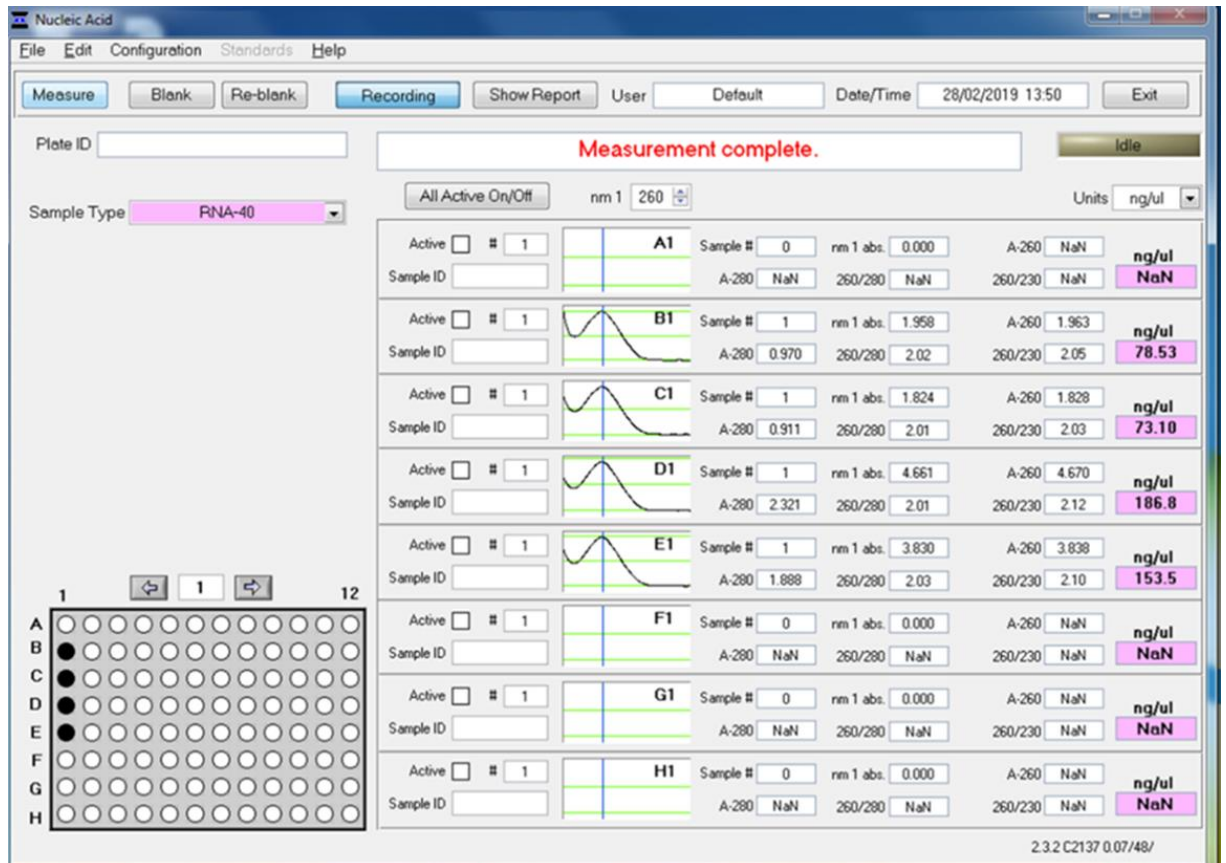
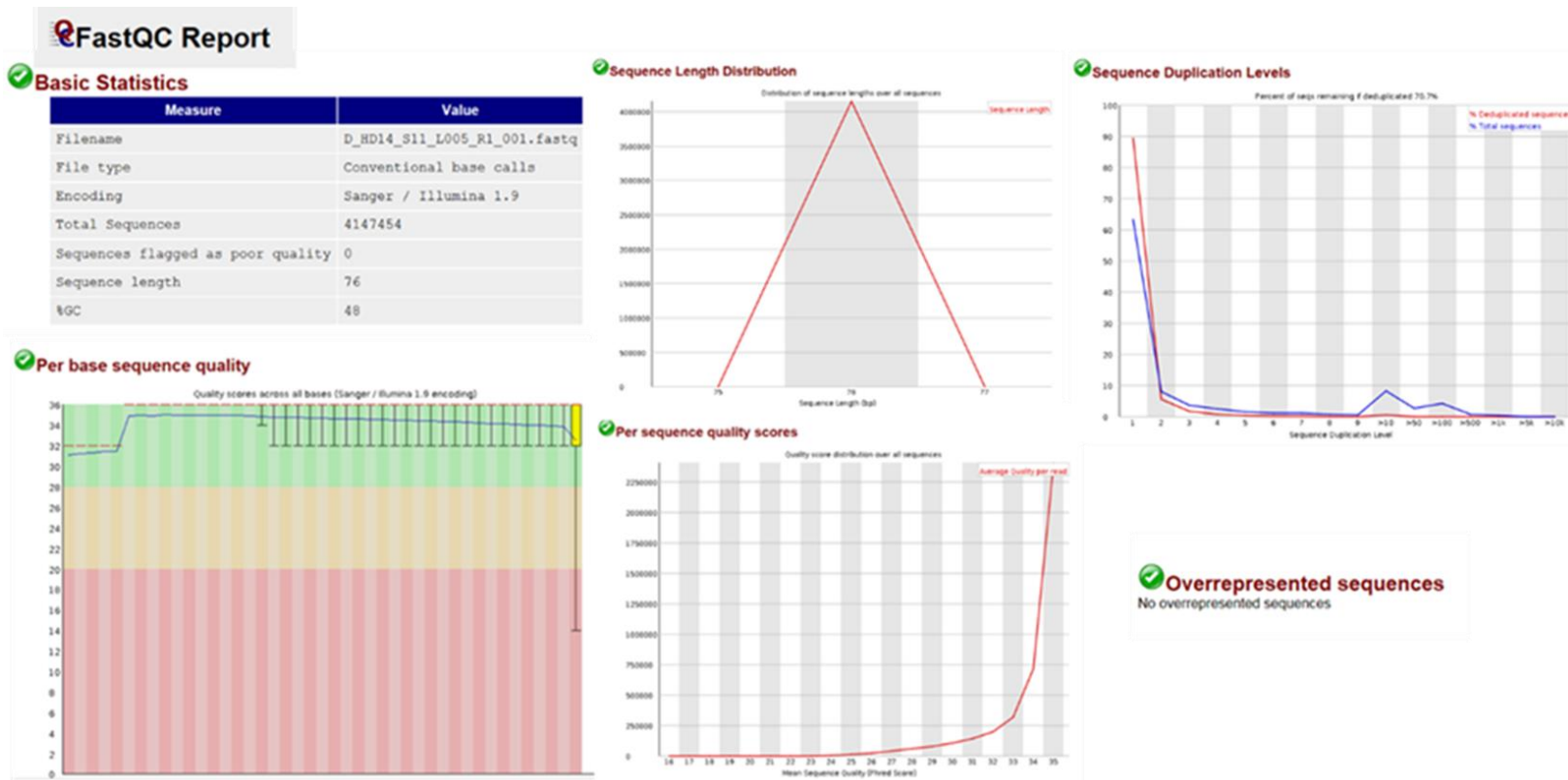
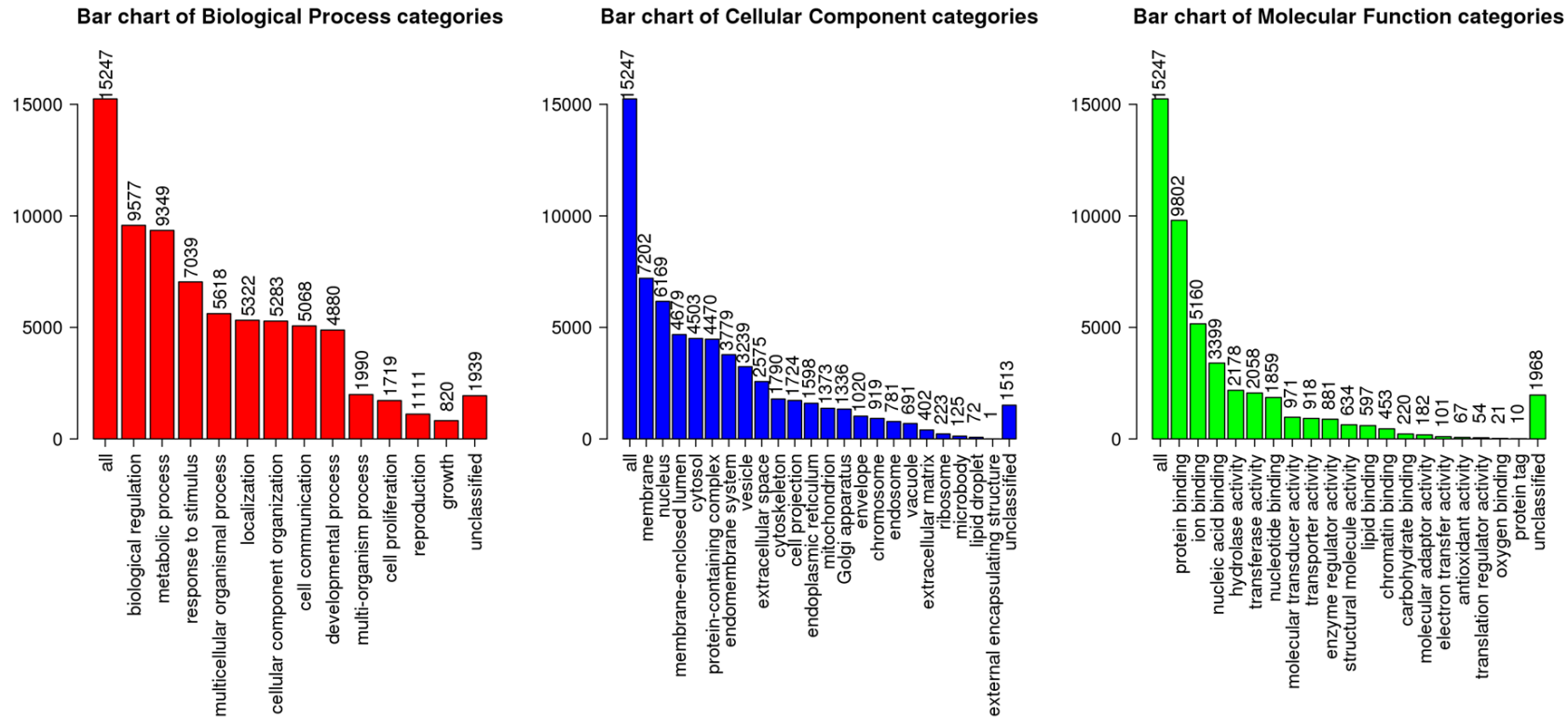




Figure (E): : Example of the graphs obtained by the FAST-QC report. The most important among them are the “per base sequence quality” and the “ overrepresented sequences”



**Figure (F1): GO terms for the whole list of genes. Each Biological Process, Cellular Component and Molecular Function category is represented by a red, blue and green bar, respectively. The height of the bar represents the number of genes in the list and also in the category.**



**Figure (F2): GO terms for the up-regulated genes. Each Biological Process, Cellular Component and Molecular Function category is represented by a red, blue and green bar, respectively. The height of the bar represents the number of up-regulated genes in each category.**

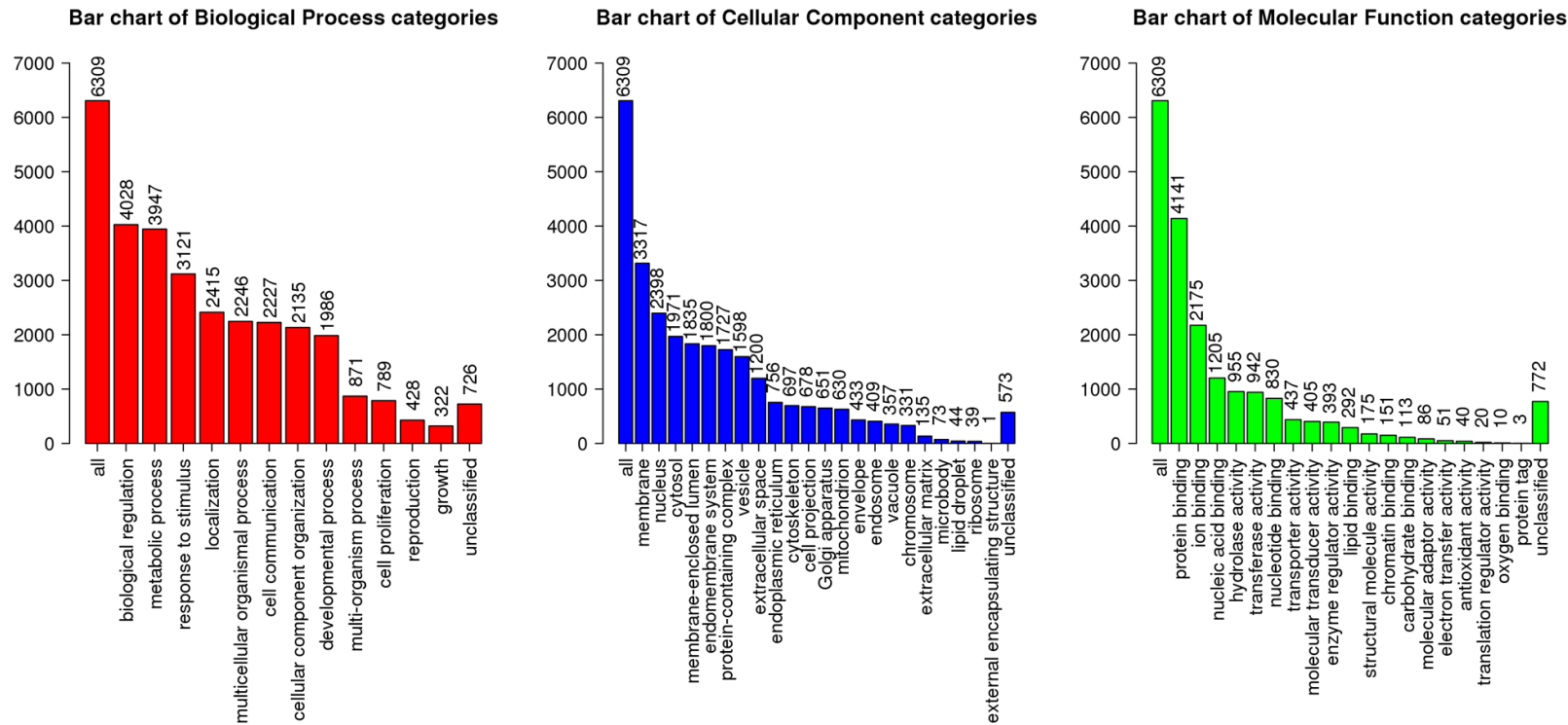
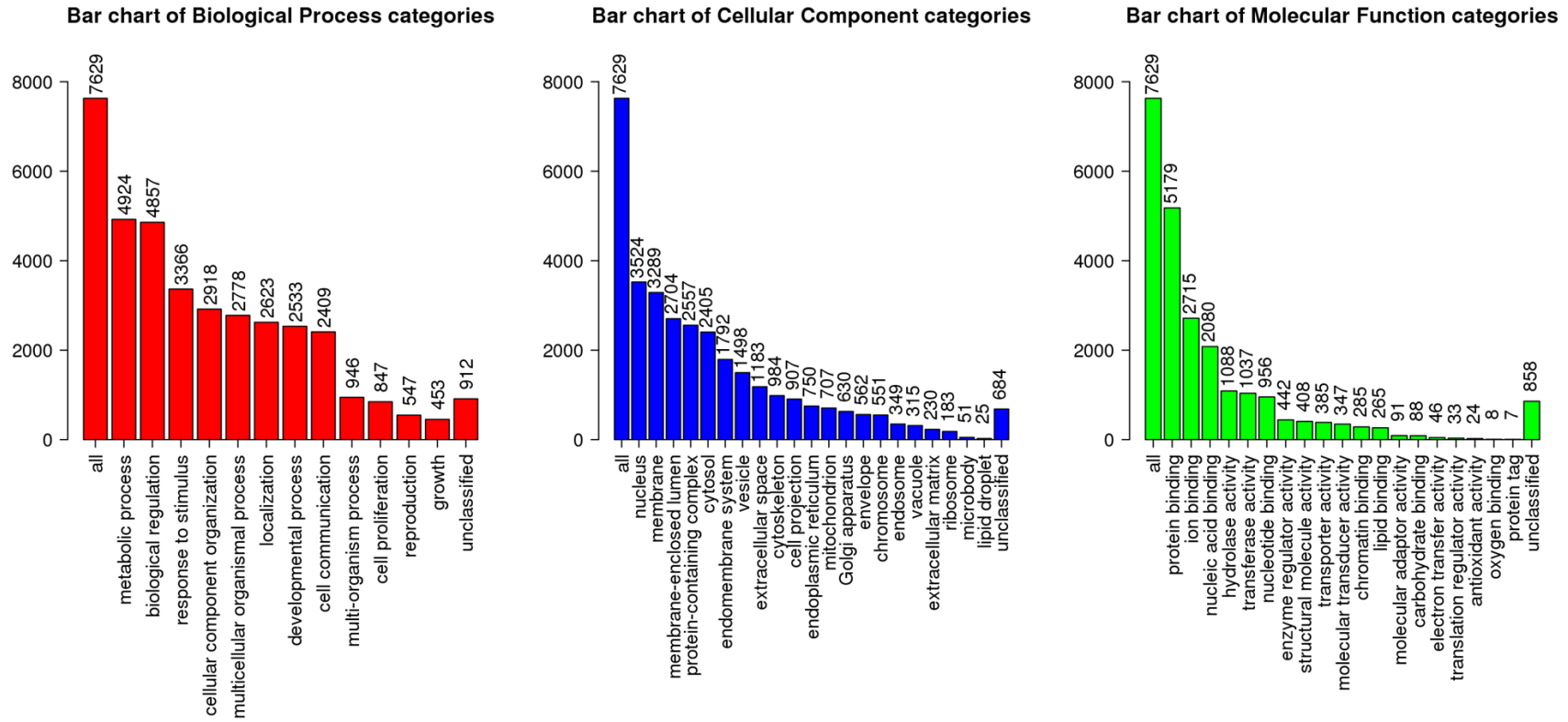


**Figure (F3): GO terms for the down-regulated genes. Each Biological Process, Cellular Component and Molecular Function category is represented by a red, blue and green bar, respectively. The height of the bar represents the number of down-regulated genes in each category.**



### **7.3 Appendix (3): Supplementary Tables**





Table (3): Summary of KEGG upregulated gene list

1	source	term_name	term_id	adjusted_p_value	negative_log10_of_adjusted_p_value	term_size	intersection_size	Genes
2	KEGG	Metabolic pathways	KEGG:01100	2.52966E-10	9.596937994	1424	640	ACO2,NAT2,CA1,AKR1B10,ACY1,CA7,PNP,NQO1,UGT1A10,HYAL2,DHCR7,PGAM1
3	KEGG	Rheumatoid arthritis	KEGG:05323	6.05788E-08	7.217679321	86	60	CXCL8,HLA-DOB,MMP1,MMP3,CXCL5,IL1B,CXCL1,TNF,IL23A,TNFSF13,ATP6V0D1,
4	KEGG	Osteoclast differentiation	KEGG:04380	6.32342E-08	7.199047955	125	80	SOCS3,SOCS1,TNFRSF11B,MAP2K6,IFNGR1,IL1B,NCF1,TYK2,PPARG,LILRA2,SIRP
5	KEGG	Tuberculosis	KEGG:05152	5.52476E-06	5.257686486	174	99	HLA-DOB,MYD88,PLK3,IFNGR1,CORO1A,IL1B,CASP8,CASP9,TNF,IL23A,IRAK2,AT
6	KEGG	Epstein-Barr virus infection	KEGG:05169	8.87685E-06	5.051741097	197	109	MYC,HLA-DOB,CR2,MYD88,CD19,CCNE2,CDKN1A,BAK1,MAP2K6,OAS1,TYK2,CXCL
7	KEGG	Influenza A	KEGG:05164	4.04211E-05	4.393392361	164	92	CXCL8,HLA-DOB,SOCS3,MYD88,BAK1,OAS1,IFNGR1,IL1B,TNFRSF10A,FDPS,TYK2
8	KEGG	TNF signaling pathway	KEGG:04668	7.42087E-05	4.12954509	110	66	SOCS3,MMP3,MAP2K6,CXCL5,IL1B,CXCL1,CREB3L4,CXCL10,CASP8,MMP9,TNF,JIU
9	KEGG	Graft-versus-host disease	KEGG:05332	7.94219E-05	4.100059993	36	28	HLA-DOB,IL1B,TNF,KLRC1,HLA-DRB5,PRF1,HLA-DMB,HLA-DQA2,HLA-E,HLA-DM
10	KEGG	Viral protein interaction with cytokine and cytokine receptor	KEGG:04061	9.15713E-05	4.038240789	98	60	CXCL13,CXCR3,TNFRSF10C,CXCL8,CCL24,CXCL5,TNFRSF10A,CXCR1,CXCL1,CXCL10,1
11	KEGG	B cell receptor signaling pathway	KEGG:04662	0.000103737	3.984064496	70	46	CD72,CD22,CR2,CD19,CD79A,VAV3,RAC2,PTPN6,FOS,CD79B,DAPP1,AKT1,PIK3CD
12	KEGG	Leishmaniasis	KEGG:05140	0.000187981	3.725886451	69	45	HLA-DOB,MYD88,IFNGR1,IL1B,NCF1,TNF,PTPN6,NCF2,NOS2,FOS,HLA-DRB5,FC
13	KEGG	Apoptosis	KEGG:04210	0.000356318	3.448162382	135	76	BAK1,BCL2L1,TNFRSF10A,CASP8,EIF2AK3,CASP9,TUBA4A,GNLY,CAPN1,LMNA,ACT
14	KEGG	Carbon metabolism	KEGG:01200	0.000412969	3.384082451	116	67	ACO2,PGAM1,IDH1,PC,GPT,SDHD,ME1,HK2,ACAT2,HKDC1,GLYCTK,SDHA,PGD,IC
15	KEGG	Hematopoietic cell lineage	KEGG:04640	0.00045175	3.345102278	93	56	HLA-DOB,CD22,CR2,CD19,CD1C,IL1B,MS4A1,ITGA2,TNF,FCER2,CD9,ANPEP,CD3E
16	KEGG	Viral myocarditis	KEGG:05416	0.000540398	3.267285934	55	37	HLA-DOB,CASP8,CASP9,ACTB,RAC2,SGCG,CD40,HLA-DRB5,PRF1,HLA-DMB,CYCS
17	KEGG	Hepatitis C	KEGG:05160	0.0008552	3.067932439	155	84	MYC,CLDN4,SOCS3,CLDN23,CDKN1A,BAK1,OAS1,OCLN,TYK2,CXCL10,CASP8,EIF2A
18	KEGG	IL-17 signaling pathway	KEGG:04657	0.001241862	2.905926532	91	54	CXCL8,MMP1,MMP3,CXCL5,IL1B,CXCL1,CXCL10,CASP8,MMP9,TNF,MAPK7,CCL17,T
19	KEGG	PD-L1 expression and PD-1 checkpoint pathway in cancer	KEGG:05235	0.001298761	2.886470715	89	53	MYD88,BATF2,MAP2K6,IFNGR1,LCK,TICAM1,PTPN6,FOS,LAT,AKT1,CD3D,PIK3CD
20	KEGG	Hepatitis B	KEGG:05161	0.001314161	2.8813515	163	87	MYC,CXCL8,MYD88,CCNE2,CDKN1A,MAP2K6,TYK2,CREB3L4,CASP8,MMP9,CASP9,
21	KEGG	Allograft rejection	KEGG:05330	0.001854461	2.731782271	34	25	HLA-DOB,TNF,CD40,HLA-DRB5,PRF1,HLA-DMB,HLA-DQA2,HLA-E,HLA-DMA,HLA
22	KEGG	Primary immunodeficiency	KEGG:05340	0.002123079	2.673033923	36	26	CD19,CD79A,LCK,TAP1,CIITA,AICDA,CD3D,UNG,ZAP70,CD40,CD8A,TNFRSF13C,C
23	KEGG	Human T-cell leukemia virus 1 infection	KEGG:05166	0.00301358	2.520917311	216	109	MYC,HLA-DOB,CCNE2,ZFP36,MMP7,SLC2A1,CDKN1A,BCL2L1,CDC20,FDPS,MAD2I
24	KEGG	Th17 cell differentiation	KEGG:04659	0.003338561	2.476440659	104	59	HLA-DOB,IFNGR1,IL1B,TYK2,LCK,IL23A,FOS,IL27RA,LAT,CD3D,IL21R,ZAP70,HLA-
25	KEGG	T cell receptor signaling pathway	KEGG:04660	0.003776726	2.422884482	100	57	TNF,VAV3,LCK,PTPN6,FOS,LAT,AKT1,CD3D,PIK3CD,ZAP70,GRAP2,CD8A,CD8B,NC
26	KEGG	NF-kappa B signaling pathway	KEGG:04064	0.004012492	2.396585847	98	56	CXCL8,MYD88,BCL2L1,IL1B,TNF,CCL4L2,LCK,TICAM1,BCL2A1,LAT,ZAP70,CD40,TN
27	KEGG	Bladder cancer	KEGG:05219	0.005318658	2.274197933	41	28	MYC,CXCL8,MMP1,CDKN1A,MMP9,DAPK2,RPS6KA5,CDH1,RASSF1,FGFR3,NRAS,F
28	KEGG	Endocytosis	KEGG:04144	0.005397395	2.267815825	244	120	CXCR1,ADRBK1,DNM2,GRK6,VPS37B,ARF6,RAB10,CAPZA1,RAB8A,ZFYVE27,CYTH
29	KEGG	Natural killer cell mediated cytotoxicity	KEGG:04650	0.005803607	2.236302019	123	67	IFNGR1,TNFRSF10A,TNF,VAV3,CD48,LCK,RAC2,PTPN6,KLRC1,KLRC3,TNFRSF10B,
30	KEGG	Legionellosis	KEGG:05134	0.006037866	2.219116499	55	35	CXCL8,MYD88,IL1B,CXCL1,CASP8,CASP9,TNF,CASP7,CASP1,CXCL3,ARF1,CXCL2,VC
31	KEGG	Peroxisome	KEGG:04146	0.006628713	2.178570772	80	47	IDH1,PEX10,PEX13,DECR2,NOS2,PECR,PEX14,PEX11G,SLC27A2,PEX26,ACAA1,SCP



#### **7.4 Appendix (4): Interstitial cell marker gene sequences**

**(1) cKit (KIT)**

**>ENST00000288135.5 Ensembl Transcript chromosome:GRCh38:4:1:190214555:1**

CGCTCGCGGCTCTGGGGGCTCGGCTTTGCCGCGCTCGCTGCACTTGGGCGAGAGCTGGAA  
 CGTGACCAGAGCTCGGATCCCATCGCAGCTACCGCGATGAGAGGCGCTCGCGGCGCCTG  
 GGATTTTCTCTGCGTTCTGCTCCTACTGCTTCGCGTCCAGACAGGCTCTTCTCAACCATC  
 TGTGAGTCCAGGGGAACCGTCTCCACCATCCATCCATCCAGGAAAATCAGACTTAATAGT  
 CCGCGTGGGCGACGAGATTAGGCTGTTATGCACTGATCCGGGCTTTGTCAAATGGACTTT  
 TGAGATCCTGGATGAAACGAATGAGAATAAGCAGAATGAATGGATCACGAAAAGGCAGA  
 AGCCACCAACACCGGCAAATACACGTGCACCAACAAACACGGCTTAAGCAATTCCATTTA  
 TGTGTTTGTAGAGATCCTGCCAAGCTTTTCTTGTGACCGCTCCTTGTATGGGAAAGA  
 AGACAACGACACGCTGGTCCGCTGTCTCTCACAGACCCAGAAGTGACCAATTATTCCCT  
 CAAGGGGTGCCAGGGGAAGCCTCTTCCAAGGACTTGAGGTTTATTCTGACCCCAAGGC  
 GGGCATCATGATCAAAGTGTGAAACGCGCCTACCATCGGCTCTGTCTGCATTGTTCTGT  
 GGACCAGGAGGGCAAGTCAGTGTGTGCGAAAAATTCATCCTGAAAGTGAGGCCAGCCTT  
 CAAAGCTGTGCCTGTTGTGTCTGTGTCCAAAGCAAGCTATCTTCTTAGGGAAGGGGAAGA  
 ATTCACAGTGACGTGCACAATAAAAGATGTGTCTAGTTCTGTGTACTCAACGTGGAAAAG  
 AGAAAACAGTCAGACTAACTACAGGAGAAATATAATAGCTGGCATCACGGTGACTTCAA  
 TTATGAACGTCAGGCAACGTTGACTATCAGTTCAGCGAGAGTTAATGATTCTGGAGTGTT  
 CATGTGTTATGCCAATAATACTTTTGGATCAGCAAATGTCACAACAACCTTGAAGTAGT  
 AGATAAAGGATTCATTAATATCTTCCCATGATAAACACTACAGTATTTGTAAACGATGG  
 AGAAAATGTAGATTTGATTGTTGAATATGAAGCATTCCCAAACCTGAACACCAGCAGTG  
 GATCTATATGAACAGAACCTTCACTGATAAATGGGAAGATTATCCCAAGTCTGAGAATGA  
 AAGTAATATCAGATACGTAAGTGAACCTCATCTAACGAGATTAAGGACCCGAAGGAGG  
 CACTTACACATTCTAGTGCCAATTCTGACGTCAATGCTGCCATAGCATTAAATGTTTA  
 TGTGAATACAAAACCAGAAATCCTGACTTACGACAGGCTCGTGAATGGCATGCTCCAATG  
 TGTGGCAGCAGGATTCCCAGAGCCCACAATAGATTGGTATTTTTGTCCAGGAACTGAGCA  
 GAGATGCTCTGCTTCTGTACTGCCAGTGGATGTGCAGACACTAACTCATCTGGGCCACC  
 GTTTGGAAAGCTAGTGGTTCAGAGTTCTATAGATTCTAGTGCATTCAAGCACAATGGCAC  
 GGTTGAATGTAAGGCTTACAACGATGTGGGCAAGACTTCTGCCTATTTTAACTTTGCATT  
 TAAAGGTAACAACAAAGAGCAAATCCATCCCACACCCTGTTCACTCCTTTGCTGATTGG  
 TTTTCGTAATCGTAGCTGGCATGATGTGCATTATTGTGATGATTCTGACCTACAAATATTT  
 ACAGAAACCCATGTATGAAGTACAGTGGAAGGTTGTTGAGGAGATAAATGGAAACAATTA  
 TGTTTACATAGACCCAACACAACCTTCTTATGATCACAATGGGAGTTTCCAGAAACAG  
 GCTGAGTTTTGGGAAAACCCTGGGTGCTGGAGCTTTCGGGAAGGTTGTTGAGGCAACTGC  
 TTATGGCTTAATTAAGTCAGATGCGGCCATGACTGTCGCTGTAAAGATGCTCAAGCCGAG  
 TGCCCATTTGACAGAACGGGAAGCCCTCATGTCTGAACTCAAAGTCCTGAGTTACCTTGG

TAATCACATGAATATTGTGAATCTACTTGGAGCCTGCACCATTGGAGGGCCACCCTGGT  
CATTACAGAATATTGTTGCTATGGTGTCTTTTGAATTTTTTGGAGAAGAAAACGTGATTC  
ATTTATTTGTTCAAAGCAGGAAGATCATGCAGAAGCTGCACTTTATAAGAATCTTCTGCA  
TTCAAAGGAGTCTTCCTGCAGCGATAGTACTAATGAGTACATGGACATGAAACCTGGAGT  
TTCTTATGTTGTCCCAACCAAGGCCGACAAAAGGAGATCTGTGAGAATAGGCTCATACAT  
AGAAAGAGATGTGACTCCCGCCATCATGGAGGATGACGAGTTGGCCCTAGACTTAGAAGA  
CTTGCTGAGCTTTTCTTACCAGGTGGCAAAGGGCATGGCTTTCCTCGCCTCCAAGAATTG  
TATTCACAGAGACTTGGCAGCCAGAAATATCCTCCTTACTCATGGTCCGATCACAAAGAT  
TTGTGATTTTGGTCTAGCCAGAGACATCAAGAATGATTCTAATTATGTGGTTAAAGGAAA  
CGCTCGACTACCTGTGAAGTGGATGGCACCTGAAAGCATTTCAACTGTGTATACACGTT  
TGAAAGTGACGTCTGGTCCTATGGGATTTTTCTTTGGGAGCTGTTCTCTTTAGGAAGCAG  
CCCCTATCCTGGAATGCCGGTCGATTCTAAGTCTACAAGATGATCAAGGAAGGCTTCCG  
GATGCTCAGCCCTGAACACGCACCTGCTGAAATGTATGACATAATGAAGACTTGCTGGGA  
TGCAGATCCCCTAAAAAGACCAACATTCAAGCAAATTGTTCACTAATTGAGAAGCAGAT  
TTCAGAGAGCACCAATCATATTTACTCCAACCTTAGCAAACCTGCAGCCCCAACCGACAGAA  
GCCCGTGGTAGACCATTCTGTGCGGATCAATTCTGTGCGCAGCACCGCTTCTCCTCCCA  
GCCTCTGCTTGTGCACGACGATGTCTGAGCAGAATCAGTGTGGTCCACCCCTCCAGGA  
ATGATCTCTTCTTTTGGCTTCCATGATGGTTATTTTCTTTTCTTTCAACTTGCATCCAAC  
TCCAGGATAGTGGGCACCCCACTGCAATCCTGTCTTTCTGAGCACACTTTAGTGGCCGAT  
GATTTTTGTCATCAGCCACCATCCTATTGCAAAGGTTCCAACCTGTATATATTCCAATAG  
CAACGTAGCTTCTACCATGAACAGAAAACATTCTGATTTGGAAAAAGAGAGGGGAGGTATG  
GACTGGGGGCCAGAGTCTTTCCAAGGCTTCTCCAATTCTGCCAAAAAATATGGTTGATA  
GTTTACCTGAATAAATGGTAGTAATCACAGTTGGCCTTCAGAACCATCCATAGTAGTATG  
ATGATAACAAGATTAGAAGCTGAAAACCTAAGTCTTTTATGTGGAAAACAGAACATCATT  
GAACAAAGGACAGAGTATGAACACCTGGGCTTAAGAAATCTAGTATTTTCATGCTGGGAAT  
GAGACATAGGCCATGAAAAAATGATCCCCAAGTGTGAACAAAAGATGCTCTTCTGTGGA  
CCTGTCATGAGCTTTTATACTACCGACCTGGTTTTTAAATAGAGTTTGCTATTAGAGCA  
TTGAATTGGAGAGAAGGCCTCCCTAGCCAGCACTTGTATATACGCATCTATAAATTGTCC  
GTGTTTACATTTGAGGGGAAAACACCATAAGGTTTTCGTTTTCTGTATACAACCCTGGCA  
TTATGTCCACTGTGTATAGAAGTAGATTAAGAGCCATATAAGTTTGAAGGAAACAGTTAA  
TACCATTTTTTAAGGAAACAATATAACCACAAAAGCACAGTTTGAACAAAATCTCCTCTTT  
TAGCTGATGAACTTATTCTGTAGATTCTGTGGAACAAGCCTATCAGCTTCAGAATGGCAT  
TGTACTCAATGGATTTGATGCTGTTTGACAAAGTTACTGATTCACTGCATGGCTCCCACA  
GGAGTGGGAAAACACTGCCATCTTAGTTTGGATTCTTATGTAGCAGGAAATAAAGTATAG  
GTTTAGCCTCCTTCGCAGGCATGTCTGGACACCGGGCCAGTATCTATATATGTGTATGT  
ACGTTTGTATGTGTAGACAAATATTGGAGGGGTATTTTTGCCCTGAGTCCAAGAGGG

TCCTTTAGTACCTGAAAAGTAACTTGGCTTTCATTATTAGTACTGCTCTTGTTTCTTTTC  
ACATAGCTGTCTAGAGTAGCTTACCAGAAGCTTCCATAGTGGTGCAGAGGAAGTGGAAGG  
CATCAGTCCCTATGTATTTGCAGTTCACCTGCACTTAAGGCACTCTGTTATTTAGACTCA  
TCTTACTGTACCTGTTCCCTTAGACCTTCCATAATGCTACTGTCTCACTGAAACATTTAAA  
TTTTACCCTTTAGACTGTAGCCTGGATATTATTCTTGTAGTTTACCTCTTTAAAAACAAA  
ACAAAACAAAACAAAAAATCCCCTTCCCTCACTGCCCAATATAAAAAGGCAAATGTGTACA  
TGGCAGAGTTTGTGTGTTGTCTTGAAAGATTGAGGTATGTTGCCTTTATGGTTTCCCCCT  
TCTACATTTCTTAGACTACATTTAGAGAAGTGTGGCCGTTATCTGGAAGTAACCATTTGC  
ACTGGAGTTCTATGCTCTCGCACCTTTCCAAAGTTAACAGATTTTGGGGTTGTGTTGTCA  
CCCAAGAGATTGTTGTTTCCATACTTTGTCTGAAAAATTCCTTTGTGTTTCTATTGACT  
TCAATGATAGTAAGAAAAGTGGTTGTTAGTTATAGATGTCTAGGTACTTCAGGGGCACTT  
CATTGAGAGTTTTGTCTTGGATATTCTTGAAAGTTTATATTTTATAATTTTTTCTTACA  
TCAGATGTTTCTTTGCAGTGGCTTAATGTTTGAATTATTTTGTGGCTTTTTTTGTAAAT  
ATTGAAATGTAGCAATAATGTCTTTTGAATATTCCAAGCCCATGAGTCCTTGAAAATAT  
TTTTATATATACAGTAACTTTATGTGTAATACATAAGCGGCGTAAGTTTAAAGGATGT  
TGGTGTTCACGTGTTTTATTCCCTGTATGTTGTCCAATTGTTGACAGTTCTGAAGAATTC  
TAATAAAATGTACATATATAAATCAA

**(2) Ano1**

**>ENST00000355303.9 Ensembl Transcript chromosome:GRCh38:11:1:135086622:1**

AAAGGCGGGCCGGCTGGCGTCCAAGTTCCTGACCAGGCGGGCCGGCCCCGCGGACCAG  
 CAGCCGGGTGGCGGCGGATCGGCCCCGAGAGGCTCAGGCGCCCCCGCATCGAGCGCGC  
 GGGCCGGGCGGGCCAGGGCGGGCGGCGGAGCGGGAGGCGCCACGTCCCCGGCGGGCCTG  
 GGCGCGGGGAGGCCCGCCCCCTGCGAGCGCGCCGCAACGCTGCGGTCTCCGCCCGCAG  
 AGGCCCGCGGGGCCGTGGATGGGGAGGGCGCGCCGCCCCGGCGGTCCCAGCGCACAGGCGG  
 CCACGATGAGGGTCAACGAGAAGTACTCGACGCTCCCCGGCCGAGGACCGCAGCGTCCACA  
 TCATCAACATCTGCGCCATCGAGGACATCGGCTACCTGCCGTCCGAGGGCAGCTGCTGA  
 ACTCCTTATCTGTGGACCCTGATGCCGAGTGCAAGTATGGCCTGTACTTCAGGGACGGCC  
 GGC GCAAGGTGGACTACATCCTGGTGTACCATCACAAGAGGCCCTCGGGCAACCGGACCC  
 TGGTCAGGAGGGTGCAGCACAGCGACACCCCCTCTGGGGCTCGCAGCGTCAAGCAGGACC  
 ACCCCCTGCCGGCAAGGGGGCGTCGCTGGATGCAGGCTCGGGGAGCCCCCGATGGACT  
 ACCACGAGGATGACAAGCGCTTCCGCAGGGAGGAGTACGAGGGCAACCTCCTGGAGGCGG  
 GCCTGGAGCTGGAGCGGGACGAGGACACTAAAATCCACGGAGTCGGGTTTGTGAAAATCC  
 ATGCCCCCTGGAACGTGCTGTGCAGAGAGGCCGAGTTTCTGAAACTGAAGATGCCGACGA  
 AGAAGATGTACCACATTAATGAGACCCGTGGCCTCCTGAAAAAATCAACTCTGTGCTCC  
 AGAAAATCACAGATCCCATCCAGCCCAAAGTGGCTGAGCACAGGCCCCAGACCATGAAGA  
 GACTCTCCTATCCCTTCTCCCGGAGAAGCAGCATCTATTTGACTTGTCTGATAAGGATT  
 CCTTTTTCGACAGCAAACCCGGAGCACGATTGTCTATGAGATCTTGAAGAGAACGACGT  
 GTACAAAAGCCAAGTACAGCATGGGCATCACGAGCCTGCTGGCCAATGGTGTGTACGCGG  
 CTGCATACCCACTGCACGATGGAGACTACAACGGTGAAAACGTCGAGTTCAACGACAGAA  
 AACTCCTGTACGAAGAGTGGGCACGCTATGGAGTTTTCTATAAGTACCAGCCCATCGACC  
 TGGTCAGGAAGTATTTTGGGGAGAAGATCGGCCTGTACTTCGCCTGGCTGGGCGTGTACA  
 CCCAGATGCTCATCCCTGCCTCCATCGTGGGAATCATTGTCTTCTGTACGGATGCGCCA  
 CCATGGATGAAAACATCCCCAGCATGGAGATGTGTGACCAGAGACACAATATCACCATGT  
 GCCCGCTTTGCGACAAGACCTGCAGCTACTGGAAGATGAGCTCAGCCTGCGCCACGGCCC  
 GCGCCAGCCACCTCTTCGACAACCCCGCCACGGTCTTCTTCTGTCTTCATGGCCCTCT  
 GGGCTGCCACCTTCATGGAGCACTGGAAGCGGAAACAGATGCGACTCAACTACCGCTGGG  
 ACCTCACGGGCTTTGAAGAGGAAGAGGAGGCTGTCAAGGATCATCCTAGAGCTGAATACG  
 AAGCCAGAGTCTTGGAGAAGTCTCTGAAGAAAGAGTCCAGAAACAAAGAGAAGCGCCGGC  
 ATATTCCAGAGGAGTCAACAAACAAATGGAAGCAGAGGGTTAAGACAGCCATGGCGGGGG  
 TGAAATTGACTGACAAAAGTGAAGCTGACATGGAGAGATCGGTTCCCAGCCTACCTACTA  
 ACTTGGTCTCCATCATCTTCATGATTGCAGTGACGTTTGCCATCGTCCTCGGCGTCATCA  
 TCTACAGAATCTCCATGGCCGCCGCTTGGCCATGAACTCCTCCCCCTCCGTGCGGTCCA  
 ACATCCGGGTACAGTCACAGCCACCGCAGTCATCATCAACCTAGTGGTCATCATCCTCC

TGGACGAGGTGTATGGCTGCATAGCCCCGATGGCTCACCAAGATCGAGGTCCCAAAGACGG  
AGAAAAGCTTTGAGGAGAGGCTGATCTTCAAGGCTTTCCTGCTGAAGTTTGTGAATTCCT  
ACACCCCCATCTTTTACGTGGCGTTCTTCAAAGGCCGTTTTGTTGGACGCCCGGGCGACT  
ACGTGTACATTTTCCGTTCCCTCCGAATGGAAGAGTGTGCGCCAGGGGGCTGCCTGATGG  
AGCTATGCATCCAGCTCAGCATCATCATGCTGGGGAAACAGCTGATCCAGAACAACCTGT  
TCGAGATCGGCATCCCGAAGATGAAGAAGCTCATCCGCTACCTGAAGCTGAAGCAGCAGA  
GCCCCCTGACCACGAGGAGTGTGTGAAGAGGAAACAGCGGTACGAGGTGGATTACAACC  
TGGAGCCCTTCGCGGGCCTCACCCAGAGTACATGGAATGATCATCCAGTTTGGCTTCG  
TCACCCTGTTTGTGCGCTCCTTCCCCCTGGCCCCACTGTTTGCCTGCTGAACAACATCA  
TCGAGATCCGCTGGACGCCAAAAAGTTTGTCACTGAGCTCCGAAGGCCGGTAGCTGTCA  
GAGCCAAAGACATCGGAATCTGGTACAATATCCTCAGAGGCATTGGGAAGCTTGCTGTCA  
TCATCAATGCCTTCGTGATCTCCTTACGTCTGACTTCATCCCGCGCCTGGTGTACCTCT  
ACATGTACAGTAAGAACGGGACCATGCACGGCTTCGTCAACCACACCCTCTCCTCCTTCA  
ACGTCACTGACTTCCAGAACGGCACGGCCCCAATGACCCCTGGACCTGGGCTACGAGG  
TGCAGATCTGCAGGTATAAAGACTACCGAGAGCCGCGTGGTCGGAAAAACAAGTACGACA  
TCTCCAAGGACTTCTGGGCCGTCTGGCAGCCCGGCTGGCGTTTTGCATCGTCTTCCAGA  
ACCTGGTCATGTTTCATGAGCGACTTTGTGGACTGGGTCATCCCGGACATCCCCAAGGACA  
TCAGCCAGCAGATCCACAAGGAGAAGGTGCTCATGGTGGAGCTGTTTCATGCGGGAGGAGC  
AAGACAAGCAGCAGCTGCTGAAAACCTGGATGGAGAAGGAGCGGCAGAAGGACGAGCCGC  
CGTGCAACCACCACAACACCAAAGCCTGCCAGACAGCCTCGGCAGCCCAGCCCCAGCC  
ATGCCTACCACGGGGGCGTCTGTAGCTATGCCAGCGGGGCTGGGCAGGCCAGCCGGGCA  
TCCTGACCGATGGGCACCCTCTCCCAGGGCAGGCGGCTTCCCGCTCCCACCAGGGCCCGG  
TGGGTCCTGGGTTTTCTGCAAACATGGAGGACCACTTTCTGATAGGACATTTTCTTTCT  
TCTTTCTGTTTTCTTCCCTTGTTTTTGCACAAAGCCATTATGCAGGGAATATTTTTTAA  
TCTGTAGTATTCAAGATGAATCAAAATGATGGCTGGTAATACGGCAATAAGGTAGCAAAG  
GCAGGTGCTTTCAGAAAAGATGCTTGAAACTTGAGTCTCCCTAGAGGTGAAAAGTGAG  
CAGAGGCCCGTAGAAACCCTCCTCTGAATCCTCCTAATTCCTTAAGATAGATGCAAAATG  
GTAAGCCGAGGCATCGCGCAAAGCTGGTGCATGCTTCAGGGAAAATGGAAAACCCACG  
CAAGAATAATGATTGATTCCGGTTCCAAAAGGTGTCACCTACCTGTTTCAGAAAAGTTAG  
ACTTTCCATCGCCTTTTCTTCCATCAGTTGAGTGGCTGAGAGAGAAGTGCCTCATCCCT  
GAGCCACACAGGGGGCGTGGGAGCATCCCAGTTATCCCTGGAAAAGCTAGAAGGGGACAGA  
GGTGTCCCTGATTAAGCAGGAAACAGCACCCCTTGGCGTCCCAGCAGGCTCCCCACTGTC  
AGCCACACACCTGCCCCATCACACCAAGCCGACCTCAGAGTTGTTTCATCTTCTTATGG  
GACAAAACCGGTTGACCAGAAAATGGGCAGAGAGAGATGACCTCGGAAGCATTTCACAG  
ATGGTGTGAGGGTTTCAAGAAGCTTAGGGCTTCCAGGGTCCCCTGGAAGCTTTAGAAT  
ATTTATGGGTTTTTTTTCAAATATCAATTATGTTAGATTGAGGATTTTTTTTTCTGTAG

CTCAAAGGTGGAGGGAGTTTATTAGTTAACCAAATATCGTTGAGAGGAATTTAAAATACT  
GTTACTACCAAAGATTTTTATTAATAAAGGCTTATATTTTGGTAACACTTCTCTATATTT  
TACTCACAGGAATGTCACTGTTGGACAATTATTTTAAAAGTGTATAAAACCAAGTCTCA  
TAAATGATATGAGTGATCTAAATTTGCAGCAATGATACTAAACAACCTCTCTGAAATTTCT  
CAAGCACCAAGAGAAAACATCATTTTAGCAAAGGCCAGGAGGAAAAATAGAAATAAATTTG  
TCTTGAAGATCTCATTGATGTGATGTTACATTCCCTTTAATCTGCCAACTGTGGTCAAAG  
TTCATAGGTGTCGTACATTTCCATTATTTGCTAAAATCATGCAATCTGATGCTTCTCTTT  
TCTCTTGTACAGTAAGTAGTTTGAAGTGGGTTTTGTATATAAATACTGTATTAATAAATTA  
GGCAATTACCAAAAATCCTTTTATGGAAACCATTTTTTTAAAAGTGAATGTACACAAAT  
CCACAGAGGACTGTGGCTGGACATTCATCTAAATAAATTTGAATATACGA

**(3) PDGFRA****>ENST00000508170.5 Ensembl Transcript chromosome:GRCh38:4:1:190214555:1**

GGTTTTTGAGCCCATTACTGTTGGAGCTACAGGGAGAGAAACAGAGGAGGAGACTGCAAG  
 AGATCATTGGAGGCCGTGGGCACGCTCTTTACTCCATGTGTGGGACATTCATTGCGGAAT  
 AACATCGGAGGAGAAGTTTCCCAGAGCTATGGGGACTTCCCATCCGGCGTTCCTGGTCTT  
 AGGCTGTCTTCTCACAGGGCTGAGCCTAATCCTCTGCCAGCTTTCATTACCCTCTATCCT  
 TCCAAATGAAAATGAAAAGGTTGTGCAGCTGAATTCATCCTTTTCTCTGAGATGCTTTGG  
 GGAGAGTGAAGTGAAGTGGCAGTACCCCATGTCTGAAGAAGAGAGCTCCGATGTGGAAAT  
 CAGAAATGAAGAAAACAACAGCGGCCTTTTTGTGACGGTCTTGAAGTGAAGCAGTGCCTC  
 GCGGCCACACAGGGTTGTACACTTGCTATTACAACCACACTCAGACAGAAGAGAATGA  
 GCTTGAAGGCAGGCACATTTACATCTATGTGCCAGACCCAGATGTAGCCTTTGTACCTCT  
 AGGAATGACGGATTATTTAGTCATCGTGAGGATGATGATTCTGCCATTATACCTTGTGC  
 CACAACCTGATCCCGAGACTCCTGTAACCTTACACAACAGTGAGGGGGTGGTACCTGCCTC  
 CTACGACAGCAGACAGGGCTTAATGGGACCTTCACTGTAGGGCCCTATATCTGTGAGGC  
 CACCGTCAAAGGAAAGAAGTTCCAGACCATCCCATTTAATGTTTATGCTTTAAAAGGTAC  
 TTGTATCATCTCCTTCTTCTTTAAATAAGAGTAACAGGCAAATCATAAGGTGCGTGTA  
 GGATTTTTTTTTTTTTTAAATCATCATCACTGGTGATCCTAAATTCTGATTTGGGGATT  
 TAGGACCCAGCTAATACAATGTCTGTGGCTATAATAAAGCTTAAAATTAATAAAGGC  
 CAAAGCTTGATTACCCATGCAAGATTTTATGTTTCATCAGTTGACTTCAAATACTGTAA  
 GGAATCTTTTCTTACATAAGCCTCTTACTTTTATTACATTCTGACTATGGCGGCCCT  
 AAAAACAAACATACACCCAGGGGGTTAGATGCCTAGATTAATTTTAGTAACCTAAGAAAA  
 GTGATTTGAAGAAAGTAGTTTAGACTTCAACCCTTTGATGTCCACAGTTAGTACGCTTGG  
 GGAAGTATAATACATGCTGAGGTCAACAGATATTTCTGAACACTATATTACATGGAGGA  
 ATGGGTAGCAGCAAGAGTACACTGTTTTAAATCAGAGCACAGCTAATTTTGTGCCAGGC  
 ACTGTGCTAGGTTCTGGGAAAGTACTGAGAATAACTGAGGAGCAGAGTGAAGAGAAGAA  
 GAGAAGAAACAATTGGATAGAAACAAAGTGTCTAGAGCAGTGTGGATCAGCAAATGTTGG  
 TTGATTAATGAATAAATTTATTAGTCAAGGAGATTGTGGACGAGTATAACCATAACTAA  
 CCCACTGCTGAGGAATGCGGTGTTCTGTTTATTGGAATTTATTTTATTGTTATTATT  
 TGTAATTCTGTATTATAACTATATGCCTAATTGTTGTACACCATCTCACAATCAAGCCTT  
 GTGAGATTTTCCAAATTTTATCTTGATCAAACCTGGTTTGCAAATTTTTTTCAGGGTTTT  
 CTTAAAAAATAAATAAATAAATAAATAAATAAATAAATAAATAAATAAATAAATAAATAA  
 GGCCCTTGATTTGTTCTTTTTTATAGCAACATCAGAGCTGGATCTAGAAATGGAAGCTC  
 TAAAACCGTGATAAGTCAGGGGAAACGATTGTGGTCACCTGTGCTGTTTTAACAATG  
 AGGTGGTTGACCTTCAATGGACTTACCCTGGAGAAGTGGTAGGTACCCTCAAACGTGCA  
 ATGGCTTGGAGCAGAGCAACAGGGCTCAGAAGACCTGCATTTGAGCTCGGTCTGTCACTG

ATGGGCACATCACTGAGTTTCTCTAGACCTTAGCTTCCCACCTCTGGGATGAACACATTT  
GATTAAATGGCCTTTAGGACTCCTTGATCAATGGGAGAGTTTGAAATGATAGTTCCTGGA  
CCAGGCCCTTCAGAATACATAAAGAGTGTGCCGTAAGCCTTCTTTTTCAGAAGTCAGACA  
GAAATAGGAAGGTTCTCTGGCTACAAGATATCAACCAAAAAA

**(4) KCNN3**

**>ENST00000271915.8 Ensembl Transcript chromosome:GRCh38:1:1:248956422:1**

TTGAGCCAGCGAGGAGTGAAGCTGAGCCTGGCCTCACACGCTCCTAGAGGACCACCTCCT  
GAGAGAGTTCTTTACCCCCTCTTCTTTCTCCAAGCTCCCCTCCTGCTCTCCCTCCCTGC  
CCAATACAATGCATTCTTGAGTGGCAGCGTCTGGACTCCAGGCAGCCCCAGAGAACCGAA  
GCAAGCCAAAGAGAGGACTGGAGCCAAGATACTGGTGGGGGAGATTGGATGCCTGGCTTT  
CTTTGAGGACATCTTTGGAGCGAGGGTGGCTTTGGGGTGGGGGCTTGTGCTGCAGGGAAT  
ACAGCCAGGCCCCAAGATGGACACTTCTGGGCACTTCCATGACTCGGGGGTGGGGGACTT  
GGATGAAGACCCCAAGTGCCCCTGTCCATCCTCTGGGGATGAGCAGCAGCAGCAGCAGCA  
GCAGCAACAGCAGCAGCAGCCACCACCGCCAGCGCCACCAGCAGCCCCCAGCAGCCCCT  
GGGACCCTCGCTGCAGCCTCAGCCTCCGCAGCTTCAGCAGCAGCAGCAGCAGCAGCAGCA  
GCAGCAGCAGCAGCAGCCACCGCATCCCCTGTCTCAGCTCGCCCAACTCCAGAGCCAGCC  
CGTCCACCCTGGCCTGCTGCACTCCTCTCCCACCGCTTTCAGGGCCCCCCCCCTTCGTCCAA  
CTCCACCGCCATCCTCCACCCTTCTCCAGGCAAGGCAGCCAGCTCAATCTCAATGACCA  
CTTGCTTGGCCACTCTCCAAGTTCCACAGCTACAAGTGGGCCTGGCGGAGGCAGCCGGCA  
CCGACAGGGCCAGCCCCCTGGTGCACCGGCGGGACAGCAACCCCTTCACGGAGATCGCCAT  
GAGCTCCTGCAAGTATAGCGGTGGGGTCATGAAGCCCCTCAGCCGCCTCAGCGCCTCCCC  
GAGGAACCTCATCGAGGCCGAGACTGAGGGCCAACCCCTCCAGCTTTTCAGCCCTAGCAA  
CCCCCGGAGATCGTCATCTCCTCCCGGAGGACAACCATGCCACCCAGACCCTGCTCCA  
TCACCCTAATGCCACCCACAACCACCAGCATGCCGGCACCCACCGCCAGCAGCACCACCTT  
CCCCAAAGCCAACAAGCGGAAAAACCAAACATTGGCTATAAGCTGGGACACAGGAGGGC  
CCTGTTTGAAAAGAGAAAGCGACTGAGTACTATGCTCTGATTTTTGGGATGTTTGGAAT  
TGTTGTTATGGTGATAGAGACCGAGCTCTCTTGGGGTTTGTACTCAAAGGACTCCATGTT  
TTCGTTGGCCCTGAAATGCCTTATCAGTCTGTCCACCATCATCCTTTTGGGCTTGATCAT  
CGCCTACCACACACGTGAAGTCCAGCTCTTCGTGATCGACAATGGCGCGGATGACTGGCG  
GATAGCCATGACCTACGAGCGCATCCTGTACATCAGCCTGGAGATGCTGGTGTGCGCCAT  
CCACCCATTCTGGCGAGTACAAGTTCTTCTGGACGGCACGCCTGGCCTTCTCCTACAC  
ACCCTCCCGGGCGGAGGCCGATGTGGACATCATCCTGTCTATCCCCATGTTCTGCGCCT  
GTACCTGATCGCCCCGAGTCATGCTGCTGCACAGCAAGCTCTTACCGATGCCTCGTCCCG  
CAGCATCGGGGCCCTCAACAAGATCAACTTCAACACCCGCTTTGTCATGAAGACGCTCAT  
GACCATCTGCCCTGGCACTGTGCTGCTCGTGTTTCAGCATCTCTCTGTGGATCATTGCTGC  
CTGGACCGTCCGTGTCTGTGAAAGGTACCATGACCAGCAGGACGTAAGTAGTAACCTTCT  
GGTGCCATGTGGCTCATCTCCATCACATTCTTTCCATTGGTTATGGGGACATGGTGCC  
CCACACATACTGTGGGAAAGGTGTCTGTCTCCTCACTGGCATCATGGGTGCAGGCTGCAC  
TGCCCTTGTGGTGGCCGTGGTGGCCCGAAAGCTGGAACCTACCAAAGCGGAGAAGCACGT

TCATAACTTCATGATGGACTCAGCTCACCAAGCGGATCAAGAATGCTGCAGCCAATGT  
CCTTCGGGAAACATGGTTAATCTATAAACACACAAAGCTGCTAAAGAAGATTGACCATGC  
CAAAGTGAGGAAACACCAGAGGAAGTTCCTCCAAGCTATCCACCAGTTGAGGAGCGTCAA  
GATGGAACAGAGGAAGCTGAGTGACCAAGCCAACACTCTGGTGGACCTTTCCAAGATGCA  
GAATGTCATGTATGACTTAATCACAGAACTCAATGACCGGAGCGAAGACCTGGAGAAGCA  
GATTGGCAGCCTGGAGTCGAAGCTGGAGCATCTCACCGCCAGCTTCAACTCCCTGCCGCT  
GCTCATCGCCGACACCCTGCGCCAGCAGCAGCAGCAGCTCCTGTCTGCCATCATCGAGGC  
CCGGGGTGTGAGCGTGGCAGTGGCACCACCCACACCCCAATCTCCGATAGCCCCATTGG  
GGTCAGCTCCACCTCCTTCCCGACCCCGTACACAAGTTCAAGCAGTTGCTAAATAAATCT  
CCCCACTCCAGAAGCATTACCCATAGGTCTTAAGATGCAAATCAACTCTCTCTGGTCGC  
TTTGCCATCAAGAAACATTCAGACCAGGGAACGGAAAGAAGAGAGACCGAGCTAATTAAC  
TAACTCATGTTCAATTCAGCGTGCTTGGTCCGACATGCCTTGAAACCAGAAATCTAATCTC  
TGTTTAGGTGCCTCTACTTGGGAGCGGGAAGAGGAGATGACAGGAAGCGACGCCTCTGGC  
AGGGCCCTTGCTGCAGAGTTGGTGGAGAACAGAAATCCACGCTCAATCTCAGGTCTTCAC  
GCGGGGGGTGGGGTTCAGATGCACTGAAGTAGCCAACAGCGAAGCCAGTCCAGAAGAGGG  
GTCCGCTGGGAGGGAGGGTTGTGTCAGGCTTGGGGGATGGGCTCTTCGCCATGGGGGTCT  
TTGAACACACCTCTCTCCTTTCTTTTGTCTACGGAAGCCTCTGGGTGACAAAAGTAAAA  
GAGAGCTGCCCACTTTGCCAAAACAGATATACTCGAATCAGACTGAAAAAAAAAAAAA  
AAGACACAGACAAATAAAAAGCCAGATTTTCCACTCGATATTAATACCCACATAAACCTG  
TGTGTTTGCAAACGTGTACATGTACACACATACACATCCCACGTTTCGCTTCAGGTCTTTT  
CTTATTTGAGCTTAATCCAAATAAAAAGGACTTGACACCTTACCCTGCATACAATAGGC  
ACCCCTTACATGTGTTTTGAGTTGGTCTGAATCTGAACATGGGGTGCTTTTCAGTTCAGGT  
AGTTAGCTAGTTCTGGCCACATTCTGAGTTTCACTGAAGATGTGGATCCCTTCAGACATA  
ATGCACATTGCTTTGCCTGGATATGCACCTTGCTTGATTTGAAATGGATGCCAAGCCAA  
AATTGTTGGCATTTCAGGAGGGATAAGCAGGCTTCTAAAATAACAGCATCTGCAGAGTTT  
TCTTCTCCATCCAAACAAGTTGTGTTTCGATGGTCCACATGACCAGGTGTATGTCTGTA  
AGTGTGGAGGGAGAGGACAAGAAATTGTGCATGTGTGTGCAGACATGCACAAACAGGAGC  
AATCCAATAACACCTTAGTGAATAGAAATATGGTTGGGGATTTGCTGAGCTGTATTTATC  
CAGCAACAGGTTTCCAGCCCCAGATGTTAGTAGTGCAAAGGGCCAAGTGCCTCAATTGT  
GAGCCTCTGAGCTAGGAGGAGAAGTGATGAAGAGTGGCCTATGTGGTCCCTTCTACCTGA  
CCTTAAGTCATCTCAAAATGAAATATTGTGAGAATGAAGGGAACCCTTAGGGAACCTTGT  
GGGTAAGGTAAGTGGACATGGATTTGTCAGTAGCCTGTTCTACTGTGCCATGTTAATCT  
TGGTGCGAAAACTATTCCAATACATCTCAAACCTCCAAGAGACTTCAGAAACATCAAGAT  
TTAGTGTAATGAGCGGCGCAGAAAAATGTTTTTATTGCTCCATAATCTGACCACACGTAA  
CATTTGTGACGTGAAAACCATGACTTTCTATTCTGAGGTCTTTGGTTTCTGCCTGTGGG  
AAATTGAATGGCACTGTATGGACTATTTTCATCTGTTGATGGTAAAACAAAAGGGTGATTT

TTTTGCTTGTGGTTGTCATCTTGGGTTTACCTTTGTAAGAAGACATCATCACCATTCTGA  
AGGCAGTGGCTTGGCATGGAGATTTTTATTCTGTAGCACTGGGCCTGTTCTTCTAAGGAC  
AGCACAAGGTAGACAATTGTAGAGCCAAGGCCACTTTTTTCAGGAAGATCTAGTCTCTTGC  
TAACCCTCTTCTTCTCTCTTGGCTATTGCTGCTGCTCTTTTGATGGTTTATAGTCTTAAT  
GGCCTGCCTTGATAATTCCTTTGAACACTTTCATTAGTTGTTTTGCATACCAGAGATGCC  
GCACCTGCTGTTGGCTTATTTTTTACTTGTCTATTAACTGTTGATTATCTGAATGTTT  
CCCCCTCCTTGTTCATGTCCCAAGAATGGTGCTCCTGTTTTCAGTGACAGTTCAGCT  
GAACATATAAGCAGATGTGTAACAGATGAAGTAACCATGCAGTTTCCTTGTGGCATTAG  
TTCCATTTACAAAAGTGAAGACCACTGGTGGGCTGATCTGAGTGTGCCAATCCTGATCAT  
TTAAACCTACAGCCTTCAACTGGTGATTCCTACCCACCGTTTTTCATTCTGCTATAACCCT  
GTGATATGTGTGCGTGTGGGTGTGAGTGTGGGTGTGTGCACATATAGAGATTTAGTCTTA  
ATTTCAACCAAATGACATGCAAGATTCCTACTGCCACTCTTCTGGCCAAAAGTGTGCACA  
GACTGTGATTTATTCAATTGTGGTCTGTGACTTTAACCCATCATTGATGCTCTCACTTAGG  
TAAACCCTAAAGACCAAACCTAGCAACACTAGTCAAGGGAGTGAAGTGGAGTTATTTCTGGT  
AGCAGTAGCCACTGGCATCCTAGAAACACATGGACATTTGTAGCATGAATTGACCTATTG  
GTAGTGCAATAGCTATACATGATTTTTATTCTTGGCAAAAAGAAAATGCTTCAAAAAAAAA  
GTGATCAAACCTGCACATTGATCCTGTAATAGCAAATGGAAGGCTATTTCTCTGTACTAG  
CATTTTCAGCTTTATGTGGGAAAGTTACCCGTTCTCCTGCAAGTACAATCAACCCTTGATG  
ACTTAAGTATTAATTATTCTGGGTGTAGCTCACCCAAGTTTTCTTCTACATCTTTTGGC  
TAATTCCACCACACCTCAGCATCACAGTCAGATGGGAAAAGGGGCAGGTGGATTCTCATG  
TCATGCCTTCTTGTACCTTATTTTCAAGTTTTGTGGTGGAGGAGTTTAATTATCTGCTC  
AAGAATCTGGTATATATAGCCAGGTGCGGTGGCTCATGCCTGTAATCCCAGGACTTTGGG  
CAAGGCGAGAGGATCACCTGAGGTGAGGAGTTCAAGACCAGCCTGGCCAACATGGCAAAA  
CCCCATCTCTACTAAAAATACAAAAATTAGCTGGGTTTGGTGGTGGACACCTGTAGTCCC  
AGCTACTTGGGAGGCTGCGGCAGGAGAATCACTTGAACCCCGGAAGTGGAGGTTGCAGTG  
AGCCAAGATCGTGCCATTGCACTCCAGCTTGGGTGACCGAGCAAGACTCCGTCTCAAAAA  
AAAAAAAAAATCGGCTATATGTAAAAACTATTAATTATGTAACCTCACTCCAATACTGT  
ACTGATCAAGATCTGCCACTCCTAGAGGACTGACCCAATGGCAGATCCCCTACTATAAT  
CTTTCTGACAACCTCAGTGACAGGTAAAATCACTCTAATATTCCTAAAATATCTAGACACT  
TGAATTAGAAATACAGAACCACCCCAACCCTGCCATTGCTTAAGCCATATTAAGCTTC  
ATGTAAGTAAAGTCAAGGATGTAAGTGTGATACTTTAAGACCACTAATCTCAGTGGAAAT  
TCAGGACATAGCATTAGTTGGTAAATTACACCAGACTAGGGGCTCACTCCTCCTTAGATT  
GAAGTCCAAATAAAAGTCTTCACCTTTGGATCAAAGGCCACATATATATGATCATCATCA  
ATAAATTGTCATAAAGTGTCTATGAACTGCTCTTGCCATCTTCTAATACGTAACCTTCAT  
GACATCATGTCTCTAGAAGTGTCTAATACAATCCAAAAGAACAAGGGGGGAAGGCCCCAA  
GTCACCCTGACCGACCTCAGCAGGGGCCAGTGGTAGAACAACAATCTTGTGAATTAGGA

GACATAGAAAATGTACGCAAAAGTAAATTCCAAGCGCTGAGCATGTACAAGCTATTTTTA  
TTATTTAAAGCCAAGAAGGAAGAGCATTGAAGAAGTAATGATTTTAATATAGTGGGGGAT  
TTCCCCCTTAAATTTTTATAATTTCTTGTGAATAACAATCATGGAAAAGAAGAAACCT  
AGTCATACAAAATCAGAATAAATAAAAATCTTAAGACTGGATCCACATCTTTGGCCAATT  
CATATAAGCACCTAATACATCAATTTCTCTGTACTTAAAATGAAGAGAATAATTAATATT  
CTTAAGTACAATGTTTTCAATAGAGAACAAAATGAAATCACCTTTGTCATCAACAGCAGCC  
CAGACTGACTGTATCTAGATCACACCTTGATGTTACGTTTGAATGCAGTCAGTAGTTACC  
AAAAAGTAATTAGTGCACATTAATAGTGGTAAAATCAGCAGGGAGAAATATGGGATTAG  
CACGTAGTTCCAGAACCTTCTCCTCCTCCAGAGTGCAACTCAACAAACAGTACACTCCA  
AATTAAGAATCAATGTTTCATCCCAGGACAAACGGTGTGCTCCCATCACAGTACCACAA  
CTGAGATACTGTGAAGTCATTGCACTACCAGTAGGTTACTACTCTTTTGAAGTTACTGTT  
TTTAAATCCTAAAATATGTCCCCAGTTTTCTACATTCATTCTTCTTCCCCTAAGAGTTGC  
TAGAAGCAGATGAAGGATCCCTATTGACTCTGCAGGGTTTGATTTTCAGTACCTTAGACAG  
CTATCTGGTGACTTCCCAGTAGGCACGAACAACCCCTTCTCTCCCCTTGCACTCGGTGGG  
CTTGATGACGCCCCAGACAGTATCCTTTCTTCTCTACTGCCGCCAAAATAAACATTAGG  
GAAATGGGATCATTAAACCACTGAGAAAAGGAGTTTACAGGGATCGCAATAGTAACTGTC  
TGCTTGTGGTAGTAGAAAGCTTGTGCCAGGCTGCATGAATAGAAATTAATGTTAAACTCC  
TGTTAGACGAGTAATATGTAGATTTTTATTGAAACAGACCACAGCTTATTA AAAAGTACT  
CAGTGCAATGGTATATACATATACAGATAGAAAAAATATAACTGTGATCTTTTTGTC  
TTACGCCATTACTGGAAACACCCAAACGTGAACTGGAGTTCCCTCTGAACAAAACCATTG  
TCAAATCTTCAACATATGACCTCCAAATCTAGGTGCCAAGTGCCCTGTGACAGTTGTTTA  
CACACCTGAAAAATGTATCCTGGAAGCTGTAATCTTGGCCTGGGCTATGTGTTGAAACA  
AGCAAAAGAGACACATCGTGACCAACCAAGCTGGTGGAGGAAAAGCACAAAATTCAACTC  
CAACCTGCAGTTAGGATCCCAAAGAGATGTTGACATTTATAGCCAAAAGAAAAAGTACA  
TATCTGAATCAGATCG  
AAGCAGCCAACGTCCAGCTTCACTCAAGAAGGACAAGGAATAAACAACATTCTCTAGCTG  
TGTCATGTTGTCTCAGTTTTTGAATCTCAACCAGGACTGATCCACCTTCATCAGATACGT  
TTTTAATGGCGCAACAACTCAATTTTGGTCCCAGACTCTCCATTCTGCACTGGCCACGA  
GAACAACAAGAGAATGACAGGATGTTAATGGAGGAAACATTTTCATGGCAAGCTCAGAAA  
CTGAAGTGTATATTCAGAATCAGATGAGCTTTAATATGAATTTGCATCTTGCCTCTGT  
ACTGCTTGCTATTTTTTAATGATAGGAGAAAAGCATAACAGTTTATTTTTAAATATGAAATA  
TATTGATATATTATAAAATATATTGTAACCTTCAATTAACATTTTGTATCAAACCTAGTGT  
TTAGCAGGTCCACTGTCAGCCTGCTCTCCAATGACTGTTTCTGAGTACACATCACTGTT  
AGTGATTGCCGGGCACCCAGAAAAAGGGTCTCCTACCACAGCCTACTGAACTGCCATAT  
TCTAATTCTCCAAGGCCTGGGTATTAGAGACAAAAGAACATTATCCAAGAGTAGAGGAA  
TAATTCTACCCTAAATTCTATCAAGCCATTTTCAGAAGAGATTTTAAAAGCCATCACTCCT

TTAGTAGCTCTGCAAAGCCAGTTTAATAAAAAGTTCAGGCTCTTTCTATATAAATTCAAAG  
GCCTCATTACATAAAATTATATAAGTCTCAAACCTAGCCAACCAGTTTTCTTTGACAATG  
TCAGAATTGGACATAAGAAAGAGTCCTGTTTTCTGTAACCTAAAATACTCAAATCCTA  
GGCATTCTGAGTTTCTCCATGTACGTGAAACCGGGTTCGGCTTTCCAAACTACACAAGGC  
CCAACAAGAGTCCAGTGTGCAGATGTGCTTTTCTAAATTGGCAATACCCTTGAGGGAGCA  
AGGTTCCCACATGTTTATCAAGGACATGGAGCCCAGCTCCTAAGGGAGTGATGGGAGGAG  
CCGGCAGGACATGAACAGCCAGAGCCAGCAAAGAGCCGGGCTGCCTTTTCTGCTAGCTTC  
CTCTAGCTGGGAGGAAATAAAGGGTCCCCTTGAGATATTGTCTTTATAGCAAATTA  
GCAACTCATGGAATCTACACCCTCTTTCTCTACAGAGCAGCTGAGACATACATGTAGAA  
GTTCTCAGTTCCCTCCTTCATATGGCTAAGGCACTACTTCTAGATGAAAACAGGATGTGT  
TCGGTTACAGAATAAAGATTTTCTAGAATCAGTGAGCCTCTTCTCACCTGGGACCCTCAC  
TTGCTGTTGTTGCTTTGGTGCAATATTGTACAGGTGCAAACCAGGTTGCATCGGGCAGA  
TTAACTGAGCCTATGTGTCTTCCCTTCCAAGCCCTGAAAATTCACATAGATTTACAG  
ATAGTGCAAAAACAACAAGTTTTCTCCTGGGAAAAGGCTGGAATCCTTCAAATTTCAATTT  
ATATGAGCTTAAAGGTATATAAGTCATGGGGCTCACTGACATTAGGTATTCATGCTGTTT  
GAAAGAGAAATGTCTAAATGCCCGTTTTTCAGTCTGTTTGTGTAGCTGAGCCCTAAGTGT  
ACACAAGTTTTCTTGTTATGGAGCTAAATCTCTCAGTGCCTGTATTACTCCTCAGTTAT  
ATGTTAGGCCGAGCTCCACTAAAGCCATCTGAACTCCAGGGCACTTGTTTTTATCAGGTT  
ACTTACTCACCGGATAATGAAATTGGCTTATTTTCAATTTTACAATTGACTGATGAATG  
TATTGGTGGTAATTGATTTATTTCTTCACTTTTTTTTTGCTACTAAATGATTTTTTCTTTT  
TTAAAATTATTATTATTATTTTGGAGATGGAGTCTCACTCTGTGCGCCAGGCTGGAGT  
GCAGTGGCGCCATCTCAGCTCACTGCAAGCTCTGCCTCCTGGGTTTCATGCAATTCTCCTG  
CCTCAGCCTCCCAGTAGCTGGGATTACAGGTGCGTGCCACCACGACCAGCTAATTTTTT  
TGTATTTTTAGTAGAGACAGGGTTTCATCATGTAAACCAGGATGGTCTCGATCTCCTGAC  
CTCGTGATCCACCTGCCTGGGCCTCCCAAAGTGAGCCACTGTGCCTGGCCAGTAAGTGC  
TTTTTCTTTTGGTTTTTCTTCTAACACTGCTCAGACCAAGACTTACATTTATAAAGAG  
CAAATATATTCTGACCTTTCCCCTCAAAGTTGTATTCCATCTAGAATCAAGGAAACAAAT  
GCAAATTCATCATTTGGGGAAAGCAGACCTCTTGACAGTAATTCAAGTCCATGGCTATAT  
GCTAACCTTGCTACTCAAAGTGTGGTCCACAGACCAGCAGCGTTAGCATCATCTGTAAG  
CTTGTTAGAAATGCAGAATCTCAGGCCCCACATCAAACCTTCTTCATCAGAATTGGCCTT  
TTAACAAATCCCAGGTGACCTGTATGCACCAGAAATATTGATAAGCACTGGCCTCACCT  
CACCGTAGTGATAACTAACCTCGTTAATAATTAGAGAATGAAGCTATCTCTTCTTGAGT  
CTCATTTACAGAATTATTTGAAGATGTGAAGGTCCTGAATGATCATAAGGATTAATAA  
TGCATCTTTAAATCCACTTGAGGTTATATAACTTGGATGGTCTACATCAAACATAATAA  
AGTCAATAAGAGATAGTCTTTTTCCGGTCTTACCTAAATAGCACTCCATATCCTTGAGCC  
ACCTCAAAGCCCCATTTTTAAGTTTTAGTCTTTTTTTTTTTAGACCAGACTAGCAAAGC

CATCAGAATATCAGGTGGAACCTCAGGGCAGGTCTCTGGAAGGCTACAGGAGTCTCTGC  
TTAGCATAGTACAGAAAATTGTTGTGTTTCTCGATCCTTGTGTTCTTCCCTTGAGGAACTC  
AGCATCTCACCAGTAAGAACTCCCCTCCCCTAGAGGAAAATAGCAAGAGAAGTTAGTTTA  
ACCATCTAGAAACATTGCTAATCTCCTTGAAGCCAATTCTTACTCATTGCACCAACA  
AGAAACTCCAAGGTGGGCAAGGAAAGACGTGAATTCTGATATTGGCGCCATAACTCGA  
TATGTACCCAGAAACAGTTATGTTCTAAATTAATGGCTTAACTGTTCAATTGAAAAAG  
TGCTTGGACTTCAATCTAAAGAGGTCAGTATAAATATGTATGTGTGTGTGACGTGTA  
TGTAGGCAAATATTTACAGATTTATACATACATAGGTGCACACACATATACCCGCACATT  
CATATATAATATACATACATATATAAATGCTTCATAATATATCATATTGCTATTCACA  
GCTCCATTTCTTTTGTCTGGTCCATGTTTATTTGTTTAGTGAGACCTTACATAGAGAG  
GTTCTATTCGGAACATTGATGATTTTTTGTGTTTACTTTTTATAAAAAGGTAA  
AGGATATTAATAAAAAAAAAAAGTCAAGTGCCTGAAGGTTTTGAATGGAGTTACGGTA  
AACTTTCTCAGGTCACCAAAGAGGAAACATTTTCTTTGGAAAACATTTTCTGTTTCA  
GTGACTTTGTTTTCCCTGGTGGTAATGCATAAATAAGAGTGGTTAAAGTGATTTTGTA  
GTTTTATTTCAATCCATTTCTGTGGTCCATAAGGCAATAGCTAAAAATTTGTTTCAGTC  
TAGTGCCAGTTTTCTCCACACATCAGCATCAGAAGGGCCCGTCTTCACATGCTCTGTG  
TGGTTTTGTTTCGCGTTGTTACTGTGTTCCCTACTAAGGAAAGGCAAATGAAATTGCAGGG  
GCTGGAGCTTAGACCAGCTCCAAATATGGCTTCCTTTGGTAACACACACAGAAGGTGGA  
CTAGTGGGAAGTCTCTCTCCCTGAAGCAGGTGGGAACCTGTGTCTTAGAAGGCAGAGGAG  
TCCCAGTGAACCTCCACAGCTCCATGGGCCCTGCCTGTCTACAGTTATACAACCTGCCTG  
TATGAGTCAGCCTTTCTCTACCTTAGCCAAAGGTCTTCTCTTTCTGTGGTGTGACAGCTT  
GTAATGAACCAACTTGCTCTGGTTAGAAGTCCCTAGAGCTCCAGGAAGAGTCGCCAGGTT  
TCCATTGCTGTGCTCAAAGCTCAAGGACACATTATACTTCTTTAAACCAACTAAATCTCT  
CTAGCTCCCTGCCCCATGGTGACACTTTCATAATAGGCAGGGCCAAGTCAGAGAGGTCA  
TGCCCTGTATACAGTGTCAATCAGAAGAGACACTGCAAATGTCAGAGGTGACCAGAAAG  
ACAACAGATCTCTCCAGCTGTCCTCACAGCTGCAGGCACATTTGTGGAATTGTGAGTAGG  
AAGGCTTGGCAGCCAGGGGATGGGAAATGAATTTCCCAAGTTGAAAACCCTGTACCCTT  
ACTTTCTTCCATAAATTTTTCTGTAGTTCTAGGTAAATAATAATAATAAAAAATGC  
AAATTAGGTGCTTTAGAAGGAGTATGTAATATCTGGGACTTTTTCTAAGTTGGTAGACCT  
AAAAATGTTTTCAAAAATATATCTAGCTGCATTTCTACTGCTGTCATTCCTTAAAGCTC  
TTCCTCAAAAACCTCCATATGAATGAATACATTTACCAACTCAGTGATTAATAATA  
GTACTTTATACTTATACACAGTAATACCTTTTCTAAGGATCTCAAATGCCAATATATT  
AGTCATCACCCGTGAAGGTGGATGACATATTATCCCATTTCCAATGGGAAAATTGGG  
CCATAGAAAACCTGAGGAGCAAATGACTCATCTACAGGAATTAATGGAAAAACAGGCTA  
GGATTTCTCAGCACACTTTAGGAGTGAATGAAAACCTTACAGGCTTCAGTTCTACTGCTGG  
CCACCATTGGATTTGTAAGATCCAGGATGTGTATTGACCACATGTGTCCAGACCCAGGCT

TAGGGCATCTGGAATGAGAGTGGTGGGCTGGTGTGTGGGTCTGAGGATCTGGATGGGAGA  
CTGCATTTTCTTCTCTGTGCAAAATATGGAAGTGTGACCTTGAAGGTGGGCTTAGTCTAT  
GGCCTCCCCACTCCTGCTTGAAGCTGGAGAGAATGGGCATTTTTAAATGTTACG  
GCATATGCTAATATAATATTATGGCATTAAATAAAAACAAGAAGAGAAGTACTGACTAAAACC  
AAAAAACCAAAAA

## References

- ABRAMOVIC, M., RADENKOVIC, G. & VELICKOV, A. 2014. Appearance of interstitial cells of Cajal in the human midgut. *Cell and tissue research*, 356, 9-14.
- AL-SHBOUL, O. A. 2013. The importance of interstitial cells of cajal in the gastrointestinal tract. *Saudi journal of gastroenterology: official journal of the Saudi Gastroenterology Association*, 19, 3.
- ALBERTS, B., JOHNSON, A., LEWIS, J., RAFF, M., ROBERTS, K. & WALTER, P. 2002. Looking at the structure of cells in the microscope. Garland Science; Molecular Biology of the Cell. 4th edition.
- ALBUQUERQUE, E. X., PEREIRA, E. F., ALKONDON, M. & ROGERS, S. W. 2009. Mammalian nicotinic acetylcholine receptors: from structure to function. *Physiological reviews*, 89, 73-120.
- ALMOND, LINDLEY, R. M., KENNY, S. E., CONNELL, M. G. & EDGAR, D. H. 2007. Characterisation and transplantation of enteric nervous system progenitor cells. *BMJ*, 56, 489-496.
- ALVES, M. M., SRIBUDIANI, Y., BROUWER, R. W., AMIEL, J., ANTIÑOLO, G., BORREGO, S., CECCHERINI, I., CHAKRAVARTI, A., FERNÁNDEZ, R. M. & GARCIA-BARCELO, M.-M. 2013. Contribution of rare and common variants determine complex diseases—Hirschsprung disease as a model. *Developmental biology*, 382, 320-329.
- AMBACHE, N. 1947. The electrical activity of isolated mammalian intestines. *The Journal of physiology*, 106, 139-153.
- AMBINDER, R. F. & MANN, R. B. 1994. Detection and characterization of Epstein-Barr virus in clinical specimens. *The American journal of pathology*, 145, 239.
- AMIEL, J. & LYONNET, S. 2001. Hirschsprung disease, associated syndromes, and genetics: a review. *Journal of medical genetics*, 38, 729-739.
- AMIEL, J., SPROAT-EMISON, E., GARCIA-BARCELO, M., LANTIERI, F., BURZYNSKI, G., BORREGO, S., PELET, A., ARNOLD, S., MIAO, X. & GRISERI, P. 2008. Hirschsprung disease, associated syndromes and genetics: a review. *Journal of medical genetics*, 45, 1-14.
- ANATOL, T., MOHAMMED, W. & RAO, C. 2008. Interstitial cells of Cajal and intestinal function in Trinidadian children. *West Indian Medical Journal*, 57, 393-397.
- ANDRAE, J., GALLINI, R. & BETSHOLTZ, C. 2008. Role of platelet-derived growth factors in physiology and medicine. *Genes & development*, 22, 1276-1312.
- ANTHONY, M. 2016. Junqueira's Basic Histology: Text and Atlas. 14.
- AULI, M., MARTINEZ, E., GALLEGO, D., OPAZO, A., ESPIN, F., MARTI-GALLOSTRA, M., JIMÉNEZ, M. & CLAVÉ, P. 2008. Effects of excitatory

- and inhibitory neurotransmission on motor patterns of human sigmoid colon in vitro. *British journal of pharmacology*, 155, 1043-1055.
- BAKER, S. A., HENNIG, G. W., SALTER, A. K., KURAHASHI, M., WARD, S. M. & SANDERS, K. M. 2013. Distribution and Ca<sup>2+</sup> signalling of fibroblast-like (PDGFR $\alpha$ +) cells in the murine gastric fundus. *The Journal of physiology*, 591, 6193-6208.
- BAKER, S. A., HENNIG, G. W., WARD, S. M. & SANDERS, K. M. 2015. Temporal sequence of activation of cells involved in purinergic neurotransmission in the colon. *The Journal of physiology*, 593, 1945-1963.
- BARAJAS-LOPEZ, C., BEREZIN, I., DANIEL, E. E. & HUIZINGA, J. 1989. Pacemaker activity recorded in interstitial cells of Cajal of the gastrointestinal tract. *American Journal of Physiology-Cell Physiology*, 257, C830-C835.
- BARSHACK, I., FRIDMAN, E., GOLDBERG, I., CHOWERS, Y. & KOPOLOVIC, J. 2004. The loss of calretinin expression indicates aganglionosis in Hirschsprung's disease. *Journal of clinical pathology*, 57, 712-716.
- BASSOTTI, G., VILLANACCI, V., CATHOMAS, G., MAURER, C. A., FISOGNI, S., CADEI, M., BARON, L., MORELLI, A., VALLONCINI, E. & SALERNI, B. 2006. Enteric neuropathology of the terminal ileum in patients with intractable slow-transit constipation. *Human pathology*, 37, 1252-1258.
- BAUER, A. J., PUBLICOVER, N. G. & SANDERS, K. M. 1985. Origin and spread of slow waves in canine gastric antral circular muscle. *American Journal of Physiology-Gastrointestinal and Liver Physiology*, 249, G800-G806.
- BAUER, S., HARTMANN, J. T., DE WIT, M., LANG, H., GRABELLUS, F., ANTOCH, G., NIEBEL, W., ERHARD, J., EBELING, P. & ZETH, M. 2005. Resection of residual disease in patients with metastatic gastrointestinal stromal tumors responding to treatment with imatinib. *International journal of cancer*, 117, 316-325.
- BAUME, M., CARIOU, A., LEVEAU, A., FESSY, N., PASTORI, F., JARRAUD, S. & PIERRE, S. 2019. Quantification of Legionella DNA certified reference material by digital droplet PCR. *Journal of microbiological methods*, 157, 50-53.
- BECKETT, E. A., Horiguchi, K., KHOYI, M., SANDERS, K. M. & WARD, S. M. 2002. Loss of enteric motor neurotransmission in the gastric fundus of Sl/Sld mice. *The Journal of physiology*, 543, 871-887.
- BECKETT, E. A., TAKEDA, Y., YANASE, H., SANDERS, K. M. & WARD, S. M. 2005. Synaptic specializations exist between enteric motor nerves and interstitial cells of Cajal in the murine stomach. *Journal of Comparative Neurology*, 493, 193-206.
- BENARROCH, E. E. 2007. Enteric nervous system: functional organization and neurologic implications. *Neurology*, 69, 1953-1957.
- BEREZIN, I., HUIZINGA, J. & DANIEL, E. 1988. Interstitial cells of Cajal in the canine colon: a special communication network at the inner border of the circular muscle. *Journal of Comparative Neurology*, 273, 42-51.

- BEREZIN, I., HUIZINGA, J. & DANIEL, E. 1990. Structural characterization of interstitial cells of Cajal in myenteric plexus and muscle layers of canine colon. *Canadian journal of physiology and pharmacology*, 68, 1419-1431.
- BERNARDINI, N., SEGNANI, C., IPPOLITO, C., DE GIORGIO, R., COLUCCI, R., FAUSSONE-PELLEGRINI, M. S., CHIARUGI, M., CAMPANI, D., CASTAGNA, M. & MATTII, L. 2012. Immunohistochemical analysis of myenteric ganglia and interstitial cells of Cajal in ulcerative colitis. *Journal of cellular and molecular medicine*, 16, 318-327.
- BERRIDGE, M. J. 2008. Smooth muscle cell calcium activation mechanisms. *The Journal of physiology*, 586, 5047-5061.
- BERTHEAU, P., CAZALS-HATEM, D., MEIGNIN, V., DE ROQUANCOURT, A., VÉROLA, O., LESOURD, A., SÉNÉ, C., BROCHERIOU, C. & JANIN, A. 1998. Variability of immunohistochemical reactivity on stored paraffin slides. *Journal of clinical pathology*, 51, 370-374.
- BETTOLLI, M., DE CARLI, C., CORNEJO-PALMA, D., JOLIN-DAHEL, K., WANG, X.-Y., HUIZINGA, J., KRANTIS, A., RUBIN, S. & STAINES, W. A. 2012. Interstitial cell of Cajal loss correlates with the degree of inflammation in the human appendix and reverses after inflammation. *Journal of pediatric surgery*, 47, 1891-1899.
- BLAIR, P., BAYGUINOV, Y., SANDERS, K. & WARD, S. 2012a. Relationship between enteric neurons and interstitial cells in the primate gastrointestinal tract. *Neurogastroenterology & Motility*, 24.
- BLAIR, P. J., BAYGUINOV, Y., SANDERS, K. M. & WARD, S. M. 2012b. Interstitial cells in the primate gastrointestinal tract. *Cell and tissue research*, 350, 199-213.
- BLAIR, P. J., RHEE, P.-L., SANDERS, K. M. & WARD, S. M. 2014. The significance of interstitial cells in neurogastroenterology. *Journal of neurogastroenterology and motility*, 20, 294.
- BLAY, J.-Y., LE CESNE, A., RAY-COQUARD, I., BUI, B., DUFFAUD, F., DELBALDO, C., ADENIS, A., VIENS, P., RIOS, M. & BOMPAS, E. 2007. Prospective multicentric randomized phase III study of imatinib in patients with advanced gastrointestinal stromal tumors comparing interruption versus continuation of treatment beyond 1 year: the French Sarcoma Group. *Journal of clinical oncology*, 25, 1107-1113.
- BONDURAND, N. & SHAM, M. H. 2013. The role of SOX10 during enteric nervous system development. *Developmental biology*, 382, 330-343.
- BORREGO, S., RUIZ-FERRER, M., FERNÁNDEZ, R. M. & ANTIÑOLO, G. 2013. Hirschsprung's disease as a model of complex genetic etiology. *Histol Histopathol*, 28, 1117-1136.
- BOYCE, R. W., DORPH-PETERSEN, K.-A., LYCK, L. & GUNDERSEN, H. J. G. 2010. Design-based stereology: introduction to basic concepts and practical approaches for estimation of cell number. *Toxicologic pathology*, 38, 1011-1025.
- BRAZ, J. C., GREGORY, K., PATHAK, A., ZHAO, W., SAHIN, B., KLEVITSKY, R., KIMBALL, T. F., LORENZ, J. N., NAIRN, A. C. & LIGGETT, S. B. J. N. M. 2004. PKC- $\alpha$  regulates cardiac contractility and propensity toward heart failure. 10, 248.

- BRELAND, A., HA, S. E., JORGENSEN, B. G., JIN, B., GARDNER, T. A., SANDERS, K. M. & RO, S. 2019. Smooth Muscle Transcriptome Browser: offering genome-wide references and expression profiles of transcripts expressed in intestinal SMC, ICC, and PDGFR $\alpha$  cells. *Scientific reports*, 9.
- BROMLEY, C. M., PALECHEK, P. L. & BENDA, J. A. 1994. Preservation of estrogen receptor in paraffin sections. *Journal of Histotechnology*, 17, 115-118.
- BULT, H., BOECKXSTAENS, G., PELCKMANS, P., JORDAENS, F., VAN MAERCKE, Y. & HERMAN, A. 1990. Nitric oxide as an inhibitory non-adrenergic non-cholinergic neurotransmitter. *Nature*, 345, 346.
- BURNS, A. J., HERBERT, T. M., WARD, S. M. & SANDERS, K. M. 1997. Interstitial cells of Cajal in the guinea-pig gastrointestinal tract as revealed by c-Kit immunohistochemistry. *Cell and tissue research*, 290, 11-20.
- BURNS, A. J., LOMAX, A., TORIHASHI, S., SANDERS, K. M. & WARD, S. M. 1996. Interstitial cells of Cajal mediate inhibitory neurotransmission in the stomach. *Proceedings of the National Academy of Sciences*, 93, 12008-12013.
- BURNSTOCK, G. 1976. Purinergic receptors. *Journal of theoretical biology*, 62, 491-503.
- BURNSTOCK, G., CAMPBELL, G., SATCHELL, D. & SMYTHE, A. 1970. Evidence that adenosine triphosphate or a related nucleotide is the transmitter substance released by non-adrenergic inhibitory nerves in the gut. *British journal of pharmacology*, 40, 668-688.
- BURRY, R. W. 2011. Controls for immunocytochemistry: an update. *Journal of Histochemistry & Cytochemistry*, 59, 6-12.
- CARRASQUILLO, M. M., MCCALLION, A. S., PUFFENBERGER, E. G., KASHUK, C. S., NOURI, N. & CHAKRAVARTI, A. 2002. Genome-wide association study and mouse model identify interaction between RET and EDNRB pathways in Hirschsprung disease. *Nature genetics*, 32, 237.
- CARSON, F. L. 2015. *Histotechnology. A Self-Instructional Text 3<sup>rd</sup> Edition*.
- CASSIDY, A. & JONES, J. 2014. Developments in in situ hybridisation. *Methods*, 70, 39-45.
- CAULFIELD, M. P. & BIRDSALL, N. J. 1998. International Union of Pharmacology. XVII. Classification of muscarinic acetylcholine receptors. *Pharmacological reviews*, 50, 279-290.
- CHABOT, B., STEPHENSON, D. A., CHAPMAN, V. M., BESMER, P. & BERNSTEIN, A. 1988. The proto-oncogene c-kit encoding a transmembrane tyrosine kinase receptor maps to the mouse W locus. *Nature*, 335, 88.
- CHALAZONITIS, A. & RAO, M. 2018. Enteric nervous system manifestations of neurodegenerative disease. *Brain research*.
- CHAN, F., LIU, Y., SUN, H., LI, X., SHANG, H., FAN, D., AN, J. & ZHOU, D. 2010. Distribution and possible role of PDGF-AA and PDGFR- $\alpha$  in the gastrointestinal tract of adult guinea pigs. *Virchows Archiv*, 457, 381-388.

- CHAN, M., LEE, C. W. & WU, M. 2013. Integrating next-generation sequencing into clinical cancer diagnostics. Taylor & Francis.
- CHARGIN, A., MORGAN, R., SUNDRAM, U., SHULTS, K., TSAY, E. L., RATTI, N. & PATTERSON, B. K. 2016. Quantification of PD-L1 and PD-1 expression on tumor and immune cells in non-small cell lung cancer (NSCLC) using non-enzymatic tissue dissociation and flow cytometry. *Cancer Immunology, Immunotherapy*, 65, 1317-1323.
- CHATTERJEE, SUMANTRA & CHAKRAVARTI, A. J. H. M. G. 2019. A gene regulatory network explains RET—EDNRB epistasis in Hirschsprung disease.
- CHATTERJEE, S., KAPOOR, A., AKIYAMA, J. A., AUER, D. R., LEE, D., GABRIEL, S., BERRIOS, C., PENNACCHIO, L. A. & CHAKRAVARTI, A. J. C. 2016. Enhancer variants synergistically drive dysfunction of a gene regulatory network in Hirschsprung disease. 167, 355-368. e10.
- CHEN, H., ORDOG, T., CHEN, J., YOUNG, D. L., BARDSLEY, M. R., REDELMAN, D., WARD, S. M. & SANDERS, K. M. 2007a. Differential gene expression in functional classes of interstitial cells of Cajal in murine small intestine. *Physiological genomics*, 31, 492-509.
- CHEN, H., REDELMAN, D., RO, S., WARD, S. M., ORDOG, T. & SANDERS, K. M. 2007b. Selective labeling and isolation of functional classes of interstitial cells of Cajal of human and murine small intestine. *American Journal of Physiology-Cell Physiology*, 292, C497-C507.
- CHEN, J., DU, L., XIAO, Y.-T. & CAI, W. 2013. Disruption of interstitial cells of Cajal networks after massive small bowel resection. *World Journal of Gastroenterology: WJG*, 19, 3415.
- CHEN, Z.-H., ZHANG, Y.-C., JIANG, W.-F., YANG, C., ZOU, G.-M., KONG, Y. & CAI, W. 2014. Characterization of interstitial Cajal progenitors cells and their changes in Hirschsprung's disease. *PLoS One*, 9, e86100.
- CHENG, H. R., GRAHAM HK, NAGY N, GOLDSTEIN AM, BELKINDGERSON J 2015. Endoscopic delivery of enteric neural stem cells to treat Hirschsprung disease. *Neurogastroenterol Motil* 27, 1509-1514.
- CHESS-WILLIAMS, R., CHAPPLE, C., YAMANISHI, T., YASUDA, K. & SELLERS, D. 2001. The minor population of M3-receptors mediate contraction of human detrusor muscle in vitro. *Journal of autonomic pharmacology*, 21, 243-248.
- CHRISTENSEN, J. 1992. A commentary on the morphological identification of interstitial cells of Cajal in the gut. *Journal of the autonomic nervous system*, 37, 75-88.
- CHRISTOPHER, S., KATHRYN L. FOWLER, MATTHEW THORNTON, SHA HUANG, IBRAHIM HAJJALI, XIAOGANG HOU, BRENDAN GRUBBS, JASON R. SPENCE, AND TRACY C. GRIKSCHEIT, 2017. Neural crest cell implantation restores enteric nervous system function and alters the gastrointestinal transcriptome in human tissue-engineered small intestine. *Stem Cell Reports*, 9, 883-896.
- CHRISTOPHI, G. P., RONG, R., HOLTZAPPLE, P. G., MASSA, P. T. & LANDAS, S. K. J. I. B. D. 2012. Immune markers and differential signaling networks in ulcerative colitis and Crohn's disease. 18, 2342-2356.

- COBINE, C. A., HENNIG, G. W., KURAHASHI, M., SANDERS, K. M., WARD, S. M. & KEEF, K. D. 2011. Relationship between interstitial cells of Cajal, fibroblast-like cells and inhibitory motor nerves in the internal anal sphincter. *Cell and tissue research*, 344, 17-30.
- COOKE, H. J. 2000. Neurotransmitters in neuronal reflexes regulating intestinal secretion. *Annals of the New York Academy of Sciences*, 915, 77-80.
- COOPER, J. E., NATARAJAN, D., MCCANN, C., CHOUDHURY, S., GODWIN, H., BURNS, A., THAPAR, N. J. N. & MOTILITY 2017. In vivo transplantation of fetal human gut-derived enteric neural crest cells. 29, e12900.
- COSTA, M., BROOKES, S. J. & HENNIG, G. W. 2000. Anatomy and physiology of the enteric nervous system. *Gut*, 47, iv15-iv19.
- COSTA, M., DODDS, K. N., WIKLENDT, L., SPENCER, N. J., BROOKES, S. J. & DINNING, P. G. 2013. Neurogenic and myogenic motor activity in the colon of the guinea pig, mouse, rabbit, and rat. *American Journal of Physiology-Gastrointestinal and Liver Physiology*, 305, G749-G759.
- COUDRY, R. A., MEIRELES, S. I., STOYANOVA, R., COOPER, H. S., CARPINO, A., WANG, X., ENGSTROM, P. F. & CLAPPER, M. L. 2007. Successful application of microarray technology to microdissected formalin-fixed, paraffin-embedded tissue. *The Journal of molecular diagnostics*, 9, 70-79.
- COYLE, D., KELLY, D. A., O'DONNELL, A. M., GILLICK, J. & PURI, P. 2016. Use of anoctamin 1 (ANO1) to evaluate interstitial cells of Cajal in Hirschsprung's disease. *Pediatric surgery international*, 32, 125-133.
- COYLE, D., O'DONNELL, A. M. & PURI, P. 2015. Altered distribution of small-conductance calcium-activated potassium channel SK3 in Hirschsprung's disease. *Journal of pediatric surgery*, 50, 1659-1664.
- CRUZ-ORIVE, L. M. & WEIBEL, E. R. 1990. Recent stereological methods for cell biology: a brief survey. *American Journal of Physiology-Lung Cellular and Molecular Physiology*, 258, L148-L156.
- DAUNORAVICIUS D, J. B., EDVARDAS ZURAUSKAS, AIDA LAURINAVICIENE, DAIVA BIRONAITE 2014. Quantification of myocardial fibrosis by digital image analysis and interactive stereology. *Diagnostic Pathology*, 114.
- DAVIS, J. S., GUPTA, V., GAGEA, M. & WU, X. 2016. An Advanced Histologic Method for Evaluation of Intestinal Adenomas in Mice Using Digital Slides. *PloS one*, 11, e0151463.
- DE LIMA, M. A., CABRINE-SANTOS, M., TAVARES, M. G., GEROLIN, G. P., LAGES-SILVA, E. & RAMIREZ, L. E. 2008. Interstitial cells of Cajal in chagasic megaesophagus. *Annals of diagnostic pathology*, 12, 271-274.
- DE MAN, J. G., DE WINTER, B. Y., SEERDEN, T. C., DE SCHEPPER, H. U., HERMAN, A. G. & PELCKMANS, P. A. 2003. Functional evidence that ATP or a related purine is an inhibitory NANC neurotransmitter in the mouse jejunum: study on the identity of P2X and P2Y purinoceptors involved. *British journal of pharmacology*, 140, 1108-1116.
- DE MELO DIAS, G. C., CASSEL, M., OLIVEIRA DE JESUS, L. W., BATLOUNI, S. R. & BORELLA, M. I. 2017. Spermatogonia, Germline Cells, and Testicular Organization in the Characiform Prochilodus

- lineatus Studied Using Histological, Stereological, and Morphometric Approaches. *The Anatomical Record*, 300, 589-599.
- DELCAMBRE, G. H., LIU, J., HERRINGTON, J. M., VALLARIO, K. & LONG, M. T. 2016. Immunohistochemistry for the detection of neural and inflammatory cells in equine brain tissue. *PeerJ*, 4, e1601.
- DER-SILAPHET, T., MALYSZ, J., HAGEL, S., ARSENAULT, A. L. & HUIZINGA, J. D. 1998. Interstitial cells of Cajal direct normal propulsive contractile activity in the mouse small intestine. *Gastroenterology*, 114, 724-736.
- DO, M. Y., MYUNG, S.-J., PARK, H.-J., CHUNG, J.-W., KIM, I.-W., LEE, S. M., YU, C. S., LEE, H. K., LEE, J.-K. & PARK, Y. S. 2011a. Novel classification and pathogenetic analysis of hypoganglionosis and adult-onset Hirschsprung's disease. *Digestive diseases and sciences*, 56, 1818-1827.
- DO, M. Y., MYUNG, S.-J., PARK, H.-J., CHUNG, J.-W., KIM, I.-W., LEE, S. M., YU, C. S., LEE, H. K., LEE, J.-K., PARK, Y. S. J. D. D. & SCIENCES 2011b. Novel classification and pathogenetic analysis of hypoganglionosis and adult-onset Hirschsprung's disease. 56, 1818-1827.
- DOLESHAL, M., MAGOTRA, A. A., CHOUDHURY, B., CANNON, B. D., LABOURIER, E. & SZAFRANSKA, A. E. 2008. Evaluation and validation of total RNA extraction methods for microRNA expression analyses in formalin-fixed, paraffin-embedded tissues. *The Journal of Molecular Diagnostics*, 10, 203-211.
- DUPONT, J. R. & SPRINZ, H. 1964. The neurovegetative periphery of the gut. A revaluation with conventional technics in the light of modern knowledge. *Developmental Dynamics*, 114, 393-402.
- DURBEC, P., MARCOS-GUTIERREZ, C. V., KILKENNY, C., GRIGORIOU, M., WARTIOWAARA, K., SUVANTO, P., SMITH, D., PONDER, B., COSTANTINI, F. & SAARMA, M. 1996. GDNF signalling through the Ret receptor tyrosine kinase. *Nature*, 381, 789.
- ECKES B, D. D., E COLUCCI-GUYON, N WANG... 1998. Impaired mechanical stability, migration and contractile capacity in vimentin-deficient fibroblasts. *Journal of cell science*, 1998 111: 1897-1907.
- EDERY, P., ATTIE, T., AMIEL, J., PELET, A., ENG, C., HOFSTRA, R. M., MARTELLI, H., BIDAUD, C., MUNNICH, A. & LYONNET, S. 1996. Mutation of the endothelin-3 gene in the Waardenburg-Hirschsprung disease (Shah-Waardenburg syndrome). *Nature genetics*, 12, 442.
- EDERY, P., LYONNET, S., MULLIGAN, L. M., PELET, A., DOW, E., ABEL, L., HOLDER, S., NIHOUL-FÉKÉTÉ, C., PONDER, B. A. & MUNNICH, A. 1994. Mutations of the RET proto-oncogene in Hirschsprung's disease. *Nature*, 367, 378.
- ELTOUM, I., FREDENBURGH, J., MYERS, R. B. & GRIZZLE, W. E. 2001. Introduction to the theory and practice of fixation of tissues. *Journal of Histotechnology*, 24, 173-190.
- EMISON, E. S., GARCIA-BARCELO, M., GRICE, E. A., LANTIERI, F., AMIEL, J., BURZYNSKI, G., FERNANDEZ, R. M., HAO, L., KASHUK, C. & WEST, K. 2010a. Differential contributions of rare and common, coding

- and noncoding Ret mutations to multifactorial Hirschsprung disease liability. *The American Journal of Human Genetics*, 87, 60-74.
- EMISON, E. S., GARCIA-BARCELO, M., GRICE, E. A., LANTIERI, F., AMIEL, J., BURZYNSKI, G., FERNANDEZ, R. M., HAO, L., KASHUK, C. & WEST, K. J. T. A. J. O. H. G. 2010b. Differential contributions of rare and common, coding and noncoding Ret mutations to multifactorial Hirschsprung disease liability. 87, 60-74.
- EMISON, E. S., MCCALLION, A. S., KASHUK, C. S., BUSH, R. T., GRICE, E., LIN, S., PORTNOY, M. E., CUTLER, D. J., GREEN, E. D. & CHAKRAVARTI, A. 2005. A common sex-dependent mutation in a RET enhancer underlies Hirschsprung disease risk. *Nature*, 434, 857.
- ENGEL, K. B. & MOORE, H. M. 2011. Effects of preanalytical variables on the detection of proteins by immunohistochemistry in formalin-fixed, paraffin-embedded tissue. *Archives of pathology & laboratory medicine*, 135, 537-543.
- EPPERSON, A., HATTON, W. J., CALLAGHAN, B., DOHERTY, P., WALKER, R. L., SANDERS, K. M., WARD, S. M. & HOROWITZ, B. 2000. Molecular markers expressed in cultured and freshly isolated interstitial cells of Cajal. *American Journal of Physiology-Cell Physiology*, 279, C529-C539.
- ESPINOSA, I., LEE, C.-H., KIM, M. K., ROUSE, B.-T., SUBRAMANIAN, S., MONTGOMERY, K., VARMA, S., CORLESS, C. L., HEINRICH, M. C. & SMITH, K. S. 2008. A novel monoclonal antibody against DOG1 is a sensitive and specific marker for gastrointestinal stromal tumors. *The American journal of surgical pathology*, 32, 210-218.
- FALAH, N., POSEY, J. E., THORSON, W., BENKE, P., TEKIN, M., TARSHISH, B., LUPSKI, J. R. & HAREL, T. J. A. J. O. M. G. P. A. 2017. 22q11. 2q13 duplication including SOX10 causes sex-reversal and peripheral demyelinating neuropathy, central dysmyelinating leukodystrophy, Waardenburg syndrome, and Hirschsprung disease. 173, 1066-1070.
- FARRUGIA, G. 2008. Interstitial cells of Cajal in health and disease. *Neurogastroenterology & Motility*, 20, 54-63.
- FAUSSONE-PELLEGRINI, M., CORTESINI, C. & PANTALONE, D. 1990a. Neuromuscular structures specific to the submucosal border of the human colonic circular muscle layer. *Canadian journal of physiology and pharmacology*, 68, 1437-1446.
- FAUSSONE-PELLEGRINI, M., PANTALONE, D. & CORTESINI, C. 1990b. Smooth muscle cells, interstitial cells of Cajal and myenteric plexus interrelationships in the human colon. *Cells Tissues Organs*, 139, 31-44.
- FAUSSONE-PELLEGRINI MS , PANTALONE D & C, C. 1989. An ultrastructural study of the interstitial cells of Cajal of the human stomach. . *Journal of Submicroscopic Cytology and Pathology*, 21, 439-460.
- FAUSSONE-PELLEGRINI, M. S. & THUNEBERG, L. 1999. Guide to the identification of interstitial cells of Cajal. *Microscopy research and technique*, 47, 248-266.
- FERNÁNDEZ, R. M., MATHIEU, Y., LUZON-TORO, B., NÚÑEZ-TORRES, R., GONZÁLEZ-MENESES, A., ANTIÑOLO, G., AMIEL, J. & BORREGO, S.

2013. Contributions of PHOX2B in the pathogenesis of Hirschsprung disease. *PloS one*, 8, e54043.
- FERNÁNDEZ, R. M., SÁNCHEZ-MEJÍAS, A., MENA, M., RUIZ-FERRER, M., LÓPEZ-ALONSO, M., ANTIÑOLO, G. & BORREGO, S. 2009. A novel point variant in NTRK3, R645C, suggests a role of this gene in the pathogenesis of Hirschsprung disease. *Annals of human genetics*, 73, 19-25.
- FORREST, A. S., ORDOG, T. & SANDERS, K. M. 2006. Neural regulation of slow-wave frequency in the murine gastric antrum. *American Journal of Physiology-Gastrointestinal and Liver Physiology*, 290, G486-G495.
- FOX, C. H., JOHNSON, F. B., WHITING, J. & ROLLER, P. P. 1985. Formaldehyde fixation. *Journal of Histochemistry & Cytochemistry*, 33, 845-853.
- FRANK, J. K.-L., HONGSHENGGUI, REESON XUWANG, TINGWENZHOU, WING HONLAI, HUNG-FATTSE, PAUL KWONG-HANGTAM1, MARIA-MERCEDESGARCIA-BARCELO, ELLY SAU-WAINGAN 2017. Correction of Hirschsprung-Associated Mutations in Human Induced Pluripotent Stem Cells Via Clustered Regularly Interspaced Short Palindromic Repeats/Cas9, Restores Neural Crest Cell Function. *Gastroenterology*, 153, 139-153.
- FRYKMAN, P. K., CHENG, Z., WANG, X. & DHALL, D. J. E. J. O. I. 2015. Enterocolitis causes profound lymphoid depletion in endothelin receptor B-and endothelin 3-null mouse models of Hirschsprung-associated enterocolitis. 45, 807-817.
- FUJITA, A., TAKEUCHI, T., JUN, H. & HATA, F. 2003. Localization of Ca<sup>2+</sup>-activated K<sup>+</sup> channel, SK3, in fibroblast-like cells forming gap junctions with smooth muscle cells in the mouse small intestine. *Journal of pharmacological sciences*, 92, 35-42.
- FURNESS, J. 2000. Types of neurons in the enteric nervous system. *Journal of the autonomic nervous system*, 81, 87-96.
- FURNESS, J. B. 2012. The enteric nervous system and neurogastroenterology. *Nature reviews Gastroenterology & hepatology*, 9, 286.
- FURNESS, J. B., RIVERA, L. R., CHO, H.-J., BRAVO, D. M. & CALLAGHAN, B. 2013. The gut as a sensory organ. *Nature reviews Gastroenterology & hepatology*, 10, 729.
- GAFFNEY, E., RIEGMAN, P., GRIZZLE, W. & WATSON, P. 2018. Factors that drive the increasing use of FFPE tissue in basic and translational cancer research. *Biotechnic & Histochemistry*, 93, 373-386.
- GALLEGO, D., GIL, V., MARTÍNEZ-CUTILLAS, M., MAÑÉ, N., MARTÍN, M. T. & JIMÉNEZ, M. 2012. Purinergic neuromuscular transmission is absent in the colon of P2Y1 knocked out mice. *The Journal of physiology*, 590, 1943-1956.
- GALLEGO, D., HERNÁNDEZ, P., CLAVÉ, P. & JIMÉNEZ, M. 2006. P2Y1 receptors mediate inhibitory purinergic neuromuscular transmission in the human colon. *American Journal of Physiology-Gastrointestinal and Liver Physiology*, 291, G584-G594.
- GARDI, J. E., NYENGAARD, J. R. & GUNDERSEN, H. J. G. 2008. The proportionator: unbiased stereological estimation using biased automatic

- image analysis and non-uniform probability proportional to size sampling. *Computers in biology and medicine*, 38, 313-328.
- GEERING, K. 2005. Function of FXYP proteins, regulators of Na, K-ATPase. *Journal of bioenergetics and biomembranes*, 37, 387-392.
- GEISLER, E. N., RYAN, M. A. & HOUSMAN, D. E. 1988. The dominant-white spotting (*W*) locus of the mouse encodes the c-kit proto-oncogene. *Cell*, 55, 185-192.
- GENESTE, O., BIDAUD, C., DE VITA, G., HOFSTRA, R. M., TARTARE-DECKERT, S., BUYS, C. H., LENOIR, G. M., SANTORO, M. & BILLAUD, M. J. H. M. G. 1999. Two distinct mutations of the RET receptor causing Hirschsprung's disease impair the binding of signalling effectors to a multifunctional docking site. 8, 1989-1999.
- GENETICIST 2018. The Pros and Cons of FFPE vs Frozen Tissue Samples. <https://www.geneticistinc.com/blog/the-pros-and-cons-of-ffpe-vs-frozen-tissue-samples>.
- GERALDINO, R., FERREIRA, A., LIMA, M., CABRINE-SANTOS, M., LAGES-SILVA, E. & RAMIREZ, L. 2006. Interstitial cells of Cajal in patients with chagasic megacolon originating from a region of old endemicity. *Pathophysiology*, 13, 71-74.
- GERSHON, M. D. 1999. The enteric nervous system: a second brain. *Hospital Practice*, 34, 31-52.
- GFROERER, S. & ROLLE, U. 2013. Interstitial cells of Cajal in the normal human gut and in Hirschsprung disease. *Pediatric surgery international*, 29, 889-897.
- GLASER, J. R. & GLASER, E. M. 2000. Stereology, morphometry, and mapping: the whole is greater than the sum of its parts. *Journal of chemical neuroanatomy*, 20, 115-126.
- GOMEZ-PINILLA, P. J., GIBBONS, S. J., BARDSLEY, M. R., LORINCZ, A., POZO, M. J., PASRICHA, P. J., DE RIJN, M. V., WEST, R. B., SARR, M. G. & KENDRICK, M. L. 2009. Ano1 is a selective marker of interstitial cells of Cajal in the human and mouse gastrointestinal tract. *American Journal of Physiology-Gastrointestinal and Liver Physiology*, 296, G1370-G1381.
- GOSAIN, A., BARLOW-ANACKER, A. J., ERICKSON, C. S., PIERRE, J. F., HENEGHAN, A. F., EPSTEIN, M. L. & KUDSK, K. A. 2015. Impaired cellular immunity in the murine neural crest conditional deletion of endothelin receptor-B model of Hirschsprung's disease. *PLoS One*, 10, e0128822.
- GOTO, K., MATSUOKA, S. & NOMA, A. 2004. Two types of spontaneous depolarizations in the interstitial cells freshly prepared from the murine small intestine. *The Journal of physiology*, 559, 411-422.
- GOWN, A. M. 2004. Unmasking the mysteries of antigen or epitope retrieval and formalin fixation. *American journal of clinical pathology*, 121, 172-174.
- GOYAL, R. K. 2013. Revised role of interstitial cells of Cajal in cholinergic neurotransmission in the gut. *The Journal of physiology*, 591, 5413-5414.

- GRAF, C., WAGER, E., BOWMAN, A., FIACK, S., SCOTT-LICHTER, D. & ROBINSON, A. 2007. Best practice guidelines on publication ethics: a publisher's perspective. *International journal of clinical practice*, 61, 1-26.
- GRAFEN, M., HOFMANN, T. R., SCHEEL, A. H., BECK, J., EMMERT, A., KÜFFER, S., DANNER, B. C., SCHÜTZ, E., BÜTTNER, R. & OSTENDORF, A. 2017. Optimized expression-based microdissection of formalin-fixed lung cancer tissue. *Laboratory Investigation*, 97, 863.
- GRONEBERG, D., LIES, B., KÖNIG, P., JÄGER, R., SEIDLER, B., KLEIN, S., SAUR, D. & FRIEBE, A. 2013. Cell-Specific Deletion of Nitric Oxide-Sensitive Guanylyl Cyclase Reveals a Dual Pathway for Nitroergic Neuromuscular Transmission in the Murine Fundus. *Gastroenterology*, 145, 188-196.
- GROVER, M., BERNARD, C. E., PASRICHA, P. J., PARKMAN, H. P., ABELL, T. L., NGUYEN, L. A., SNAPE, W., SHEN, K. R., SARR, M. & SWAIN, J. 2012. Platelet-derived growth factor receptor  $\alpha$  (PDGFR $\alpha$ )-expressing "fibroblast-like cells" in diabetic and idiopathic gastroparesis of humans. *Neurogastroenterology & Motility*, 24, 844-852.
- GRUBIŠIĆ, V. & GULBRANSEN, B. D. 2017. Enteric glia: the most alimentary of all glia. *The Journal of physiology*, 595, 557-570.
- GULBRANSEN, B. D. & SHARKEY, K. A. 2009. Purinergic neuron-to-glia signaling in the enteric nervous system. *Gastroenterology*, 136, 1349-1358.
- GULLEY, M. L. 2001. Molecular diagnosis of Epstein-Barr virus-related diseases. *The Journal of molecular diagnostics*, 3, 1-10.
- GUNADI, SUNARDI, M., BUDI, N. Y. P., KALIM, A. S., ISKANDAR, K. & DWIHANTORO, A. 2018. The impact of down-regulated SK3 expressions on Hirschsprung disease. *BMC Medical Genetics*, 19, 24.
- GUNDERSEN, H. J. G., BOYSEN, M. & REITH, A. 1981. Comparison of semiautomatic digitizer-tablet and simple point counting performance in morphometry. *Virchows Archiv B*, 37, 317-325.
- HA, S. E., LEE, M. Y., KURAHASHI, M., WEI, L., JORGENSEN, B. G., PARK, C., PARK, P. J., REDELMAN, D., SASSE, K. C. & BECKER, L. S. 2017. Transcriptome analysis of PDGFR $\alpha$ + cells identifies T-type Ca<sup>2+</sup> channel CACNA1G as a new pathological marker for PDGFR $\alpha$ + cell hyperplasia. *PloS one*, 12, e0182265.
- HAHN, S., BAUER, S., HEUSNER, T. A., EBELING, P., HAMAMI, M. E., STAHL, A., FORSTING, M., BOCKISCH, A. & ANTOCH, G. 2011. Postoperative FDG-PET/CT staging in GIST: is there a benefit following R0 resection? *European journal of radiology*, 80, 670-674.
- HANANI, M. & FREUND, H. 2000a. Interstitial cells of Cajal—their role in pacing and signal transmission in the digestive system. *Acta physiologica scandinavica*, 170, 177-190.
- HANANI, M. & FREUND, H. 2000b. Interstitial cells of Cajal—their role in pacing and signal transmission in the digestive system. *Acta Physiologica*, 170, 177-190.
- HARA, Y., KUBOTA, M. & SZURSZEWski, J. H. 1986. Electrophysiology of smooth muscle of the small intestine of some mammals. *The Journal of Physiology*, 372, 501-520.

- HARRINGTON, A., HUTSON, J. & SOUTHWELL, B. 2007a. Immunohistochemical localisation of cholinergic muscarinic receptor subtype 1 (M1r) in the guinea pig and human enteric nervous system. *Journal of chemical neuroanatomy*, 33, 193-201.
- HARRINGTON, A., HUTSON, J. & SOUTHWELL, B. 2008. Immunohistochemical localisation of pre-synaptic muscarinic receptor subtype-2 (M2r) in the enteric nervous system of guinea-pig ileum. *Cell and tissue research*, 332, 37-48.
- HARRINGTON, A., PECK, C., LIU, L., BURCHER, E., HUTSON, J. & SOUTHWELL, B. 2010a. Localization of muscarinic receptors M1R, M2R and M3R in the human colon. *Neurogastroenterology & Motility*, 22, 999-e263.
- HARRINGTON, A. M., HUTSON, J. & SOUTHWELL, B. R. 2007b. High affinity choline transporter immunoreactivity in rat ileum myenteric nerves. *Cell and tissue research*, 327, 421-431.
- HARRINGTON, A. M., HUTSON, J. M. & SOUTHWELL, B. R. 2010b. Cholinergic neurotransmission and muscarinic receptors in the enteric nervous system. *Progress in histochemistry and cytochemistry*, 44, 173-202.
- HE, L., LONG, L. R., ANTANI, S. & THOMA, G. R. 2012. Histology image analysis for carcinoma detection and grading. *Computer methods and programs in biomedicine*, 107, 538-556.
- HEALEY, A., SEVDALIS, N. & VINCENT, C. 2006. Measuring intra-operative interference from distraction and interruption observed in the operating theatre. *Ergonomics*, 49, 589-604.
- HEANUE, T. A. & PACHNIS, V. 2007. Enteric nervous system development and Hirschsprung's disease: advances in genetic and stem cell studies. *Nature Reviews Neuroscience*, 8, 466.
- HEDEGAARD, J., THORSEN, K., LUND, M. K., HEIN, A.-M. K., HAMILTON-DUTOIT, S. J., VANG, S., NORDENTOFT, I., BIRKENKAMP-DEMTRÖDER, K., KRUHØFFER, M. & HAGER, H. 2014. Next-generation sequencing of RNA and DNA isolated from paired fresh-frozen and formalin-fixed paraffin-embedded samples of human cancer and normal tissue. *PloS one*, 9, e98187.
- HELANDER, K. G. 1994. Kinetic studies of formaldehyde binding in tissue. *Biotechnic & Histochemistry*, 69, 177-179.
- HENDERSON, P., VAN LIMBERGEN, J. E., SCHWARZE, J. & WILSON, D. C. 2010. Function of the intestinal epithelium and its dysregulation in inflammatory bowel disease. *Inflammatory bowel diseases*, 17, 382-395.
- HEUCKEROTH, R. O. 2018. Hirschsprung disease—integrating basic science and clinical medicine to improve outcomes. *Nature reviews Gastroenterology & hepatology*, 15, 152.
- HEUCKEROTH, R. O. & SCHÄFER, K.-H. 2016. Gene-environment interactions and the enteric nervous system: Neural plasticity and Hirschsprung disease prevention. *Developmental biology*, 417, 188-197.
- HEWITT, S. M., LEWIS, F. A., CAO, Y., CONRAD, R. C., CRONIN, M., DANENBERG, K. D., GORALSKI, T. J., LANGMORE, J. P., RAJA, R. G. & WILLIAMS, P. M. 2008. Tissue handling and specimen preparation in

- surgical pathology: issues concerning the recovery of nucleic acids from formalin-fixed, paraffin-embedded tissue. *Archives of pathology & laboratory medicine*, 132, 1929-1935.
- HIRST, G., BRAMICH, N., TERAMOTO, N., SUZUKI, H. & EDWARDS, F. 2002. Regenerative component of slow waves in the guinea-pig gastric antrum involves a delayed increase in  $[Ca^{2+}]_i$  and  $Cl^-$  channels. *The Journal of physiology*, 540, 907-919.
- HIRST, G. D. S. & EDWARDS, F. R. 2004. Role of interstitial cells of Cajal in the control of gastric motility. *Journal of pharmacological sciences*, 96, 1-10.
- HOFSTRA, R., VALDENNAIRE, O., ARCH, E., OSINGA, J., KROES, H., LÖFFLER, B.-M., HAMOSH, A., MEIJERS, C. & BUYS, C. 1999. A loss-of-function mutation in the endothelin-converting enzyme 1 (ECE-1) associated with Hirschsprung disease, cardiac defects, and autonomic dysfunction. *American journal of human genetics*, 64, 304.
- HORIGUCHI, K. & KOMURO, T. 2000. Ultrastructural observations of fibroblast-like cells forming gap junctions in the W/W<sup>v</sup> mouse small intestine. *Journal of the autonomic nervous system*, 80, 142-147.
- HORISAWA, M., WATANABE, Y. & TORIHASHI, S. 1998. Distribution of c-Kit immunopositive cells in normal human colon and in Hirschsprung's disease. *Journal of pediatric surgery*, 33, 1209-1214.
- HORVÁTH, V. J., VITTAL, H., LÖRINCZ, A., CHEN, H., ALMEIDA-PORADA, G., REDELMAN, D. & ÖRDÖG, T. 2006. Reduced stem cell factor links smooth myopathy and loss of interstitial cells of cajal in murine diabetic gastroparesis. *Gastroenterology*, 130, 759-770.
- HOSHINO, M., OMURA, N., YANO, F., TSUBOI, K., KASHIWAGI, H. & YANAGA, K. 2013. Immunohistochemical study of the muscularis externa of the esophagus in achalasia patients. *Diseases of the Esophagus*, 26, 14-21.
- HOUGAARD, C., ERIKSEN, B., JØRGENSEN, S., JOHANSEN, T., DYHRING, T., MADSEN, L., STRØBAEK, D. & CHRISTOPHERSEN, P. 2007. Selective positive modulation of the SK3 and SK2 subtypes of small conductance  $Ca^{2+}$ -activated  $K^+$  channels. *British journal of pharmacology*, 151, 655-665.
- HOWAT, W. J. & WILSON, B. A. 2014. Tissue fixation and the effect of molecular fixatives on downstream staining procedures. *Methods*, 70, 12-19.
- HUIZINGA, J. D. 1999. Gastrointestinal peristalsis: joint action of enteric nerves, smooth muscle, and interstitial cells of Cajal. *Microscopy research and technique*, 47, 239-247.
- HUIZINGA, J. D., BEREZIN, I., SIRCAR, K., HEWLETT, B., DONNELLY, G., BERCIK, P., ROSS, C., ALGOFI, T., FITZGERALD, P. & DER, T. 2001. Development of interstitial cells of Cajal in a full-term infant without an enteric nervous system. *Gastroenterology*, 120, 561-567.
- HUIZINGA, J. D. & CHEN, J.-H. 2014. The myogenic and neurogenic components of the rhythmic segmentation motor patterns of the intestine. *Frontiers in neuroscience*, 8, 78.

- HUIZINGA, J. D., CHEN, J., MIKKELSEN, H. B., WANG, X.-Y., PARSONS, S. & ZHU, Y. 2013. Interstitial cells of Cajal, from structure to function. *Frontiers in neuroscience*, 7, 43.
- HUIZINGA, J. D. & LAMMERS, W. J. 2009. Gut peristalsis is governed by a multitude of cooperating mechanisms. *American Journal of Physiology-Gastrointestinal and Liver Physiology*, 296, G1-G8.
- HUIZINGA, J. D., MARTZ, S., GIL, V., WANG, X.-Y., JIMENEZ, M. & PARSONS, S. 2011. Two independent networks of interstitial cells of Cajal work cooperatively with the enteric nervous system to create colonic motor patterns. *Frontiers in neuroscience*, 5, 93.
- HULZINGA, J. D., THUNEBERG, L., KLÜPPEL, M., MALYSZ, J., MIKKELSEN, H. B. & BERNSTEIN, A. 1995. *W/kit* gene required for interstitial cells of Cajal and for intestinal pacemaker activity. *Nature*, 373, 347.
- HWANG, S. J., BLAIR, P. J., BRITTON, F. C., O'DRISCOLL, K. E., HENNIG, G., BAYGUINOV, Y. R., ROCK, J. R., HARFE, B. D., SANDERS, K. M. & WARD, S. M. 2009. Expression of anoctamin 1/TMEM16A by interstitial cells of Cajal is fundamental for slow wave activity in gastrointestinal muscles. *The Journal of physiology*, 587, 4887-4904.
- HWANG, S. J., BLAIR, P. J., DURNIN, L., MUTAFOVA-YAMBOLIEVA, V., SANDERS, K. M. & WARD, S. M. 2012. P2Y1 purinoreceptors are fundamental to inhibitory motor control of murine colonic excitability and transit. *The Journal of physiology*, 590, 1957-1972.
- IINO, S., HORIGUCHI, K., HORIGUCHI, S. & NOJYO, Y. 2009. c-Kit-negative fibroblast-like cells express platelet-derived growth factor receptor  $\alpha$  in the murine gastrointestinal musculature. *Histochemistry and cell biology*, 131, 691-702.
- IINO, S., HORIGUCHI, K. & NOJYO, Y. 2008. Interstitial cells of Cajal are innervated by nitrergic nerves and express nitric oxide-sensitive guanylate cyclase in the guinea-pig gastrointestinal tract. *Neuroscience*, 152, 437-448.
- IINO, S. & NOJYO, Y. 2009. Immunohistochemical demonstration of c-Kit-negative fibroblast-like cells in murine gastrointestinal musculature. *Archives of histology and cytology*, 72, 107-115.
- IKEDA, S. 2018. Novel and simple method of double-detection using fluorescence in situ hybridization and fluorescence immunostaining of formalin-fixed paraffin-embedded tissue sections. *Oncology letters*, 15, 1084-1088.
- IMAIZUMI, M. & HAMA, K. 1969. An electron microscopic study on the interstitial cells of the gizzard in the love-bird (*Uroloncha domestica*). *Cell and Tissue Research*, 97, 351-357.
- INOUE, K., TANABE, Y. & LUPSKI, J. R. 1999. Myelin deficiencies in both the central and the peripheral nervous systems associated with a SOX10 mutation. *Annals of Neurology: Official Journal of the American Neurological Association and the Child Neurology Society*, 46, 313-318.
- IPPOLITO, C., SEGNANI, C., DE GIORGIO, R., BLANDIZZI, C., MATTII, L., CASTAGNA, M., MOSCATO, S., DOLFI, A. & BERNARDINI, N. 2009. Quantitative evaluation of myenteric ganglion cells in normal human left

- colon: implications for histopathological analysis. *Cell and tissue research*, 336, 191-201.
- ISHII, M. & KURACHI, Y. 2006. Muscarinic acetylcholine receptors. *Current pharmaceutical design*, 12, 3573-3581.
- IVANCHUK, S. M., MYERS, S. M., ENG, C. & MULLIGAN, L. M. 1996. De novo mutation of GDNF, ligand for the RET/GDNFR- $\alpha$  receptor complex, in Hirschsprung disease. *Human molecular genetics*, 5, 2023-2026.
- IWASHITA, T., KUROKAWA, K., QIAO, S., MURAKAMI, H., ASAI, N., KAWAI, K., HASHIMOTO, M., WATANABE, T., ICHIHARA, M. & TAKAHASHI, M. J. G. 2001. Functional analysis of RET with Hirschsprung mutations affecting its kinase domain. 121, 24-33.
- JAIN, D., MOUSSA, K., TANDON, M., CULPEPPER-MORGAN, J. & PROCTOR, D. D. 2003. Role of interstitial cells of Cajal in motility disorders of the bowel. *The American journal of gastroenterology*, 98, 618-624.
- JANEVSKA, V., QERIMI, A., BASHESKA, N., STOJKOVA, E., JANEVSKI, V., JOVANOVIĆ, R., ZHIVADINOVIC, J. & SPASEVSKA, L. 2015. Superficial leiomyomas of the gastrointestinal tract with interstitial cells of Cajal. *International journal of clinical and experimental pathology*, 8, 15977.
- JENG, Y.-M., MAO, T.-L., HSU, W.-M., HUANG, S.-F. & HSU, H.-C. 2000. Congenital interstitial cell of cajal hyperplasia with neuronal intestinal dysplasia. *The American journal of surgical pathology*, 24, 1568-1572.
- JIAO, Y., SUN, Z., LEE, T., FUSCO, F. R., KIMBLE, T. D., MEADE, C. A., CUTHBERTSON, S. & REINER, A. 1999. A simple and sensitive antigen retrieval method for free-floating and slide-mounted tissue sections. *Journal of neuroscience methods*, 93, 149-162.
- JOHNSON, L. R. 1977. Gastrointestinal hormones and their functions. *Annual Review of Physiology*, 39, 135-158.
- JULIE E. COOPER, CONOR J. MCCANN, DIPAN NATARAJAN, SHANAS CHOUDHURY, WEREND BOESMANS, JEAN-MARIE DELALANDE, PIETER VANDEN BERGHE, ALAN J. BURNS & THAPAR, N. 2016. In Vivo Transplantation of Enteric Neural Crest Cells into Mouse Gut; Engraftment, Functional Integration and Long-Term Safety. *PLoS One* 11, e0147989.
- JUNQUERA, C., MARTÍNEZ-CIRIANO, C., CASTIELLA, T., SERRANO, P., AZANZA, M. J. & RAMÓN Y CAJAL JUNQUERA, S. 2007. Immunohistochemical and ultrastructural characteristics of interstitial cells of Cajal in the rabbit duodenum. Presence of a single cilium. *Journal of cellular and molecular medicine*, 11, 776-787.
- KARAKUŞ, O. Z., ULUSOY, O., AKTÜRK, G., ATEŞ, O., OLGUN, E. G., DALGIÇ, M., HAKGÜDER, G., ÖZER, E., OLGUNER, M. & AKGÜR, F. M. 2016. The density of interstitial cells of Cajal is diminished in choledochal cysts. *Digestive diseases and sciences*, 61, 900-904.
- KEEF, K., MURRAY, D., SANDERS, K. & SMITH, T. 1997. Basal release of nitric oxide induces an oscillatory motor pattern in canine colon. *The Journal of Physiology*, 499, 773-786.

- KENNY, S., VANDERWINDEN, J.-M., RINTALA, R., CONNELL, M., LLOYD, D., VANDERHAEGEN, J. & DE LAET, M.-H. 1998. Delayed maturation of the interstitial cells of Cajal: a new diagnosis for transient neonatal pseudoobstruction. Report of two cases. *Journal of pediatric surgery*, 33, 94-98.
- KENNY, S. E., TAM, P. K. & GARCIA-BARCELO, M. Hirschsprung's disease. *Seminars in pediatric surgery*, 2010. Elsevier, 194-200.
- KIM, H. J. 2011. A functional role for the 'fibroblast-like cells' in gastrointestinal smooth muscles (J Physiol 2011; 589 [Pt 3]: 697-710). *Journal of neurogastroenterology and motility*, 17, 425.
- KIM, T. W., KOH, S. D., ÖRDÖG, T., WARD, S. M. & SANDERS, K. M. 2003. Muscarinic regulation of pacemaker frequency in murine gastric interstitial cells of Cajal. *The Journal of physiology*, 546, 415-425.
- KING, D., DUKES, J., REID, S., EBERT, K., SHAW, A., MILLS, C., BOSWELL, L. & FERRIS, N. 2008. Prospects for rapid diagnosis of foot-and-mouth disease in the field using reverse transcriptase-PCR. British Medical Journal Publishing Group.
- KLEIN, S., SEIDLER, B., KETTENBERGER, A., SIBAEV, A., ROHN, M., FEIL, R., ALLESCHER, H.-D., VANDERWINDEN, J.-M., HOFMANN, F. & SCHEMANN, M. 2013. Interstitial cells of Cajal integrate excitatory and inhibitory neurotransmission with intestinal slow-wave activity. *Nature communications*, 4, 1630.
- KLEMM, M. F. & LANG, R. J. 2002. Distribution of Ca<sup>2+</sup>-activated K<sup>+</sup> channel (SK2 and SK3) immunoreactivity in intestinal smooth muscles of the guinea-pig. *Clinical and experimental pharmacology and physiology*, 29, 18-25.
- KLÜPPEL, M., HUIZINGA, J. D., MALYSZ, J. & BERNSTEIN, A. 1998. Developmental origin and kit-dependent development of the interstitial cells of cajal in the mammalian small intestine. *Developmental Dynamics*, 211, 60-71.
- KNOWLES, C. H. & FARRUGIA, G. 2011. Gastrointestinal neuromuscular pathology in chronic constipation. *Best Practice & Research Clinical Gastroenterology*, 25, 43-57.
- KOBAYASHI, S., FURNESS, J. B., SMITH, T. K. & POMPOLO, S. 1989. Histological identification of the interstitial cells of Cajal in the guinea-pig small intestine. *Archives of histology and cytology*, 52, 267-286.
- KOH, S. D., SANDERS, K. M. & WARD, S. M. 1998. Spontaneous electrical rhythmicity in cultured interstitial cells of Cajal from the murine small intestine. *The Journal of Physiology*, 513, 203-213.
- KOH, S. D., WARD, S. M. & SANDERS, K. M. 2012. Ionic conductances regulating the excitability of colonic smooth muscles. *Neurogastroenterology & Motility*, 24, 705-718.
- KOMURO, T., SEKI, K. & HORIGUCHI, K. 1999. Ultrastructural characterization of the interstitial cells of Cajal. *Archives of histology and cytology*, 62, 295-316.
- KRAICHELY, R. & FARRUGIA, G. 2007. Mechanosensitive ion channels in interstitial cells of Cajal and smooth muscle of the gastrointestinal tract. *Neurogastroenterology & Motility*, 19, 245-252.

- KUBOTA, M., ITO, Y. & IKEDA, K. 1983. Membrane properties and innervation of smooth muscle cells in Hirschsprung's disease. *American Journal of Physiology-Gastrointestinal and Liver Physiology*, 244, G406-G415.
- KUBOTA, Y., KAJIOKA, S., BIERS, S. M., YOKOTA, E., KOHRI, K. & BRADING, A. F. 2004. Investigation of the effect of the c-kit inhibitor Glivec on isolated guinea-pig detrusor preparations. *Autonomic Neuroscience*, 115, 64-73.
- KULKARNI, S., MICCI, M.-A., LESER, J., SHIN, C., TANG, S.-C., FU, Y.-Y., LIU, L., LI, Q., SAHA, M. & LI, C. J. P. O. T. N. A. O. S. 2017. Adult enteric nervous system in health is maintained by a dynamic balance between neuronal apoptosis and neurogenesis. 114, E3709-E3718.
- KUMRAL, D. & ZFASS, A. M. 2018. Gut Movements: A Review of the Physiology of Gastrointestinal Transit. *Digestive diseases and sciences*, 63, 2500-2506.
- KURAHASHI, M., MUTAFOVA-YAMBOLIEVA, V., KOH, S. D. & SANDERS, K. M. 2014. Platelet-derived growth factor receptor- $\alpha$ -positive cells and not smooth muscle cells mediate purinergic hyperpolarization in murine colonic muscles. *American Journal of Physiology-Cell Physiology*, 307, C561-C570.
- KURAHASHI, M., NAKANO, Y., HENNIG, G. W., WARD, S. M. & SANDERS, K. M. 2012. Platelet-derived growth factor receptor  $\alpha$ -positive cells in the tunica muscularis of human colon. *Journal of cellular and molecular medicine*, 16, 1397-1404.
- KURAHASHI, M., NAKANO, Y., PERI, L. E., TOWNSEND, J. B., WARD, S. M. & SANDERS, K. M. 2013. A novel population of subepithelial platelet-derived growth factor receptor  $\alpha$ -positive cells in the mouse and human colon. *American Journal of Physiology-Gastrointestinal and Liver Physiology*, 304, G823-G834.
- KURAHASHI, M., ZHENG, H., DWYER, L., WARD, S. M., DON KOH, S. & SANDERS, K. M. 2011. A functional role for the 'fibroblast-like cells' in gastrointestinal smooth muscles. *The Journal of physiology*, 589, 697-710.
- KUSAFUKA, T. & PURI, P. 1997. Altered RET gene mRNA expression in Hirschsprung's disease. *Journal of pediatric surgery*, 32, 600-604.
- LAKE, J. I. & HEUCKEROTH, R. O. 2013. Enteric nervous system development: migration, differentiation, and disease. *American Journal of Physiology-Gastrointestinal and Liver Physiology*, 305, G1-G24.
- LANGTON, P., WARD, S., CARL, A., NORELL, M. & SANDERS, K. 1989. Spontaneous electrical activity of interstitial cells of Cajal isolated from canine proximal colon. *Proceedings of the National Academy of Sciences*, 86, 7280-7284.
- LECCI, A., SANTICIOLI, P. & MAGGI, C. A. 2002. Pharmacology of transmission to gastrointestinal muscle. *Current opinion in pharmacology*, 2, 630-641.
- LECOIN, L., GABELLA, G. & LE DOUARIN, N. 1996. Origin of the c-kit-positive interstitial cells in the avian bowel. *Development*, 122, 725-733.
- LEE, H. T., HENNIG, G. W., FLEMING, N. W., KEEF, K. D., SPENCER, N. J., WARD, S. M., SANDERS, K. M. & SMITH, T. K. 2007. The mechanism

- and spread of pacemaker activity through myenteric interstitial cells of Cajal in human small intestine. *Gastroenterology*, 132, 1852-1865.
- LEE, H. T., HENNIG, G. W., PARK, K. J., BAYGUINOV, P. O., WARD, S. M., SANDERS, K. M. & SMITH, T. K. 2009. Heterogeneities in ICC Ca<sup>2+</sup> activity within canine large intestine. *Gastroenterology*, 136, 2226-2236.
- LEE, J. I., PARK, H., KAMM, M. A. & TALBOT, I. C. 2005. Decreased density of interstitial cells of Cajal and neuronal cells in patients with slow-transit constipation and acquired megacolon. *Journal of gastroenterology and hepatology*, 20, 1292-1298.
- LEE, J. S., OH, J.-T., KIM, J.-H., SEO, J.-M., KIM, D.-Y., PARK, K.-W., KIM, H.-Y., JUNG, K., PARK, B. L. & KOH, I. 2016. Association analysis of SLC6A20 polymorphisms with Hirschsprung disease. *Journal of pediatric gastroenterology and nutrition*, 62, 64-70.
- LEE, M. Y., HA, S. E., PARK, C., PARK, P. J., FUCHS, R., WEI, L., JORGENSEN, B. G., REDELMAN, D., WARD, S. M. & SANDERS, K. M. 2017. Transcriptome of interstitial cells of Cajal reveals unique and selective gene signatures. *PloS one*, 12, e0176031.
- LEONARD, C., SYED, J. & RADI, Z. 2016. Comparison and impact of various whole body perfusion techniques on tissue preservation quality and immunorecognition. *Journal of Histotechnology*, 39, 39-46.
- LEVY, S., SUTTON, G., NG, P. C., FEUK, L., HALPERN, A. L., WALENZ, B. P., AXELROD, N., HUANG, J., KIRKNESS, E. F. & DENISOV, G. 2007. The diploid genome sequence of an individual human. *PLoS biology*, 5, e254.
- LIM, M. D., DICKHERBER, A. & COMPTON, C. C. 2010. Before you analyze a human specimen, think quality, variability, and bias. ACS Publications.
- LIN, L., XU, L.-M., ZHANG, W., GE, Y.-B., TANG, Y.-R., ZHANG, H.-J., LI, X.-L. & CHEN, J. D. 2009. Roles of stem cell factor on the depletion of interstitial cells of Cajal in the colon of diabetic mice. *American Journal of Physiology-Gastrointestinal and Liver Physiology*, 298, G241-G247.
- LIU, A. & POLLARD, K. 2015. Biobanking For personalized medicine. *Biobanking in the 21st Century*. Springer.
- LIU, L., THUNEBERG, L. & HUIZINGA, J. D. 1994. Selective lesioning of interstitial cells of Cajal by methylene blue and light leads to loss of slow waves. *American Journal of Physiology-Gastrointestinal and Liver Physiology*, 266, G485-G496.
- LIU, W., ZHANG, L., WU, R. J. D. & BIOLOGY, C. 2018. Enteric Neural Stem Cells Expressing Insulin-Like Growth Factor 1: A Novel Cellular Therapy for Hirschsprung's Disease in Mouse Model. 37, 642-648.
- LIU, Y.-A., CHUNG, Y.-C., PAN, S.-T., HOU, Y.-C., PENG, S.-J., PASRICHA, P. J. & TANG, S.-C. 2012. 3-D illustration of network orientations of interstitial cells of Cajal subgroups in human colon as revealed by deep-tissue imaging with optical clearing. *American Journal of Physiology-Gastrointestinal and Liver Physiology*, 302, G1099-G1110.
- LONG, D. J. & BUGGS, C. 2008. Microwave oven-based technique for immunofluorescent staining of paraffin-embedded tissues. *Journal of molecular histology*, 39, 1-4.

- LÜDER RIPOLI, F., MOHR, A., CONRADINE HAMMER, S., WILLENBROCK, S., HEWICKER-TRAUTWEIN, M., HENNECKE, S., MURUA ESCOBAR, H. & NOLTE, I. 2016. A comparison of fresh frozen vs. formalin-fixed, paraffin-embedded specimens of canine mammary tumors via branched-DNA assay. *International journal of molecular sciences*, 17, 724.
- LYFORD, G., HE, C., SOFFER, E., HULL, T., STRONG, S., SENAGORE, A., BURGART, L., YOUNG-FADOK, T., SZURSZEWSKI, J. & FARRUGIA, G. 2002. Pan-colonic decrease in interstitial cells of Cajal in patients with slow transit constipation. *Gut*, 51, 496-501.
- MAEDA, H., YAMAGATA, A., NISHIKAWA, S., YOSHINAGA, K., KOBAYASHI, S. & NISHI, K. 1992. Requirement of c-kit for development of intestinal pacemaker system. *Development*, 116, 369-375.
- MAHMOOD, R. & MASON, I. 2008. In-situ hybridization of radioactive riboprobes to RNA in tissue sections. *Molecular Embryology*. Springer.
- MALYSZ, J., GIBBONS, S. J., SARAVANAPERUMAL, S. A., DU, P., EISENMAN, S. T., CAO, C., OH, U., SAUR, D., KLEIN, S. & ORDOG, T. 2016. Conditional genetic deletion of *Ano1* in interstitial cells of Cajal impairs  $Ca^{2+}$  transients and slow waves in adult mouse small intestine. *American Journal of Physiology-Gastrointestinal and Liver Physiology*, 312, G228-G245.
- MANDARIM-DE-LACERDA, C. A. 2003. Stereological tools in biomedical research. *Anais da Academia brasileira de Ciências*, 75, 469-486.
- MANNESCHI, L. I., PACINI, S., CORSANI, L., BECHI, P. & FAUSSONE-PELLEGRINI, M. 2004. Interstitial cells of Cajal in the human stomach: distribution and relationship with enteric innervation. *Histology and histopathology*, 19, 1153-1164.
- MAO, Y., WANG, B. & KUNZE, W. 2006. Characterization of myenteric sensory neurons in the mouse small intestine. *Journal of neurophysiology*, 96, 998-1010.
- MAZZIA, C., PORCHER, C., JULÉ, Y., CHRISTEN, M.-O. & HENRY, M. 2000. Ultrastructural study of relationships between c-kit immunoreactive interstitial cells and other cellular elements in the human colon. *Histochemistry and cell biology*, 113, 401-411.
- MAZZONE, A., BERNARD, C. E., STREGE, P. R., BEYDER, A., GALIETTA, L. J., PASRICHA, P. J., RAE, J. L., PARKMAN, H. P., LINDEN, D. R. & SZURSZEWSKI, J. H. 2011. Altered expression of *Ano1* variants in human diabetic gastroparesis. *Journal of Biological Chemistry*, jbc.M110.196089.
- MCCANN, C. J., COOPER, J. E., NATARAJAN, D., JEVANS, B., BURNETT, L. E., BURNS, A. J. & THAPAR, N. J. N. C. 2017. Transplantation of enteric nervous system stem cells rescues nitric oxide synthase deficient mouse colon. 8, 15937.
- MCCANN, C. J., HWANG, S.-J., BAYGUINOV, Y., COLLETTI, E. J., SANDERS, K. M. & WARD, S. M. 2013. Establishment of pacemaker activity in tissues allotransplanted with interstitial cells of C ajal. *Neurogastroenterology & Motility*, 25, e418-e428.
- MCCLAIN, J. L., FRIED, D. E. & GULBRANSEN, B. D. 2015. Agonist-evoked  $Ca^{2+}$  signaling in enteric glia drives neural programs that regulate

- intestinal motility in mice. *Cellular and molecular gastroenterology and hepatology*, 1, 631-645.
- MCCLAIN, J. L., GRUBIŠIĆ, V., FRIED, D., GOMEZ-SUAREZ, R. A., LEINNINGER, G. M., SÉVIGNY, J., PARPURA, V. & GULBRANSEN, B. D. 2014. Ca<sup>2+</sup> responses in enteric glia are mediated by connexin-43 hemichannels and modulate colonic transit in mice. *Gastroenterology*, 146, 497-507. e1.
- MCHUGH ML 2012. Interrater reliability: the kappa statistic. *Biochemia medica*, 22, 276-282.
- MCKERNAN, K. J., PECKHAM, H. E., COSTA, G. L., MCLAUGHLIN, S. F., FU, Y., TSUNG, E. F., CLOUSER, C. R., DUNCAN, C., ICHIKAWA, J. K. & LEE, C. C. 2009. Sequence and structural variation in a human genome uncovered by short-read, massively parallel ligation sequencing using two-base encoding. *Genome research*, 19, 1527-1541.
- MCNICOL, A. & RICHMOND, J. 1998. Optimizing immunohistochemistry: antigen retrieval and signal amplification. *Histopathology*, 32, 97-103.
- MEINDS, R., VAN DER STEEG, A., SLOOTS, C., WITVLIET, M., DE BLAAUW, I., VAN GEMERT, W., TRZPIS, M. & BROENS, P. 2019. Long-term functional outcomes and quality of life in patients with Hirschsprung's disease. *British Journal of Surgery*.
- MIGUEL, C., EDUARDO VILAR, SU-YI TSAI, KYLE CHANG, SADAF AMIN, TARA SRINIVASAN, TUO ZHANG, NINA H PIPALIA, HUANHUAN JOYCE CHEN, MAVEE WITHERSPOON, MIRIAM GORDILLO, JENNY ZHAOYING XIANG, FREDERICK R MAXFIELD, STEVEN LIPKIN, TODD EVANS & CHEN, S. 2017. Colonic organoids derived from human induced pluripotent stem cells for modeling colorectal cancer and drug testing. *Nature Medicine*, 23, 878-884.
- MIKKELSEN, H. B. 2010. Interstitial cells of Cajal, macrophages and mast cells in the gut musculature: morphology, distribution, spatial and possible functional interactions. *Journal of cellular and molecular medicine*, 14, 818-832.
- MINERVA M. CARRASQUILLO, ANDREW S. MCCALLION, ERIK G. PUFFENBERGER, CARL S. KASHUK, & N. N. & CHAKRAVARTI, A. 2002. Genome-wide association study and mouse model identify interaction between RET and EDNRB pathways in Hirschsprung disease. *Nature Genetics*, 32, 237-244.
- MIYAMOTO-KIKUTA, S., EZAKI, T. & KOMURO, T. 2009. Distribution and morphological characteristics of the interstitial cells of Cajal in the ileocaecal junction of the guinea-pig. *Cell and tissue research*, 338, 29.
- MOORE, S., JOHNSON, G. & SCHNEIDER, J. J. E. J. O. P. S. 2000. Elevated tissue immunoglobulins in Hirschsprung's disease-indication of early immunologic response. 10, 106-110.
- MORGAN, J., NAVABI, H., SCHMID, K. & JASANI, B. 1994. Possible role of tissue-bound calcium ions in citrate-mediated high-temperature antigen retrieval. *The Journal of pathology*, 174, 301-307.
- NAKAHARA, M., ISOZAKI, K., HIROTA, S., MIYAGAWA, J.-I., HASE-SAWADA, N., TANIGUCHI, M., NISHIDA, T., KANAYAMA, S., KITAMURA, Y. & SHINOMURA, Y. 1998. A novel gain-of-function

- mutation of c-kit gene in gastrointestinal stromal tumors. *Gastroenterology*, 115, 1090-1095.
- NAKAMURA, H. & PURI, P. 2019. Altered ryanodine receptor gene expression in Hirschsprung's disease. *Pediatric surgery international*.
- NEMETH, L., MADDUR, S. & PURI, P. 2000. Immunolocalization of the gap junction protein Connexin43 in the interstitial cells of Cajal in the normal and Hirschsprung's disease bowel. *Journal of pediatric surgery*, 35, 823-828.
- NEWGREEN, D. & YOUNG, H. M. 2002. Enteric nervous system: development and developmental disturbances—part 1. *Pediatric and Developmental Pathology*, 5, 224-247.
- NEWMAN, C. J., LAURINI, R., LESBROS, Y., REINBERG, O. & MEYRAT, B. 2003. Interstitial cells of Cajal are normally distributed in both ganglionated and aganglionic bowel in Hirschsprung's disease. *Pediatric surgery international*, 19, 662-668.
- O'DONNELL, A.-M., COYLE, D. & PURI, P. 2016. Deficiency of platelet-derived growth factor receptor- $\alpha$ -positive cells in Hirschsprung's disease colon. *World journal of gastroenterology*, 22, 3335.
- O'DONNELL, A.-M. & PURI, P. 2008. Deficiency of purinergic P2Y receptors in aganglionic intestine in Hirschsprung's disease. *Pediatric surgery international*, 24, 77-80.
- O'DONNELL, A. M., NAKAMURA, H., TOMUSCHAT, C., MARAYATI, N. F. & PURI, P. 2019a. Abnormal Scn1b and Fxyd1 gene expression in the pulled-through ganglionic colon may influence functional outcome in patients with Hirschsprung's disease. *Pediatric surgery international*, 35, 9-14.
- O'DONNELL, A. M., NAKAMURA, H., TOMUSCHAT, C., MARAYATI, N. F. & PURI, P. 2019b. Altered expression of KCNG3 and KCNG4 in Hirschsprung's disease. *Pediatric surgery international*, 35, 193-197.
- OLSSON, C. & HOLMGREN, S. 2001. The control of gut motility. *Comparative Biochemistry and Physiology Part A: Molecular & Integrative Physiology*, 128, 479-501.
- ORDOG, T., REDELMAN, D., HOROWITZ, N. N. & SANDERS, K. M. 2004. Immunomagnetic enrichment of interstitial cells of Cajal. *American Journal of Physiology-Gastrointestinal and Liver Physiology*, 286, G351-G360.
- ÖRDÖG, T., REDELMAN, D., HORVÁTH, V. J., MILLER, L. J., HOROWITZ, B. & SANDERS, K. M. 2004. Quantitative analysis by flow cytometry of interstitial cells of Cajal, pacemakers, and mediators of neurotransmission in the gastrointestinal tract. *Cytometry Part A: The Journal of the International Society for Analytical Cytology*, 62, 139-149.
- ÖRDÖG, T., WARD, S. M. & SANDERS, K. M. 1999. Interstitial cells of Cajal generate electrical slow waves in the murine stomach. *The Journal of Physiology*, 518, 257-269.
- OTALI, D., STOCKARD, C. R., OELSCHLAGER, D. K., WAN, W., MANNE, U., WATTS, S. A. & GRIZZLE, W. E. 2009. Combined effects of formalin fixation and tissue processing on immunorecognition. *Biotechnic & Histochemistry*, 84, 223-247.

- OZANICH, R. M., COLBURN, H. A., VICTRY, K. D., BARTHOLOMEW, R. A., ARCE, J. S., HEREDIA-LANGNER, A., JARMAN, K., KREUZER, H. W. & BRUCKNER-LEA, C. J. 2017. Evaluation of PCR systems for field screening of *Bacillus anthracis*. *Health security*, 15, 70-80.
- PAAVILAINEN, L., EDVINSSON, Å., ASPLUND, A., HOBER, S., KAMPF, C., PONTÉN, F. & WESTER, K. 2010. The impact of tissue fixatives on morphology and antibody-based protein profiling in tissues and cells. *Journal of Histochemistry & Cytochemistry*, 58, 237-246.
- PARDI, D. S., MILLER, S. M., MILLER, D. L., BURGART, L. J., SZURSZEWSKI, J. H., LENNON, V. A. & FARRUGIA, G. 2002. Paraneoplastic dysmotility: loss of interstitial cells of Cajal. *The American journal of gastroenterology*, 97, 1828.
- PARISI, M. A. 2015. Hirschsprung disease overview.
- PARISI, M. A. & KAPUR, R. P. 2000. Genetics of Hirschsprung disease. *Current opinion in pediatrics*, 12, 610-617.
- PARK, K. J., HENNIG, G. W., LEE, H.-T., SPENCER, N. J., WARD, S. M., SMITH, T. K. & SANDERS, K. M. 2006. Spatial and temporal mapping of pacemaker activity in interstitial cells of Cajal in mouse ileum in situ. *American Journal of Physiology-Cell Physiology*, 290, C1411-C1427.
- PARK, S.-H., MIN, H., CHI, J. G., PARK, K. W., YANG, H. R. & SEO, J. K. 2005. Immunohistochemical studies of pediatric intestinal pseudo-obstruction: bcl2, a valuable biomarker to detect immature enteric ganglion cells. *The American journal of surgical pathology*, 29, 1017-1024.
- PARSONS, S. P., KUNZE, W. A. & HUIZINGA, J. D. 2011. Maxi-channels recorded in situ from ICC and pericytes associated with the mouse myenteric plexus. *American Journal of Physiology-Cell Physiology*, 302, C1055-C1069.
- PASTERNAK, A., GIL, K., MATYJA, A., GAJDA, M., SZTEFKO, K., WALOCHA, J. A., KULIG, J. & THOR, P. 2013. Loss of gallbladder interstitial Cajal-like cells in patients with cholelithiasis. *Neurogastroenterology & Motility*, 25, e17-e24.
- PERI, L. E., SANDERS, K. M. & MUTAFOVA-YAMBOLIEVA, V. N. 2013. Differential expression of genes related to purinergic signaling in smooth muscle cells, PDGFR $\alpha$ -positive cells, and interstitial cells of Cajal in the murine colon. *Neurogastroenterology & Motility*, 25.
- PIERI, L., VANNUCCHI, M. G. & FAUSSONE-PELLEGRINI, M. S. 2008. Histochemical and ultrastructural characteristics of an interstitial cell type different from ICC and resident in the muscle coat of human gut. *Journal of cellular and molecular medicine*, 12, 1944-1955.
- PILERI, S. A., RONCADOR, G., CECCARELLI, C., PICCIOLI, M., BRISKOMATIS, A., SABATTINI, E., ASCANI, S., SANTINI, D., PICCALUGA, P. P. & LEONE, O. 1997. Antigen retrieval techniques in immunohistochemistry: comparison of different methods. *The Journal of Pathology: A Journal of the Pathological Society of Great Britain and Ireland*, 183, 116-123.
- PIOTROWSKA, A. P., SOLARI, V., DE CALUWÉ, D. & PURI, P. 2003a. Immunocolocalization of the heme oxygenase-2 and interstitial cells of

- Cajal in normal and aganglionic colon. *Journal of pediatric surgery*, 38, 73-77.
- PIOTROWSKA, A. P., SOLARI, V. & PURI, P. 2003b. Distribution of Ca<sup>2+</sup>-Activated k<sup>+</sup> channels, SK2 and SK3, in the normal and Hirschsprung's disease bowel. *Journal of pediatric surgery*, 38, 978-983.
- PK NAKANE, G. P. J. 1966. Enzyme-labeled antibodies: preparation and application for the localization of antigens. *Journal of Histochemistry & Cytochemistry*, 14, 929-931.
- PLUJÀ, L., FERNÁNDEZ, E. & JIMÉNEZ, M. 1999. Neural modulation of the cyclic electrical and mechanical activity in the rat colonic circular muscle: putative role of ATP and NO. *British journal of pharmacology*, 126, 883-892.
- POPESCU, L., GHERGHICEANU, M., HINESCU, M., CRETOIU, D., CEAFALAN, L., REGALIA, T., POPESCU, A., ARDELEANU, C. & MANDACHE, E. 2006. Insights into the interstitium of ventricular myocardium: interstitial Cajal-like cells (ICLC). *Journal of cellular and molecular medicine*, 10, 429-458.
- PRAKASH, V. & HUSSEIN, M. 2018. HISTOLOGICAL STUDY-THE EFFECTS OF VARIOUS FIXATIVES ON KIDNEY Dr. *INDIAN JOURNAL OF APPLIED RESEARCH*, 8.
- PRATO, A. P., ROSSI, V., AVANZINI, S., MATTIOLI, G., DISMA, N. & JASONNI, V. 2011. Hirschsprung's disease: what about mortality? *Pediatric surgery international*, 27, 473-478.
- PUFFENBERGER, E. G., HOSODA, K., WASHINGTON, S. S., NAKAO, K., YANAGISAWA, M. & CHAKRAVARTI, A. 1994. A missense mutation of the endothelin-B receptor gene in multigenic Hirschsprung's disease. *Cell*, 79, 1257-1266.
- PURI, P. & FRIEDMACHER, F. 2018. Hirschsprung's disease. *Rickham's Neonatal Surgery*. Springer.
- PUSHKAREV, D., NEFF, N. F. & QUAKE, S. R. 2009. Single-molecule sequencing of an individual human genome. *Nature biotechnology*, 27, 847.
- RADENKOVIC, G., ILIC, I., ZIVANOVIC, D., VLAJKOVIC, S., PETROVIC, V. & MITROVIC, O. 2010a. C-kit-immunopositive interstitial cells of Cajal in human embryonal and fetal oesophagus. *Cell and tissue research*, 340, 427-436.
- RADENKOVIC, G., RADENKOVIC, D. & VELICKOV, A. 2018. Development of interstitial cells of Cajal in the human digestive tract as the result of reciprocal induction of mesenchymal and neural crest cells. *Journal of cellular and molecular medicine*, 22, 778-785.
- RADENKOVIC, G., SAVIC, V., MITIC, D., GRAHOVAC, S., BJELAKOVIC, M. & KRSTIC, M. 2010b. Development of c-kit immunopositive interstitial cells of Cajal in the human stomach. *Journal of cellular and molecular medicine*, 14, 1125-1134.
- RAIT, V. K., O'LEARY, T. J. & MASON, J. T. 2004a. Modeling formalin fixation and antigen retrieval with bovine pancreatic ribonuclease A: I—Structural and functional alterations. *Laboratory investigation*, 84, 292.

- RAIT, V. K., XU, L., O'LEARY, T. J. & MASON, J. T. 2004b. Modeling formalin fixation and antigen retrieval with bovine pancreatic RNase A II. Interrelationship of cross-linking, immunoreactivity, and heat treatment. *Laboratory investigation*, 84, 300.
- RAMOS-VARA, J. 2005. Technical aspects of immunohistochemistry. *Veterinary pathology*, 42, 405-426.
- RAMOS-VARA, J. A. & BEISSENHERZ, M. E. 2000. Optimization of immunohistochemical methods using two different antigen retrieval methods on formalin-fixed, paraffin-embedded tissues: experience with 63 markers. *Journal of Veterinary Diagnostic Investigation*, 12, 307-311.
- REHFELD, J. F. 1998. The new biology of gastrointestinal hormones. *Physiological reviews*, 78, 1087-1108.
- ROBINSON, T. L., SIRCAR, K., HEWLETT, B. R., CHORNEYKO, K., RIDDELL, R. H. & HUIZINGA, J. D. 2000. Gastrointestinal stromal tumors may originate from a subset of CD34-positive interstitial cells of Cajal. *The American journal of pathology*, 156, 1157-1163.
- ROLLE, U., PIASECZNA-PIOTROWSKA, A. & PURI, P. 2007. Interstitial cells of Cajal in the normal gut and in intestinal motility disorders of childhood. *Pediatric surgery international*, 23, 1139-1152.
- ROLLE, U., PIOTROWSKA, A. P., NEMETH, L. & PURI, P. 2002. Altered distribution of interstitial cells of Cajal in Hirschsprung disease. *Archives of pathology & laboratory medicine*, 126, 928-933.
- ROMEO, G., RONCHETTO, P., LUO, Y., BARONE, V., SERI, M., CECCHERINI, I., PASINI, B., BOCCIARDI, R., LERONE, M. & KÄÄRIÄINEN, H. 1994. Point mutations affecting the tyrosine kinase domain of the RET proto-oncogene in Hirschsprung's disease. *Nature*, 367, 377.
- RØMERT, P. & MIKKELSEN, H. B. 1998. c-kit immunoreactive interstitial cells of Cajal in the human small and large intestine. *Histochemistry and cell biology*, 109, 195-202.
- ROSENBAUM, S. T., SVALØ, J., NIELSEN, K., LARSEN, T., JØRGENSEN, J. C. & BOUCHELOUCHE, P. 2012. Immunolocalization and expression of small-conductance calcium-activated potassium channels in human myometrium. *Journal of cellular and molecular medicine*, 16, 3001-3008.
- RUIZ-FERRER, M., TORROGLOSA, A., NÚÑEZ-TORRES, R., DE AGUSTÍN, J. C., ANTIÑOLO, G. & BORREGO, S. 2011. Expression of PROKR1 and PROKR2 in human enteric neural precursor cells and identification of sequence variants suggest a role in HSCR. *PLoS One*, 6, e23475.
- RUMESSEN, J. J. 1994. Identification of interstitial cells of Cajal. Significance for studies of human small intestine and colon. *Danish medical bulletin*, 41, 275-293.
- RUMESSEN, J. J., MIKKELSEN, H. B., QVORTRUP, K. & THUNEBERG, L. 1993. Ultrastructure of interstitial cells of Cajal in circular muscle of human small intestine. *Gastroenterology*, 104, 343-350.
- RUMESSEN, J. J., MIKKELSEN, H. B. & THUNEBERG, L. 1992. Ultrastructure of interstitial cells of Cajal associated with deep muscular plexus of human small intestine. *Gastroenterology*, 102, 56-68.

- RUMESSEN, J. J. & THUNEBERG, L. 1991. Interstitial cells of cajal in human small intestine Ultrastructural identification and organization between the main smooth muscle layers. *Gastroenterology*, 100, 1417-1431.
- RUMESSEN, J. J., THUNEBERG, L. & MIKKELSEN, H. B. 1982. Plexus muscularis profundus and associated interstitial cells. II. Ultrastructural studies of mouse small intestine. *The Anatomical Record*, 203, 129-146.
- RUMESSEN, J. J., VANDERWINDEN, J.-M., HANSEN, A. & HORN, T. 2013. Ultrastructure of interstitial cells in subserosa of human colon. *Cells Tissues Organs*, 197, 322-332.
- RUMESSEN, J. J., VANDERWINDEN, J.-M., RASMUSSEN, H., HANSEN, A. & HORN, T. 2009. Ultrastructure of interstitial cells of Cajal in myenteric plexus of human colon. *Cell and tissue research*, 337, 197-212.
- SAFFREY, M. J. 2013. Cellular changes in the enteric nervous system during ageing. *Developmental biology*, 382, 344-355.
- SALOMON, R., ATTIE, T., PELET, A., BIDAUD, C., ENG, C., AMIEL, J., SARNACKI, S., GOULET, O., RICOUR, C. & NIHOUL-FÉKÉTÉ, C. 1996. Germline mutations of the RET ligand GDNF are not sufficient to cause Hirschsprung disease. *Nature genetics*, 14, 345.
- SANCHEZ-MEJIAS, A., FERNÁNDEZ, R. M., LOPEZ-ALONSO, M., ANTIÑOLO, G. & BORREGO, S. 2010. New roles of EDNRB and EDN3 in the pathogenesis of Hirschsprung disease. *Genetics in Medicine*, 12, 39.
- SÁNCHEZ-MEJÍAS, A., NÚÑEZ-TORRES, R., FERNÁNDEZ, R. M., ANTIÑOLO, G. & BORREGO, S. 2010a. Novel MLPA procedure using self-designed probes allows comprehensive analysis for CNVs of the genes involved in Hirschsprung disease. *BMC medical genetics*, 11, 71.
- SÁNCHEZ-MEJÍAS, A., WATANABE, Y., FERNÁNDEZ, R. M., LÓPEZ-ALONSO, M., ANTIÑOLO, G., BONDURAND, N. & BORREGO, S. 2010b. Involvement of SOX10 in the pathogenesis of Hirschsprung disease: report of a truncating mutation in an isolated patient. *Journal of molecular medicine*, 88, 507-514.
- SANDERS, K., KOH, S., ÖRDÖG, T. & WARD, S. 2004. Ionic conductances involved in generation and propagation of electrical slow waves in phasic gastrointestinal muscles. *Neurogastroenterology & Motility*, 16, 100-105.
- SANDERS, K. M. 1996. A case for interstitial cells of Cajal as pacemakers and mediators of neurotransmission in the gastrointestinal tract. *Gastroenterology*, 111, 492-515.
- SANDERS, K. M., KITO, Y., HWANG, S. J. & WARD, S. M. 2016. Regulation of gastrointestinal smooth muscle function by interstitial cells. *Physiology*, 31, 316-326.
- SANDERS, K. M., KOH, S. D., RO, S. & WARD, S. M. 2012a. Regulation of gastrointestinal motility—insights from smooth muscle biology. *Nature reviews Gastroenterology & hepatology*, 9, 633.
- SANDERS, K. M., KOH, S. D. & WARD, S. M. 2006. Interstitial cells of Cajal as pacemakers in the gastrointestinal tract. *Annu. Rev. Physiol.*, 68, 307-343.
- SANDERS, K. M., WARD, S. M. & KOH, S. D. 2014. Interstitial cells: regulators of smooth muscle function. *Physiological reviews*, 94, 859-907.

- SANDERS, K. M., ZHU, M. H., BRITTON, F., KOH, S. D. & WARD, S. M. 2012b. Anoctamins and gastrointestinal smooth muscle excitability. *Experimental physiology*, 97, 200-206.
- SAYEGH, A. I. & WASHINGTON, M. C. 2012. Back to Basics: Regulation of the Gastrointestinal Functions. *J Gastroint Dig Syst*, 2, 118.
- SCALIA, C. R., BOI, G., BOLOGNESI, M. M., RIVA, L., MANZONI, M., DESMEDT, L., BOSISIO, F. M., RONCHI, S., LEONE, B. E. & CATTORETTI, G. 2017. Antigen masking during fixation and embedding, dissected. *Journal of Histochemistry & Cytochemistry*, 65, 5-20.
- SCHEPPACH, W. 1994. Effects of short chain fatty acids on gut morphology and function. *Gut*, 35, S35-S38.
- SERI, M., YIN, L., BARONE, V., BOLINO, A., CELLI, I., BOCCIARDI, R., PASINI, B., CECCHERINI, I., LERONE, M. & KRISTOFFERSSON, U. 1997. Frequency of RET mutations in long-and short-segment Hirschsprung disease. *Human mutation*, 9, 243-249.
- SHAN-RONG SHI, R. J. C., CLIVE R. TAYLOR 2001. Antigen Retrieval Techniques: Current Perspectives. *Journal of Histochemistry and Cytochemistry*, 49, 931-937.
- SHANG-JIE XIAO, X.-C. Z., HUA DENG, WEI-PING ZHOU, WEN-YI YANG, LI-KE YUAN, JIANG-YU ZHANG, SONG TIAN, LU XU, LIANG ZHANG, HUI-MIN XIA 2018. Gene expression profiling coupled with Connectivity Map database mining reveals potential therapeutic drugs for Hirschsprung disease. *Journal of Pediatric Surgery*, 53, 1716-1721.
- SHI, S.-R., COTE, R. J. & TAYLOR, C. R. 1997. Antigen retrieval immunohistochemistry: past, present, and future. *Journal of Histochemistry & Cytochemistry*, 45, 327-343.
- SHI, S.-R., LIU, C., POOTRAKUL, L., TANG, L., YOUNG, A., CHEN, R., COTE, R. J. & TAYLOR, C. R. 2008. Evaluation of the value of frozen tissue section used as "gold standard" for immunohistochemistry. *American journal of clinical pathology*, 129, 358-366.
- SHI, S.-R., LIU, C. & TAYLOR, C. R. 2007. Standardization of immunohistochemistry for formalin-fixed, paraffin-embedded tissue sections based on the antigen-retrieval technique: from experiments to hypothesis. *Journal of Histochemistry & Cytochemistry*, 55, 105-109.
- SHI, S.-R., SHI, Y. & TAYLOR, C. R. 2011. Antigen retrieval immunohistochemistry: review and future prospects in research and diagnosis over two decades. *Journal of Histochemistry & Cytochemistry*, 59, 13-32.
- SHIN, H., KALAPURAKAL, S. K., LEE, J. J., RO, J. Y., HONG, W. K. & LEE, J. S. 1997. Comparison of p53 immunoreactivity in fresh-cut versus stored slides with and without microwave heating. *Modern pathology: an official journal of the United States and Canadian Academy of Pathology, Inc*, 10, 224-230.
- SHUTTLEWORTH, C., XUE, C., WARD, S., DE VENETE, J. & SANDERS, K. 1993. Immunohistochemical localization of 3', 5'-cyclic guanosine monophosphate in the canine proximal colon: responses to nitric oxide

- and electrical stimulation of enteric inhibitory neurons. *Neuroscience*, 56, 513-522.
- SINGH, B., MAL, G., BISSI, L. & MAROTTA, F. 2016. Journal of Gastrointestinal & Digestive System.
- SINGH, R. D., GIBBONS, S. J., SARAVANAPERUMAL, S. A., DU, P., HENNIG, G. W., EISENMAN, S. T., MAZZONE, A., HAYASHI, Y., CAO, C. & STOLTZ, G. J. 2014. Ano1, a Ca<sup>2+</sup>-activated Cl<sup>-</sup> channel, coordinates contractility in mouse intestine by Ca<sup>2+</sup> transient coordination between interstitial cells of Cajal. *The Journal of physiology*, 592, 4051-4068.
- SIRCAR, K., HEWLETT, B., HUIZINGA, J., CHORNEYKO, K., BEREZIN, I. & RIDDELL, R. 1999. Interstitial cells of Cajal as precursors of gastrointestinal stromal tumors. *The American journal of surgical pathology*, 23, 377-389.
- SMITH, C. J. & OSBORN, A. M. 2009. Advantages and limitations of quantitative PCR (Q-PCR)-based approaches in microbial ecology. *FEMS microbiology ecology*, 67, 6-20.
- SMITH, T. K., REED, J. B. & SANDERS, K. M. 1987. Interaction of two electrical pacemakers in muscularis of canine proximal colon. *American Journal of Physiology-Cell Physiology*, 252, C290-C299.
- SOLARI, V., PIOTROWSKA, A. P. & PURI, P. 2003. Histopathological differences between recto-sigmoid Hirschsprung's disease and total colonic aganglionosis. *Pediatric surgery international*, 19, 349-354.
- SOUTHARD-SMITH, E. M., KOS, L. & PAVAN, W. J. 1998. Sox10 mutation disrupts neural crest development in Dom Hirschsprung mouse model. *Nature genetics*, 18, 60.
- SPECHT, K., RICHTER, T., MÜLLER, U., WALCH, A., WERNER, M. & HÖFLER, H. 2001. Quantitative gene expression analysis in microdissected archival formalin-fixed and paraffin-embedded tumor tissue. *The American journal of pathology*, 158, 419-429.
- SPENCER, N. J., HENNIG, G. W. & SMITH, T. K. 2002. Electrical rhythmicity and spread of action potentials in longitudinal muscle of guinea pig distal colon. *American Journal of Physiology-Gastrointestinal and Liver Physiology*, 282, G904-G917.
- SPOUGE, D. & BAIRD, P. 1985. Hirschsprung disease in a large birth cohort. *Teratology*, 32, 171-177.
- SRINIVASAN, M., SEDMAK, D. & JEWELL, S. 2002. Effect of fixatives and tissue processing on the content and integrity of nucleic acids. *The American journal of pathology*, 161, 1961-1971.
- STERNINI, C., SU, D., GAMP, P. D. & BUNNETT, N. W. 1995. Cellular sites of expression of the neurokinin-1 receptor in the rat gastrointestinal tract. *Journal of Comparative Neurology*, 358, 531-540.
- STREUTKER, C., HUIZINGA, J., DRIMAN, D. & RIDDELL, R. 2007. Interstitial cells of Cajal in health and disease. Part I: normal ICC structure and function with associated motility disorders. *Histopathology*, 50, 176-189.
- SUTCLIFFE, J., SUGARMAN, I. & LEVITT, M. 2013. Anorectal anomalies and Hirschsprung disease (including stomas). *Surgery-Oxford International Edition*, 31, 631-638.

- SUZUKI, H., TAKANO, H., YAMAMOTO, Y., KOMURO, T., SAITO, M., KATO, K. & MIKOSHIBA, K. 2000. Properties of gastric smooth muscles obtained from mice which lack inositol trisphosphate receptor. *The Journal of Physiology*, 525, 105-111.
- SUZUKI, H., WARD, S., BAYGUINOV, Y., EDWARDS, F. & HIRST, G. 2003. Involvement of intramuscular interstitial cells in nitrenergic inhibition in the mouse gastric antrum. *The Journal of physiology*, 546, 751-763.
- SYRBU, S. I. & COHEN, M. B. 2011. An enhanced antigen-retrieval protocol for immunohistochemical staining of formalin-fixed, paraffin-embedded tissues. *Signal Transduction Immunohistochemistry*. Springer.
- SZYLBERG, Ł. & MARSZAŁEK, A. 2014. Diagnosis of Hirschsprung's disease with particular emphasis on histopathology. A systematic review of current literature. *Przegląd gastroenterologiczny*, 9, 264.
- TAGUCHI, T., SUITA, S., MASUMOTO, K. & NADA, O. 2003. Universal distribution of c-kit-positive cells in different types of Hirschsprung's disease. *Pediatric surgery international*, 19, 273-279.
- TAGUCHI, T., SUITA, S., MASUMOTO, K. & NAGASAKI, A. 2005. An abnormal distribution of C-kit positive cells in the normoganglionic segment can predict a poor clinical outcome in patients with Hirschsprung's disease. *European journal of pediatric surgery*, 15, 153-158.
- TAM, P. K. & GARCIA-BARCELÓ, M. J. P. S. I. 2009. Genetic basis of Hirschsprung's disease. 25, 543-558.
- TANG, C. S.-M., NGAN, E. S.-W., TANG, W.-K., SO, M.-T., CHENG, G., MIAO, X.-P., LEON, T. Y.-Y., LEUNG, B. M.-C., HUI, K.-J. W. & LUI, V. H.-C. 2012. Mutations in the NRG1 gene are associated with Hirschsprung disease. *Human genetics*, 131, 67-76.
- TANG, W., LI, B., TANG, J., LIU, K., QIN, J., WU, W., GENG, Q., ZHANG, J., CHEN, H. & XU, X. 2013. Methylation analysis of EDNRB in human colon tissues of Hirschsprung's disease. *Pediatric surgery international*, 29, 683-688.
- TARAVIRAS, S., MARCOS-GUTIERREZ, C. V., DURBEC, P., JANI, H., GRIGORIOU, M., SUKUMARAN, M., WANG, L.-C., HYNES, M., RAISMAN, G. & PACHNIS, V. J. D. 1999. Signalling by the RET receptor tyrosine kinase and its role in the development of the mammalian enteric nervous system. 126, 2785-2797.
- TAYLOR, C. 2006. Standardization in immunohistochemistry: the role of antigen retrieval in molecular morphology. *Biotechnic & Histochemistry*, 81, 3-12.
- TAYLOR, C. & BURNS, J. 1974. The demonstration of plasma cells and other immunoglobulin-containing cells in formalin-fixed, paraffin-embedded tissues using peroxidase-labelled antibody. *Journal of clinical pathology*, 27, 14-20.
- TAYLOR, C. R., SHI, S.-R., CHEN, C., YOUNG, L., YANG, C. & COTE, R. J. 1996. Comparative study of antigen retrieval heating methods: microwave, microwave and pressure cooker, autoclave, and steamer. *Biotechnic & histochemistry*, 71, 263-270.

- THUNEBERG, L. 1999. One hundred years of interstitial cells of Cajal. *Microscopy research and technique*, 47, 223-238.
- THUNEBERG, L., RUMESSEN, J. & MIKKELSEN, H. 1982. Interstitial cells of Cajal-an intestinal impulse generation and conduction system? *Scandinavian journal of gastroenterology. Supplement*, 71, 143-4.
- TIMMERMANS, J.-P. 2001. Interstitial cells of Cajal: is their role in gastrointestinal function in view of therapeutic perspectives underestimated or exaggerated? *Folia morphologica*, 60, 1-10.
- TJADEN, N. E. B. & TRAINOR, P. A. 2013. The developmental etiology and pathogenesis of Hirschsprung disease. *Translational Research*, 162, 1-15.
- TOMAN, J., TURINA, M., RAY, M., PETRAS, R. E., STROMBERG, A. J. & GALANDIUK, S. 2006. Slow transit colon constipation is not related to the number of interstitial cells of Cajal. *International journal of colorectal disease*, 21, 527-532.
- TORIHASHI, S., HORISAWA, M. & WATANABE, Y. 1999a. c-Kit immunoreactive interstitial cells in the human gastrointestinal tract. *Journal of the autonomic nervous system*, 75, 38-50.
- TORIHASHI, S., KOBAYASHI, S., GERTHOFFER, W. T. & SANDERS, K. M. 1993. Interstitial cells in deep muscular plexus of canine small intestine may be specialized smooth muscle cells. *American Journal of Physiology-Gastrointestinal and Liver Physiology*, 265, G638-G645.
- TORIHASHI, S., NISHI, K., TOKUTOMI, Y., NISHI, T., WARD, S. & SANDERS, K. M. 1999b. Blockade of kit signaling induces transdifferentiation of interstitial cells of Cajal to a smooth muscle phenotype. *Gastroenterology*, 117, 140-148.
- TORIHASHI, S., WARD, S. M., NISHIKAWA, S.-I., NISHI, K., KOBAYASHI, S. & SANDERS, K. M. 1995. c-kit-Dependent development of interstitial cells and electrical activity in the murine gastrointestinal tract. *Cell and tissue research*, 280, 97-111.
- TORIHASHI, S., WARD, S. M. & SANDERS, K. M. 1997. Development of c-Kit-positive cells and the onset of electrical rhythmicity in murine small intestine. *Gastroenterology*, 112, 144-155.
- TORIHASHI\*, S., NISHI‡, K., TOKUTOMI‡, Y., NISHI\*, T., WARD§, S. & SANDERS§, K. M. Blockade of kit signaling induces transdifferentiation of interstitial cells of Cajal to a smooth muscle phenotype. *Gastroenterology*, 117, 140-148.
- TORROGLOSA, A., ALVES, M., FERNÁNDEZ, R. M., ANTIÑOLO, G., HOFSTRA, R. & BORREGO, S. 2016. Epigenetics in ENS development and Hirschsprung disease. *Developmental biology*, 417, 209-216.
- TOSHIHIDE IWASHITA, G. M. K., RICARDO PARDAL, , MARK J. KIEL & MORRISON, S. J. 2003. Hirschsprung Disease Is Linked to Defects in Neural Crest Stem Cell Function. *Science*, 301, 972-976.
- TRAVAGLI, R. A., HERMANN, G. E., BROWNING, K. N. & ROGERS, R. C. 2006. Brainstem circuits regulating gastric function. *Annu. Rev. Physiol.*, 68, 279-305.
- TRUPP, M., ARENAS, E., FAINZILBER, M., NILSSON, A.-S., SIEBER, B.-A., GRIGORIOU, M., KILKENNY, C., SALAZAR-GRUESO, E., PACHNIS,

- V. & ARUMÄE, U. 1996. Functional receptor for GDNF encoded by the c-ret proto-oncogene. *Nature*, 381, 785.
- V. ASHLEY CANTRELL, SARAH E. OWENS, RONALD L. CHANDLER, DAVID C. AIREY, KEVIN M. BRADLEY, JEFFREY R. SMITH & SOUTHARD-SMITH, E. M. 2004. Interactions between Sox10 and EdnrB modulate penetrance and severity of aganglionosis in the Sox10Dom mouse model of Hirschsprung disease. *Human Molecular Genetics*, 13, 2289-2301.
- VAN DER STAAY, F., FANELLI, R., BLOKLAND, A. & SCHMIDT, B. 1999. Behavioral effects of apamin, a selective inhibitor of the SKCa-channel, in mice and rats. *Neuroscience & Biobehavioral Reviews*, 23, 1087-1110.
- VAN HELDEN, D. F., LAVER, D. R., HOLDSWORTH, J. & IMTIAZ, M. S. 2010. Generation and propagation of gastric slow waves. *Clinical and Experimental Pharmacology and Physiology*, 37, 516-524.
- VANDERWINDEN, J.-M., RUMESSEN, J. J., DE KERCHOVE D'EXAERDE, A., GILLARD, K., PANTHIER, J.-J., LAET, M.-H. & SCHIFFMANN, S. N. 2002. Kit-negative fibroblast-like cells expressing SK3, a Ca<sup>2+</sup>-activated K<sup>+</sup> channel, in the gut musculature in health and disease. *Cell and tissue research*, 310, 349-358.
- VANDERWINDEN, J.-M., RUMESSEN, J. J., DE LAET, M.-H., VANDERHAEGHEN, J.-J. & SCHIFFMANN, S. N. 2000. CD34 immunoreactivity and interstitial cells of Cajal in the human and mouse gastrointestinal tract. *Cell and tissue research*, 302, 145-153.
- VANDERWINDEN, J.-M., RUMESSEN, J. J., DE, M. L., VANDERHAEGHEN, J.-J. & SCHIFFMANN, S. N. 1999. CD34+ cells in human intestine are fibroblasts adjacent to, but distinct from, interstitial cells of Cajal. *Laboratory investigation; a journal of technical methods and pathology*, 79, 59-65.
- VANDERWINDEN, J. M., RUMESSEN, J. J., LIU, H., DESCAMPS, D., DE LAET, M. H. & VANDERHAEGHEN, J. J. 1996. Interstitial cells of Cajal in human colon and in Hirschsprung's disease. *Gastroenterology*, 111, 901-910.
- VANNUCCHI, M. G., DE GIORGIO, R. & FAUSSONE-PELLEGRINI, M. S. 1997. NK1 receptor expression in the interstitial cells of Cajal and neurons and tachykinins distribution in rat ileum during development. *Journal of Comparative Neurology*, 383, 153-162.
- VANNUCCHI, M. G. & TRAINI, C. 2016. Interstitial cells of Cajal and telocytes in the gut: twins, related or simply neighbor cells? *Biomolecular concepts*, 7, 93-102.
- VANNUCCHI, M. G., TRAINI, C., MANETTI, M., IBBA-MANNESCHI, L. & FAUSSONE-PELLEGRINI, M. S. 2013. Telocytes express PDGFR  $\alpha$  in the human gastrointestinal tract. *Journal of cellular and molecular medicine*, 17, 1099-1108.
- VILLANACCI, V., BASSOTTI, G., NASCIMBENI, R., ANTONELLI, E., CADEI, M., FISOGNI, S., SALERNI, B. & GEBOES, K. 2008. Enteric nervous system abnormalities in inflammatory bowel diseases. *Neurogastroenterology & Motility*, 20, 1009-1016.

- WALLACE, A. S. & BURNS, A. J. 2005. Development of the enteric nervous system, smooth muscle and interstitial cells of Cajal in the human gastrointestinal tract. *Cell and tissue research*, 319, 367-382.
- WALLACE, A. S., BURNS, A. J. J. C. & RESEARCH, T. 2005. Development of the enteric nervous system, smooth muscle and interstitial cells of Cajal in the human gastrointestinal tract. 319, 367-382.
- WANG, F., FLANAGAN, J., SU, N., WANG, L.-C., BUI, S., NIELSON, A., WU, X., VO, H.-T., MA, X.-J. & LUO, Y. 2012. RNAscope: a novel in situ RNA analysis platform for formalin-fixed, paraffin-embedded tissues. *The Journal of Molecular Diagnostics*, 14, 22-29.
- WANG, H., SU, N., WANG, L.-C., WU, X., BUI, S., NIELSEN, A., VO, H.-T., LUO, Y. & MA, X.-J. 2014a. Dual-color ultrasensitive bright-field RNA in situ hybridization with RNAscope. *In Situ Hybridization Protocols*. Springer.
- WANG, H., SU, N., WANG, L.-C., WU, X., BUI, S., NIELSEN, A., VO, H.-T., LUO, Y. & MA, X.-J. 2014b. Quantitative ultrasensitive bright-field RNA in situ hybridization with RNAscope. *In Situ Hybridization Protocols*. Springer.
- WANG, H., ZHANG, Y., LIU, W., WU, R., CHEN, X., GU, L., WEI, B. & GAO, Y. 2009. Interstitial cells of Cajal reduce in number in recto-sigmoid Hirschsprung's disease and total colonic aganglionosis. *Neuroscience letters*, 451, 208-211.
- WANG, J., MOU, Y., ZHANG, Q., ZHANG, F., YANG, H., ZHANG, W. & LI, A. 2013a. Expression and significance of neuroligins in myenteric cells of Cajal in Hirschsprung's disease. *PloS one*, 8, e67205.
- WANG, L. L., FAN, Y., ZHOU, F. H., LI, H., ZHANG, Y., MIAO, J. N., GU, H., HUANG, T. C. & YUAN, Z. W. 2011. Semaphorin 3A expression in the colon of Hirschsprung disease. *Birth Defects Research Part A: Clinical and Molecular Teratology*, 91, 842-847.
- WANG, L. M., MCNALLY, M., HYLAND, J. & SHEAHAN, K. 2008. Assessing interstitial cells of Cajal in slow transit constipation using CD117 is a useful diagnostic test. *The American journal of surgical pathology*, 32, 980-985.
- WANG, X., YUAN, C., XIANG, L., LI, X., ZHAO, Z. & JIN, X. 2013b. The clinical significance of pathological studies of congenital intestinal atresia. *Journal of pediatric surgery*, 48, 2084-2091.
- WANG, X. Y., PATERSON, C. & HUIZINGA, J. 2003. Cholinergic and nitrenergic innervation of ICC-DMP and ICC-IM in the human small intestine. *Neurogastroenterology & Motility*, 15, 531-543.
- WANG, X. Y., SANDERS, K. M. & WARD, S. M. 1999. Intimate relationship between interstitial cells of Cajal and enteric nerves in the guinea-pig small intestine. *Cell and tissue research*, 295, 247-256.
- WARD, S., ÖRDÖG, T., KOH, S., BAKER, S. A., JUN, J., AMBERG, G., MONAGHAN, K. & SANDERS, K. 2000a. Pacemaking in interstitial cells of Cajal depends upon calcium handling by endoplasmic reticulum and mitochondria. *The Journal of Physiology*, 525, 355-361.
- WARD, S. M., BECKETT, E. A., WANG, X., BAKER, F., KHOYI, M. & SANDERS, K. M. 2000b. Interstitial cells of Cajal mediate cholinergic

- neurotransmission from enteric motor neurons. *Journal of Neuroscience*, 20, 1393-1403.
- WARD, S. M., BURNS, A. J., TORIHASHI, S., HARNEY, S. C. & SANDERS, K. M. 1995. Impaired development of interstitial cells and intestinal electrical rhythmicity in steel mutants. *American Journal of Physiology-Cell Physiology*, 269, C1577-C1585.
- WARD, S. M., BURNS, A. J., TORIHASHI, S. & SANDERS, K. M. 1994a. Mutation of the proto-oncogene c-kit blocks development of interstitial cells and electrical rhythmicity in murine intestine. *The Journal of Physiology*, 480, 91-97.
- WARD, S. M., BURNS, A. J., TORIHASHI, S. & SANDERS, K. M. 1994b. Mutation of the proto-oncogene c-kit blocks development of interstitial cells and electrical rhythmicity in murine intestine. *The Journal of physiology*, 480, 91-97.
- WARD, S. M. & SANDERS, K. M. 2001. Interstitial cells of Cajal: primary targets of enteric motor innervation. *The Anatomical Record: An Official Publication of the American Association of Anatomists*, 262, 125-135.
- WARD, S. M. & SANDERS, K. M. 2006. Involvement of intramuscular interstitial cells of Cajal in neuroeffector transmission in the gastrointestinal tract. *The Journal of physiology*, 576, 675-682.
- WERNER, M., CHOTT, A., FABIANO, A. & BATTIFORA, H. 2000. Effect of formalin tissue fixation and processing on immunohistochemistry. *The American journal of surgical pathology*, 24, 1016-1019.
- WEST, R. B., CORLESS, C. L., CHEN, X., RUBIN, B. P., SUBRAMANIAN, S., MONTGOMERY, K., ZHU, S., BALL, C. A., NIELSEN, T. O. & PATEL, R. 2004. The novel marker, DOG1, is expressed ubiquitously in gastrointestinal stromal tumors irrespective of KIT or PDGFRA mutation status. *The American journal of pathology*, 165, 107-113.
- WESTER, K., WAHLUND, E., SUNDSTRÖM, C., RANEFALL, P., BENGTSSON, E., RUSSELL, P. J., OW, K. T., MALMSTRÖM, P.-U. & BUSCH, C. 2000. Paraffin section storage and immunohistochemistry: effects of time, temperature, fixation, and retrieval protocol with emphasis on p53 protein and MIB1 antigen. *Applied Immunohistochemistry & Molecular Morphology*, 8, 61-70.
- WHEELER, D. A., SRINIVASAN, M., EGHOLM, M., SHEN, Y., CHEN, L., MCGUIRE, A., HE, W., CHEN, Y.-J., MAKHIJANI, V. & ROTH, G. T. 2008. The complete genome of an individual by massively parallel DNA sequencing. *nature*, 452, 872.
- WIIG, H. & SWARTZ, M. A. 2012. Interstitial fluid and lymph formation and transport: physiological regulation and roles in inflammation and cancer. *Physiological reviews*, 92, 1005-1060.
- WILLIAMS, J., MEPHAM, B. & WRIGHT, D. 1997. Tissue preparation for immunocytochemistry. *Journal of clinical pathology*, 50, 422-428.
- WISSE, E., BRAET, F., DUMIEL, H., VREULS, C., KOEK, G., DAMINK, S. W. O., VAN DEN BROEK, M. A., DE GEEST, B., DEJONG, C. H. & TATENO, C. 2010. Fixation methods for electron microscopy of human and other liver. *World Journal of Gastroenterology: WJG*, 16, 2851.

- WON, K.-J., SANDERS, K. M. & WARD, S. M. 2005. Interstitial cells of Cajal mediate mechanosensitive responses in the stomach. *Proceedings of the National Academy of Sciences*, 102, 14913-14918.
- WORBY, C. A., VEGA, Q. C., ZHAO, Y., CHAO, H. H.-J., SEASHOLTZ, A. F. & DIXON, J. E. 1996. Glial cell line-derived neurotrophic factor signals through the RET receptor and activates mitogen-activated protein kinase. *Journal of Biological Chemistry*, 271, 23619-23622.
- XIE, R., CHUNG, J.-Y., YLAYA, K., WILLIAMS, R. L., GUERRERO, N., NAKATSUKA, N., BADIE, C. & HEWITT, S. M. 2011. Factors influencing the degradation of archival formalin-fixed paraffin-embedded tissue sections. *Journal of Histochemistry & Cytochemistry*, 59, 356-365.
- XUE, C., WARD, S. M., SHUTTLEWORTH, C. W. & SANDERS, K. M. 1993. Identification of interstitial cells in canine proximal colon using NADH diaphorase histochemistry. *Histochemistry*, 99, 373-384.
- YADAK, R., BREUR, M. & BUGIANI, M. 2019. Gastrointestinal Dysmotility in MNGIE: from thymidine phosphorylase enzyme deficiency to altered interstitial cells of Cajal. *Orphanet journal of rare diseases*, 14, 33.
- YAMASHIRO, M., KOUUDA, W., KONO, N., TSUNEYAMA, K., MATSUI, O. & NAKANUMA, Y. 1998. Distribution of intrahepatic mast cells in various hepatobiliary disorders. *Virchows Archiv*, 433, 471-479.
- YAMASHITA, S. 2007. Heat-induced antigen retrieval: mechanisms and application to histochemistry. *Progress in histochemistry and cytochemistry*, 41, 141-200.
- YAMATAKA, A., KATO, Y., TIBBOEL, D., MURATA, Y., SUEYOSHI, N., FUJIMOTO, T., NISHIYE, H. & MIYANO, T. 1995. A lack of intestinal pacemaker (c-kit) in aganglionic bowel of patients with Hirschsprung's disease. *Journal of pediatric surgery*, 30, 441-444.
- YAMATAKA, A., OHSHIRO, K., KOBAYASHI, H., FUJIWARA, T., SUNAGAWA, M. & MIYANO, T. 1997. Intestinal pacemaker C-KIT+ cells and synapses in allied Hirschsprung's disorders. *Journal of pediatric surgery*, 32, 1069-1074.
- YAMAZAWA, T. & IINO, M. 2002. Simultaneous imaging of Ca<sup>2+</sup> signals in interstitial cells of Cajal and longitudinal smooth muscle cells during rhythmic activity in mouse ileum. *The Journal of physiology*, 538, 823-835.
- YANG, J., DUAN, S., ZHONG, R., YIN, J., PU, J., KE, J., LU, X., ZOU, L., ZHANG, H. & ZHU, Z. 2013a. Exome sequencing identified NRG3 as a novel susceptible gene of Hirschsprung's disease in a Chinese population. *Molecular neurobiology*, 47, 957-966.
- YANG, X.-J., XU, J.-Y., SHEN, Z.-J. & ZHAO, J. 2013b. Immunohistochemical alterations of cajal-like type of tubal interstitial cells in women with endometriosis and tubal ectopic pregnancy. *Archives of gynecology and obstetrics*, 288, 1295-1300.
- YAO, H., FAN, J., CHENG, Y. J., CHEN, X. M., JI, C. C., LIU, L. J., ZHENG, Z. H. & WU, S. H. 2018. SCN 1B $\beta$  mutations that affect their association with Kv4. 3 underlie early repolarization syndrome. *Journal of cellular and molecular medicine*, 22, 5639-5647.

- YONEDA, S., FUKUI, H. & TAKAKI, M. 2004. Pacemaker activity from submucosal interstitial cells of Cajal drives high-frequency and low-amplitude circular muscle contractions in the mouse proximal colon. *Neurogastroenterology & Motility*, 16, 621-627.
- YOUNG, H., CIAMPOLI, D., SOUTHWELL, B. & NEWGREEN, D. 1996. Origin of interstitial cells of Cajal in the mouse intestine. *Developmental biology*, 180, 97-107.
- YOUNG, H., MCCONALOGUE, K., FURNESS, J. & DE VENETE, J. 1993. Nitric oxide targets in the guinea-pig intestine identified by induction of cyclic GMP immunoreactivity. *Neuroscience*, 55, 583-596.
- YOUNG, H. M. 1999. Embryological origin of interstitial cells of Cajal. *Microscopy Research and Technique*, 47, 303-308.
- YUN, H.-Y., SUNG, R., KIM, Y. C., CHOI, W., KIM, H. S., KIM, H., LEE, G. J., YOU, R. Y., PARK, S.-M. & YUN, S. J. 2010. Regional distribution of interstitial cells of Cajal (ICC) in human stomach. *The Korean Journal of Physiology & Pharmacology*, 14, 317-324.
- ZANNI, E., ADAMO, A., BELLIGNI, E., LERONE, M., MARTUCCIELLO, G., MATTIOLI, G., PRATO, A. P., RAVAZZOLO, R., SILENGO, M. & BACHETTI, T. J. B. E. B. A.-M. B. O. D. 2017. Common PHOX2B poly-alanine contractions impair RET gene transcription, predisposing to Hirschsprung disease. 1863, 1770-1777.
- ZHANG, R. X., WANG, X. Y., CHEN, D. & HUIZINGA, J. 2011. Role of interstitial cells of Cajal in the generation and modulation of motor activity induced by cholinergic neurotransmission in the stomach. *Neurogastroenterology & Motility*, 23, e356-e371.
- ZHANG, W., SEGURA, B. J., LIN, T. R., HU, Y. & MULHOLLAND, M. W. 2003. Intercellular calcium waves in cultured enteric glia from neonatal guinea pig. *Glia*, 42, 252-262.
- ZHANG, Y., HE, Q., ZHANG, R., ZHANG, H., ZHONG, W. & XIA, H. 2017. Large-scale replication study identified multiple independent SNPs in RET synergistically associated with Hirschsprung disease in Southern Chinese population. *Aging (Albany NY)*, 9, 1996.
- ZHAO, J., ZHU, Y., XIE, X., YAO, Y., ZHANG, J., ZHANG, R., HUANG, L., CHENG, J., XIA, H. & HE, J. J. A. 2019. Pleiotropic effect of common PHOX2B variants in Hirschsprung disease and neuroblastoma. 11, 1252.
- ZHENG, H., PARK, K. S., KOH, S. D. & SANDERS, K. M. 2014. Expression and function of a T-type Ca<sup>2+</sup> conductance in interstitial cells of Cajal of the murine small intestine. *American Journal of Physiology-Cell Physiology*, 306, C705-C713.
- ZHI-WEN PAN, J.-C. L. 2012. Advances in Molecular Genetics of Hirschsprung's Disease  
*THE ANATOMICAL RECORD*, 295, 1628-1638.
- ZHOU, D.-S. & KOMURO, T. 1992a. The cellular network of interstitial cells associated with the deep muscular plexus of the guinea pig small intestine. *Anatomy and embryology*, 186, 519-527.

- ZHOU, D.-S. & KOMURO, T. 1992b. Interstitial cells associated with the deep muscular plexus of the guinea-pig small intestine, with special reference to the interstitial cells of Cajal. *Cell and tissue research*, 268, 205-216.
- ZHU, M. H., KIM, T. W., RO, S., YAN, W., WARD, S. M., KOH, S. D. & SANDERS, K. M. 2009. A Ca<sup>2+</sup>-activated Cl<sup>-</sup> conductance in interstitial cells of Cajal linked to slow wave currents and pacemaker activity. *The Journal of physiology*, 587, 4905-4918.
- ZHU, M. H., SUNG, I. K., ZHENG, H., SUNG, T. S., BRITTON, F. C., O'DRISCOLL, K., KOH, S. D. & SANDERS, K. M. 2011. Muscarinic activation of Ca<sup>2+</sup>-activated Cl<sup>-</sup> current in interstitial cells of Cajal. *The Journal of physiology*, 589, 4565-4582.
- ZHU, M. H., SUNG, T. S., O'DRISCOLL, K., KOH, S. D. & SANDERS, K. M. 2015. Intracellular Ca<sup>2+</sup> release from endoplasmic reticulum regulates slow wave currents and pacemaker activity of interstitial cells of Cajal. *American Journal of Physiology-Cell Physiology*, 308, C608-C620.
- ZHU, Y. F., WANG, X.-Y., LOWIE, B.-J., PARSONS, S., WHITE, L., KUNZE, W., PAWELKA, A. & HUIZINGA, J. D. 2014. Enteric sensory neurons communicate with interstitial cells of Cajal to affect pacemaker activity in the small intestine. *Pflügers Archiv-European Journal of Physiology*, 466, 1467-1475.